Synthetic Methodologies for Intermolecular Radical Difunctionalizations of Alkenes and Application of Artemisinin in an Acrylamide Polymerization

Inaugural-Dissertation

zur Erlangung des Doktorgrades

der Mathematisch-Naturwissenschaftlichen Fakultät

der Universität zu Köln

vorgelegt von

Marcel Lux

aus Siegen

2021

Berichterstatter: PD Dr. Martin Klußmann

         Prof. Dr. Albrecht Berkessel

Tag der mündlichen Prüfung: 17. Februar 2021

Erklärung zur Dissertation

gemäß der Promotionsordnung vom 12. März 2020

Hiermit versichere ich an Eides statt, dass ich die vorliegende Dissertation selbstständig und ohne die Benutzung anderer als der angegebenen Hilfsmittel und Literatur angefertigt habe. Alle Stellen, die wörtlich oder sinngemäß aus veröffentlichten und nicht veröffentlichten Werken dem Wortlaut oder dem Sinn nach entnommen wurden, sind als solche kenntlich gemacht. Ich versichere an Eides statt, dass diese Dissertation noch keiner anderen Fakultät oder Universität zur Prüfung vorgelegen hat; dass sie - abgesehen von unten angegebenen Teilpublikationen und eingebundenen Artikeln und Manuskripten - noch nicht veröffentlicht worden ist sowie, dass ich eine Veröffentlichung der Dissertation vor Abschluss der Promotion nicht ohne Genehmigung des Promotionsausschusses vornehmen werde. Die Bestimmungen dieser Ordnung sind mir bekannt. Darüber hinaus erkläre ich hiermit, dass ich die Ordnung zur Sicherung guter wissenschaftlicher Praxis und zum Umgang mit wissenschaftlichem Fehlverhalten der Universität zu Köln gelesen und sie bei der Durchführung der Dissertation zugrundeliegenden Arbeiten und der schriftlich verfassten Dissertation beachtet habe und verpflichte mich hiermit, die dort genannten Vorgaben bei allen wissenschaftlichen Tätigkeiten zu beachten und umzusetzen. Ich versichere, dass die eingereichte elektronische Fassung der eingereichten Druckfassung vollständig entspricht.

Teilpublikationen:

(1)   W. Shao, M. Lux, M. Klussmann *Org. Chem. Front.* **2019**, *6*, 1796–1800. [Ref. [1]]

(2)   M. Lux, M. Klussmann *Org. Lett.* **2020**, *22*, 3697–3701. [Ref. [2]]

18. Dezember 2020, Marcel Lux,

Datum, Name und Unterschrift

III

Abstract

An introduction is given to the topics of photoredox catalysis and intermolecular radical difunctionalizations of alkenes. Radical difunctionalizations transform C–C double (multiple) bonds by generating two new σ bonds in one reaction. Starting from general models in this research field, applications of α-carbonyl and acyl radicals are described. In addition, methodologies, which use the consecutive 1,2-addition of a radical as well as a nucleophile are addressed.

An application of artemisinin as a radical co-initiator in acrylamide polymerizations in aqueous medium was developed. The assessment of reaction conditions, leading to the formation and characterization of polymer mixtures is described. Hydrochloric acid as well as iron species are used as co-initiators. Furthermore, results from an *electron paramagnetic resonance* (EPR) experiment with the initiator system were pointing towards the involvement of a by December 2020 unknown radical in the chemistry of artemisinin.

A joined project is discussed, elaborating a method for Brønsted acid catalyzed γ-cyanoketone formations. The difunctionalization implements α-ketonyl radical formation from condensation of ketones with *tert*-butylhydroperoxide[3] and methanesulfonyl cyanide.[1] Contributions to learn about the application scope of formed γ-cyanoketones, subsequent transformations and from a noticed difference in diastereoselectivity compared to the previously reported γ-peroxyketone synthesis[3] are described.

An investigation of photoredox catalyzed alkene difunctionalization using a consecutive addition of acyl radicals and nucleophilic *N*-alkylindoles is summarized.[2] In the Ir(ppy)$_3$ catalyzed reaction, simple starting materials, namely aldehydes, *N*-alkylindoles and styrenes were employed. Moreover, a base is needed for successful product formation. The reaction is based on a Ir(III)/Ir(IV) catalytic cycle and *tert*-butyl perbenzoate as oxidant as well as precursor for *tert*-butoxyl radicals. Acyl radicals were generated by hydrogen atom transfer. Aryl as well as aliphatic aldehydes were suitable substrates. Investigations of the reaction scope, description of mechanistic indications and discussions in the scientific context are presented.

Die Einleitung behandelt die Themen Photoredoxkatalyse und intermolekulare, radikalische Difunktionalisierung von Alkenen. Mit Hilfe radikalischer Difunktionalisierung kann eine C–C Doppelbindung (Mehrfachbindung) in zwei neue σ-Bindungen an den entsprechenden C-Atomen umgesetzt werden. Ausgehend von Erläuterungen allgemeiner Modelle auf diesem Forschungsgebiet, werden Anwendungen von α-Carbonyl- und Acylradikalen beschrieben. Darüber hinaus, werden Synthesemethoden angesprochen, welche die aufeinanderfolgende 1,2-Addition eines Radikals sowie eines Nukleophils verwenden.

Eine Anwendung von Artemisinin als radikalischer Co-Initiator bei Acrylamidpolymerisationen im wässrigen Medium wurde entwickelt. Eine Untersuchung der Reaktionsbedingungen hin zur Synthese und Charakterisierung von Polymermischungen wird beschrieben. Salzsäure sowie Eisenspezies werden als Co-Initiatoren verwendet. Darüber hinaus, deuten die Ergebnisse eines EPR-Experiments (Electron Paramagnetic Resonance) mit dem Initiatorsystem auf die Beteiligung eines bis Dezember 2020 unbekannten Radikals in diesem Artemisinin-Initiatorsystem hin.

Ein gemeinsam durchgeführtes Projekt wird diskutiert, in dem eine Methode zur Brønsted-Säure-katalysierten Bildung von γ-Cyanoketonen entwickelt wurde. Die Difunktionalisierung implementiert die Bildung von α-Ketonylradikalen aus der Kondensation von Ketonen mit *tert*-Butylhydroperoxid[3] und Methansulfonylcyanid.[1] Beiträge zum Reaktionsumfang gebildeter γ-Cyanoketone, zum Verständnis von Folgereaktionen und beobachteter Diastereoselektivitäten werden beschrieben.

Eine Studie zur Photoredox-katalysierte Alkendifunktionalisierung unter aufeinanderfolgender Addition von Acylradikalen und nukleophilen *N*-Alkylindolen wird zusammengefasst.[2] Bei der Ir(ppy)₃-katalysierten Reaktion wurden schlichte Edukte, nämlich Aldehyde, *N*-Alkylindole und Styrole, eingesetzt. Zusätzlich wird für eine erfolgreiche Produktbildung eine Base benötigt. Die Reaktion basiert auf einem Ir(III)/Ir(IV)-Katalysezyklus und *tert*-Butylperbenzoat als Oxidationsmittel sowie Vorstufe für *tert*-Butoxylradikale. Acylradikale wurden durch Wasserstoffatomtransfer erzeugt. Geeignete Substrate waren sowohl aromatische als auch aliphatische Aldehyde. Eine Untersuchung des Reaktionsumfangs, Erläuterungen zu mechanistischen Indizien und eine Einordnung in den wissenschaftlichen Kontext werden vorgestellt.

Abbreviations

A_{iso}	Isotropic hyperfine coupling constant
AgOAc	Silver (I) acetate
Ag_2CO_3	Silver (I) carbonate
$AgNO_3$	Silver (I) nitrate
AM	Acrylamide
ATP	Adenosine triphosphate
$B(Ar^F)_4^-$	Tetrakis(3,5-bis(trifluoromethyl)phenyl)borate
$B(C_6F_5)_3$	Tris(pentafluorophenyl)borane
Boc	*tert*-Butyloxycarbonyl (pg)
BOX	Bisoxazoline
bpy	2,2'-Bipyridyl
CHP	α,α-Cumyl hydroperoxide
Conc.	Concentrated
Conv.	Conversion
CTA	Chain-transfer-agent
CuCl	Copper (I) chloride, cuprous chloride
δ	Chemical shift /ppm
d	Doublet
dd	Doublet of doublet
DBU	1,8-Diazabicyclo[5.4.0]undec-7-ene
DCE	1,2-Dichloroethane

DCM	Dichloromethane
DCP	Di-α,α-cumyl peroxide
DFO	Deferoxamine
DFT	Density functional theory
DIPEA	Diisopropylethylamine
DMDC	Dimethyl dicarbonate
DMA	Dimethylacetamide
DMF	Dimethylformamide
d.r.	Diastereomeric ratio
DTBP	Di-*tert*-butyl peroxide
e.e.	Enantiomeric excess
e.r.	Enantiomeric ratio
ET	Electron transfer
equiv.	Equivalent
fac	Facial
g_{iso}	Isotropic Landé factor
GC/MS	Gas chromatography/mass spectrometry
hept	Heptet
HOMO	highest occupied molecular orbital
HPLC	High performance liquid chromatography
HSi(TMS)$_3$	Tris(trimethylsilyl)silane

IEFPCM	Integral Equation Formalism of Polarizable Continuum Model
iPr$_2$NEt	Bis(isopropyl)ethylamine
[Ir(dF-CF$_3$-ppy)$_2$(dtbbpy)]PF$_6$	[4,4′-*Bis*(1,1-dimethylethyl)-2,2′-bipyridine-*N*1,*N*1′]*bis*[3,5-difluoro-2-[5-(trifluoromethyl)-2-pyridinyl-*N*]phenyl-*C*]Iridium(III) hexafluorophosphate
[Ir(dtbbpy)(ppy)$_2$]PF$_6$	[4,4′-*Bis*(1,1-dimethylethyl)-2,2′-bipyridine-*N1,N1′*]bis[2-(2-pyridinyl-N)phenyl-*C*]iridium(III) hexafluorophosphate
Ir(ppy)$_3$	*fac*-Tris[2-phenylpyridinato-*C2,N*]iridium(III)
KIE	Kinetic isotope effect
K$_2$S$_2$O$_8$	Potassium peroxodisulfateL
LC	Ligand-centered electronic excitation
LC/MS	Liquid chromatography/mass spectroscopy
LED	Light-emitting diode
LHMDS	Lithium hexamethyl disilyl amide
LMCT	Ligand-to-metal-charge-transfer
LPO	Lauroyl peroxide
LSF	Late stage functionalization
LUMO	Lowest unoccupied molecular orbital
M$_n$	number-average molar mass
M$_w$	weight-average molar mass
M$_z$	z-average molar mass
MC	Metal-centered electronic excitation

MeCN	Acetonitrile
MeCN-d_3	Trideutero-acetonitrile
mer	Meridonal
MLCT	Metal-to-ligand-charge-transfer
MMA	Methyl methacrylate
MTBE	*tert*-Butylmethylether
NBS	*N*-Bromosuccinimide
NaSO$_2$CF$_3$	Sodium trifluoromethylsulfinate
OAc	Acetate
o.d.	Outer diameter
PAM	Polyacrylamide
PCET	Proton-coupled-electron-transfer
Pd(OAc)$_2$	Palladium (II) acetate
PDI	Polydispersity index
pg	Protecting group
Ph	Phenyl
phen	1,10-Phenanthroline
PhH	Benzene
PhCl	Chlorobenzene
PhCF$_3$	Trifluoromethylbenzene
PMP	*para*-Methoxyphenyl

PRE	Persistent radical effect
*p*TsOH	*para*-Toluene sulfonic acid
$Rh_2(esp)_2$	Bis($\alpha,\alpha,\alpha',\alpha'$-tetramethyl-1,3-benzenedipropionate)-dirhodium
$Ru(bpy)_3(B(Ar^F)_4)_2$	Tris(2,2′-bipyridine)ruthenium(II) (tetrakis(3,5-bis(trifluoromethyl)phenyl)borate)
$Ru(bpy)_3Cl_2$	Tris(2,2′-bipyridine)ruthenium(II) chloride
$Ru(bpy)_3(PF_6)_2$	Tris(2,2′-bipyridine)ruthenium(II) hexafluorophosphate
SET	Single electron transfer
SOMO	Single occupied molecular orbital
r.t.	Room temperature
TBHP	*tert*-Butyl hydroperoxide
TBPA	*tert*-Butyl peracetate
TBPB	*tert*-Butyl perbenzoate
TBS	(*tert*-Butyl)dimethylsilyl
TEMPO	2,2,6,6-Tetramethylpiperidinyloxyl radical
TLC	Thin-layer chromatography
TMSCN	Trimethylsilyl cyanide
$TMSN_3$	Trimethylsilyl azide
Tf	Triflyl, trifluoromethylsulfonyl (pg)
theo.	Theoretically; based on theoretical calculations
THF	Tetrahydrofuran

TMS	Trimethylsilyl
TR-EPR	Time-resolved electron paramagnetic resonance spectroscopy
TPP	Triphenylpyrylium (TPP^+)
TPSS functional	Tao–Perdew–Staroverov–Scuseria *functional*
Ts	Tosyl, *p*-toluylsulfonyl (pg)
wt%	Weight percentage
X_n	Number-average degree of polymerization
y	Yield (isolated yield, if not stated otherwise)

Table of Contents

1 Introduction

1.1 Photoredox catalysis

1.1.1 Fundamentals

Compounds, that, after electronic excitation by photonic energy, deliver chemical energy in interaction with co-catalysts and/or substrates are called photocatalysts.[4] With this momentum the substrates can follow different reaction paths, which are not commonly accessible by thermal means.[4-5] It is also understood that the excited state (from here on an electronical excited state is referred simply as excited state) of a catalyst differs not only by its energy, but due to differing electronic features in more physical and thus chemical properties.[4,6] There are different forms, in which photocatalysts can act or, with other words to which category they could be assigned. Catalysts could serve in processes of (i) energy transfer, (ii) organometallic excitation, (iii) light-induced atom transfer, (iv) photoredox catalysis.[4]

Over 40 years photoredox catalysis engages topics of water splitting[7], carbon dioxide reduction[8] or material science in solar cell applications[9]. Avenue to synthetic chemistry came with more understanding and research of polypyridyl metal (also known as polyimine) complexes and organic dyes.[4] These special designed catalysts can transfer the gained energy by photonic excitation into chemical processes by single electron transfers (SET).[4,6] In contrast to traditional redox catalysis photoexcited catalysts, especially polypyridyl complexes, bear the potential, that they gained higher qualities both as oxidant and as reductant compared to their electronic ground state.[4] Exemplary customarily used photoredox catalyst fac-Tris[2-phenylpyridinato-$C2,N$]iridium(III) (Ir(ppy)$_3$, see chapter 7 for structure) has in its ground state a reduction potential of $E_{1/2}(M/M^-) = -2.19$ V and an oxidation potential of $E_{1/2}(M^+/M) = 0.77$ V while in photoexcitation the reduction potential is given by $E_{1/2}(M^*/M^-) = 0.31$ V and the oxidation potential is given by $E_{1/2}(M^+/M^*) = -1.73$ V (all redox potentials are given as reduction potentials of the redox pair; all are referred against a saturated calomel electrode (SCE); solvent used was MeCN).[10] In a concrete catalytic application, only one of these abilities is used according to the (more) favorable electrochemical potential. Thus in a catalytic cycle the excited state is used in an oxidative quenching or a reductive quenching mode (referring to the oxidation state change in catalyst (Figure 1)).[10b]

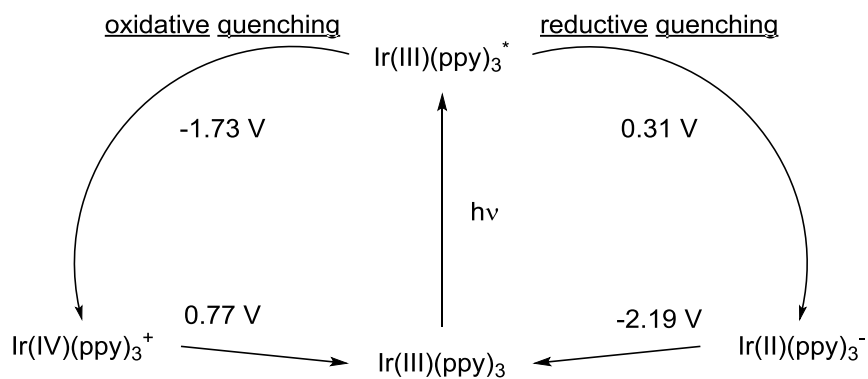Figure 1. Photoredox cycle of Tris(2-phenylpyridinato-*C2,N*)iridium.

In an octahedral ligand field, d^6 metals show an energetic splitting of the former d orbitals by an amount of Δ. The splitting can approximately be characterized by a higher e_g term (2 orbitals) and a lower t_{2g} term (3 orbitals, Figure 2).[6]
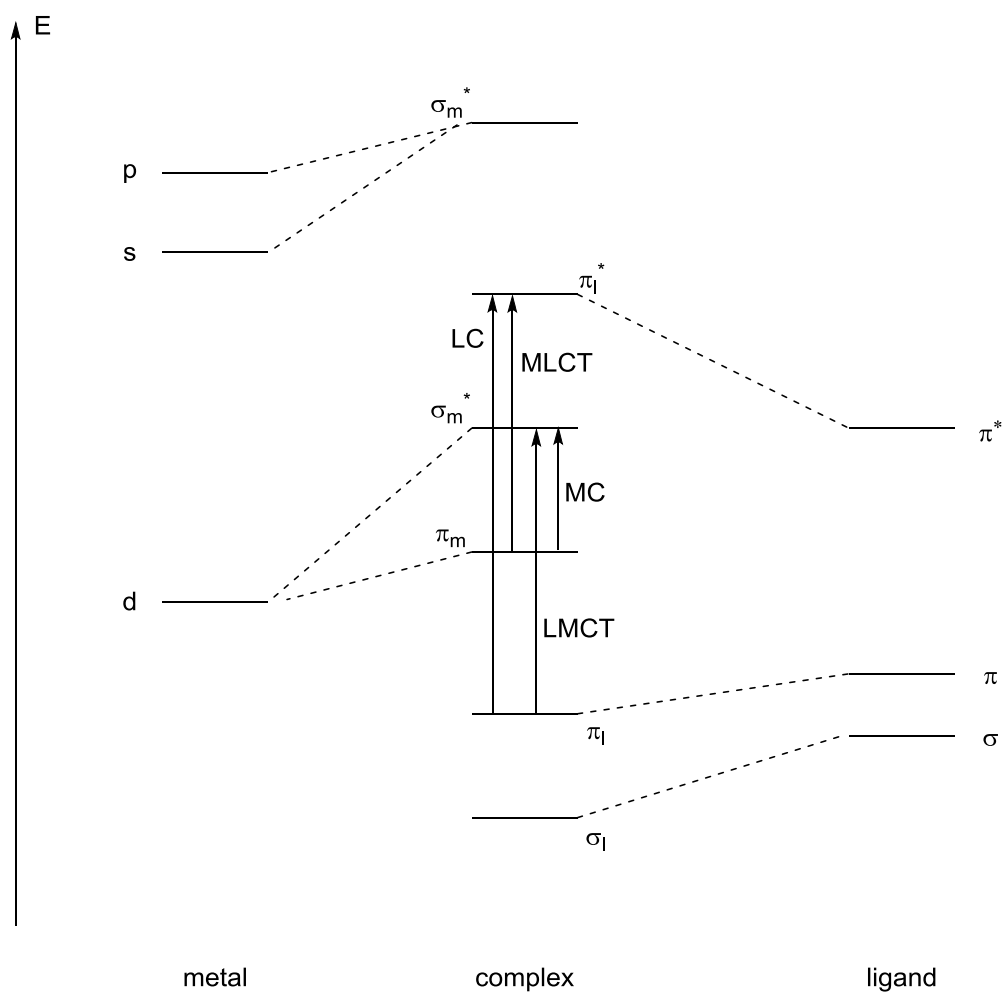
Figure 2. Schematic Jablonski diagram of an octahedral d^6-metal complex.

The t_{2g} orbitals are herein fully occupied and can be considered as the energetically highest occupied molecular orbitals (HOMO niveau) while the e_g term is unoccupied.[6]

In comparison to *3d* or *4d* metal complexes like Fe(II) or Ru(II), respectively, for *5d* polypyridine complexes of Ir(III) the energy gap Δ between the terms is higher (as for *4d* compared to *3d* due to orbital size).[11] In a Jablonski diagram of such complexes, metal based outer *s* and *p* orbitals can be considered and would show a higher energy than the *d* orbitals. They would therefore contribute to antibonding metal based σ^*_M orbitals in the complex. From the aromatic ligand side occupied low lying σ and π orbitals would contribute as well as higher unoccupied π^* orbitals. While the former two orbital types would result in fully occupied ligand based σ_L and π_L terms of the complexes orbitals, the latter one would result in unoccupied ligand based π^*_L. In theory the energetic arrangement of the terms gives possibilities for either a ligand based or a metal based π orbital to be the higherst occupied molecular orbital (HOMO) niveau and either a ligand based antibonding π^*_L or a metal based σ^*_M term to be the lowest unoccupied molecular orbital (LUMO) niveau. Depending on this array an electronic excitation from HOMO to LUMO niveau (by visible light absorption) can be (a) metal-centered (MC), (b) ligand-centered (LC), or charge transfer from (c) ligand-to-metal (LMCT) or (d) metal-to-ligand (MLCT) (Figure 2).[6] As remarked for Ir(III) the orbital size of the *d* orbitals contribute to the energy level arrangement, as well as the ligand's influence on the electronic repulsion according to the trend of the spectrochemical series. Cyclometalating ppy ligands are considered to have a strong influence on increasing Δ.[11] Furthermore, high lying occupied orbitals based on either metal or ligand are constitution for the metal complexes tendency of oxidation, while low lying unoccupied orbitals express the ease of reduction, respectively.[6] For Ir(III) in conclusion MLCT and LC transitions can be matched by UV-Vis spectroscopy.[11] For Ir(ppy)$_3$ the broad absorption band extended into the visible light region is typical for a spin-allowed (singlet state) MLCT.[12] In toluene the absorption maximum for this lowest-energy electronic transition was around $\lambda = 375$ nm.[13]

The deactivation of the excitation can take place intramolecularly (radiative or non-radiative)[6] or intermolecularly. In the second-order kinetic process, energy or electron transfers are the most encountered interactions. The diffusion controlled processes demand excited state life times of $>10^{-9}$ s and are therefore in metal complexes practically realizable for the lowest excited-state.[6] From luminescence experiments the excited state life time was estimated to be 2.0 µs in degassed toluene or acetonitrile (MeCN) and 0.1 µs in dichloromethane (DCM).[13a]

The electron transfer is described by the Marcus theory[14] and variations thereof[15]. The kinetic rate constant is dependent on different factors. The activation energy for instance is connected to the difference in free Gibbs energy of the states (before and after electron transfer) as well as the so-called reorganization energy. The reorganization energy (λ) respects the change in internal (λ_i) as well as external reorganization (λ_s) which occur on a molecular level along the course of the electron transfer reaction. Internal reorganization takes place for exemplary changes in orbital sizes, external reorganization occurs in solution by allignement of the solvent molecules to the novel constitution of charges.[14b]

$$\lambda = \lambda_i + \lambda_s$$

The driving force for the process is its exergonicity ($\Delta G_0 < 0$), derived practically from the redox potentials of the reaction partners.[16]

$$\Delta G = -n\ F\ \Delta E_{rct}$$

$$\Delta E_{rct} = E_{1/2}^{red} - E_{1/2}^{ox}$$

with ΔG – difference in free Gibbs energy

n – molar number of transferred electrons per total process

F – Faraday constant

ΔE_{rct} – reaction potential

$E_{1/2}^{red}$ – redox potential of the reduction process

$E_{1/2}^{ox}$ – redox potential of the oxidation process

Ir(ppy)$_3$ can be synthesized either starting from IrCl$_3$ via a dinuclear chloro-ligands-bridged intermediate[13a,17] or from Ir(acac)$_3$ by successive ligand substitution.[18] The thermodynamic product is the *fac*-configurational isomer, caused by the "trans-influence" which opposed C–Ir and Ir–N bonds to each other.[11]

1.1.2 Modern Synthesis Applications

In this century discoveries attributed to photoredox catalysis in synthesis increased the attraction of chemists towards this research field. A short selection of studies on synthetic methodology developments is presented hereafter.[10b,19]

The T. Yoon group used a system of Ru(bpy)$_3$Cl$_2$ and LiBF$_4$ as Lewis acid to cyclize bis(α,β-unsaturated ketones) (Scheme 1).[20] Mechanistically the photoexcited Ru(II) was reduced by electron transfer from diisopropylethylamine (DIPEA). In turn, the activated enone was reduced by recyclization of the catalyst to form a β-enolate radical. The radical engages the intramolecular cyclization. The generation of the final 1,2-dicarbonylcyclobutane from this reduced species was not clarified. The control experiments showed that amine, LiBF$_4$, photoredox catalyst and irradiation were necessary to perform this cyclization.[20]
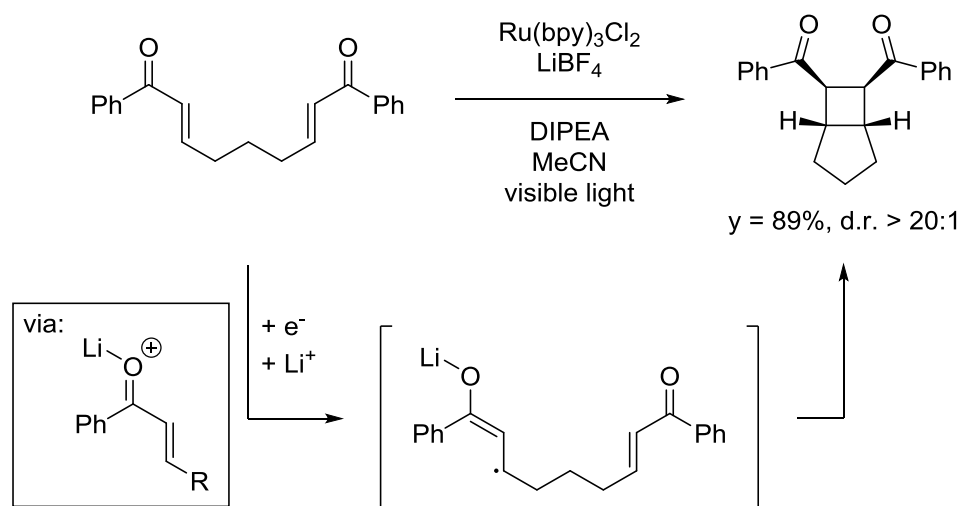
Scheme 1. Ru(bpy)$_3$$^{2+}$-photoredox catalyzed, Li$^+$-assisted, cyclization.

MacMillan *et al.* showed also in 2008 the dual-catalysis of photoredox and organo catalysis to succeed in asymmetric α-alkylation of aldehydes (Scheme 2).[21] Ru(bpy)$_3$Cl$_2$ was used to photoreductively cleave the bromide anion from α-carbonyl bromides (and 1,3-dicarbonyl-2-bromides). The gained α-carbonyl alkyl radical attacked the enamine, formed from imidazolidinone and aldehyde, preferentially at the Si-face of the *E*-enamine (underlined by comparative DFT calculations). The reaction proceeded with 2,6-lutidine as base in DMF solution and is an example for organo-single-occupied-molecular-orbital (SOMO)-catalysis. A Ru(I) species was suggestively formed from Ru(II)* by electron-donation of the radical-enamine-adduct forming a respective iminium intermediate.[21]

6
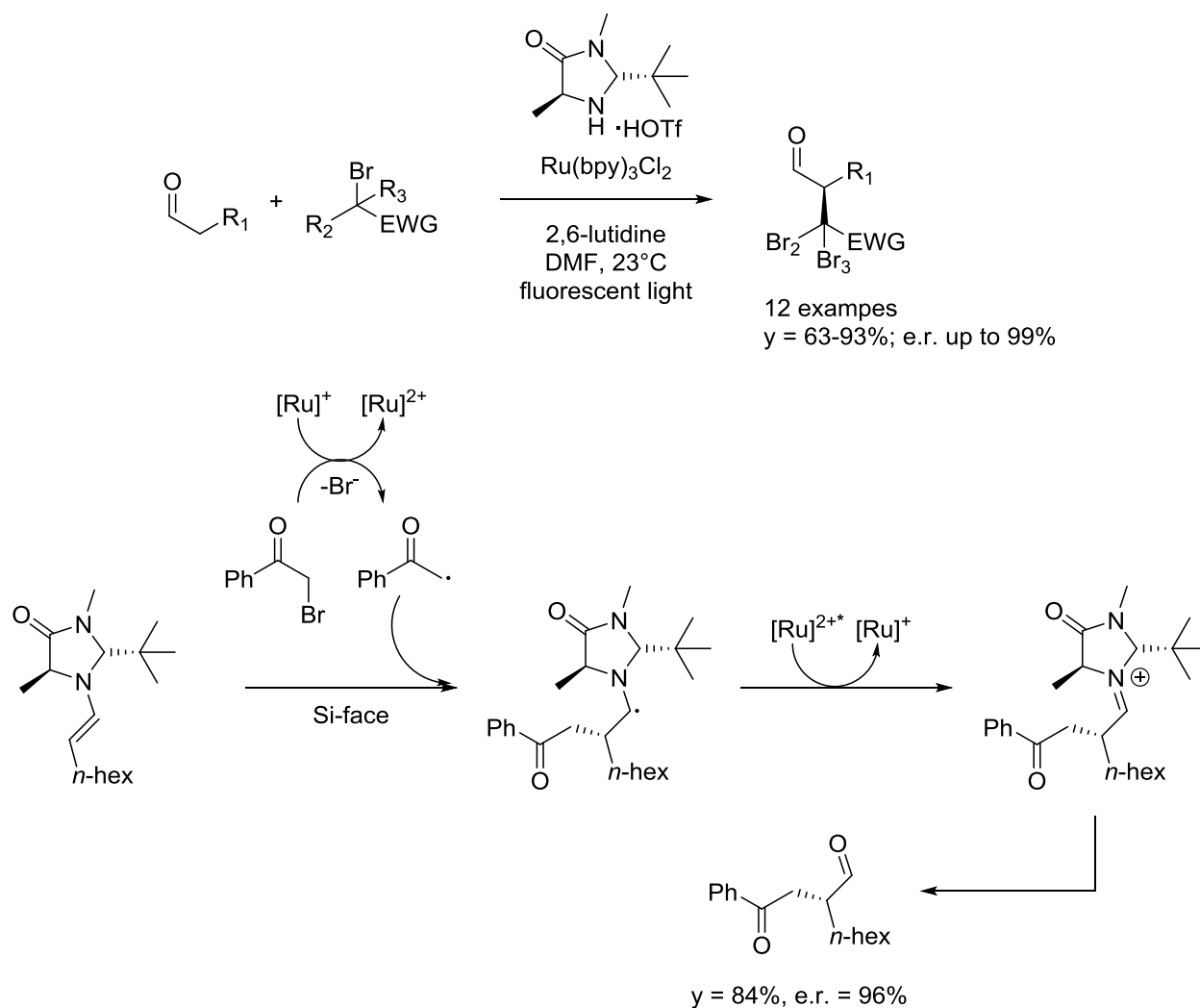
Scheme 2. Organo-SOMO-catalysis with $Ru(bpy)_3^{2+}$.

In 2011, the MacMillan group found in an automated screening process that α-amino-C-H arylations of *tertiary* amines could be performed with electron-deficient cyano arenes under $Ir(ppy)_3$ catalysis (Scheme 3).[22] The process was carried out in DMA and in presence of NaOAc as base at r.t.. Successfully amine substrates were found with pyrrolidines, piperidines, piperazines, morpholines, azepanes and acyclic diethylphenylamine. The reaction was valid for a great variety of substrates.[22]
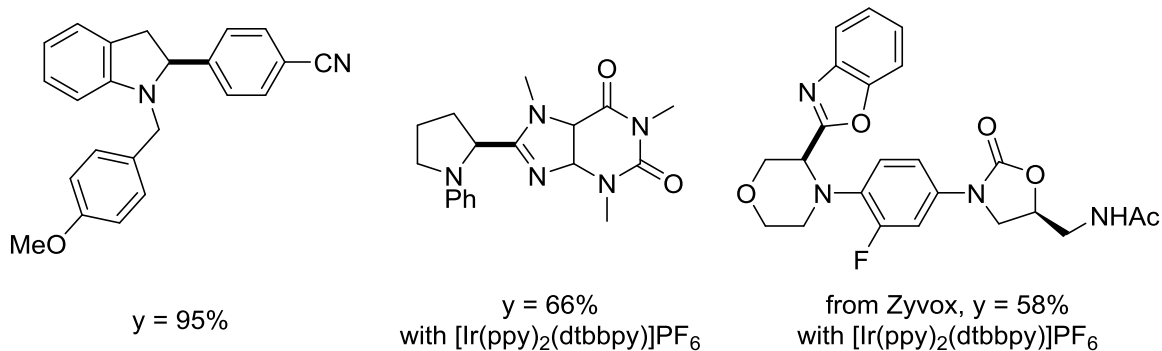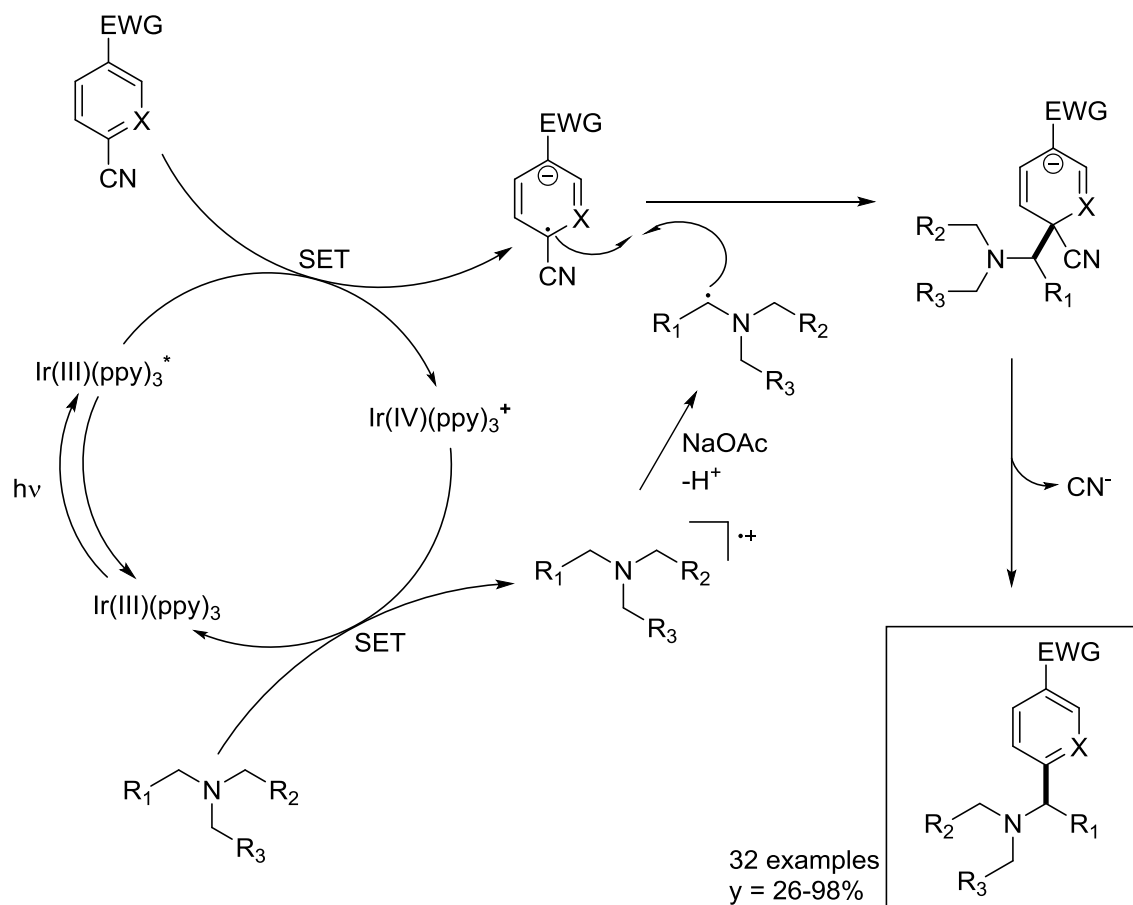
Scheme 3. Photoredox catalyzed α-amino-arylation.

In 2013 the Knowles group began publishing studies on photoredox catalyzed proton-coupled-electron-transfers (PCET) processes.[23] Their first finding in this field was the intramolecular ketyl-olefin cyclization to five-membered rings from aryl ketones with a tethered alkene.[24] They had used $Ru(bpy)_3(BAr^F_4)_2$ as reducing catalyst and diphenylphosphoric acid as protic catalyst.

2-Phenyldihydrobenzothiazoline (or a Hanztsch ester) was used as terminal reductant and proton supply.[24] The separation of electron and proton transfer decouples this activation strategy from homolytic bond strength dependencies compared to a hydrogen atom transfer (HAT), so that especially weak covalent hydrogen bonds can be established[24] or especially strong covalent hydrogen bonds can be cleaved[25].

To place this into a context, it is also important to get an idea where visible-light enabled electron transfers were used to enable the synthesis of molecules that are known from natural abundance or are used in pharmaceutical, medicinal chemistry or different industrial horizons.[19,26]

The group of Stephenson showed that (+)-catharanthine could be cleaved oxidatively between carbons 2 and 3 by a SET to photoexcited [Ir(dF-CF$_3$-ppy)$_2$(dtbbpy)]PF$_6$ in methanol (Scheme 4a).[27] The generated iminium ion radical was nucleophilic attacked in the presence of trimethylsilyl cyanide (TMSCN) and the resonance stabilized C centered radical was reduced to the corresponding anion by SET from the formed Ir(II) species, followed by protonation (Scheme
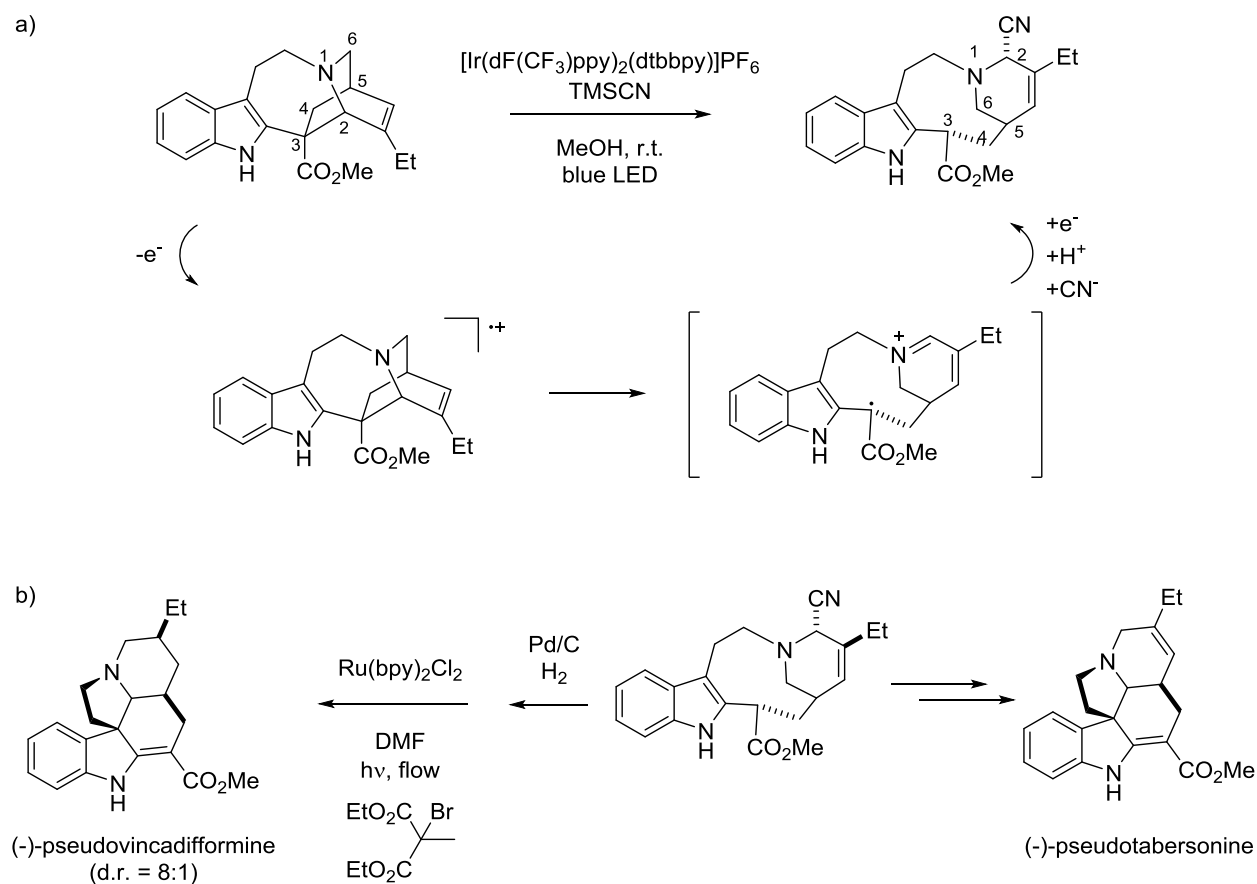
Scheme 4. Photoredox catalysis applied in alkaloid scaffold alternation.

9

4a). With this technique and proposed reaction steps the chemists obtained an α-amino nitrile in high yield (either as batch or in flow reactor) and which could be used to synthesize (-)-pseudotabersonine or (-)-pseudovincadifformine (Scheme 4b). (-)-Pseudotabersonine was gained by acidic treatment at elevated temperature. (-)-Pseudovincadifformine was synthesized in three steps (2 pots) from the α-amino nitrile. After a Pd catalyzed hydrogenation of the contained double bond, a reductive cyanide cleavage was performed. The final product was then obtained by another photoredox catalyzed (Ru(bpy)$_3$Cl$_2$) intramolecular nucleophilic cyclization in the presence of diethyl-2-bromo-2-methyl malonate as oxidant (Scheme 4b).[27]

After an synthetic access to *trans*-clerodane involving a reductive, decarboxylative phthalimidoxycarbonyl cleavage to form the alkyl radical using a system of Ru photoredox catalyst with reductants DIPEA and Hanztsch ester in 2015[28], the Overman group presented a redox neutral variant using the corresponding oxalate as alkyl radical precursor and [Ir(dF-CF$_3$-ppy)$_2$(dtbbpy)]PF$_6$ as catalyst (Scheme 5).[29] Mechanistically the cesium decahydronaphthalen-1-yl-oxalate was oxidized by SET to photoexcited Ir(III) catalyst. After decarboxylation, the resulting alkyl radical was added in terminal position to 4-vinylfuran-2(*5H*)-one. After SET from Ir(II), protonation and isomerization in basic solution the product was obtained in 78% yield over the two steps (Scheme 5).[29]
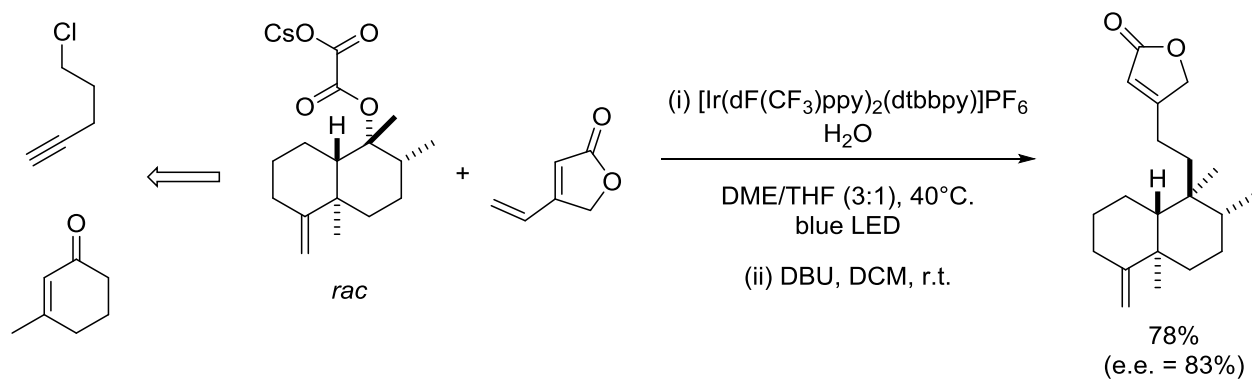
Scheme 5. Oxalate activation by an Ir photoredox system.

10

In 2018 Y. Qin and coworkers reported a 20-step synthesis of (+)-actinophyllic acid using two photoredox catalytic steps (Scheme 6).[30] From *N*-protected 4-amino-*n*-butanal, asymmetric α-alkylation with dimethyl-malonate-α,α'-alkyl radical (from bromide) was performed following the presented organo-SOMO-catalysis procedure of MacMillan *et al*. (see Scheme 2) with Ir(ppy)$_3$ and imidazolidinone catalysts. Further, the α-functionalized aldehyde was reduced to the corresponding 1° alcohol, which underwent an intramolecular transesterification. By α-bromination of the γ-lactone the substrate for a Ru photoredox catalyzed 3-methylindole attack was furnished. Reductive SET from Ru(II) catalyst followed by bromide cleavage suggestively
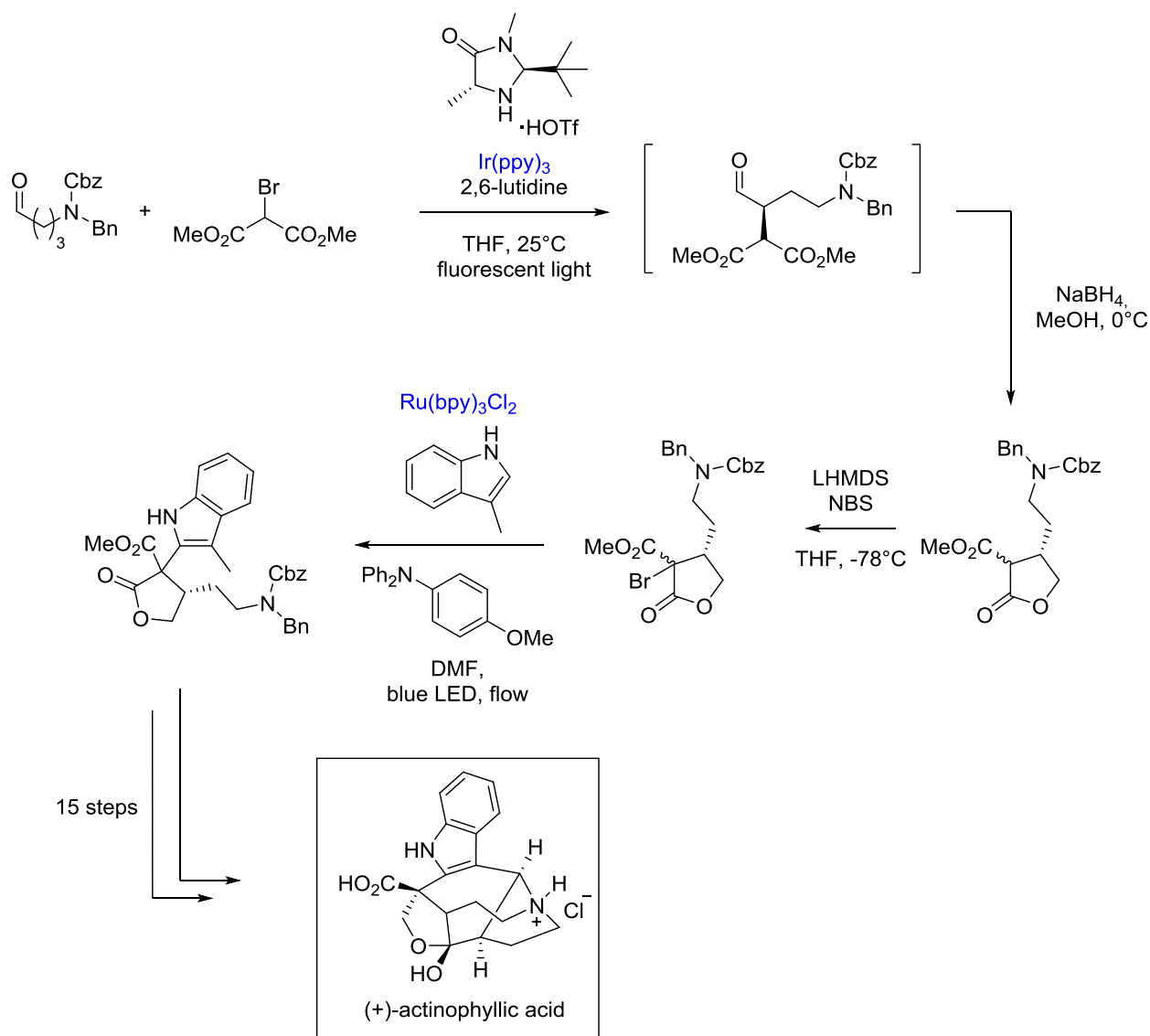
Scheme 6. Applications of photoredox catalyzed steps in the total synthesis of actinophyllic acid.

11

resulted in the lactone derived α-alkyl radical. The radical added to the indole in 2-position and after SET from this radical-adduct intermediate to Ru(III) and rearomatization the next step towards (+)-actinophyllic acid was successfully achieved (Scheme 6).[30]

1.2 Intermolecular Radical Alkene Difunctionalizations

The transformation of a C–C double bond to two new sp^3-C centered σ bonds within a single reaction, involving radicals, attracted interest in the last decade. Synthetic techniques of this kind are step economic towards target molecules and thus are considered valuable alternatives in synthesis design towards sustainable processes.[31]

Moreover, the high reactivity and thus often high chemoselectivity of radicals led in several examples to success in reacting complex molecules. This feature connects radical based approaches often to a suitability for late stage functionalizations (LSF).[32] Yet, it is not practical and simply does not suit every example, generalizing radical approaches as potential LSF.[32b] Analogously, photoredox chemistry is not automatically atom-economic and energy-efficient. Although many reactions are performed near room temperature, visible-light is a different form of energy, consuming today mostly electrical energy and that in turn is also delivered by combustion energy. Despite the necessity evaluating concrete radical approaches in terms of sustainability, it is without doubt that they deliver a different portfolio of possibilities, which is by nature divergent from closed-shell reactivities. On this note, radical difunctionalizations stand out from difunctionalizations via nucleo-palladation of alkenes.[33]

There are two major working models for radical difunctionalizations.[31] There is the possibility of two consecutive additions of radicals to the alkene. More precisely this first mechanism (type 1, Scheme 7) is a radical addition to a double bond, generating a new σ bond between the interacting atoms and leaving an intermediary radical, centered at the neighboring carbon atom of the former C–C π bond (**I1**). This radical-alkene-adduct **I1** could in the next elementary step
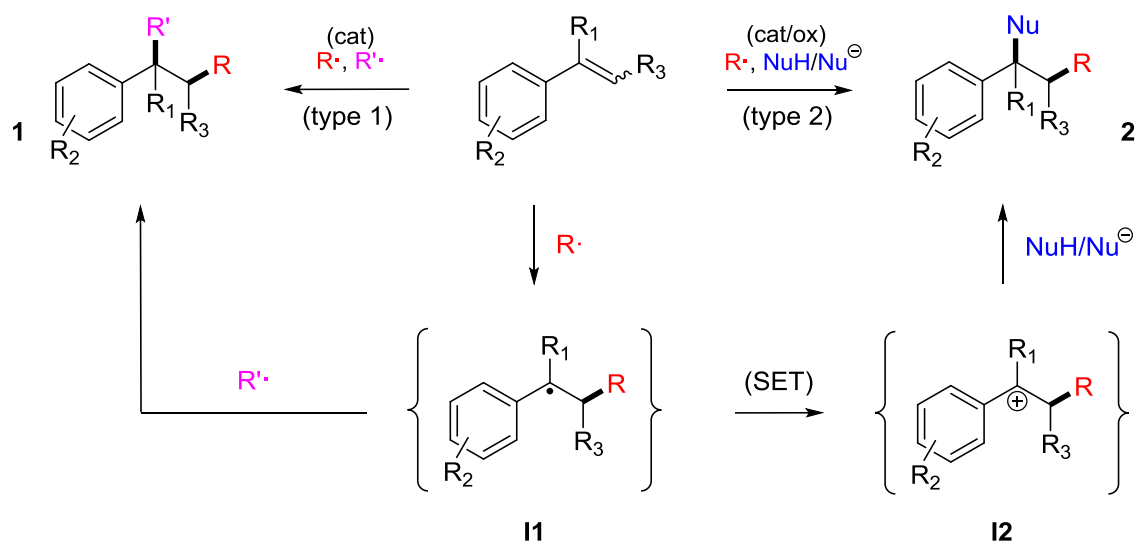
Scheme 7. Models for intermolecular radical difunctionalizations of styrenes.

combine with a second radical, which could be of the same kind as the first, or a different one.[31] The reaction of two radicals to form a σ bond is considered to be an incident that is depending on the relative life-time of the two radicals under reaction conditions.[34] According to the classical persistent radical effect (PRE)[34a-c] a high possibility for a cross-coupling is given, if one radical exhibits practically no tendency for self-combination. In a cage of inert solvent molecules, the life-time of a radical is limited by its tendency to combine with a second radical.[35] If one radical is only converted by cross-coupling and the second one in addition by self-combination, over time the concentration of the non-self-combining radical will rise. At a specific concentration of this long-lived, persistent radical, the radical-radical cross coupling with the short-lived, transient radical is kinetically favored compared to the self-combination of the latter. New formed transient radical is at this point practically immediately reacted with the persistent radical, leading to a kinetically controlled selectivity of the transient radical to combine with the persistent radical.[34a-c] Recently in 2020, Studer showcased another interpretation.[36] It was derived, that the highest possibilities of cross-coupling between two differing radicals is given, when the rate of their formation is equal.[36-37] Furthermore, if the formation rates of the two radicals are quite

13

equal, the more long-lived radical does not need to be persistent to obtain a high possibility for cross-coupling. Rather a significant high difference for rates of self-combination needs to be given.[36-37] Returning to radical difunctionalizations, the combination of a radical-alkene-adduct **I1** with another radical to obtain a 1,2-difunctionalization product of the former alkene could be governed by one of these principles. In difunctionalizations with two radical species often a metal catalyst is used, which changes the situation.[31] However, in the methodology for γ-peroxyketone formation[3] of the Klußmann group (see chapter 1.2.2) the *tert*-butylperoxyl-benzyl radical combination could possibly match an interpretation of the persistent radical effect.[3,38]

Further, there is the working model to form the corresponding carbocation **I2** from the radical-alkene-adduct **I1**. The second functionalization is then realized by a nucleophilic attack (type 2, Scheme 7).

In the following section some aspects of C centered radical addition to double bonds are given on this mechanistic step. Moreover, a more in depth description of α-carbonyl radicals (see chapter 1.2.2) and acyl radicals (see chapter 1.2.4) in the context of alkene difunctionalization and nucleophile involving difunctionalizations of alkenes with amines (see chapter 1.2.5.1), alkyl nitriles (see chapter 1.2.5.2) and indoles (see chapter 1.2.5.3) will follow. These are focused on C centered radicals.

1.2.1 Radical Addition to Alkenes

The addition of a radical to a C–C double bond forms a σ bond from a π bond, making this an exothermic process.[39] The exothermic reaction is described by an early transition state along the reaction coordinate.[39-40] The descriptions in this section are considering additions of C centered radicals to mono- or 1,1-disubstituted alkenes in solution.

From the Arrhenius equation[16] $k = A\ e^{E_A/RT}$ follows, for a given temperature and alkene, the rate constants for the additions of different radicals differ in two possible quantities: the frequency factor A and the activation energy E_A.[39] For radical additions to alkenes relatively little variations by frequency factors are reported, yet decreasing with steric demand.[39] The more essential difference of rate constants at the same temperature is caused by a difference in activation energy. The activation energy is for small reactants influenced by three major aspects of the

reaction: the steric repulsion, the overall reaction enthalpy (corresponding to bond formation) and the polar substituent effects on the reactants.[39,41] In general, the alkene substituents at the attacked carbon atom show a much higher influence than more remote ones. This often results in regioselectivity of the radical additions.[39-40] General reaction enthalpies H_r typically range between -180 and -20 kJ mol^{-1}.[39] Activation energies show low variation roughly 0 to 42 kJ mol^{-1}.[39] By polar substituent effects the actual barrier is shifted to a lower energy.[39]

The result of polar substituent effects is a relative fast addition of the radical to the matching alkene. Using frontier molecular orbital (FMO) theory, this is plausible for the SOMO of an electron-donor substituted radical (relatively high energy) interacting with a LUMO of an electron-acceptor substituted alkene (relatively low energy).[39] Energetically close frontier orbitals deliver a relatively low energy of the transition state towards radical addition. In the transition state a partial charge transfer of the radical to the alkene is supposed and the radical is showing a nucleophilic character. Analogously for an electron-acceptor substituted radical the SOMO (of relatively low energy) interacts more vividly with the HOMO of an electron-donor substituted alkene (relatively high energy). For this case, in the transition state towards radical addition, a partial charge transfer from the alkene to the radical is in act. The latter exhibit an electrophilic character.[39-40] Also an impact on the activation energy are suspected by either the magnitude of alkene's triplet excitation energy[42] and the alkene's (and radical's) geometry[43].

The methyl and the benzyl radical for example are considered to have no such enhanced interactions to alkenes. Rate constants of addition vary only little. At near room temperature the rate constants for benzyl radical are 100-1000 times lower than for the methyl radical.[39,44] C centered radicals adjacent to one cyano or one ester group are considered ambiphilic. Their selectivity towards alkenes (relative rate) is similar to the methyl radical.[45,39] Electron-donor substituted radicals are nucleophilic and show the highest rate differences in additions to different alkenes.[39,46] Near room temperature, variations of rate constants for different alkenes by 3-5 orders of magnitude are possible.[39] The rate constant strongly increases with increasing electron-accepting ability of the alkene. Often they even show higher rate constants in reactions with electron-acceptor substituted alkenes than with phenyl substituted alkenes, despite the bigger exothermicity of reaction with the latter.[39] Benzoyl radicals could be assigned as moderate nucleophilic.[47] However, information about rate constants of acyl radicals for addition to alkenes are scarce.[48] Electrophilic radicals are less selective than the methyl radical.[39,49]

15

1.2.2 Carbon-Radicals in α-Carbonyl Position

During kinetic analysis of acid-catalyzed oxidative coupling of cyclopentanone to xanthene under autoxidative conditions, an unexpectedly rapid reaction was observed by the Klußmann group.[50] The coupling reaction proceeded on a higher rate than the formation of the supposed intermediate, the *secondary* hydroperoxidation product of xanthene.[50] A different mechanism was in act, suggestively forming radicals from ketones and hydroperoxides under acid mediation.[50] Transforming the system into an organic medium with the use of *tert*-butyl hydroperoxide (TBHP) instead of oxygen, the unsuspected α-carbonyl radical, derived from the ketone could be added to styrenes. With *p*-toluenesulfonic acid as catalyst, TBHP, ketone and styrene formed γ-peroxyketones **3**, products of free-radical difunctionalization with α-ketonyl and *tert*-butyl peroxyl radicals.[3] Besides styrenes, allylbenzene could be used for the procedure with acetone, yielding the product in 12%. From the results, the ketonyl radical formation was proposed to run over an acid-catalyzed condensation of ketone and hydroperoxide to generate an alkenyl peroxide

28 examples, y = 18-75%
d.r. up to 1:1.5

3a, 74%   **3b**, 37%   **3c**, 59%, d.r. = 1:1.5
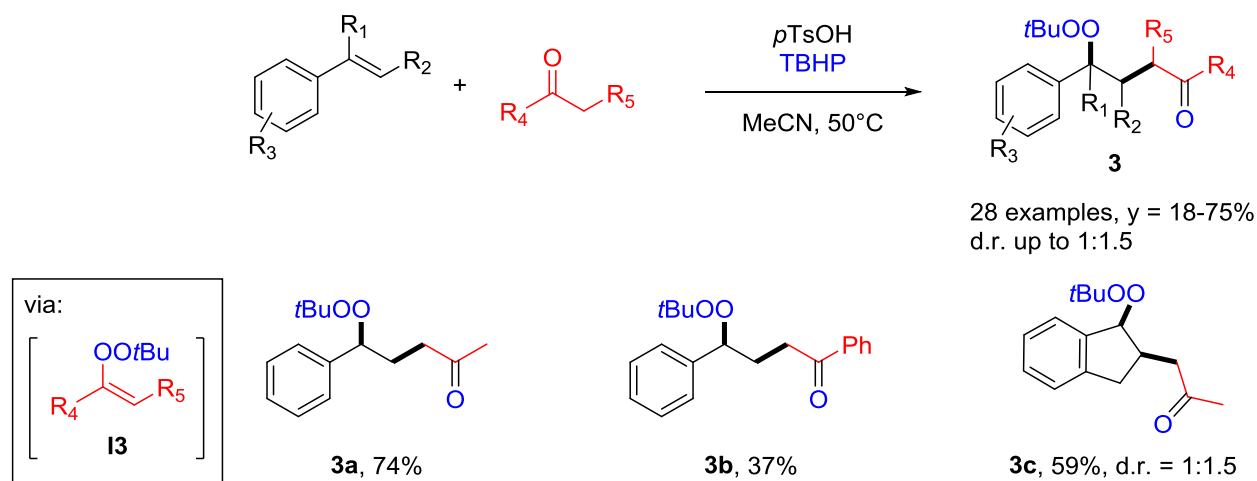
Scheme 8. Alkylation-peroxidation via acid-catalyzed formation of alkenyl peroxides.

intermediate **I3**.[3] The described **I3** is a proposed species[51], which arguably decomposes quite fast to generate the resonance-stabilized α-ketonyl radical by O–O bond cleavage.[3] By-product *tert*-butoxyl radical can form the *tert*-butylperoxyl radical in a HAT reaction with TBHP.[52]

Contrary, in the field of alkene difunctionalizations, α-carbonyl radicals were mostly formed from the respective α-bromo carbonyl compounds.[53]

1.2.3　Intermolecular Radical Carbocyanations of Alkenes

The Inoue group reported in 2012 a Cu catalyzed chloromethylation-cyanation procedure of aliphatic alkenes bearing a benzoyloxy group.[54] Mechanistically they suggested after homolytic cleavage of the chloro-substituent and addition of the cyanomethyl radical to the double bond, an intramolecular cyano group transfer to get to the final cyanide product. The role of the Cu catalyst was not further clarified (Scheme 9).[54]
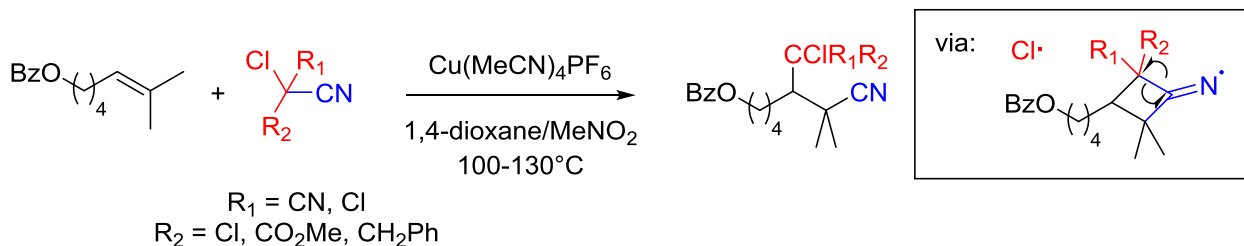
Scheme 9. Cu catalyzed chloroalkylation-cyanation involving group transfer.

In the group of G. Liu an enantioselective trifluoromethylation-cyanation of styrenes was developed (Scheme 10).[55] They used a Cu catalyst with an enantiopure bisoxazoline (BOX)-type
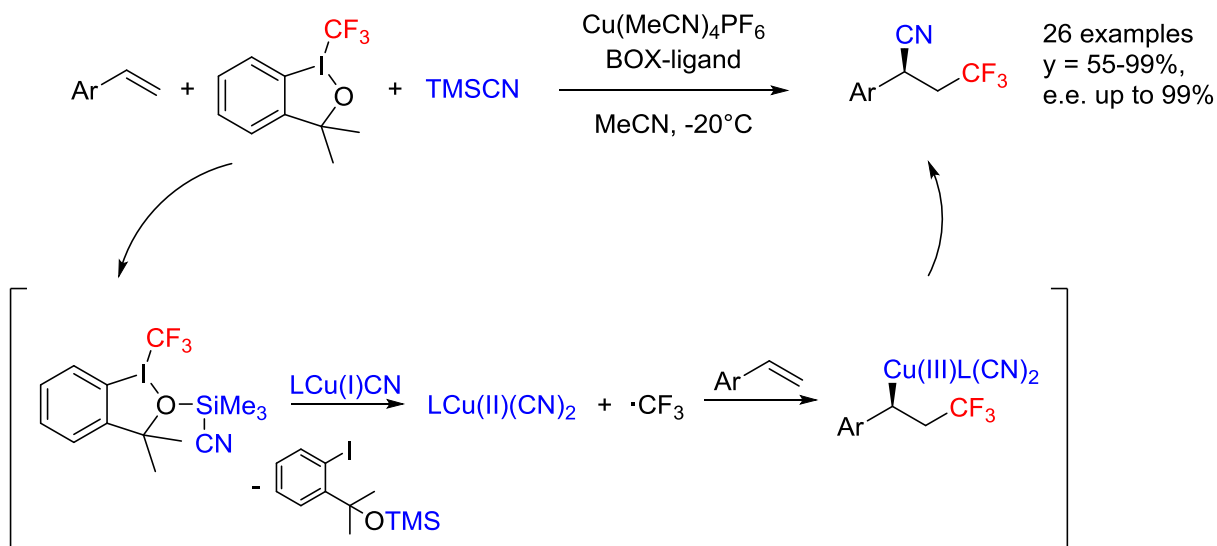
Scheme 10. Cu catalyzed trifluoromethylation-cyanation.

ligand, Togni's reagent as radical and TMSCN as cyanide source. For the mechanism, they proposed a Cu(I) attributed activation of a complex of TMSCN-Tognis's reagent to form the trifluoromethyl radicals and Cu(II) cyanide complexes. Radical-styrene-adduct and Cu(II) form a C(III) complex to release the enantioenriched cyanide product upon reductive elimination. Aliphatic alkenes could also be difunctionalized via this procedure, but with at best minor

17

enantioselectivities.[55] The group later could show that β,γ-unsaturated carbonyl compounds could be added to the scope of this enantioselective trifluoromethylation-cyanation technique.[56]

Inspired by the above work of G. Liu, Y. Pan and coworkers presented, that using a combination of Cu-BOX-complex and Ir(ppy)$_3$ photoredox catalysis gave access to an enantioselective alkylation-cyanation technique.[57] The alkyl radicals were derived from corresponding phthalimid-*N*-yl-esters upon electron-donation of photoexcited Ir(ppy)$_3$[*]. Nine different (*primary*, *secondary* and *tertiary*) alkyl radical precursors could be implemented in the method to functionalize monosubstituted styrenes (Scheme 11).[57]
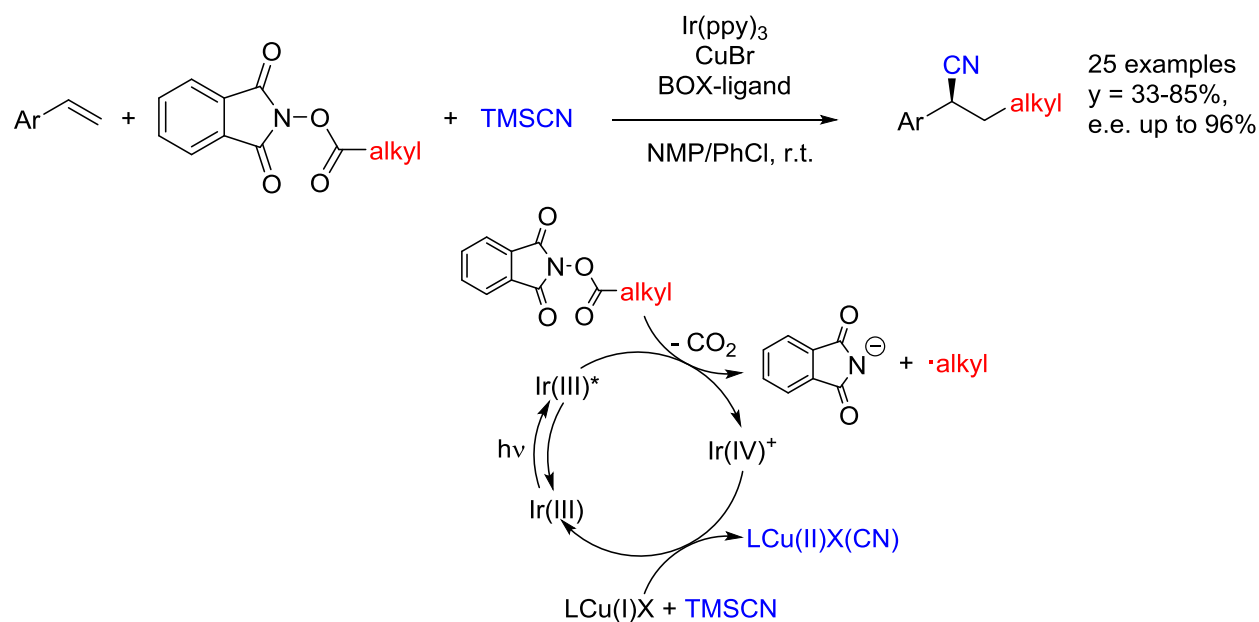
Scheme 11. Metalophotoredox catalyzed alkylation-cyanation.

18

The Landais group initially found that with the help of di-*tert*-butyl hyponitrite and bis(trimethyltin) alkyl radicals (from α-carbonylalkyliodides or α-cyano alkyliodides) and cyano groups (from *p*-toluenesulfonyl cyanide (*p*TsCN)) could be regioselectively attached to unsymmetric substituted cyclopropenes in a moderate diastereoselective fashion (Scheme 12a).[58]
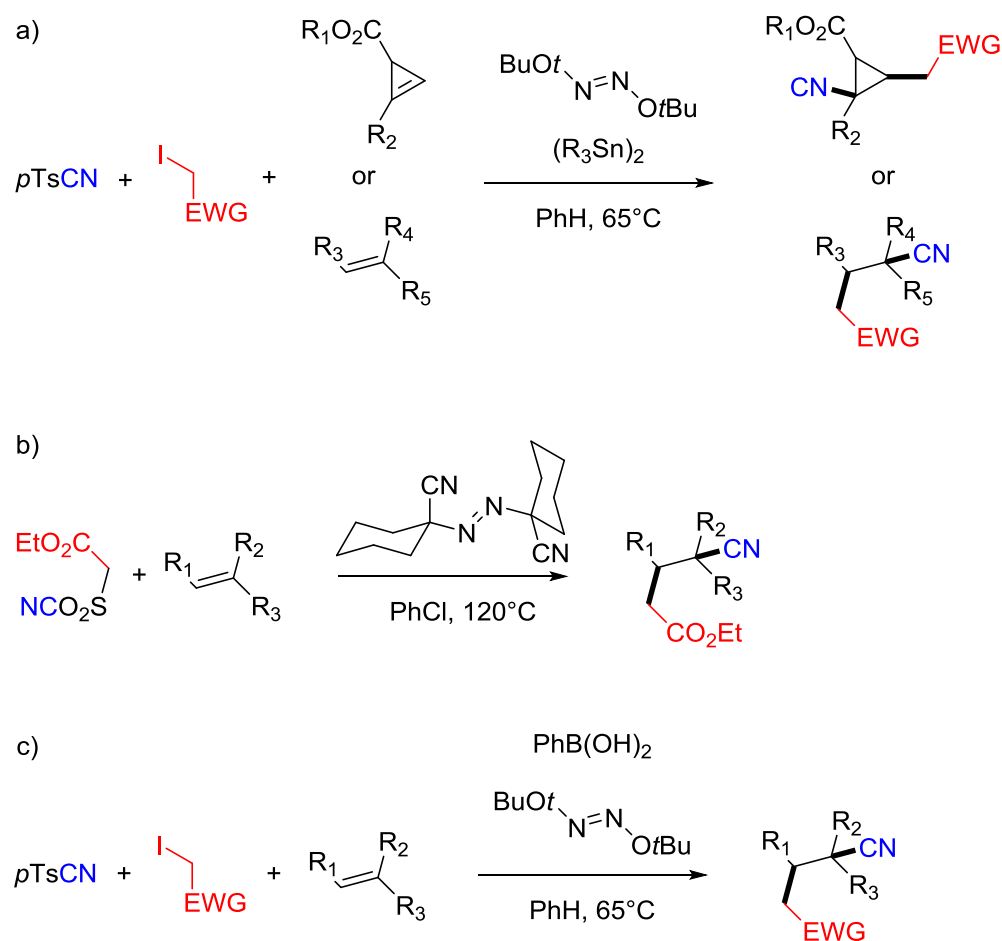
Scheme 12. Evolution of carbocyanation strategies by the Landais group.

The synthetic method was also viable for the difunctionalization of aliphatic alkenes.[59] To avoid the use of a tin reagent, a special designed 2-cyanosulfonyl acetate could upon thermal activation with a diazo initiator deliver alkyl and cyanidyl radicals. The technique was proven viable in alkylation-cyanation of aliphatic alkenes (Scheme 12b).[59] Finally the Landais group managed to return to the simple *p*TsCN reagent without the use of a tin reagent in alkylation-cyanation of aliphatic alkenes. Additives di-*tert*-butyl hyponitrite and phenylboronic acid were used to perform the reaction (Scheme 12c).[60]

Chemists of the H. Bao group succeeded in transforming 1,3-enynes in Cu catalyzed 1,4-radical additions to α-alkylated allene cyanides (Scheme 13).[61] TMSCN was used as cyanidyl and alkyl diacyl peroxides as alkyl radical sources. Furthermore, by addition of an activated alkyl iodide, the hereof derived radicals added preferentially to the enynes in the difunctionalization process compared to the alkyl radicals generated from the diacyl peroxides. From DFT calculations the cyanation was suggested to proceed by transfer from a *N* bonded Cu cyanide complex to the allenic radical.[61]
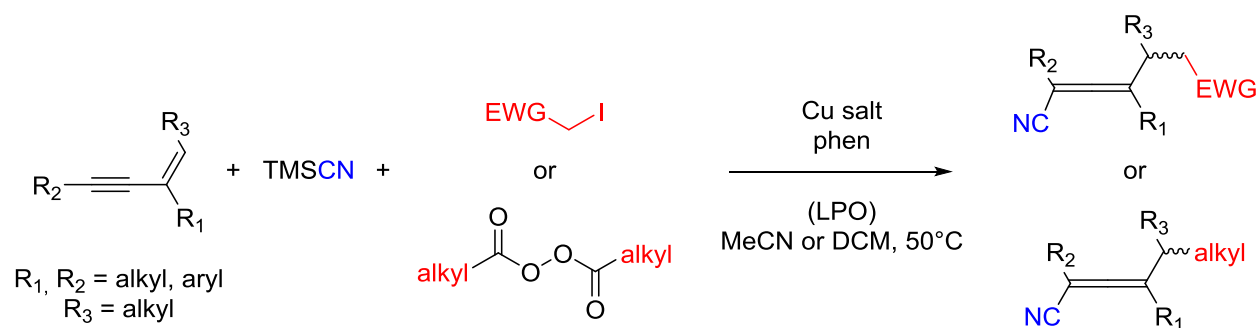
Scheme 13. Cu catalyzed carbocyanations of 1,3-enynes.

1.2.4 Acyl Radicals

1.2.4.1 Generation and some Applications of Acyl Radicals and Alternatives

A range of possibilities is known about the formation of acyl radicals from different starting materials and using different techniques.[62] Some examples are presented, pointing out the variety of possibilities. Scheme 14 depicts some ways to form acyl radicals on the top half and applications on the bottom half. Matching colors between bottom and top half show application
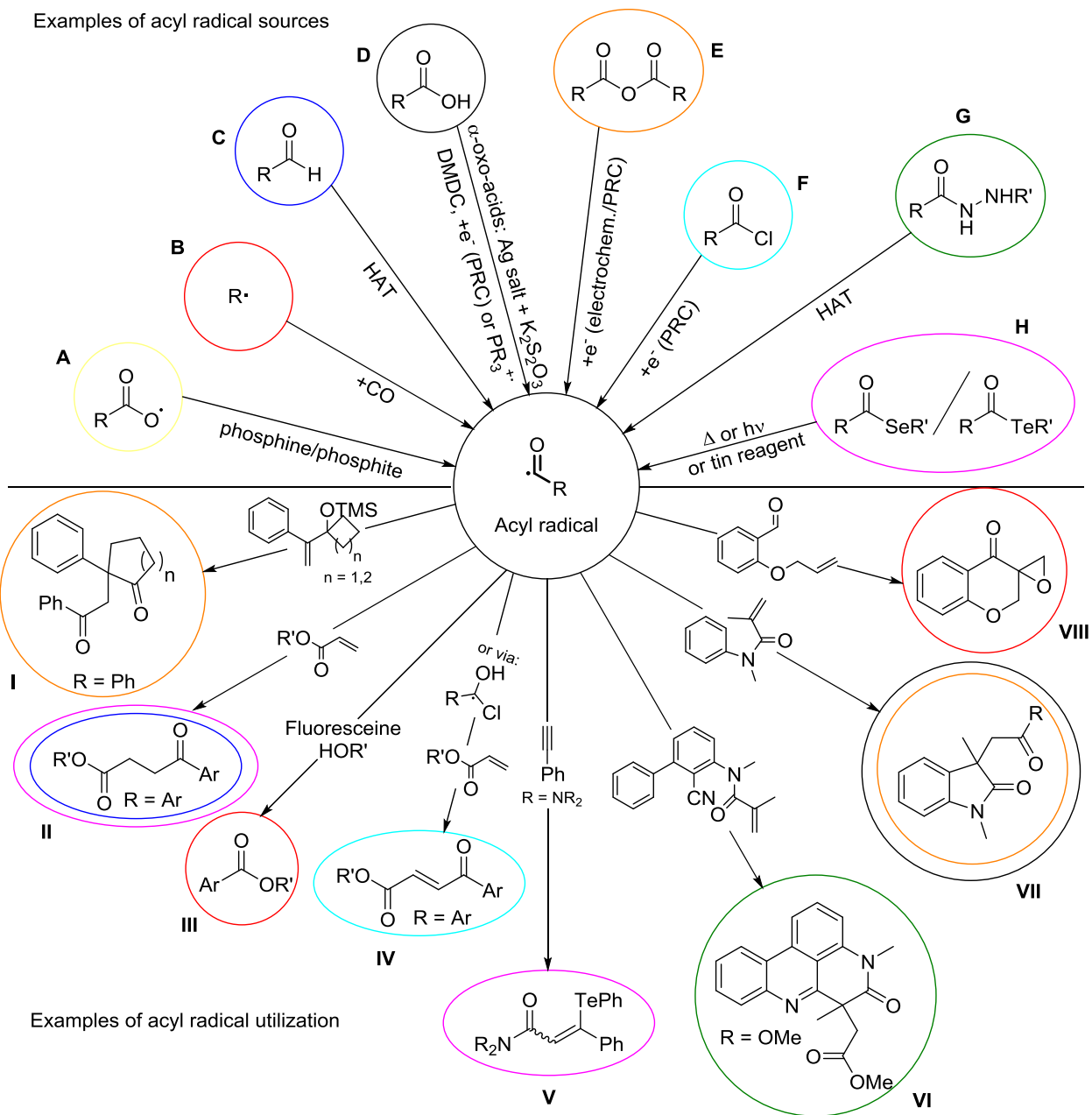
Scheme 14. Acyl radical. HAT = hydrogen atom transfer; DMDC= dimethyl dicarbonate; PRC = photoredox catalysis.

and some of their known radical sources. In the following examples, the matching of radical source and application is indicated by the connection of letter and roman numeral.

Benzoyloxyl radicals (e.g. from homolysis of corresponding peroxides or nitroxides) could be trapped with phosphines or phosphites and the adduct in turn could undergo fragmentation with generation of acyl radicals and stable P–O double bonds (**A**, Scheme 14).[63] With the same driving force nucleophilic attack of (alcohols or) carboxylic acids on the radical-cation of phosphines could yield the corresponding (alkyl or) acyl radicals (**D**).[64]

One classical way to generate acyl radicals is the use of organometallic/metalloide compounds. Especially the use of acyl tellurides and selenides was common. The respective radicals were most often released by means of heat, irradiation or also from reactions with tin reagents.[62a,65] Regarding that these reagents were applied for some decades now, the frame of these applications seem still to be restricted to hydroacylations (**HIII**),[62a] group transfer-radical addition to C–C multiple bonds (**HV**),[66] and radical addition in tandem with intramolecular cyclizations[67].[68] On the one hand, the often harsh reaction conditions probably restrict the use of sensitive substrates, on the other hand, this is also a sign for the chemists considerations towards sustainability, waste- and energy-efficiency. The specific organometallic compounds could be considered as prefunctionalized starting material and thus elongate potential synthesis routes, consuming time. Nevertheless, acyl tellurides and selenides found applications in relatively modern radical synthesis steps. In MacMillan's total synthesis of (-)-vincorin in 2013 the thermal cleavage of the acyl telluride at 200°C was initiation of an intramolecular cyclization and ketene formation with a α-thioether-acetylene unit.[69] García-Díaz' group used a trialkylstannane to perform an intramolecular hydroacylation and within construct the tetracyclic scaffold of uleine or strychnos alkaloids.[70]

An approach from carboxylic hydrazines[71] was further refined by Sun *et al*., who showed in 2017 that hydrazine carboxylates could be activated by photoredox mediated hydrogen atom transfer (HAT) using Eosin Y and TBHP under white light irradiation at r.t..[72] The alkoxycarbonyl radicals were used to trigger a cascade cyclization upon addition to a cyanide bearing *N*-biarylmethacrylamide leading to a phenanthridine scaffold (**GVI**).[72]

In 2015 the chemists of W.-J. Xiao's group reported the use of photocatalyst Fluorescein (blue light irradiation) to reductively (SET) cleave aryldiazonium salts at r.t. to the sp^2-aryl radicals.[73]

Under carbonmonoxide atmosphere the corresponding acyl radicals were formed. These in turn were oxidized by the radical cation of Fluorescein (restoring uncharged Fluorescein) to the analogous ylidyneoxonium cation. Nucleophilic attack by *primary* and *secondary* aliphatic alcohols achieved an alkoxycarbonylation of the aryl radical (**BIII**).[73]

In 1983 Scheffold and Orlinski found that carboxylic anhydrides could in the presence of vitamine B_{12} as mediator reductively form acyl radicals under electrochemical and photochemical reaction conditions.[74] With this technique, they performed hydroacylations of electron-deficient alkenes. The hydrogen atom was transferred from solvent *N,N*-dimethylformamide. They had reported that the corresponding acid chlorides delivered low yields.[74] The photoredox catalytic formation of acyl radicals from carboxylic anhydrides and acids however, was driven forward by the Wallentin group. In 2015 they could use aromatic acids via *in situ* anhydride formation with dimethyl dicarbonate (DMDC) and by $Ir(ppy)_3$ catalysis under visible light irradiation at r.t for this purpose (**DVII**).[75] In 2016 they presented the direct use of symmetric aromatic anhydrides for the same reaction outcome under similar reaction conditions (**EVII**).[76] Furthermore the acyl radicals were used to trigger a semipinacol rearrangement upon addition on double bonds of TMS-protected α-(1-hydroxycycloalkyl)styrenes (**EI**).[76]

The Ngai group used aromatic carboxylic acid chlorides as radical precursor in a $Ir(ppy)_3$ photoredox catalyzed (pyridine assisted) so-called radical Heck-type functionalization of stabilized alkenes (**FIV**).[77] This often is proposed with an oxidation-deprotonation sequence from the radical-alkene-adduct **I1** (here from acyl).[31] However, DFT calculations in hand, the chemists depicted a modified mechanism, starting with a proton-coupled-electron-transfer (PCET) from catalyst to chloride. An aryl-chloro-hydroxymethyl-radical was formulated to be the central intermediate and to add to the alkene double bond.[77]

As an abundant source of acyl radicals, aldehydes could give the radical species after a HAT process. In 2010 the Caddick group showed that hydroacylations of acrylate derivatives could be achieved with aldehyde under oxygen atmosphere in 1,4-dioxane.[78] The acyl radicals were assumingly generated by HAT to oxygen. Acyl radicals were then in competition between proceeding autoxidation towards carbonic acids via acylperoxyl radicals and the addition to the alkene's double bond.[78]

In 2017 the Jana group used a system of TBHP with Ru(bpy)$_3$Cl$_2$ (blue light irradiated) at r.t. with cooperative catalyst Pd(OAc)$_2$ and in MeCN solution to perform 2-acylations of *N*-(2-pyrimidinyl)indoles.[79] The pyrimidine substituent suggestively facilitates the C–H activation in 2-position of the indole upon precoordination and thus transfer of the acyl radical.[79] In 2014 the J.-H. Li group presented the use of *primary* alcohols as acylation reagents. Involving HAT they presented a more unlikely source and alternative way for acylation.[80]

Although already in early development phases, simple solutions for acyl radical formations were suggested, anticipated and studied,[81] it needed a new inspiration to get the radical chemistry, and so the radical acylation chemistry back going. The increase in research in the second decade of the 21th century, could be attributed to perpsectives, which photoredox catalysis offers, evidently from the more recent examples of the above presented and also from latest review articles concerning radical acylations[62b,62d,82].

1.2.4.2   Intermolecular Alkene Difunctionalizations involving Acylation

In the field of intermolecular difunctionalization reactions of alkenes the Zh. Li group[83] made in a seminal study use of a system containing *tert*-butylhydroperoxide (TBHP) and an Fe(II) chloride catalyst to form β-peroxy-ketones. The peroxy-ketones could be transformed to α,β-epoxy-ketones upon treatment with basic 1,8-diazabicyclo[5.4.0]undec-7-ene (DBU) (Scheme 15a). Catalytic Fe formed in reaction with TBHP *tert*-butoxyl (and peroxyl) radicals, which in turn could engage in the HAT from aldehydes. The acyl radicals where added along with *tert*-butylperoxyl radicals to styrenes (and 1,3-butadiene).[83] The reaction could also be performed enantioselectively by using a (*S*)-*N*-substituted proline based organocatalyst with styrenes and aromatic aldehydes (as well as *n*-hexanal) in MeCN at r.t., published by the Siva group (Scheme 15b).[84] The procedure led predominantly to the (*S,S*)-α,β-epoxy-ketones in enantiomeric ratios of up to e. r. = 99:1. The use of *n*-hexanal was also documented successfully but with lower e.r.. Interestingly, the activation of TBHP was under the used conditions claimed to be achieved by thermal homolysis.[84]

Y. Wang *et al.* published studies of peroxy-acylation of acrylates by using TBHP and catalytic bis(α,α,α',α'-tetramethyl-1,3-benzenedipropionate)-dirhodium Rh$_2$(esp)$_2$. The reaction was carried out in 1,2-dichloroethane (DCE) at r.t.. The group presented aromatic aldehydes only in these transformations (Scheme 15c).[85]

a)
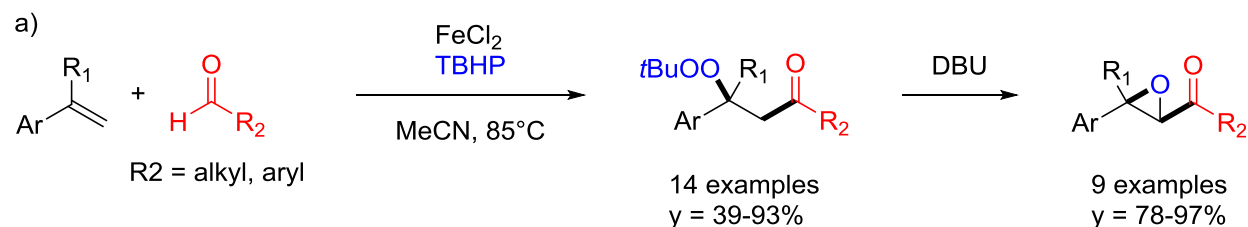
b) enantioselctive α,β-epoxyacylation of styrenes without metal, without DBU, at r.t.

catalyst:

17 examples
y = 53-95%
e.e. up to 99%
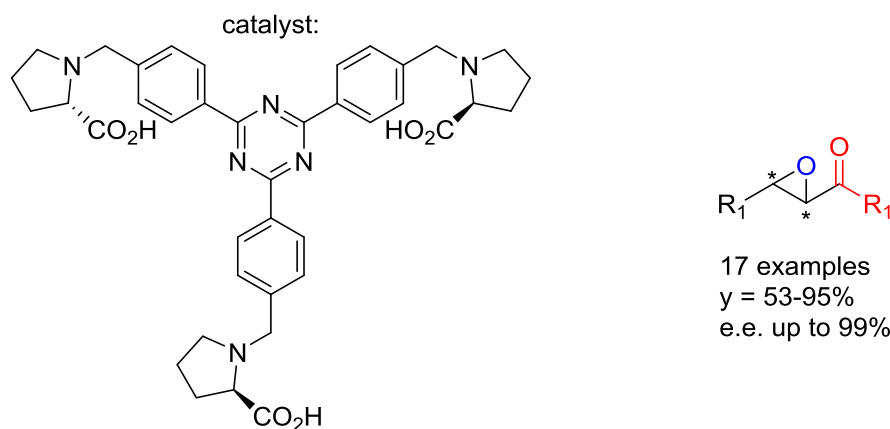
c) Peroxydation-acylation of α,β-unsaturated esters

22 examples
y = 39-78%
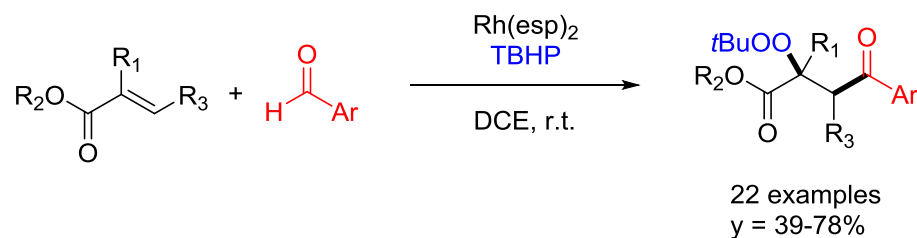
Scheme 15. Catalyzed peroxidation-acylations.

H. Bao *et al*. were able to replace the peroxygroup with radical alternatives. With a Cu(I) complex and TBHP as radical precursor a cyano group (TMSCN source) together with an acyl group could be introduced to styrenes (Scheme 16a).[86] From density functional theory (DFT) based calculations of intermediate and transition state geometries, the scientists gave insight on a possible mechanism. They proposed that upon TBHP cleavage, the resulting Cu(II)OH complex

25

formed TMSOH (also observed by GC/MS) in reaction with TMSCN. The now Cu bond cyano ligand was supposingly transferred to the acyl radical-alkene-adduct forming the benzylic cyanide (without Cu(III) complex formation).[86] With an Fe catalyst and TBHP present styrenes,
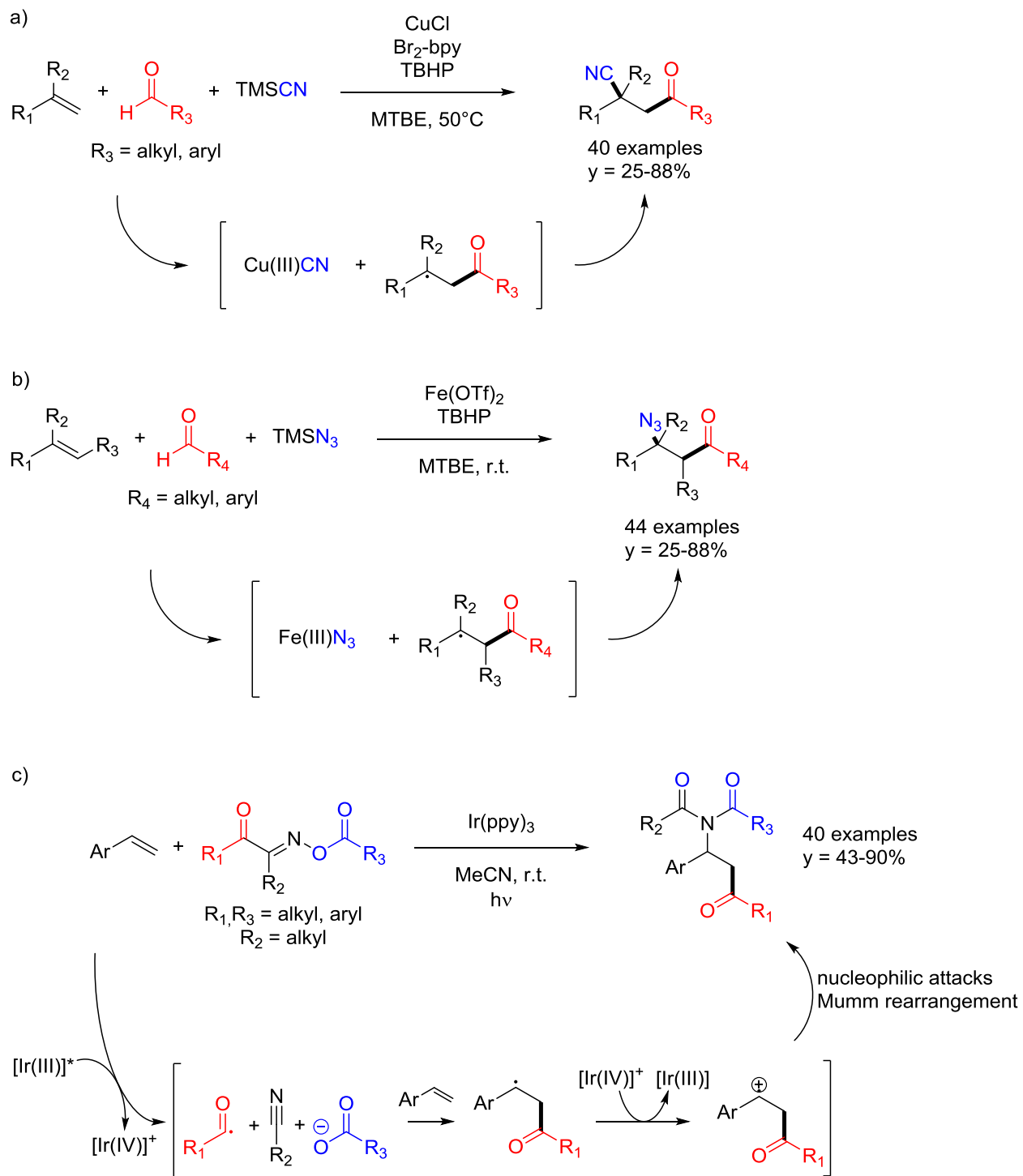
Scheme 16. Examples of difunctionalizations involving an acylation. Br_2-bpy = 4,4'dibromo-bipyridin-2,2'-yl.

26

α,β-unsaturated carbonyl compounds or 4-phenylbut-1-ene could be functionalized in MTBE at r.t. (Scheme 16b) with an acyl group and an azido group (TMSN$_3$ source).[87] Mechanistically, similarly to the acylation-cyanation a group transfer from an Fe(III) azide complex to the benzylic radical intermediate was suggested.[87]

Photoredox catalyzed intermolecular difunctionalizations using aldehyde derived radicals dealt so far only with the generation of α,β-epoxy-ketones using Ruthenium[88] or methylene blue[89] catalysts. The D. Z. Wang group reported in 2015 that Ru(bpy)$_3$Cl$_2$ (white light irradiated) was in photoexcited state suitable for a SET to TBHP in MeCN at r.t..[88] The resulting *tert*-butoxyl radical served as H-acceptor from aromatic aldehydes. Benzoyl and *tert*-butylperoxyl radicals were subsequently added to the styrenes double bond. The present Cs$_2$CO$_3$ transformed the β-peroxyketone to the final product. The recyclization of the Ru(II) was proposed to take place by SET from a *tert*-butylperoxide anion to the Ru(III) species, also forming a *tert*-butylperoxyl radical.[88] The Salles group used methylene blue as photoredox catalyst with K$_2$S$_2$O$_8$ and air oxygen as oxidants and radical precursors in aqueous medium at r.t. with K$_2$CO$_3$ as a base present.[89] Since the absence of oxygen led to worse product yield, they considered also oxygen involved in the reaction course. Yet, they had not a comprehensive understanding about the role of the two oxidants present. Their mechanistic proposal consisted of a SET from a hydroperoxide anion (generated in alkaline hydrolysis of persulfate) to photoexcited methylene blue. The so generated hydroperoxyl radical was believed to be involved in HAT from aldehydes as well as radical-radical-cross-coupling with the benzyl radical intermediate to form a benzylic hydroperoxide. The reoxidation to methylene blue was believed to be achieved by SET to either oxygen or peroxosulfate.[89]

The L. Yang group found a dual difunctionalization with two olefins. One electron deficient alkene and one styrene were coupled with each other as well as with an acyl (or alkyl radical after decarbonylation[90]) and a *tert*-butylperoxyl radical to yield 1,5-diketones in basic medium.[91] Using di-*tert*-butyl-peroxide (DTBP) and an Fe catalyst at elevated temperature aliphatic aldehydes could be used as radical alkylating agent after decarbonylation of the corresponding acyl radical in an azido-alkylation reaction of styrenes.[92]

In the laboratories of L.-Z. Wu a synthetic technique for acylation-imidation of styrenes was found, using special acyl oxime ester substrates (Scheme 16c).[93] Upon SET of photoexcited Ir(ppy)$_3$ the substrate fragmentates to acyl radical, alkyl nitrile and carboxylate anion. The acyl-styrene-adduct was oxidized by Ir(IV), regenerating the catalyst and generating the corresponding carbocation intermediate. Nucleophilic attack of MeCN could lead to a nitrilium cation, which could form an imidate with the carboxylate. A Mumm rearrangement[94] led to the respective imide product.[93]

1.2.5 Intermolecular Difunctionalizations with Nucleophiles

1.2.5.1 Amine Nucleophiles

In 2017 J.-H. Li and coworkers described the usage of α-cyano alkyl radicals and amines (1° or 2°) to difunctionalize styrenes (Scheme 17).[95] The alkylation-amination was realized by mediation of oxidation agent Ag$_2$CO$_3$ (2 equiv.) in alkyl nitrile solvent at 120°C. Radical generation from alkyl nitriles as well as oxidation of the radical-alkene-adduct **I1** to the corresponding benzylic carbocation **I2** was accomplished. An Fe species enhanced the yield for the difunctionalization process. The reaction of *p*-methoxystyrene with acetonitrile and dibenzylamine was shown to run also in satisfactory yield in PhCF$_3$ with excess acetonitrile.[95] In MeCN, *p*-methoxystyrene was functionalized with cyclic amines (morpholine as standard amine), *primary* amines, and sulfonamides.[95]
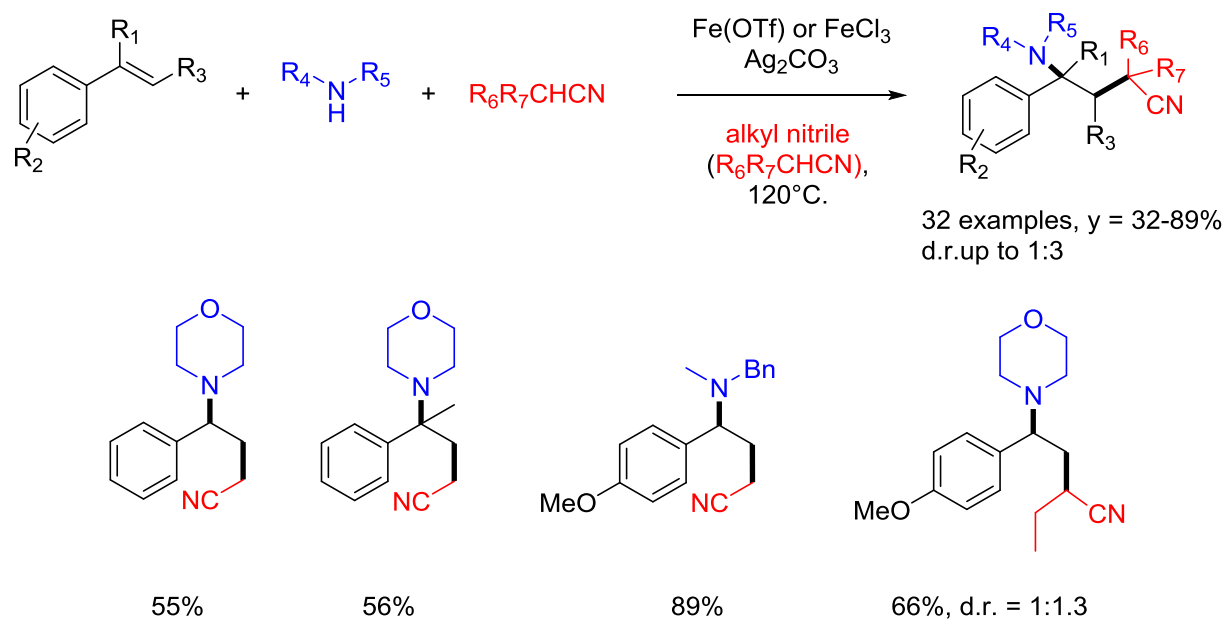
Scheme 17. Fe catalyzed α-cyanoalkylation-amination.

28

Morpholine and MeCN could be used to difunctionalize plain styrene and some functionalized styrenes, 1,1-disubstituted ethylenes and trisubstituted ethylenes. *p*-Cyanostyrene and hept-1-ene were revealed to be incompatible alkenes in the method.[95] The usage of MeCN-*d₃* instead of MeCN resulted in a slower difunctionalization of *p*-methoxystyrene with dibenzylamine. The KIE of $k_H/k_D = 2.7$ led the scientists to the assumption, that the H- abstraction of the alkyl nitrile is the rate controlling step in the reaction mechanism.[95]

Further difunctionalization methods with amines were reported in combinations with C centered radicals derived from α-bromoalkyl esters[53a,96] or from alkyl *N*-hydroxyphthalimide esters (photocatalytic alkyl radical formation)[97]. Depending on the reaction conditions (polar solvent favorable) and on substrates, procedures with α-alkylester radicals and Cu catalysts could directly obtain intramolecular lactam formations.[53a,96b] The Li group found access to a vicinal alkylation-amination method for styrenes under Ru(bpy)$_3$Cl$_2$ (1 mol%) photoredox catalysis in DMSO at r.t..[97] While irradiation and photoredox catalyst were necessary for the reaction to proceed the presence of a Lewis acid delivered a yield improvement. The source of alkyl radicals were corresponding alkyl *N*-hydroxyphthalimide esters, forming besides the radical, carbondioxide and phthalimide anion upon photoredox catalytic single electron reduction.[97] Standard substrates used in the transformation were *p*-methoxystyrene, *tertiary*-C-adamantyl *N*-hydroxyphthalimide ester and *o,m*-dimethylaniline (or aniline). In contrast to the other techniques of this segment, this method presented no electron-deficient styrenes in the reaction scope.[97]

1.2.5.2   Amidation via Alkyl Nitriles

Greaney and coworkers published in 2013 a synthetic technique, which allows the addition of aryl radicals together with mainly alkoxy groups from nucleophilic addition of alcohols (methanol, *n*-butanol, 1,2-diethoxyethane, *iso*-propanol; y = 33-70%) onto styrenes. Also two examples of arylation-amidation by addition of the phenyl radicals together with acetonitrile (y = 53%) or benzonitrile (y = 36%) in Ritter reactions were presented.[98] The reaction was catalyzed by Ir(ppy)$_3$ under white light irradiation at r.t.. The general radical source was the diaryliodonium tetrafluoroborate salt, which released the aryl radicals upon single electron reduction in reaction with the catalyst.[98]

König *et al.* elaborated the arylation-amidation of styrenes with aryldiazonium tetrafluoroborate salts and alkyl nitriles in 2014.[99] The reaction was catalyzed by Ru(bpy)$_3$Cl$_2$ (0.5 mol%) under blue light irradiation at 20°C in the presence of 1 equiv. water. Common Cu catalysts for Meerwein arylations could not replace the Ru catalyst. Light was essential to the reaction progress and without Ru catalyst only 5% yield of a phenylated styrene in acetonitrile were obtained. The alkyl nitrile was used as solvent but could seemingly be used in excess (10 equiv.) in DCM solution.[99] In MeCN, styrene could be arylated with a range of phenyldiazonium salts (*p*-ethoxycarbonyl, *p*-trifluoromethyl, *p*-methoxy, *p*-bromo, *m*-nitro, etc.; y = 50-92%).[99] With *p*-nitrophenyldiazonium tetrafluoroborate and styrene, primary, secondary and tertiary alkyl nitriles were found viable alternatives to MeCN.[99] In MeCN, *p*-nitrophenyldiazonium tetrafluoroborate could be used to difunctionalize some *p*-substituted styrenes (methyl, chloro, carboxyl; y = 55-97%) and internal aryl-substituted (*E*)-alkenes (stilbene, β-methylstyrene, β-methoxycarbonylstyrene, β-acetylstyrene).[99]

In 2013 Koike and Akita presented synthetic results on a trifluoromethylation-amidation reaction of styrenes (Scheme 18).[100] The chemists found Ir(ppy)$_3$ and Ru(bpy)$_3$(PF$_6$)$_2$ almost equally efficient in this transformation and chose the latter (0.5 mol%), as less expensive material, for further investigations in the study. Umemoto's reagent (1 equiv., alkene in 1.2 equiv. amount) was an effective source of the trifluoromethyl radical upon single electron reduction with Ru(II)[*]
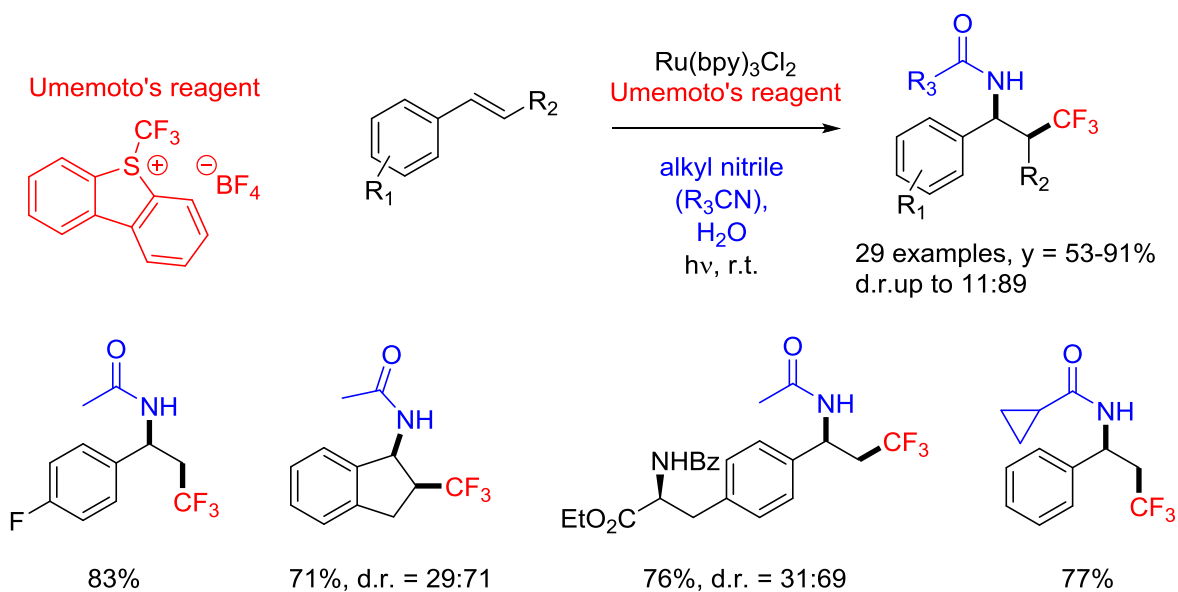
Scheme 18. Ru photoredox catalyzed trifluoromethylation-amidation.

30

photoredox catalyst. The nucleophile MeCN was used as solvent, but it was shown for different alkyl nitriles, DCM could be used as major solvent with alkyl nitrile cosolvent (9:1 v/v mixture).[100] Photoredox catalyst as well as visible-light irradiation were essential for the reaction to proceed.[100] Alkyl nitriles could be readily varied in the trifluoromethylation-amination of styrene.[100] In MeCN, exemplary alkylated, halogenated, *p*-trifluoromethylated, *m*-formylated or *m*-*N*-Boc-amino styrenes in application showed the broad substrate range of the technique. While no concrete alkoxylated styrene was presented, *p*-acetoxystyrenes was suitable. The scientists considered the method to have prospect to late-stage functionalizations when they discovered that a vinylated estrone-derivative and a protected vinylated tyrosine-derivative to react according to the procedure.[100]

In 2017 the group of H. Bao described the use of MeCN as both H-donor for radical generation and as nucleophile in the difunctionalizations of alkenes (Scheme 19).[101] With a Cu catalyst (5 mol%), BPO as proposed precursor for phenyl radicals (via benzoyloxy decarbonylation) and HPF$_6$ (60 mol%) as additive, the reactions were carried out in MeCN at 70°C. The article
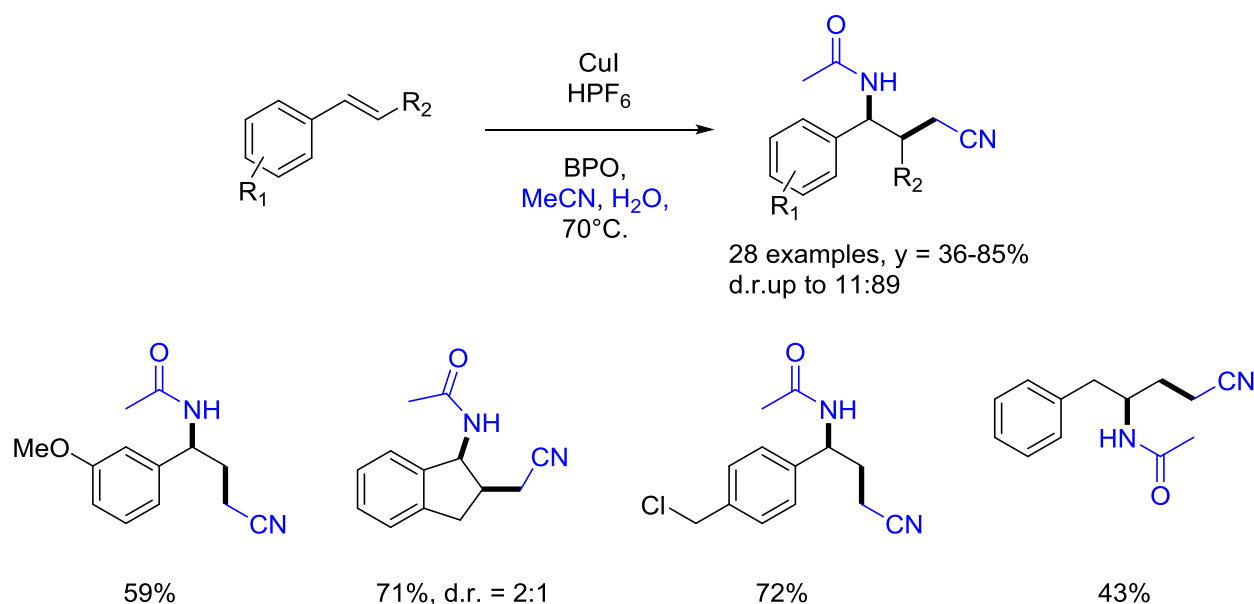
Scheme 19. Cu catalyzed α-cyanomethylation-amidation.

presented MeCN as only nucleophile and radical source for the difunctionalization in use and could derive numerous products from different alkenes.[101] The procedure established the difunctionalization for styrenes with different aryl-substitution patterns, including alkyl, halogen, chloromethyl, carboxyl or aryl groups. Acetoxy groups were also viable. Methoxy groups were established in *m*-position to the vinyl substituent. Furthermore β-alkyl- or aryl-substituted

styrenes were viable and difunctionalizations of some aliphatic alkenes were accomplished with the technique. In the latter cases α-cyanomethylated alkenes were yielded as side-products.[101]

1.2.5.3 Difunctionalizations with Indole Nucleophile

Masson and coworkers made in 2014 efforts towards the trifluoromethylation-arylation of styrenes.[102] Using catalytic $Ru(bpy)_3(PF_6)_2$ (5 mol%) they could under blue light irradiation reductively generate trifluoromethyl radicals from Umemoto's reagent and oxidize the radical-styrene-adduct in turn (Scheme 20). Designed for trimethoxybenzene as nucleophile Masson *et al.* showed that besides 2-vinylnaphthalene some styrenes were viable substrates for the procedure in DCM at r.t.. Namely styrenes with *p*-methoxy, *p*-acetoxy-, *p*-*tert*-butyl-, *p*-chloro-, *m*-methyl-, *o*-bromo-, *β*-methyl-, *β*-phenyl- and interestingly a *p*-hydroxy-substituent were practicable to derivatize in this method. Different substituted (multi)methoxybenzenes were used.[102]

8 examples[a], y = 31-99%

82%   52%   31%
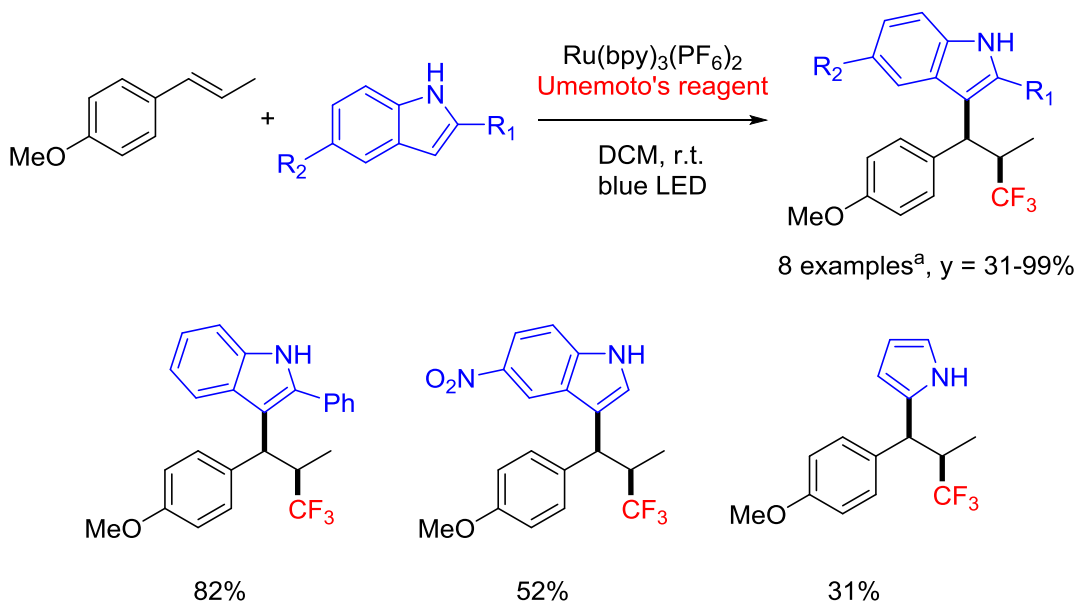
Scheme 20. Ru photoredox catalyzed trifluoromethylation-arylation ([a]including pyrrole and benzofuran products).

Turning their interest towards heteroarene nucleophiles the chemists could show that the methodology holds using (*E*)-β-methyl-*p*-methoxystyrene as alkene (Scheme 20). The double bond could be functionalized with indole, substituted indoles (5-nitro, 5-bromo, 5-methoxy, 2-

methyl, 2-phenyl) as well as with pyrrole and with benzofuran. The indoles and benzofuran were thereby functionalized at 3-position while the shown pyrrole attacked at 2-position.[102]

The J.-H. Li group showed in 2016 that α-carbonyl alkyl bromides could be reductively cleaved to add the resulting α-carbonyl centered radicals together with *N*-protected indoles to styrenes (Scheme 21).[53c]
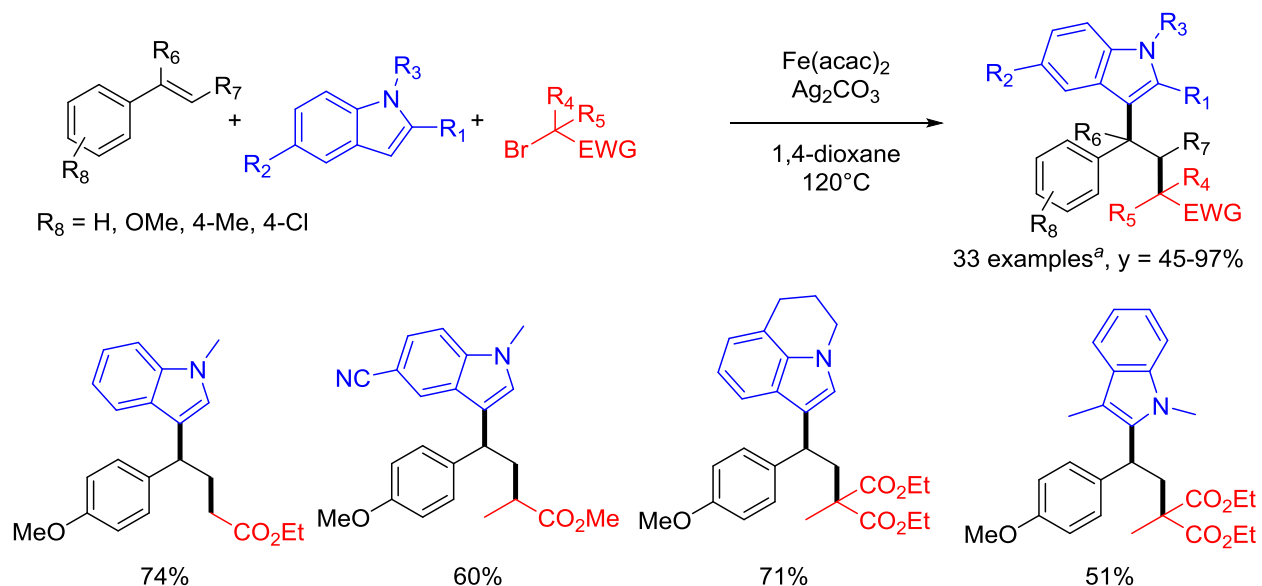
Scheme 21. Ag mediated addition of a-carbonyl radicals and indoles ([a]inclusing 2-indolyl product).

The electrons for the cleavage were provided by Ag_2CO_3 at harsh reaction temperatures of 120°C in 1,4-dioxane (chlorobenzene could serve as an almost alike effective reaction medium). A $Ag(II)CO_3$ species was believed to be the present oxidant to transform the intermediary radical-styrene-adduct **I1** to the corresponding benzylic carbocation **I2**. Despite this proposed redox cycle Ag_2CO_3 (2 equiv.) could not be applied in catalytic amounts (neither in the presence of an alternative base). A non-essential but yield improving additive was found with $Fe(acac)_2$, believed to act as an Lewis acid for radical stabilization (ferrous and ferric chlorides and $Cu(acac)_2$ did not affect the yield positively). The researchers studied the reaction with *p*-methoxybenzene and *N*-methylindole to find a range of α-bromides derived from esters (1°, 2° and 3° (malonates)) and ketones (aryl and aliphatic) to work well (y = 60-96%). The highest yield was reached with diethyl-2-bromo-2-methylmalonate, the lowest yield with bromomethyl-phenyl-ketone.[53c] With *p*-methoxystyrene and diethyl-2-bromo-2-methylmalonate the aryl-

substitution on *N*-methylindole had an influence on the product yield. A superior convenience was suggested for electron-donating substituents compared to electron-withdrawing ones. 3-substituted indole connected in 2-position with the styrene-derived benzylic cation **I2**. It was found that besides methyl also benzyl and Boc group could be used for the *N*-protection, while unprotected *N*-H indole would not lead to a difunctionalization.[53c] The portfolio of *p*-substituted styrenes showed the highest yield for a *p*-methoxy substituent (y = 90%), good yields for *p*-chloro-(y = 80%), *p*-methyl groups (y = 75%) while *p*-cyanostyrene was incompatible to the method.[53c] For *p*-methylstyrene competition experiments between 5-methyl- and 5-cyano-*N*-methylindole were presented. The results showed that along the time course of the reaction the 5-methyl substituted indole was distinctively used in advance of the 5-cyano derivative. These time resoluted reactions were indicating that the indole attack is rather an ionic process.[53c]

The J.-H. Li group published in 2016 another difunctionalization of styrenes with mainly indoles and α-carbonyl centered radicals derived from the corresponding bromide (Scheme 22).[103] Compared to the technique above, photocatalyst Ir(ppy)$_3$ (1 mol%) controlled in MeCN at r.t. the difunctionalizations. Also a base (K$_2$CO$_3$ with best results) is mandatory in this procedure to receive the difunctionalized styrene in quantifiable amounts.[103] Asides *N*-methylindole some derivatives (methylated, 5-bromo, 5-cyano, y = 39-79%) showed to be applicable. A methyl group in 2-position showed to have a positive influence on the yield (y = 79%). A competitive reactivity of 2- and 3-position was not further described. While plain indole was only producing trace amounts of difunctionalization product, *N*-benzylindole proved to be a good nucleophile (y =71%). In addition also some strongly substituted pyrroles (3-acetyl-1,2,4-trimethyl, 3-acetyl-1-benzyl-2,4-dimethyl; y = 69-77%) were successfully applied.[103]
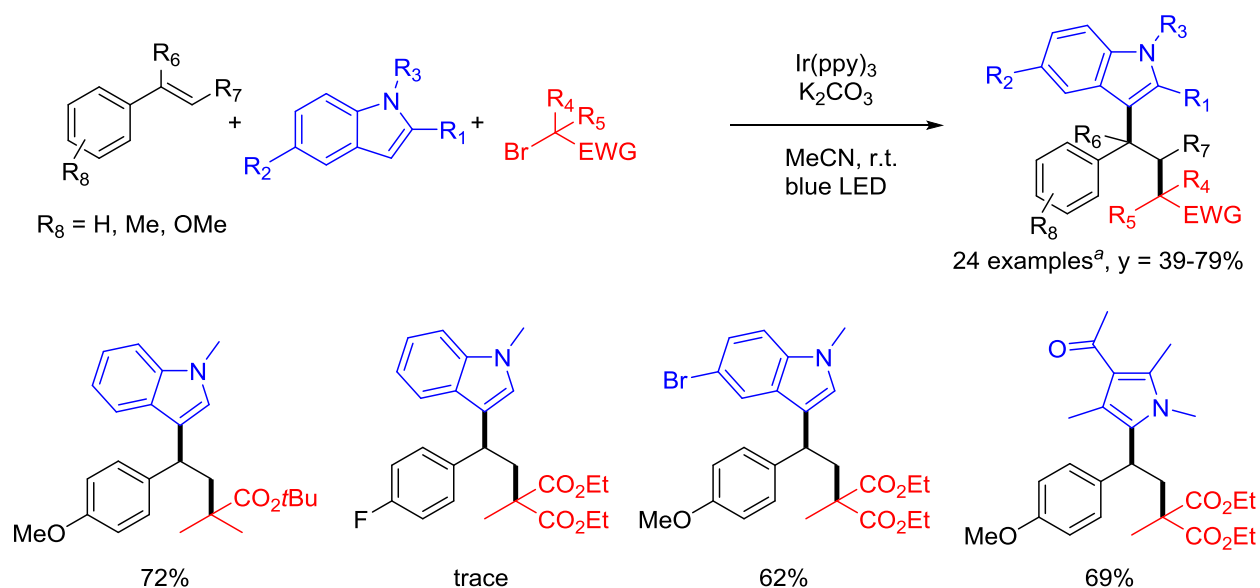
Scheme 22. Photoredox catalyzed addition of α-carbonyl radicals and indoles ([a]including pyrrole and 2-indolyl products).

Regarding the scope of the alkenes, it was shown that especially methoxy substituents were present in the practicable styrenes. Simply styrene (y = 44%), 4-methylstyrene (y = 48%) and α-methylstyrene (y = 40%) showed to perform, with slightly diminished yields for their difunctionalization products. 4-Fluoro- and 4-cyanostyrene could not be functionalized in the described manner. The authors described styrenes with electron-donating groups as well as some aliphatic alkenes as inert to the reaction conditions.[103] With the use of 3-deuterated-*N*-methylindole in combination with *p*-methoxystyrene and diethyl-2-bromo-2-methylmalonate a kinetic isotope effect (KIE) of $k_H/k_D = 1.13/1$ was used to question the involvement of a HAT from the indole to a radical in the reaction course.[103]

C. Zhu *et al.* described also in 2016 a technique to add diflouroketomethyl groups besides indoles to styrenes.[104] The α-carbonyl centered radicals were formed from single electron reduction of corresponding difluoroketomethyl bromides by the photoredox catalyst Ir(ppy)$_3$ in the presence of AgOAc under visible white light irradiation and at r.t.. The typical bromide used was ethyl-bromodifluoroacetate. *p*-Methoxystyrene along with *N*-methylindole were used as standard substrates. In addition to irradiation and Ir(ppy)$_3$ also a base was necessary to obtain a difunctionalization process.[104] In terms of alkenes *p*-methoxy, *o*-methoxy and *p*-methylstyrenes as well as 1,2-dihydronaphthalene were found to lead to difunctionalizations with *N*-methylindole and ethyl-bromodifluoroacetate. *p*-Chloro-, *p*-bromostyrene, pentafluorophenylethylene as well

as plain styrene and α-methylstyrene were insuccesfully tested in this difunctionalization strategy.[104]

In 2017 the groups of J.-H. Li and S. Luo disclosed a synthetic method to silylate alkenes in 1,2-difunctionalizations.[105] Initially amines were the presented nucleophiles, but the intrinsic features of this method made a more vaste range of N- and C-nucleophile applicable (Scheme 23). The silylation was derived from silanes, which were transformed to their corresponding radicals by
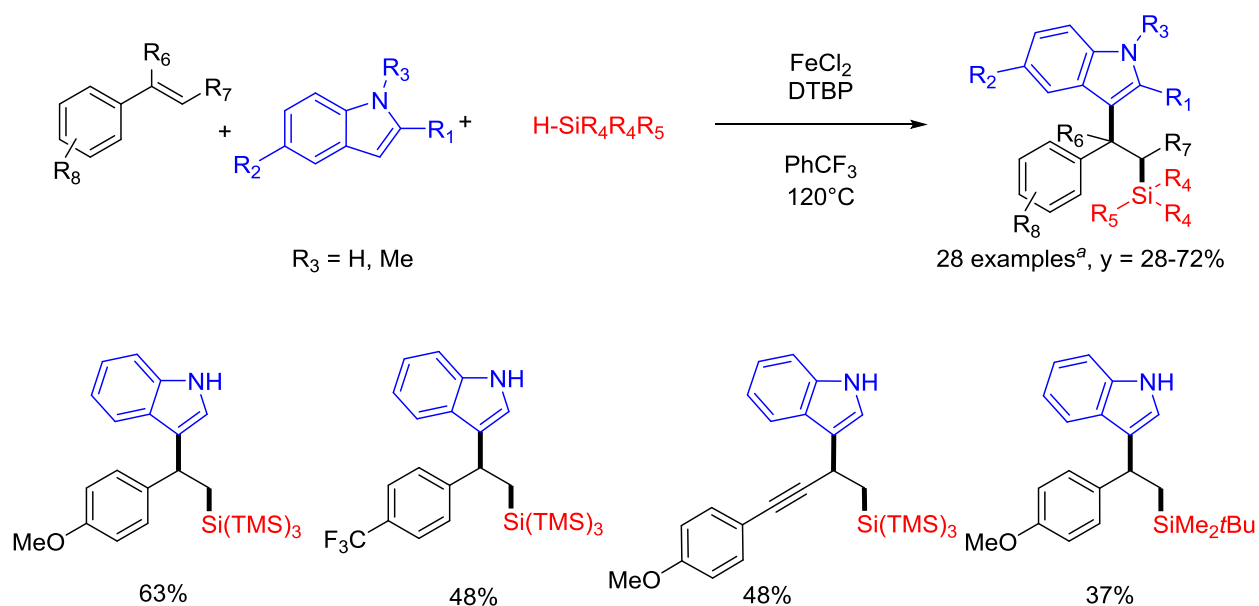
Scheme 23. Fe catalyzed silylation-arylation ([a]including pyrrole and conjugated alkene products).

H-abstraction. As a H-acceptor *tert*-butoxyl radical was used anon formed by means of FeCl$_2$ catalysis from DTBP at 120°C in PhCF$_3$. The here used Fe(II) species was believed to be recycled after electron transfer from intermediary silyl-radical-alkene-adduct **I1** to the Fe(III) species. Secondary amines (morpholine, piperidine, pyrrolidine, diethylamine, 3-phenylpropylamine) as well as a number of primary amines, amides and a phthalimide were tolerated.[105] With *p*-methoxybenzene and *N-H* indole, HSi(TMS)$_3$ (y = 63%) brought the most efficient difunctionalization. Further *tertiary* alkylated, hydroxodiphenylsilane and *primary* phenylsilane were successful integrated into difunctionalizations.[105] With HSi(TMS)$_3$ and *p*-methoxybenzene *N-H* indoles with electron-donating and –withdrawing substituents as well as pyrrole served as nucleophile for the benzylic arylation.[105] A variety of monosubstituted styrenes, conjugated

alkenes, α-methylstyrene and two internal alkenes with lower yields were shown to work in this difunctionalization with *N-H* indole and HSi(TMS)$_3$.[105]

In 2018 the J.-H. Li group described a Ir(ppy)$_3$ photoredox catalyzed vicinal diarylation of styrenes (Scheme 24).[106] The C(sp^2)-aryl radicals were formed reductively from aryldiazonium salts, as nucleophiles mainly multimethoxybenzenes and in addition some indoles could be used. The reaction was carried out in chlorobenzene at r.t. with blue light irradiation. Furthermore the authors described that the employment of a base, namely 2,2'-bipyridyl (bpy), was necessary in order to observe a difunctionalization. Some experiments suggested that the influence of the base mainly lied in the suppression of competitive hydroarylation of the styrenes. The addition of a Lewis acid like Sc(OTf)$_3$ to the reaction mixture in contrary favored the hydroarylation reaction course.[106]
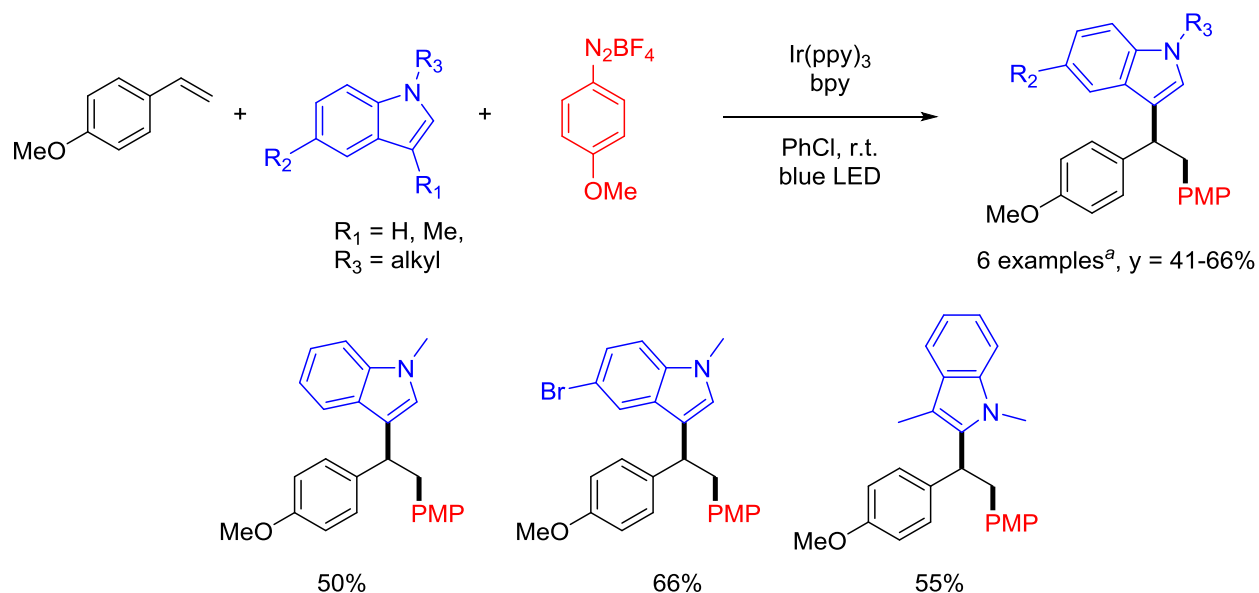
Scheme 24. Photoredox catalyzed 1,2-diarylation ([a]including 2-indolyl product).

The substitution pattern of trimethoxybenzenes (y = 30-76%) could have a quite important role on the product yield. In general, the electron-poorer methoxybenzenes showed a lack of reactivity.[106] On *p*-methoxystyrene and with the *p*-methoxyphenyl diazonium tetrafluoroborate as radical source some *N*-alkylindoles were alternative nucleophiles. The electronic influence of a 5-substituent seemed to have a lower impact on the product yield, while for 1,3-dimethoxybenzenes a further substituents could determine about the difunctionalization to proceed.[106]

For 1,3,5-trimethoxybenzenes alkenes were not showing a clear trend depending on the electronic features. Oct-1-ene was tested unsuccessfully in the difunctionalization method. 1,1-diphenylethylene was transformed to 1,1-diphenyl-2-(*p*-methoxyphenyl)ethylene under the reaction conditions by monofunctionalization with the diazonium salt.[106]

Also in 2018 the J.-H. Li group established a technique to add radicals derived from alkyl nitriles together with indoles to styrenes (Scheme 25).[107]
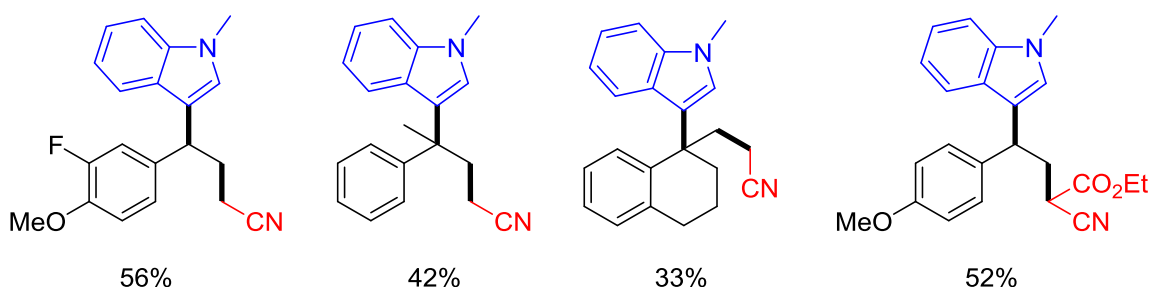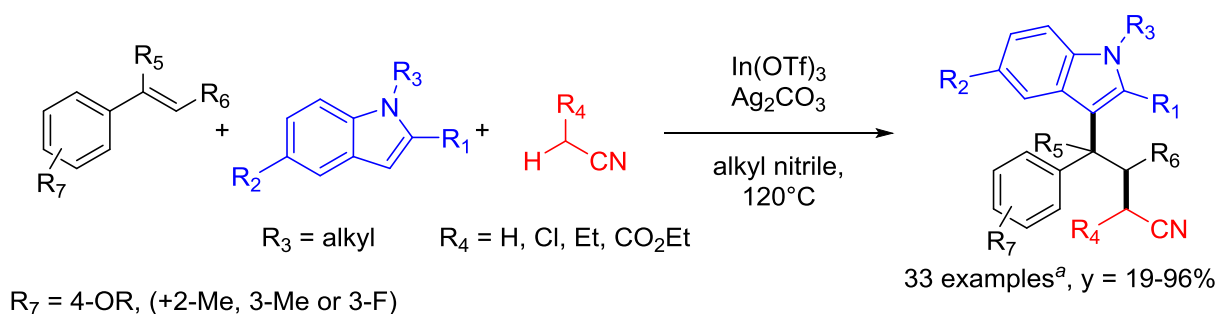
Scheme 25. Ag mediated cyanomethylation-arylation ([a]including pyrrole and 2-indolyl products).

The alkyl nitrile was directly employed as solvent and Ag_2CO_3 (2 equiv.) was used as mediator at 120°C to cleave the α-C(sp^3)–H bond of the nitrile oxidatively and to oxidize the intermediary radical-alkene-adduct **I1** to the corresponding benzylic cation **I2**. Furthermore, application of Lewis acid In(OTf)$_3$ in the reaction was found to improve the reaction yield. In contrast to the Ag salt the Lewis acid is not essential for the difunctionalization to occur.[107] *p*-Methoxystyrene was also difunctionalized (in MeCN) using functionalized *N*-methylindoles, whereby the electron-poorer indoles show lower product yields. While benzofuran, thiophene and benzo[b]thiophene failed to lead to difunctionalizations, *N*-protected pyrroles could be implemented to the methodology.[107] With *N*-methylindole (in MeCN) difunctionalizations of styrenes bearing alkoxy groups on the aromatic ring, substituted 2-vinylthiophene, α-substituted styrenes, as well as dihydronaphthalene were presented while oct-1-ene failed.[107]

Furthermore the J.-H. Li group presented the synthetic procedure for difunctionalization of styrenes with the use of ether molecules, which form radicals upon C–H bond cleavage in α-position to the ether-oxygen.[108] Standard alkene was again p-methoxybenzene, N-methylindole the nucleophile and 1,4-dioxane solvent and radical precursor (Scheme 26).
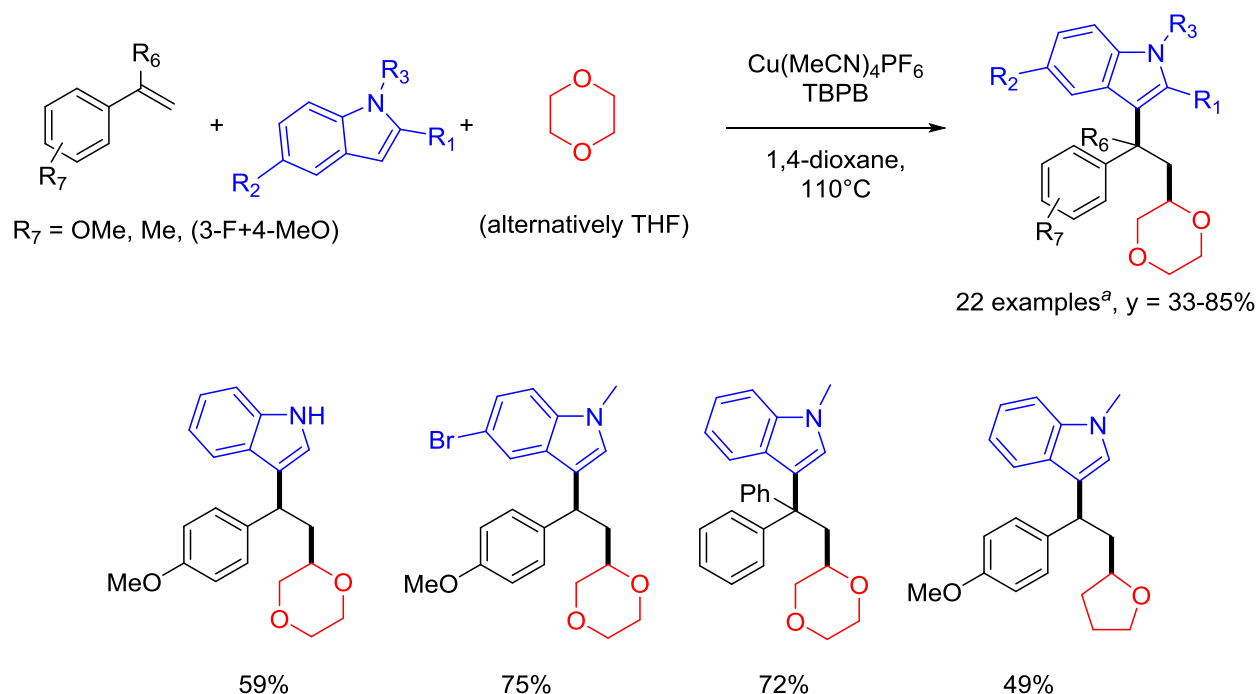
Scheme 26. Cu catalyzed addition of α-ether alkyl radicals and indoles ([a]including pyrrole and 2-indolyl products).

The methodology describes the use of catalytic Cu(MeCN)$_4$PF$_6$ (10 mol%), tert-butyl peroxybenzoate (TBPB) as source for tert-butoxyl radicals, which are the present H-acceptors in the system or more generally work as oxidant at 110°C. Cu catalyst as well as peroxide were indispensable for the reaction to proceed (alternatively di-α-cumyl peroxide (DCP), di-tert-butyl peroxide (DTBP), tert-butyl hydroperoxide (TBHP), α-cumyl hydroperoxide (CHP) suitable, resulting in lower difunctionalizaton yields).[108]

Glorius *et al.* have used *N*-benzylic Katritzky salts (tetrafluoroborate) and indoles to difunctionalize styrenes under [Ir(dtbbpy)(ppy)$_2$]PF$_6$ photoredox catalytic conditions (blue light) in MeCN at r.t. (Scheme 27).[109]
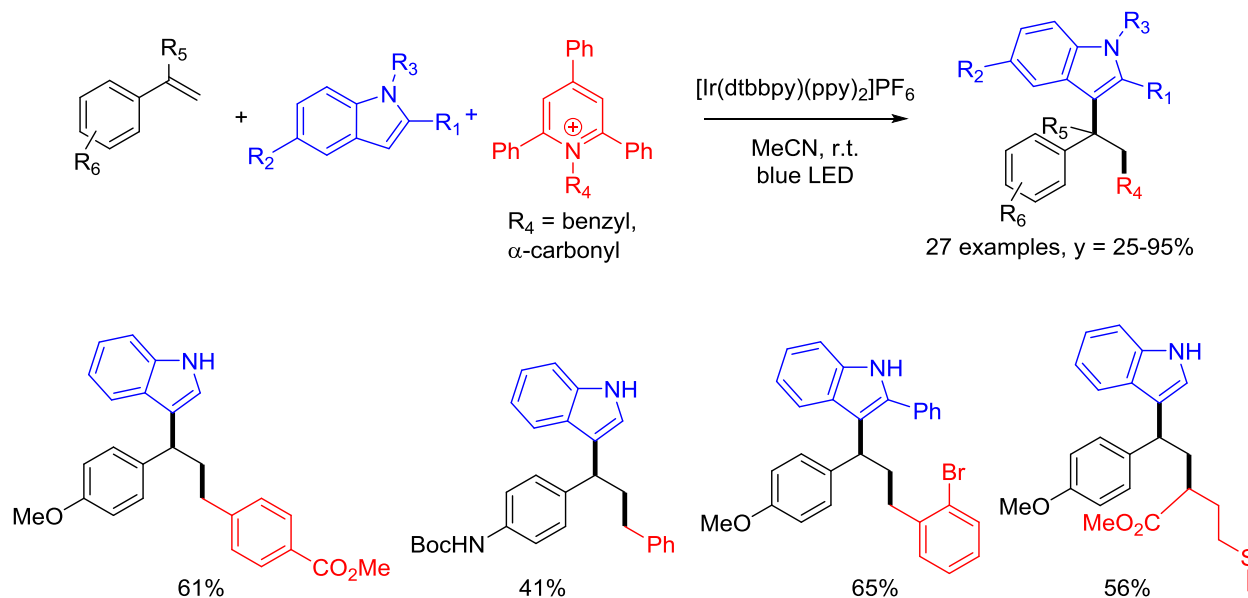
Scheme 27. Photoredox catalyzed addition of benzyl radicals and indoles.

The Katritzky salt represents an alternative to benzylic halide to produce benzylic radicals in a reductive fashion. In comparison to the latter pyridinium salts feature more positive reduction potentials and therefore should deliver more easily the corresponding radical. Furthermore this operation circumvents the generation of acid by-products which in turn could have a great impact on the reaction system (e.g. side-reaction hydroarylation).[109]

The employment of a variation of Katritzky salts showed that substituted benzylic radicals show reasonable suitability to add to *p*-methoxystyrene together with *N-H* indole. Furthermore, pyridinium salts derived from α-amino acids could be used to functionalize *p*-methoxystyrene with the corresponding α-carbonyl radicals.[109] In terms of nucleophiles 5-iodoindole, *N*-methylindole, 2-phenylindole and *N*-methylaniline were alternatives presented to react with *p*-methoxystyrene and toluyl radicals from the pyridinium salt source.[109]

In 2019 the J.-H. Li group reported a CuCl-catalyzed 1,2-trifluoromethylation-arylation of styrenes using NaSO$_2$CF$_3$ as source for trifluoromethyl radicals at 50°C MeCN.[110] The generation of radicals was observed only in the presence of a Cu catalyst (10 mol%) and an oxidant (3 equiv.), for which TBPB was found to be most efficient. Also K$_2$S$_2$O$_8$ (10 mol%) was a yield

improving additive. Arylation was achieved by using several indole and some pyrrole derivatives.[110] With NaS_2O_8 and *N-H* indole, some styrenes were shown to be implemented in the technique. Among viable monosubstituted alkenes only alkoxylated styrenes and a substituted 2-vinylthiophene were present in the scope. β-phenyl-*p*-methoxystyrene did not yield the difunctionalization product.[110]

1.3   Artemisinin in Action

Artemisinin (quinghaosu) and derivatives are today the first choice to treat malaria diseases caused by parasites of the plasmodia family.[111] Especially, since the occurance of multi drug resistances by plasmodia towards antimalarials of type quinolone, its importance rose.[112] Due to an often fast metabolism and fast excretion, artemisinin and derivatives were more and more chosen to be part in a combinatory therapy together with a more long-lived antimalarial to hinder new resistances and overcome monotherapy failures.[113] To the start of drug researches on artemisinins, the structural pharmacophore was identified as the endoperoxide bridge.[114] Whereas, deoxygenated derivatives showed no specific antimalarial activity.[114] The endoperoxide function drew attention towards radical based mechanisms of action. *In vitro* experimental applications suggested, that artemisinins antimalarial activities were antagonized in the presence of a radical scavenger, while the presence of radical initiators gave better results.[115] Reactions of artemisinin with malaria parasite Plasmodium falciparum resulted in transformations of a vaste spectrum of protein cell segments.[116] Synthetic evidence from different studies for fragmentation of artemisinin derivatives under Fe mediated conditions[117], paired with successful EPR spin-trapping experiments[118] fired discussions and assumptions concerning the mechanism, according to which artemisinin and its derivatives display its activity/activities.[113,116b,119] Initial suggestions of Posner based on experimental isolations of degradation products of an artemisinin model molecule after reaction in the presence of Fe species.[120] Formed products in this study were partially in line with known thermal decomposition products[121] of artemisinin.[120] In Posner's experiments, Fe mediation was conducted, because of the knowledge of abundance of Fe in malaria parasites (like P. falciparum). Malaria parasites' harmful effect on its mammal host is based on the digestion of red blood cell hemoglobin units to hematin and hemozoin (malarial pigment). Hemozoin is the crystalline product of dimerization processes of heme units and is also stored in the digestion vacuole of P. falciparum.[122] The concept of Fe mediation for trioxane cleavage was soon assumed and further tested.[118b] Furthermore, among Fe mediated artemisinin

degradation, heme is more effective than hemoglobin, hemin or inorganic Fe salts.[123] Yet, there is also evidence that mammal parasites, that do not contain Fe based species are inhibited by artemisinin derivatives.[124] Nevertheless, until today the proposal of Posner on the mechanistic behavior of artemisinin in malarial parasites is discussed and considered.[116b] The formed radicals in turn are on this basis supposed to be the causes for parasite apoptosis and the medicative effect of artemisinin derivatives in malarial diseases.

The Fe based activation was suggested to start on a reductive O–O bond cleavage of the endoperoxide bridge (Scheme 28a). The electron is theoretically transferred to either of the two oxygen atoms leading to two branches of this mechanistic consideration (**4→J1** or **4→J4**, respectively). When the initial radical is centered on the *tertiary* oxygen (**J1**) a 1,5-HAT could lead to a *secondary* alkyl radical **J2** which in turn could be an intermediate for observed products (4-hydroxy deoxyartemisinin **J3** etc.).[116b] Along the other proposed reaction path, a formed oxyl radical adjacent to the acetale group in **J4** is believed to undergo a homolytic β-cleavage[125] forming a *primary* alkyl radical (and carbonyl formation of acetyl, **J5**), that led to the observed tetrahydrofuran moiety in isolated products **J6**.[116b]

In addition, another point of view is that the so formed C centered radicals are too reactive and thus too transient to interfere with vital biomolecules and cell organelles of the parasite. In this case, they would not be involved in the pharmacological effect of artemisinin.[119] This standpoint is also backed up by antimalarial activity resulting from scaffolds structurally impaired or unable to form analogous C centered radicals.[126] On that note and some basic experimental findings an heterolytic trioxane cleavage was alternatively proposed (Scheme 28b).[127] Yet, the formation of a *tertiary* hydroperoxide (**J8** or **J10**, respectively) along this mechanistic path could lead to some radical intermediates (**J9**) in the interplay with hemin or Fe based activation apart from heterolytic actions.[116b]
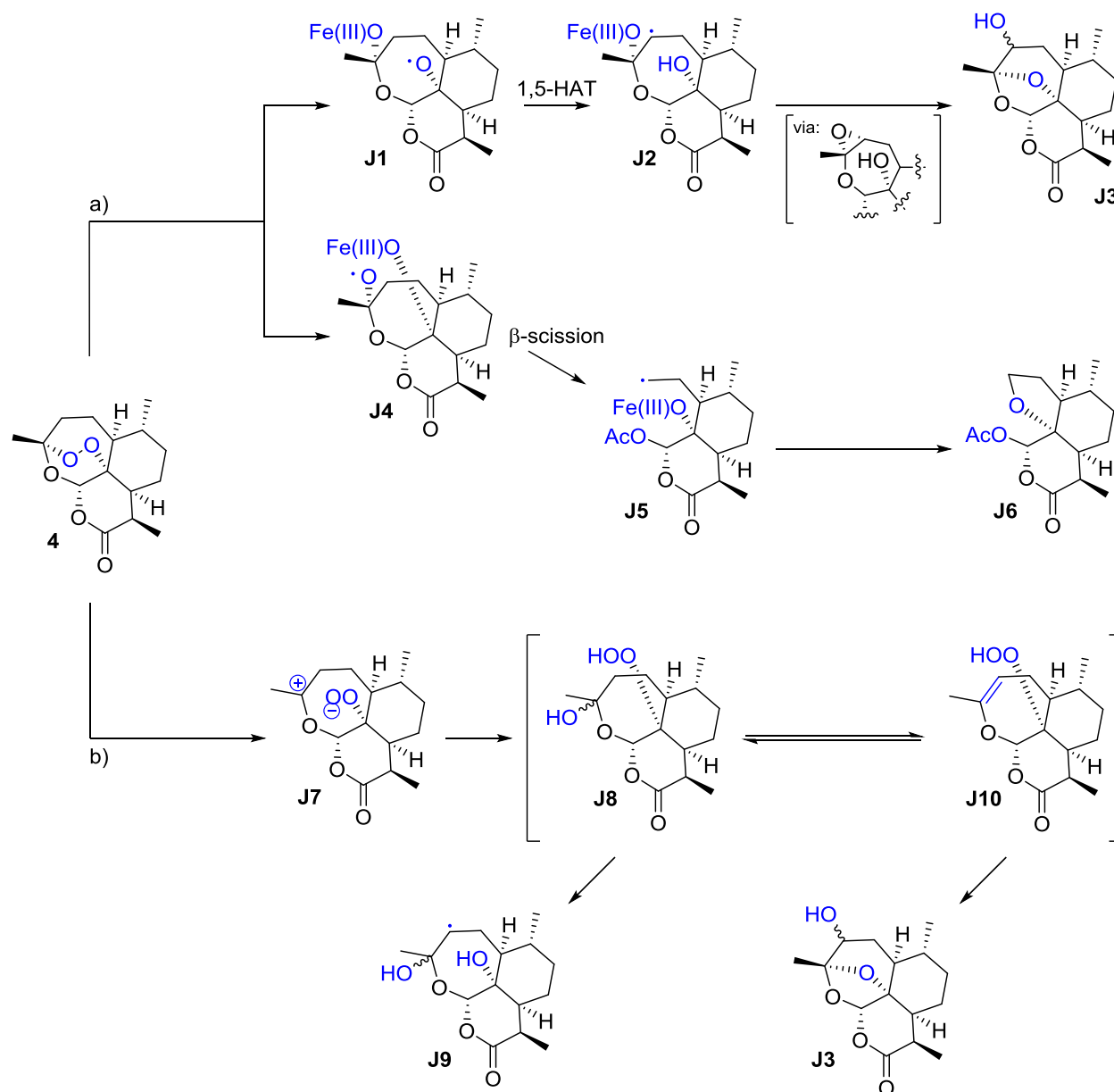
Scheme 28. Proposed mechanisms of action of antimalarial artemisinin.

Artemisinin derivatives were also associated with anti-cancer treatments bearing antiproliferative activities. They are believed to be a source of reactive oxygen species (ROS) that in different cells dysregulate specifically redox processes which are involved in cancer initiation or progression.[128] Its activities were believed to lay in the specifically interference with cancer cells, showing a relatively targeted cytotoxicity.[128a] Interestingly, ozonide or tetraoxane alternatives either retain similar characteristics as artemisinin in regard to antimalarial/anticancer activity or distinguishably display solely improvements as antimalarials or antiproliferative drugs compared to **4**.[128a,129]

2 Objectives

2.1 Artemisinin Application in Radical Chemistry

The remarkable applications of artemisinin and derivatives in medicine as antimalarial or in anticancer treatment are great achievements and are helping many people around the world.[112-113,128] Up to now and in future, these molecules received and will receive great attraction in order to develop the next generation of drugs and therapies.[116b] Although artemisinin has been in the center of examinations since the 1970s to this day[112], there is no fulfilling understanding, especially on how found reactivities are related to its activity in desease therapy. It is causing a controversial debate on its mechanism of action.[116b,119,130] For several years, investigations on radical chemistry of artemisinin were undertaken in the Klußmann group and were pointing towards an application as radical initiator in methyl methacrylate oligomerizations. It was my privilege to explore the chemistry, refining it towards an application and get more information about artemisinin, this molecule of great curiosity.

2.2 Alkene Difunctionalization with α-Ketonyl and Cyanidyl Radicals

The generation of α-ketonyl radicals from ketones in the presence of *tert*-butyl hydroperoxide by Brønsted acid-catalysis could be harnessed to form γ-peroxyketones from styrenes in the Klußmann group.[3] An ongoing investigation in the Klußmann group (see chapter 3.2.1 for a more general classification of principles and challenges in this study), which Dr. Wen Shao discovered and mainly investigated, dealt with a radical alkene difunctionalization with α-ketonyl and cyanidyl radicals. After I joined the project, our first goal was to further broaden the covered space of the application and realizing that, by demonstrating a validity for aliphatic alkenes besides styrenes.[1] After the departure of Dr. Wen Shao from the group, further acquired product characterizations, identifications as well as synthesis led me to a brief comparison of diastereoselectivities between the peroxidation and cyanation procedures.

2.3 Alkene Difunctionalization Involving a Nucleophilic Attachement

After first alkene difunctionalizations in the Klußmann group, achieving alkylation-peroxidation[3] and alkylation-cyanation[1], the focus was shifted towards methods, which supposingly merge a radical β-functionalization and an ionic nucleophilic α-functionalization of the styrene.[31] The general approach bears possibilities to make use of techniques and reagents of both radical and ionic disciplines of chemistry. In the first place, such a concept is rich in variety to find access to new molecules or complementary ways to known synthesis. In addition, the rather new and growing field of radical difunctionalizations showed in various examples to hold unexpected limitations or outcomes, which made the approach worthy for deeper investigations and the known reactions of this kind interesting to analyze. I embraced the challenge to succeed in a complex reaction system, merging, coordinating and largely controlling radical, ionic and redox chemistry in order to achieve the formation of two new σ bonds from the alkene's C–C double bond in one reaction. The course of my investigations and developments brought me to the opportunity to use aldehydes as source of acyl radicals and *N*-alkylindoles as nucleophiles for the purpose.

3 Results and Discussion

3.1 Artemisinin as Radical Initiator in Aqueous Acrylamide Polymerization

The here presented results were to the date of this thesis unpublished and will be included in a future article of the research groups of Dr. Alexander Schnegg and Dr. Martin Klußmann.

3.1.1 Investigation of Reaction Conditions

Previous unpublished studies in the Klußmann group showed that artemisinin and acid (especially MsOH), each in 2 mol% amounts, dissolved in methyl methacrylate (MMA) could lead to a solidification of the reaction mixture at temperatures higher than 45°C over the course of 3 days.[131]

Interested in the cause and possible meaning of this reactivity, my investigations were started to obtain more details in a related reaction. In order to bring the research topic closer to conditions in the human body, the polymerization attempts were constrained to a reaction temperature of 37°C and water as the reaction solvent. Homopolymerizations in aqueous solution are known processes for the related monomer acrylamide (AM).[132] This chapter is opened with the description of polymerization condition evaluations, proceeds with molar mass characterizations and leads to findings that outline some of the causes for reactivity. Among these investigations, it was demonstrated, that slight amounts of Fe species were necessary for the polymerization to occur.

Starting from the idea of polymerization in aqueous medium, solutions of acrylamide (450 mg, 6.3 mmol, 1 equiv.) in deionized water (1.1 mL) were treated with artemisinin (9 mg, 0.032 mmol, 0.5 mol%) and a variety of different acids (2.5 mol%,) in a GC vial (Scheme 29). The solubility of artemisinin in (acidified) water is quite low and not easy to determine on a small scale. Hence, in the following descriptions of polymerization attempts, only a small fraction of the used artemisinin was dissolved and the major proportion was present heterogeneously in the reaction mixture. The artemisinin could be detected via TLC from the reaction solution or reaction mixture/gel, but on the other hand could also often be observed as sediment after high conversion of monomer. Statements about artemisinin concentrations or its molar amounts in reaction descriptions and schemes are referring to the weighed-in quantity. Furthermore, already after rather low conversions of monomer (15-20%) the viscosity of the reaction mixture was sufficient to fully hinder the rotation of a stirring bar in small scale reactions of this screening.

All shown reactions were carried out without the use of stirring bars, meaning that further dissolution and distribution processes of artemisinin molecules in the mixtures were driven by thermal diffusion. Certainly, chain propagations were in these states driven by diffusion.

Using no acid, artemisinin alone could not initiate the polymerization (entry 1, Scheme 29) under the described conditions.
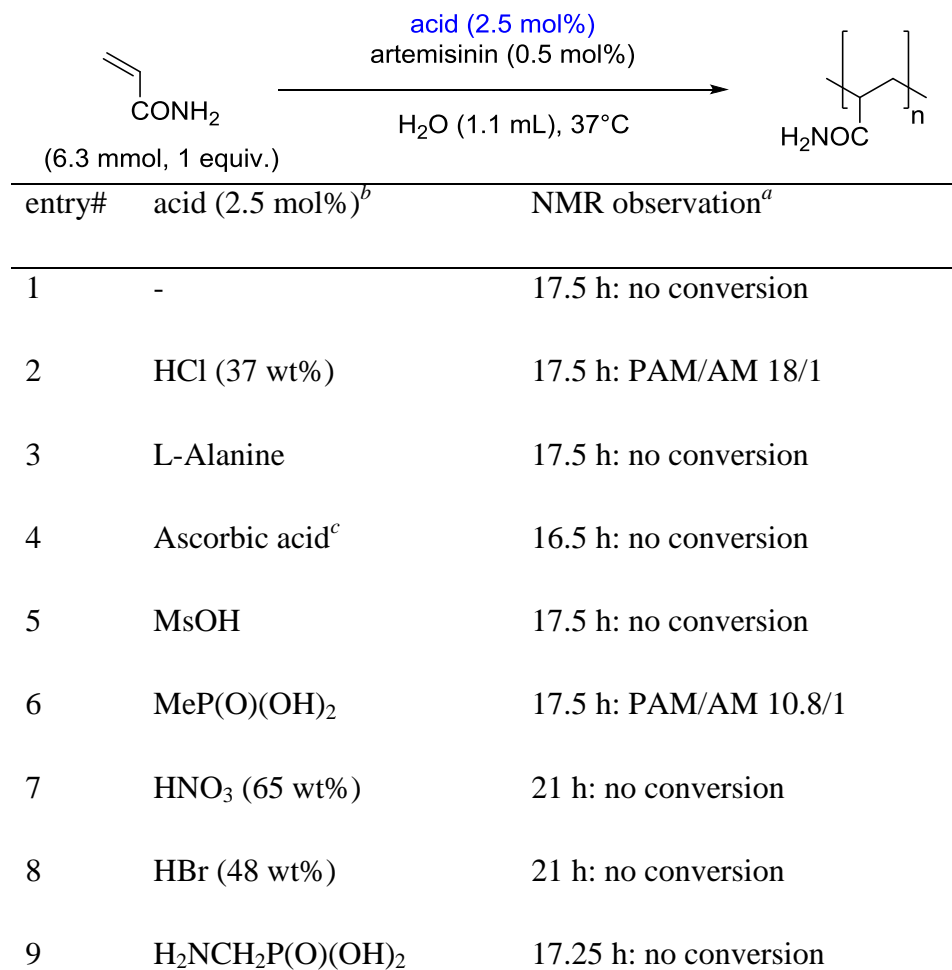
entry#	acid (2.5 mol%)[b]	NMR observation[a]
1	-	17.5 h: no conversion
2	HCl (37 wt%)	17.5 h: PAM/AM 18/1
3	L-Alanine	17.5 h: no conversion
4	Ascorbic acid[c]	16.5 h: no conversion
5	MsOH	17.5 h: no conversion
6	MeP(O)(OH)$_2$	17.5 h: PAM/AM 10.8/1
7	HNO$_3$ (65 wt%)	21 h: no conversion
8	HBr (48 wt%)	21 h: no conversion
9	H$_2$NCH$_2$P(O)(OH)$_2$	17.25 h: no conversion

[a]From ^{1}H NMR analysis. [b] note that all starting materials were used as commercially received; [c]8.7 mol% were used; PAM = polyacrylamide, AM = acrylamide.

Scheme 29. Acids of common commercial purity as co-initiator.

The first successful polymerization process was observed using conc. HCl (entry 2, Scheme 29). The mixture was already a viscous gel after 4 h reaction time and after 17.5 h a stiff jelly. For most evaluated acids the viscosity of the reaction mixture had not changed and aliquots of these mixtures dissolved homogeneously in D$_2$O for ^{1}H NMR analysis (>16 h). Reaction attempts in

which corresponding aliquotes were totally dissolved and NMR spectra showed no sign of polyacrylamide (PAM) were at this stage of the study assigned to feature no AM conversion and the used acids were not active as co-initiator (Scheme 29 and Scheme 30).
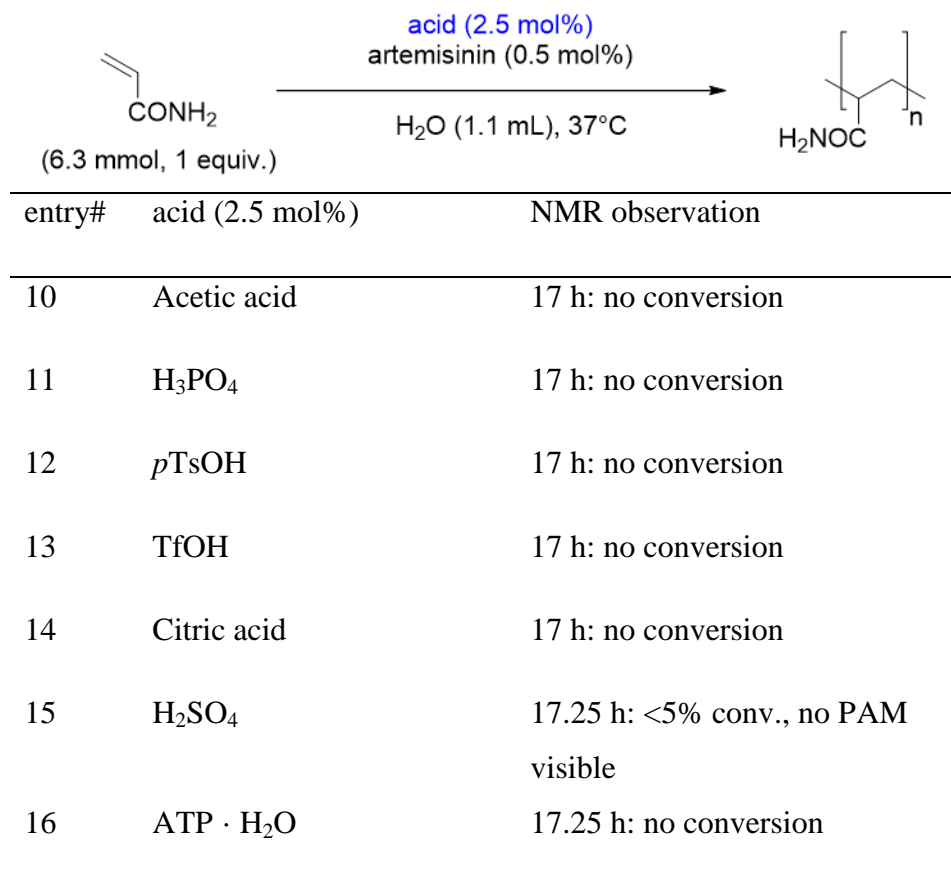
acid (2.5 mol%)
artemisinin (0.5 mol%)
H_2O (1.1 mL), 37°C

CONH₂
(6.3 mmol, 1 equiv.)

entry#	acid (2.5 mol%)	NMR observation
10	Acetic acid	17 h: no conversion
11	H_3PO_4	17 h: no conversion
12	pTsOH	17 h: no conversion
13	TfOH	17 h: no conversion
14	Citric acid	17 h: no conversion
15	H_2SO_4	17.25 h: <5% conv., no PAM visible
16	ATP · H_2O	17.25 h: no conversion

[a]From ^{1}H NMR analysis.[b]note that all starting materials were used as commercially received; PAM = polyacrylamide, AM = acrylamide.

Scheme 30. Continuation of acids of common commercial purity as co-initiator.

Some acids occurring in biological contexts like L-alanine, ascorbic acid, citric acid or adenosine triphosphate (ATP) as well as strong organic acids like pTsOH, MsOH, TfOH and strong inorganic acids like HNO_3 , H_2SO_4 or HBr showed to be incapable to initiate polymerization in this system (see Scheme 29 and Scheme 30). For reactions with HCl (entry 2, Scheme 29) and methylphosphonic acid (entry 6, Scheme 29) the polymerization could be qualitatively proven. Here, aliquotes were partially dissolved in D_2O revealing broad signals for the methylene (~1.4-2.0 ppm) and CH groups (~2.1-2.5 ppm) of oligomerized/polymerized vinyl units in NMR spectroscopy. Since the addition of 2,2,6,6-tetramethylpiperidinyloxyl radical (TEMPO) to the

reaction inhibited the polymer formation, a radical pathway was assumed (for more control experiments, see chapter 3.1.3). Polyacrylamide radical chains tend to form networks by intra-(backbiting)[133] and intermolecular HAT processes, chain transfers. These networks or hydrogels show lower solubility in water than linear polymer chains.[132a,134] A known way to avoid this behavior is the addition of a chain-transfer-agent (CTA) to the reaction, which in an optimal case prevents network formation by offering a different termination process to slower growing polymer chain ends.[132a] With the use of sodium thioglycolate as CTA and sufficiently high acid and artemisinin concentrations in the reaction, polymer mixtures were completely soluble in water. The CTA enabled a quantitative analysis of the polymer aliquots by NMR spectroscopy (sodium toluylsulfonate as internal standard) and lay the foundation for molecular weight determinations (see chapter 3.1.2).

In reactions with HCl, concentrations of 0.25 and 0.50 $mg \cdot mL^{-1}$ of sodium thioglycolate were sufficient to achieve a convenient solubility of the resulting polymers (conversions >89%, 17.5). For mass concentrations of 2.5 $mg \cdot mL^{-1}$ and 5 $mg \cdot mL^{-1}$ at reaction times around 17 h the observed conversions were even higher (>97%). Since the lower concentrations of this toxic reagent were already appropriate to achieve full solubility, a 0.50 $mg \cdot mL^{-1}$ concentration for ensuing experiments was chosen.

In presence of the CTA, 1.1 mol% HCl provided a 89% AM conversion already after 3 h reaction time. For a lower amount of acid (0.6 mol%) the conversion after 3 h reached 45% and after 17 h a 91% conversion. The solubility was again slightly worse. This could mean that the decreased acid concentration led to lower (steady-state) radical concentration in the mixture and therefore longer polymer chains, which again tend to higher network formation when diffusion is strongly limited at higher conversions. Decreasing the HCl amount further (0.2 mol%) the conversion dropped slighly for a reaction time of 18 h to 84%.

Using 1.1 mol% HCl, and varying the artemisinin amount in the polymerization mixture from 0.5 mol% to 0.25 mol%, decreased similarly the supplied conversion after 3 h to 54% (compared to 89%) while at 17 h a high conversion of 94% was achieved, but the solubility of the polymer mixtue was worsened. When going to higher artemisinin concentrations (1 mol% or 1.5 mol%) the conversion could be slightly increased (3 h: by 1% or 4%, respectively; 17.5 h: by 3% or 9%, respectively). Since 0.5 mol% artemisinin delivered a highly soluble polymer, yet left space for

49

improvements in terms of yield for further investigations of reaction conditions, this artemisinin amount was chosen. It was the lowest amount to yield a polymer mixture of high conversion that could be dissolved within 1 h (in 0.5 mL D_2O) in the test series and by that an efficient choice.

For acid amounts of 1 mol% in the presence of sodium thioglycolate (0.5 mg·mL^{-1}), some additional AM polymerizations were carried out (Scheme 31). Experiments revealed that HClO$_4$, HPF$_6$ and HI (entries 2, 4 and 3, respectively) were not able to act as a co-initiator. Further, the proteolytic enzymes trypsin (from porcine pancreas) and pepsin (from porcine gastric mucosa) could not succeed in polymerization initiation (up to 3 d). Asides HCl and MeP(O)(OH)$_2$, *o*-benzodisulfonimide (entry 5) was found to initiate the AM polymerization in combination with artemisinin. The results suggested that the choice of acid has a particular impact and only a few acids were found to enable a polymerization under the evaluated conditions. Especially the inability of HI and HBr in comparison to HCl to start the reaction and in general no direct identifiable pattern from the nature of the acids were reasons for further investigations on the cause of the observed acid activities (see chapter 3.1.3).

For HCl usages, increasing the amount of solvent (stock solution, 1.5 mL-3.6 mL) resulted in AM conversions of lower than 65% after 18 h reaction time. When increasing the amount of CTA to 2.5 mg·mL^{-1}, an simultaneous increase in HCl concentration to 5 mol% led to conversions of 68% and 86% after reaction times of 3 h and 17 h, respectively. This polymer mixture showed again a slightly worse solubility.

acid (1 mol%)
artemisinin (0.5 mol%)
sodium thioglycolate (0.5 mg mL^{-1})

$CONH_2$ (6.3 mmol, 1 equiv.) → H_2NOC ... n

H$_2$O (1 mL), 37°C

entry#	acid (1 mol%)[b]	observation	conversion (PAM/AM)[a]
1[c]	HCl	2.25 h: gel	3 h: 89% (~6/1)
		17.5 h: gel	17.5 h: 89% (~8.6/1)
2[c]	HClO$_4$	17.25 h: no gel formation	17.25 h: no conversion
3[c]	HI	17.25 h: no gel formation	17.25 h: no conversion
4[c]	HPF$_6$	17.25 h: no gel formation	17.25 h: no conversion
5[c]	o-benzodisulfonimide	2.25 h: gel	2.25 h: 77% (~2.5/1)
		17.25 h:gel	17.25: 84% (~5.1/1)
6[c]	MeP(O)(OH)$_2$	3.11 h: gel	3.11 h: 75% (~5/1)
		16 h: gel	16 h: ~94% (~15.6/1)
7	trypsin (0.1 mol%)	19 h: dispersion	19 h: no conversion
8	pepsin (0.1 mol%)	19 h: dispersion	19 h: no conversion

[a]From ^{1}H NMR analysis; [b]note that all starting materials were used as commercially received; [c]sodium thioglycolate (0.5 mg mL^{-1}); PAM = polyacrylamide, AM = acrylamide; HI was applied as concentrated solution (57wt%), HPF$_6$ was used as solution in water (55wt%).

Scheme 31. Further acid screenings with sodium thioglycolate in reaction mixture.

3.1.2 Characterization by Molecular Weight Determinations

Via NMR analysis of polymerization mixtures, a good understanding about influencing factors for conversion and solubility of the resulting polymer at high conversion states could be identified. The presence of sodium thioglycolate led to better soluble polymers for high conversion mixtures. This is probably the result of a low amount of branched polymer chains in these reactions. The influence of this reagent on chain terminations and (steady-state) radical

chain concentrations should also have an impact on the average molecular weights of the polymers. Thus polymerizations initiated by artemisinin/HCl, with different mass concentrations of the CTA present, were compared by results from NMR (entries 1 and 2, Scheme 32) and gel permeation chromatography (GPC, Figure 3). Like described before, the kind of acid used in the procedure had a big impact on the success of the polymerization. With this information the three active acids HCl, methylphosphonic acid and *o*-benzodisulfonimide were comparatively applied in the polymerization (entries 1,3 and 4, Scheme 32) and the resulting polymer mixtures analyzed by GPC (Figure 3).

While the reactions with HCl and different CTA concentrations (entries 1 and 2) showed at 3 h (>89%) and 17.5 h (>89%) quite high conversions of AM, polymerizations with *o*-benzodisulfonimide and methylphoshonic acid co-initiators (entries 3 and 4) featured lower yields after 3 h (77% and 75%, respectively).

The samples had been sent to PSS company for GPC measurements after reaching high AM conversions (≥94%). The measurements were carried out from diluted samples (~3 mg mL^{-1} in eluent 0.1 M NaNO$_3$) on PSS Suprema columns (stationary phase: modified acrylate copolymer, for more details see chapter 5.1) at 30°C.

$$\text{acid (1 mol\%)}$$
$$\text{artemisinin (0.5 mol\%)}$$
$$\text{sodium thioglycolate (0.5 or 2.5 mg mL}^{-1})$$

CONH$_2$ (6.3 mmol, 1 equiv.) $\xrightarrow{\text{H}_2\text{O (1 mL), 37°C}}$ H$_2$NOC—[ ]$_n$
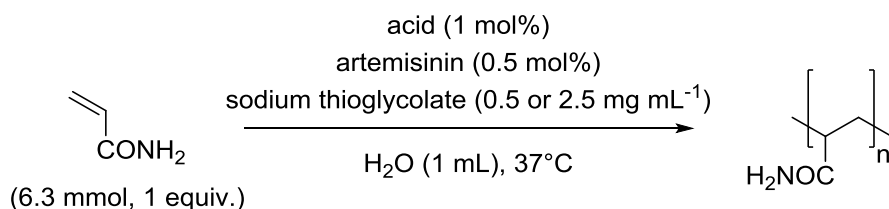
entry#	acid (1 mol%)[b]	sodium thioglycolate [mg · mL^{-1}]	conversion[a]
1	HCl	0.5	17.5 h: 89% final: 96%
2[c]	HCl	2.5	17.5 h: 97% final: 99%
3[c]	o-benzodisulfonimide	0.5	17.25 h: 84% final: 99%
4	MeP(O)(OH)$_2$ (2.5 mol%)	0.5	16 h: 94%

[a]From ^{1}H NMR analysis; [b] note that all starting materials were used as commercially received; [c] final refers to last measurement before sending.

Scheme 32. Polymerizations analyzed by GPC.

For the four samples broad molar mass distributions were determined with polydispersity indices PDI) ≥ 3.25 (Figure 3). The broad distributions are another indication for the radical mechanism, next to the polymer network forming (e.g. without CTA presence) and the polymerization inhibition by radical scavenger TEMPO. For the polymerization with HCl co-initiator and a lower CTA concentration (entry 1) a number-average molecular mass of $M_n = 100,000$ Da, a mass-average molecular mass of $M_w = 476,000$ Da, a z-average molecular mass of $M_z = 1,620,000$ Da and a PDI $= 4.74$ were determined. This result implied a number-average degree of polymerization[135] of $X_n = 1,406$. For the polymerization with HCl and the higher CTA concentration (entry 2) in turn average molecular weights were $M_n = 31,400$ Da, $M_w = 102,000$ Da and $M_z = 206,000$ Da, resulting in a PDI $= 3.25$ and a $X_n = 441$.

53

entry 1:
$M_w = 476000$ Da
PDI = 4.74

entry 2:
$M_w = 102000$ Da
PDI = 3.25

entry 4:
$M_w = 480000$ Da
PDI = 3.71

entry 3:
$M_w = 1010000$ Da
PDI = 4.48

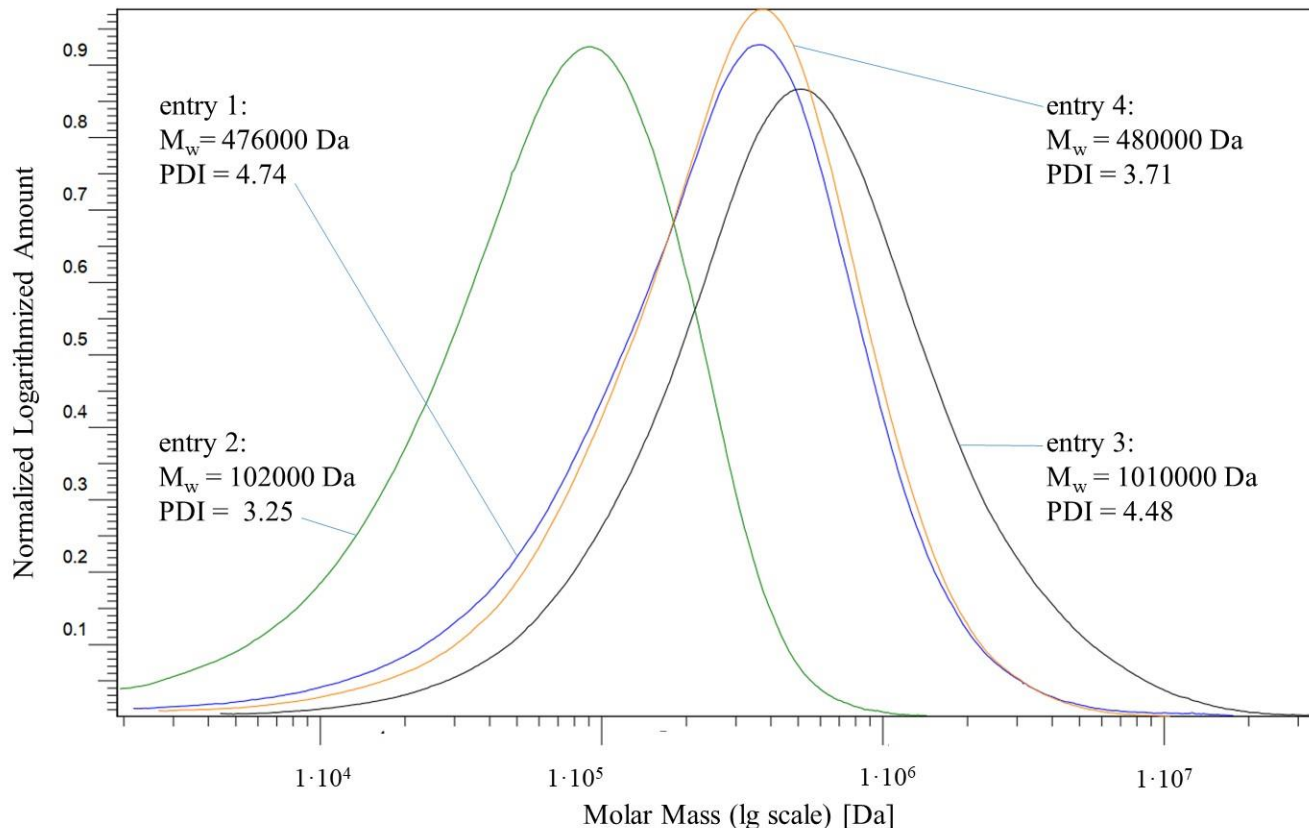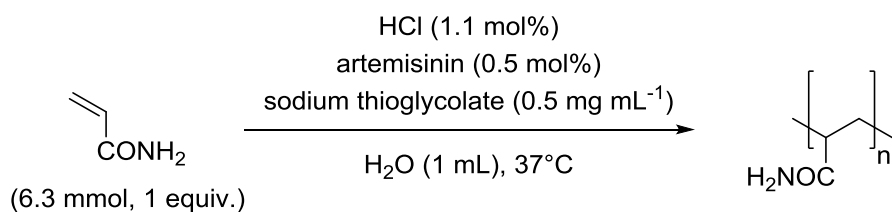Normalized Logarithmized Amount

Molar Mass (lg scale) [Da]

Figure 3. Molar mass distributions for polyacrylamides (refer to Scheme 32)

The higher concentration of CTA resulted in more rapid termination by H-donation to polymer chain ends and accordingly to lower average molecular weights and average degree of polymerization. Using *o*-benzodisulfonimide and the low CTA concentration, polymers were characterized by $M_n = 225,000$ Da, $M_w = 1,010,000$ Da and $M_z = 3,990,000$ Da, as well as by a PDI = 4.48 and a $X_n = 3,165$. Setting this side by side with results from the polymer mixture obtained with HCl co-initiator (entry 1), applying *o*-benzodisulfonimide eventuated in increased average molecular weights and number-average degree of polymerization by more than the factor 2. When using methylphosphonic acid (2.5 mol%) under otherwise unchanged conditions, the resulting polymer mixture attributed $M_n = 129,000$ Da, $M_w = 480,000$ Da and $M_z = 1,160,000$ Da, as well as a PDI = 3.71 and a $X_n = 1,814$. The general higher polydispersities suggest that the radical initiations were rather slow compared to the chain propagation and polymer chains were started not exactly at the same time.

54

3.1.3 Initiation Process with Artemisinin

From the findings, questions arose about the origin of the reactivity in this system and which tasks are occupied by the reagents, especially in the radical initiation. Here, outcomes from control experiments are presented. In Scheme 33 the standard polymerization conditions with HCl as acid are depicted and on the basis of this, experiments with deviated conditions were conducted and are listed. By replacing HCl with respective alkaline metal salts (entries 2 and 3), a reactivity based on the chloride anion could be ruled out. When leaving out either artemisinin (entry 4) or HCl without replacement (entry 5), no sign of any AM conversion could be observed.


HCl (1.1 mol%)
artemisinin (0.5 mol%)
sodium thioglycolate (0.5 mg mL^{-1})

CONH$_2$
(6.3 mmol, 1 equiv.)

H$_2$O (1 mL), 37°C

H$_2$NOC
n

entry#	deviations[b]	observation	Conversion[a]
1	TEMPO[d] additive	18.5 h: : no gel formation	18.5 h: no conversion
2[c]	NaCl instead HCl	17.25 h: : no gel formation	17.25 h: no conversion
3[c]	KCl instead HCl	17.25 h: : no gel formation	17.25 h: no conversion
4	no artemisinin	17.5 h: : no gel formation	17.5 h: no conversion
5	no acid	17.5 h: : no gel formation	17.5 h: no conversion

[a]From ^{1}H NMR analysis; [b]deviations refer to conditions: acrylamide (6.3 mmol), artemisinin (0.5 mol%), HCl (37wt%, 1.1 mol%), 1.0 mL H$_2$O, 37°C; note that all starting materials were used as commercially received; [c]sodium thioglycolate (0.5 mg mL^{-1}); [d]1.0 mol%.

Scheme 33. Control experiments for acrylamide polymerization.

In conclusion the radical initiation is dependent on both artemisinin and the acid and both co-initiators could be used in small amounts, less than 1 mol%. Although the reactions presented to this point and the previous studies in the working group might give the impression, that acid is the only co-initiator needed, there is no precedent of radical formation from artemisinin effected by acid in literature. In reports that describe reactions of artemisinin and acid, heterolytic transformations were outlined to rationalize product formations by rearrangements and hydrolysis.[136] Artemisinin's radical chemistry is in most scientists opinion connected to Fe based activation (see chapter 1.3). In order to check if Fe species on impurity level were involved, deferoxamin (DFO), an Fe chelator, was added to the successful polymerization conditions with HCl (entry 1), methylphosphonic acid (entry 2) and o-benzodisulfonimide (entry 3, Scheme 34).
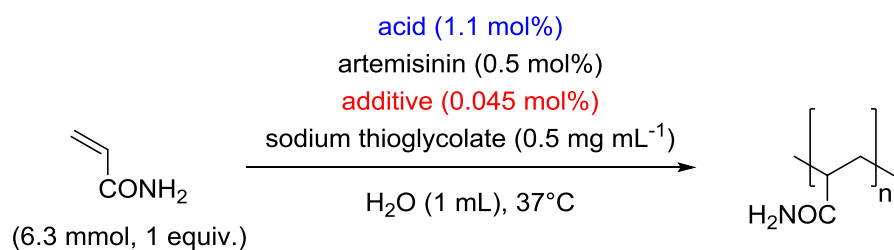
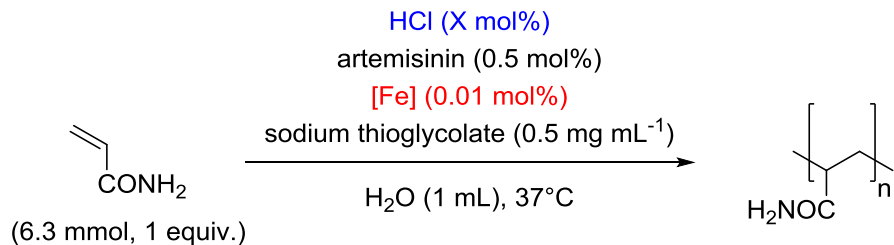| entry#	additive[b]/acid[c]	observation	Conversion[a] (PAM/AM)
1	DFO / HCl	20 h: no gel formation	20 h: no conversion
2	DFO / MeP(O)(OH)$_2$	20 h: no gel formation	20 h: no conversion
3	DFO / o-benzodisulfonimide	20 h: no gel formation	20 h: no conversion
4	HCl (tmg)	3 h: no gel formation	3 h: <5% conv.
		20 h: gel	20 h: 17% conv., (0.0333:1)

[a]From ^{1}H NMR analysis; [b]0.045 mol%; [c]1.1 mol%; DFO = deferoxamine, tmg = trace metal grade, PAM = polyacrylamide, AM = acrylamide.

Scheme 34. Reducing Fe concentration in acrylamide polymerization.

In consequence, in all three cases the polymerization was inhibited. The DFO experiments enlightened that for the successful radical initiation an Fe species had to be present. Complexation of this co-initiator, prevented the reaction. This rose the question, if the acids were obligatory for the initiation to proceed, if they had a function on their own or if certain

commercial acids deliver immanent potent Fe species, which were the actual co-initiator. At first instance, this question was addressed by using a highly pure HCl, so-called trace metal grade (tmg, entry 4, Scheme 34). While the commonly used HCl of ACS grade was specified with 0.2 ppm Fe impurities, the one used of tmg was specified with less than 1 ppb Fe. Using the latter in the polymerization showed that the polymerization proceeds, but slower, with 17% conversion after 20 h (compared to 89% after 17.5 h with ACS grade purity). This suggested that the reagent mixture of acrylamide, sodium thioglycolate and artemisinin contained some Fe impurities. It is legit to assume that the HCl of tmg should lead to higher purity (in regard of Fe) reaction mixtures than most evaluated polymerization attempts with acids of standard purity quality (see Scheme 29, Scheme 30 and Scheme 31). By this, it stood out, that in the described system HCl bears a feature, which enables the radical initiation from artemisinin with trace amounts of Fe present in contrast to most other acids. Investigating the potency of Fe in this system, the polymerization was studied applying $Fe(SO_4)_2$ as a homogeneous and Fe_2O_3 as a heterogeneous alternative (Scheme 35). Fe_2O_3 was also chosen, because it is a common Fe impurity under air conditions and potentially could be partially dissolved in aqueous media effected by strong acids. In reactions with $Fe(SO_4)_2$ the Fe species was added as freshly prepared stock solution to the mixture. Fe_2O_3 was directly weighed-in in the corresponding reactions.

The experiments implementing the external Fe species and no HCl (entries 1 and 4, Scheme 35), showed no conversion of monomer after 20 h. From these results, it was possible to deduce that also a fairly higher catalytic amount of homogeneous or heterogenous Fe (0.01 mol% in respect to AM, 2 mol% in respect to artemisinin) was incapable to start the polymerization in the system together with only artemisinin. In experiments, in which the same amount of additional Fe species was applied together with HCl (1.1 mol%, entries 2, 3, 5 and 6, Scheme 35), the conversion of AM to homopolymers was achieved. Here it is to mention, that the conversions differ from the reaction without additional Fe (after 3 h, as well as after 20 h). The Fe thereby showed an impact in the reaction and the reaction conditions were, regarding the AM conversion, more suited for the smaller amounts of Fe, brought as reagent impurities into the reaction mixtures. Interestingly, in certain experiments (entries 2, 5 and 6) no conversion after 3 h was observed, but convenient polymer formation after 20 h (56%, 59% and 71% conversion, respectively). The radical initiation seemed to comprise an induction period.

Scheme conditions:
HCl (X mol%)
artemisinin (0.5 mol%)
[Fe] (0.01 mol%)
sodium thioglycolate (0.5 mg mL^{-1})
H$_2$O (1 mL), 37°C

CONH$_2$ (6.3 mmol, 1 equiv.) → polymer (H$_2$NOC ...)$_n$

entry#	external Fe (mol%)	HCl (mol%)	observation	Conversion (PAM/AM) [a]
1	Fe(SO$_4$)$_2$·7H$_2$O (0.01)	-	20 h: no gel formation	20 h: no conversion
2	Fe(SO$_4$)$_2$·7H$_2$O (0.01)	1.1	20 h: mostly jelly	3 h: no conversion 20 h: ~56%., (1.02/1)
3	Fe(SO$_4$)$_2$·7H$_2$O (0.01)	1.1 (tmg)	3 h: gel-jelly 20 h: gel-jelly	3 h: ~37% , (0.25/1) 20 h ~89% , (7.3/1)
4	Fe$_2$O$_3$ (het., 0.01)	-	20 h: no gel formation	20 h: no conversion
5	Fe$_2$O$_3$ (het.,0.01)	1.1	3 h: no gel formation 20 h: gel	3 h: .no conversion 20 h: ~59%, (0.24)
6	Fe$_2$O$_3$ (het., 0.01)	1.1 (tmg)	20 h: gel	3 h: .no conversion 20 h: ~71%, (0.52/1)

[a]From ^{1}H NMR analysis; het. = heterogeneous, tmg = trace metal grade, PAM = polyacrylamide, AM = acrylamide.

Scheme 35. External Fe co-initiators.

The participation of Fe species in the polymerization of MMA could be anticipated. This should be investigated in the future.

3.1.4 Analysis of the Polymerization System by EPR Spectroscopy

Several approaches were pursued to trap formed radicals based on the artemisinin (0.05 mol)/HCl system with trace amounts of Fe species present in (partially) aqueous media. The use of slightly overstoichiometric acrylamide (referring to artemisinin and HCl) alone or in combination with styrene failed to produce identifyable formed species. When using an organic reagent like styrene, the polar medium prevented homogenization of the mixture, an inconvenience that potentially contributed to unreactive styrene in these approaches. In addition, methanol as co-solvent proved in the case of styrene to bring about no particular solubility improvement in the acidified mixtures. When using purely methanol as solvent, it had been proven that the underlying polymerization of acrylamide with the use of aqueous HCl or acetyl chloride and artemisinin could not be realized. Methanol was not a beneficial solvent for the trapping experiments with acrylamide and/or styrene.

Initial experiments based on radical addition (from HCl/artemisinin) to C–C(N) multiple bonds (1,1-diphenylstyrene, acrylamide, phenylacetylene or pTsCN) and trapping adducts with certain reagents (TEMPO, BHT, pTsCN or 1-phenyl-1-trimethylsiloxyethylene) in water/MeOH mixed or aqueous media (at 37 or 55°C) were unsuccessful in terms of forming an isolatable product. Some cases thereof also suffer from bad homogenization (pTsCN and phenylacetylene especially). Further, experimental strategies to synthetically trap radicals were based on the addition of lepidine or pyrrole to a mixture of artemisinin/HCl in an organic solvent (MeCN, THF, DMA, DMF, MeOH, PhH, DCM) at 37 or 55°C. In these procedures, sketched to perform reactions of Minisci-type[137], the heteroarenes were hardly reacting and the only product that could be isolated was a trimerization product of pyrrole (2,5-di(1H-pyrrol-2-yl)pyrrolidine, y = 0.05% from 2 mL pyrrole with 20 μL HCl, (30 mg artemisinin) at 37°C, 17 h).[138]

Since the radical initiation in the system has proven to be reliant on a complex interplay between acid, Fe species and artemisinin and these co-initiators were used in small quantities, a synthetic way of identifying involved radicals in the polymerization transpired as a difficult task. In addition, the conversion of artemisinin was never completed in any polymerization nor in executed radical trapping experiments, which reduced the amount of stoichiometric formed radicals produced by the system.

An alternative way to get insight in the present radicals, was the observation of corresponding reaction mixtures by *electron paramagnetic resonance* (EPR) spectroscopy. This analysis was carried out by Dr. Shannon Bonke and Dr. Sonia Chabbra from the working group of Dr. Alexander Schnegg at MPI für Energiekonversion in Mülheim an der Ruhr, Germany.

In a first attempt, a standard polymerization mixture adapted from my research towards EPR spectroscopic conditions was analyzed. To a dispersion, consisting of artemisinin (9 mg, 0.032 mmol, 0.5 mol%) and sodium dodecylsulfate (100 mg) in water (930 µL), acrylamide (450 mg, 6.3 mmol, 1 equiv.) and an aqueous stock solution of HCl (1 M, 70.6 µL, 0.071 mmol, 1.0 mol%) were added. After a brief heating at 40°C, ~50 µL of the dispersion was transferred into an EPR tube (o.d. 1.6 mm). The measurement was conducted at 40°C over the weekend, but no signal could be detected (for more details on EPR measurements, see chapter 5.1).

In another attempt, they setup a mixture of artemisinin, sodium dodecalsulfate, 5,5-dimethylpyrrolidinone-*N*-oxide (DMPO) and HCl in water by following the above description with replacing acrylamide by the addition of DMPO (5 µL, 0.045 mmol, 0.7 mol%) instead. After a short warming phase at 40°C, ~50 µL of the mixture was transferred into an EPR tube (o.d. 1.6 mm). The measurement was again undertaken at 40°C.

Within 12 min a signal consisting of 4 lines of intensity ratio 1:2:2:1 (quartet) emerged (Figure 4b). By simulation, the corresponding Hamiltonian parameters were adapted as $g_{iso} = 2.0062$, $^{H}A_{iso} = 41.1$ MHz and $^{N}A_{iso} = 41.0$ MHz ($B_0 = 337.5$ mT, field sweep of 15 mT). The resonance spectrum and parameters were in accordance to a reported spectrum of DMPO/HO• spin adduct.[139] Within 30 min the signal decreased and was overlayed (Figure 4a) by a 6 line signal with all equal relative intensity (sextet, marked with asterisk in Figure 4a, deconvoluted in Figure 4c). In the simulation the Hamiltonian parameters were adapted to $g_{iso} = 2.0061$, $^{H}A_{iso} = 58.2$ MHz (20.7 G) and $^{N}A_{iso} = 43.2$ MHz (15.4 G).
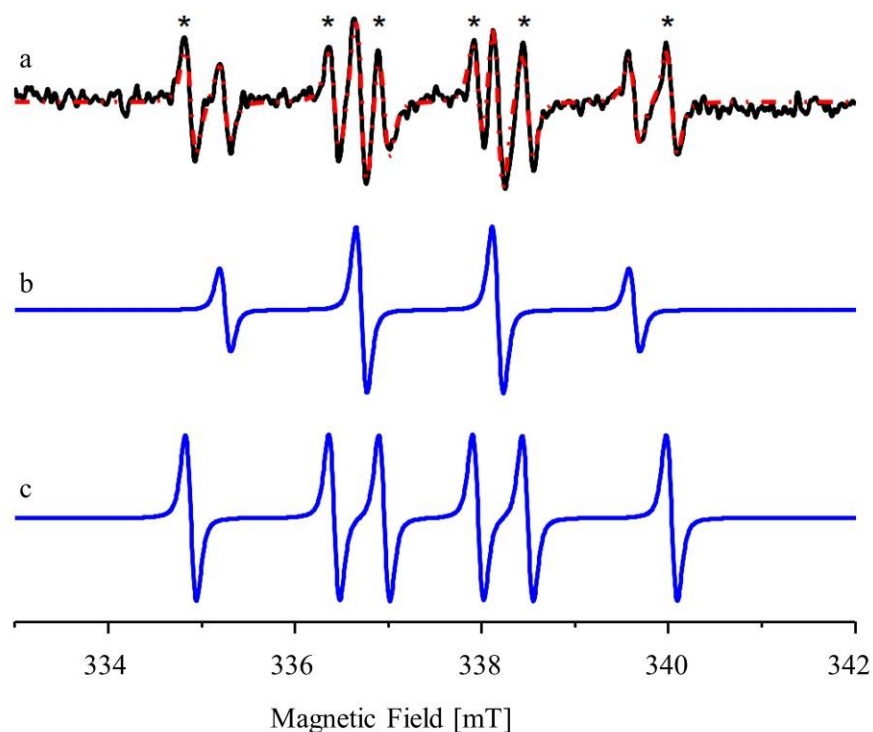
Figure 4. EPR spectrum of DMPO spin trapped radicals in artemisinin/HCl/[Fe]-system after 70 min at 40°C (black) with simulation (red) and deconvolution (blue).
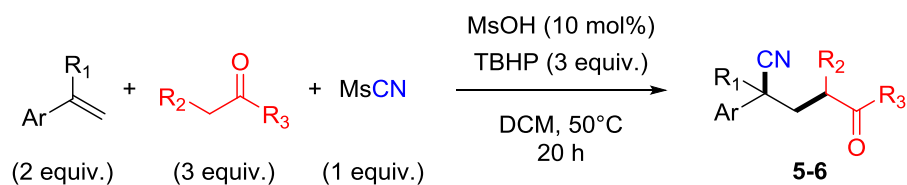
The used parameters g-factor and hyperfine coupling constants and an intensity ratio of 45%:55% (DMPO/HO·:DMPO/R·) were in good accordance to the measured spectrum. In regard of literature reports, there is to the best of our knowledge so far no clear equivalent to identify the DMPO/R· spin adduct. In an overview article[140] on DMPO spin trapped radicals, hyperfine coupling constants for α-hydroxyethyl (in water, $^H A_{iso} = 15.8$ G, $^N A_{iso} = 22.8$ G)[141] and *tertiary* β-valinyl (in water, pH = 7.4, $^H A_{iso} = 15.5$ G, $^N A_{iso} = 20.0$ G)[142] radicals could be considered as closest related examples to the ones causing the above spectrum.

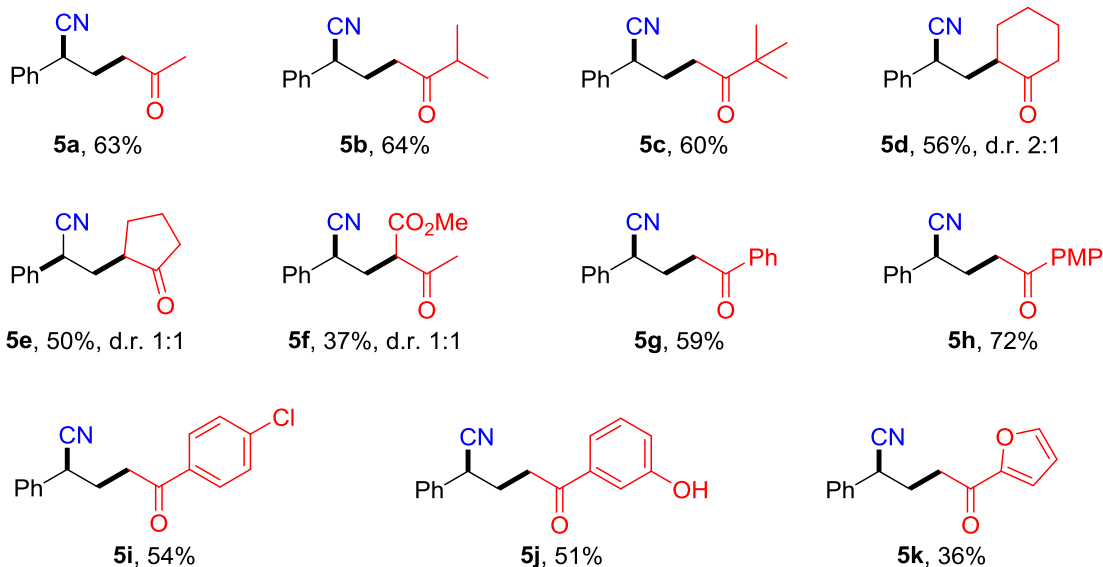## 3.2 Radical Alkene Difunctionalizations with Ketone-derived and Cyanidyl Radicals

The reaction of alkenes with α-ketonyl and cyanidyl radicals to form γ-cyanoketones was discovered by Dr. Wen Shao during his time in the Klußmann group. My contributions were in support of the project progress during his time in the group and after his departure for achieving project completion. Results presented in this chapter were partially published before and thus, the following contains discussions of the same meaning (Ref [1]).

### 3.2.1 The Technique and Vinylarene Applications

In the synthetic methodology for generating γ-peroxyketones (see Scheme 8)[3], α-ketonyl radicals were formed from ketones by Brønsted acid-catalysis in the presence of TBHP. The generation of these ketone-derived radicals under acidic conditions was suggested to proceed via condensation of ketone and TBHP forming an intermediary alkenyl peroxide. The O–O bond cleavage of such an unstable species[51] would release the α-ketonyl radical as well as a *tert*-butoxyl radical.[3] TBHP is also engaged by the latter in a HAT reaction to generate *tert*-butyl peroxyl radical and *tert*-butanol.[52] In this section the described procedure is referred as alkylation-peroxidation. From this point, a goal in the Klußmann group was to find an alternative alkene difunctionalization technique, that implements the use of α-ketonyl radicals together with another radical. A challenge in finding a new application by so formed α-ketonyl radicals, was to add a further radical (source) to this multicomponent system, which on the one hand would be kinetically inferior to the α-ketonyl radical in the addition to alkene double bonds under suitable conditions. On the other hand, this radical (source) needed to be kinetically competitive to the *tert*-peroxyl radical in combining with the intermediary transient ketonyl-radical-alkene-adduct. When TEMPO was applied on the initial alkylation-peroxidation procedure with acetone and styrene, the peroxidation product was not formed, but neither the benzyl radical nor the ketonyl radical was verifiably trapped.[3] Also a quite persistent radical could fail the task in such a multi radical mixture.
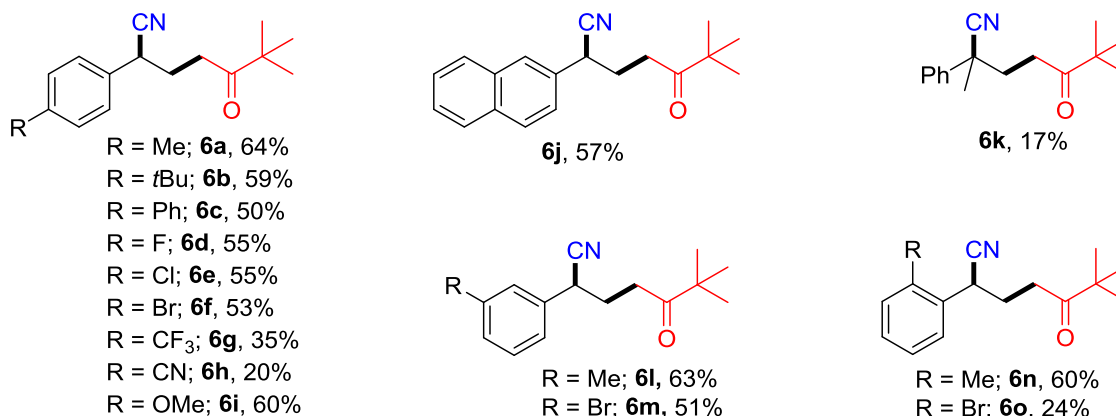
Scheme 36. Addition of ketones and cyanide to vinylarenes (W.S.).

Dr. Wen Shao (W.S.) found that with sulfonyl cyanides a benzylic cyanation was superior to the peroxidation. Mesyl cyanide (MsCN) was synthesized by oxidation of methyl thiocyanate.[59] The sulfonyl cyanide was used as limiting reagent with 2 equiv. of styrene and 3 equiv. of each ketone and TBHP. The best results were found for a 0.25 mmol scale reaction in DCM (1 mL) at 50°C using MsCN as substrate and MsOH (10 mol%) as acid catalyst (Scheme 36). This technique is in this section referred to as alkylation-cyanation. For *p*TsCN as cyanation reagent in the reaction of

acetone with styrene utilization of solvents EtOAc, *i*PrOAc and DCE delivered comparable, but slightly lower product yields. Side-products were the corresponding peroxidation product and difunctionalization products incorporating the mesyl (sulfonyl) radical at the less substituted end of the styrene double bond together with the *tert*-butylperoxyl radical at the adjacent carbon atom of the alkene.

3.2.2 Behavior of Aliphatic Alkenes in Radical Alkylation-Cyanation

Seeing the approach of my coworker, I (M. L.) was in terms of the ketone scope interested in the fact that the use of cyclohexanone (**5d**) resulted in the expression of a (certain) diastereoselectivity in contrast to cyclopentanone (**5e**). Substrate methyl 3-oxo-1-butoxylate (**5f**) could not lead to a diastereoselective reaction. Yet, the reaction of another small open-chain ketone, without the extra functional group in comparison to **5f**, was investigated (Scheme 37).
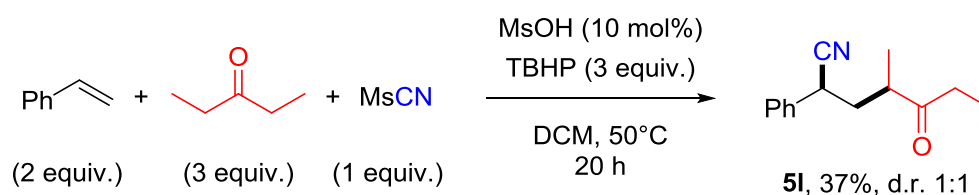

Scheme 37. 3-Pentanone in the alkylation-cyanation of styrene (M.L.).

In my first contribution to the project, 3-pentanone was added to the ketone scope for styrene difunctionalization (**5l**). The reaction featured no diastereoselectivity, but the products could be separated by column chromatography (silica, eluent: hexane/EtOAc v/v = 7/1). In sum the four examples (**5d**-**5f**, **5l**) stated, that for the addition of small ketone based *secondary* radicals, the cyanation did not run with a particularly face discrimination on the radical-styrene-adduct. The cyclohexanone product **5d** gave a hint, that a little more expanded and spatial substitution could already trigger a diastereodiscrimination in the cyanation process. In further investigations on this topic, I contributed especially in the diastereomer separation from each other and identification by NMR analysis (see section 3.2.3).

A target that was attractive for me to tackle, was the alkylation-cyanation of aliphatic alkenes (Scheme 38). We found that the same reaction conditions as for vinylarene substrates were suitable to perform the alkylation-cyanation on less stabilized alkenes. I first made approaches in investigating demanding monosubstituted alkenes in the procedure. 6-cyanohex-1-ene (**7a**, 58%), 5-methylhex-1-ene (**7b**, 18%) and 5-bromopent-1-ene (**3c**, 23%) were evaluated successfully in

the method. In addition (*R*)-limonene was successfully difunctionalized at the exo-cyclic double bond (**7d**, 22%, d.r. = 1:1), showing that also natural occurring terminal alkenes have potential to be functionalized by this technique.
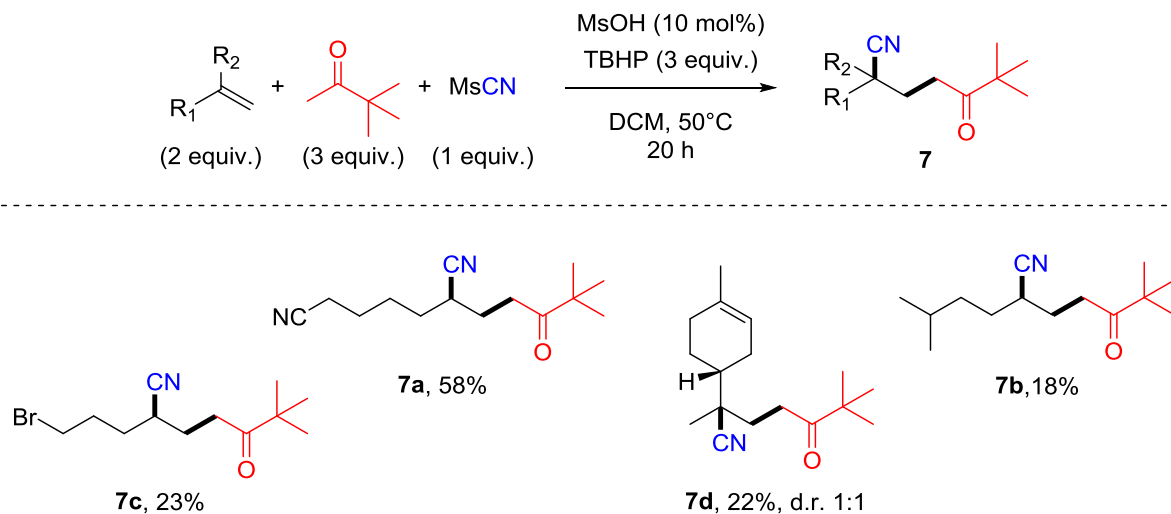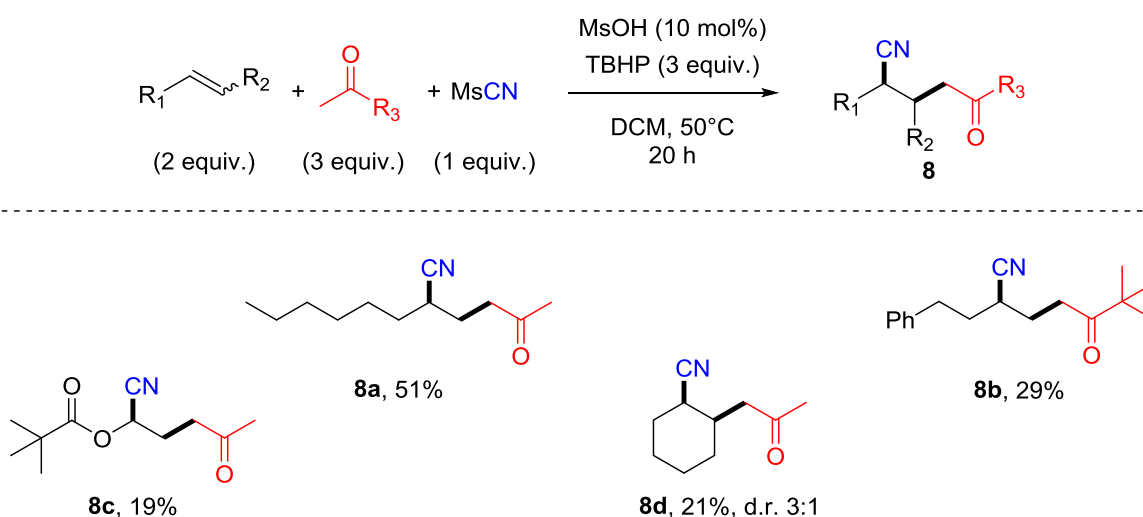

Scheme 38. Alkylation-cyanation of aliphatic alkenes (M.L.).

In contrast to the use of vinylarenes, the crude NMR mixtures did not reveal diagnostic signals for the formation of these difunctionalization products. The α-cyano proton resonances were in the conducted cases shifted upfield compared to vinylarene-derived analogues and overlayed by signals of aliphatic protons. Analyzing crude reaction mixtures for product formation and for finding product separation methods, the thin-layer chromatography (TLC) was used and a stain needed (with acidic ceric ammonium molybdate solution). During these reaction examinations, it was observed that the reaction mixtures of aliphatic alkenes contained less product species of significant amount. It was of special interest that the sulfonylation-peroxidation side-products could not be found from the reaction mixtures (neither by TLC, nor by fraction collection at suspected elution volumes during chromatography).

Compared to styrene substrates, the addition of radicals to aliphatic alkenes features a lower ΔG profile.[39] For sulfonyl radical additions, this difference in free Gibbs energy (and activation energy) is of relative low magnitude anyway.[143] The use of aliphatic alkenes could lead in this alkylation-cyanation system to a relative enhancement of sulfonyl radical cleavage rate from the radical-alkene-adduct compared to the α-ketonyl radical cleavage from the corresponding radical-alkene-adduct. The rate for the alkylation-cyanation could therefore be increased relatively to the sulfonylation-peroxidation.

Dr. Wen Shao added further aliphatic alkenes to the reaction range (Scheme 39). He found that hex-1-ene (**8a**, 51%), 4-phenylbut-1-ene (**8b**, 29%), vinylpivalate (**8c**, 19%) and cyclohexene (**8d**, 21%, d.r. = 3:1) could be used. Common for the use of aliphatic alkenes in the alkylation-cyanation was a lower yield. A possible reason for this could be the lower thermodynamic advantage in radical additions to aliphatic alkenes, synonymously for a more reactive radical-alkene-adduct intermediate. However, alternative product formation of the more reactive intermediates could not be observed.

Scheme 39. Further aliphatic alkenes suitable for alkylation-cyanation (W.S.).

66

As mentioned all alkylation-cyanation procedures with aliphatic alkenes led to less on TLC observable species. For rationalization, this could mean that the reactive intermediates were not particularly selective in their reaction path under the reaction conditions and quite low concentrations of numerous indistinct products were present in the reaction mixture after consumption of the alkene. Reactions of further aliphatic alkenes were conducted in accordance to the procedure, but led to no distinct observable reaction products at all (Scheme 40).
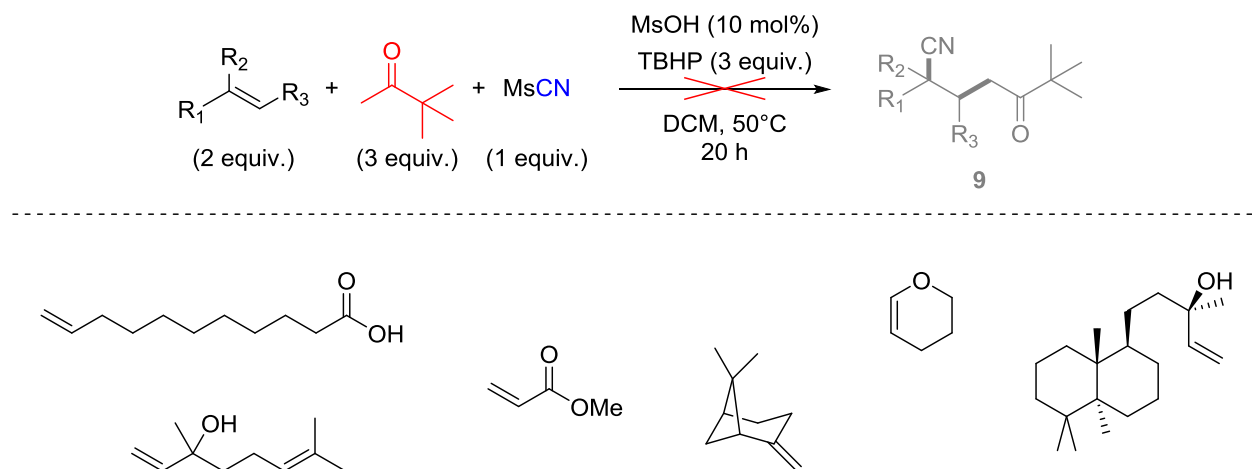
Scheme 40. Unsuccessful aliphatic alkenes in alkylation-cyanation methodology (M.L.).

Dr. Wen Shao found more substrates to be inconsistent with the method (see Supporting Information Ref. [1]). Possible reasons for the limitations could originate from effects on the radical addition, different reactivities of intermediary radical-alkene-adducts, like inter- or intramolecular HAT processes, oligomerizations or radical scissions. From the structure of the respective aliphatic alkenes no obvious characteristic or feature could be used to deduce or predict if the consecutive addition of α-ketonyl and cyanidyl radical could be accomplished.

3.2.3 Diastereomer Identification and Comparison on Diastereoselectivity

Dr. Wen Shao could show that more complex steroid based ketones like epiandrosterone (for **10**) and pregnenolone (for **11**) were viable ketone substrates in the technique (Figure 5). The reactions proceded not with a particular diastereoselectivity, mixtures with two diastereomers each were isolated (d.r. determined from crude reaction mixtures).
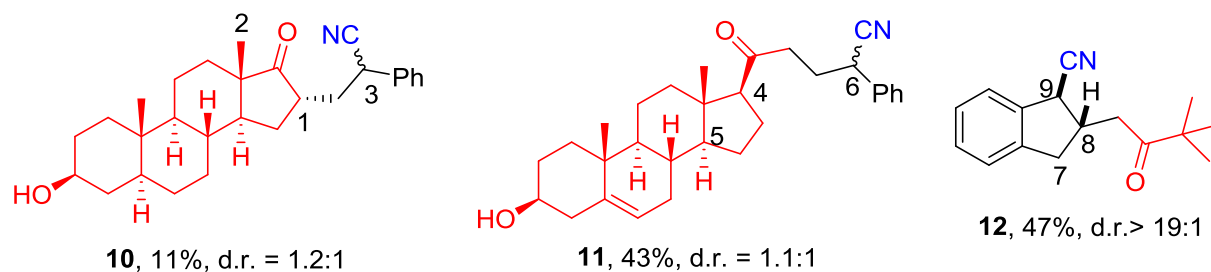

Figure 5. Application of more complex ketones and alkenes (W.S.).

A NOESY NMR experiment (M.L.) showed for both diastereomers of **10** a cross signal of the proton at α-carbonyl position (no. 1) with the methyl group protons (no. 2) at the other α-carbonyl position. The proton should therefore have the same spatial orientation as the methyl group on the cyclopentanone ring, which gives a total (*S*) configuration for both diastereomers at α-positioned center (no. 1) of the γ-cyanoketones. Thus, the isolated diastereomers differ in the configuration at the cyanide bearing carbon atom (no. 3).

For the isolated diastereomers of **11** a NOESY NMR experiment (M.L.) revealed for one diastereomer, that the proton at carbon no. 4 is oriented to the same side as proton no. 5. The relative low difference between the chemical shifts of carbons no. 4 (125 MHz, CDCl$_3$, 63.14 vs 62.94 ppm) suggested the same configuration for both diastereomers at this atom. An epimerization was not assumed or observed and the diastereomers differ in their configuration at the cyanide bearing carbon no. 6.

For the difunctionalization of indene with pinacolone in contrast, a much more diastereoselective reaction was achieved (d.r. > 19:1, **12**). In fact, only one diastereomer was isolated (W.S.). A NOESY NMR experiment (M.L) showed cross signals between the proton at carbon no. 9 to one proton at no.7 and between the opposing proton at no. 7 to the proton at no. 8. In total, a *trans* orientation of the cyano group to the ketone bearing substituent on the cyclopentene ring was suggested in product **12**.

Changing the ketone to cyclohexanone in the alkylation-cyanation process led again to low diastereoselectivity (d.r. = 1.6:1, **13**, W.S.). Similarly, the NOESY NMR experiment (M.L.) showed that protons at carbon no.1 and carbon no 2 (Scheme 41) exhibited stronger or exclusively cross signals to one proton at carbon no. 3 in both diastereomers. The protons at no. 1 and no. 2 showed these cross signals to the opposed protons of no. 3 compared to each other. The two diastereomers featured therefore *trans* orientated cyano group and ketone bearing substituent on the cyclopentene ring.
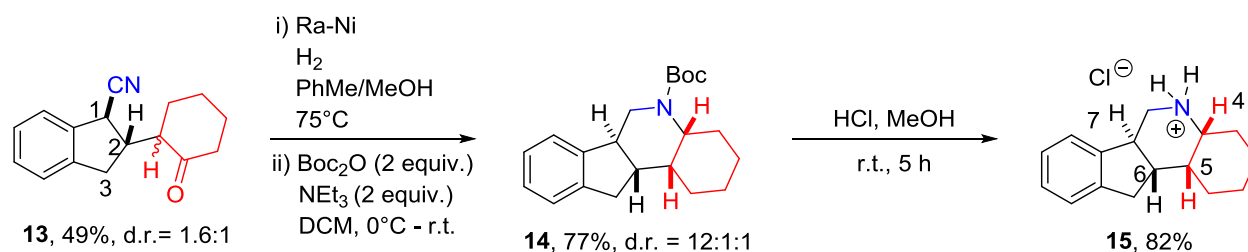
Scheme 41. Hydrogenation-cyclization sequence of γ-cyanoketone **13** to piperidine **14**.

Dr. Wen Shao transformed product **13** by a reaction sequence of hydrogenation and Boc-protection to the tetracyclic piperidine **14** in a 77% yield. The product mixture showed a d.r = 12:1:1 (Scheme 41). To confirm the relative configurations of the stereogenic centers of the major diastereomer, the hydrochloride **15** was targeted by a deprotection in acidic medium (M.L.). The hydrochloric salt of the amine precipitated from the reaction mixture (y = 97%) and after a recrystallization from methanol/Et$_2$O, crystals suitable for X-ray diffractometry were obtained (y = 82%). ^{1}H NMR analysis of the hygroscopic crystals revealed that just one diastereomer was incorporated in the crystal lattice. In regard of the yield this diastereomer should be derived from the major diastereomer of **14** and thus should exhibit the same relative configurations of the stereogenic centers. Crystallographic data revealed that the unity cell contained both enantiomers of the diastereomer in a monoclinic system of P2$_1$/n space group. Torsion angles of one enantiomer over 4 atoms (3 bonds) were determined as α[H(4)-H(5)] = - 56.3°, α[H(6)-H(5)] = 52.1°, α[H(7)-H(6)] = 175.6° (see **15**, Scheme 41, for numbering). This expressed a *cis* (*syn-clinal*) relation between protons no. 4 and no. 5, as well as no. 5 and no 6. Protons no. 6 and no. 7 are *trans* oriented relative to each other.

Dr. Wen Shao showed that the analogous hydrogenation-Boc-protection-sequence generated piperidines **16** from alkylation-cyanation product **5h** in 81% yield (Scheme 42).
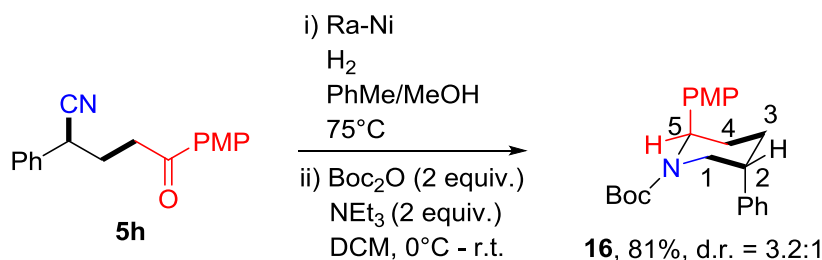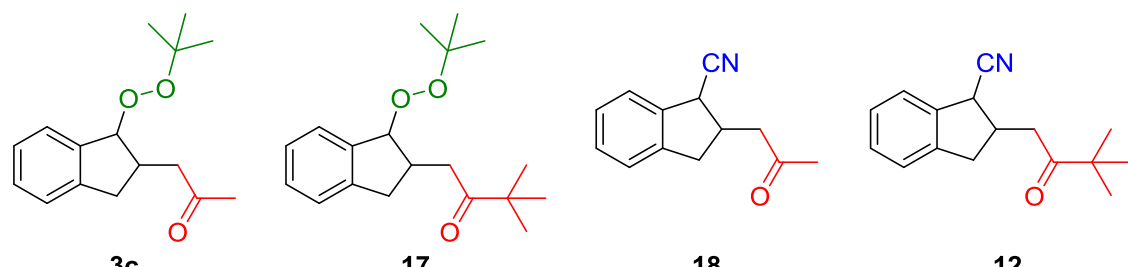

Scheme 42. Piperidine formation by cyclizing of alkylation-cyanation product **5h** (W.S.).

From the isolated diastereomer mixture ¹H NMR coupling constants and a NOESY experiment (M.L.) were used to determine the relative configurations at carbons no. 2 and no. 5 in the major diastereomer. The proton at carbon no. 5 showed two $^3J^{\text{H-H}}$ coupling constants of 4.6 Hz in ¹H NMR (CDCl₃), indicating a *syn-clinal* relation to both protons connected to carbon no. 4. This stated an equatorial orientation of the proton no. 5 in the major diastereomer. This equatorial orientation on the piperidine ring sets an axial orientation for the *p*-methoxyphenyl (PMP) substituent at carbon no. 5. NOESY cross signals of the proton at carbon no. 2 with all neighboring protons suggested also an equatorial orientation. Consequently, both aryl substituents on the piperidine ring were assigned as axial oriented and relative *trans* to each other.

The circumstance that both relatively bulky aryl substituents were oriented in axial position in the major diastereomer was further investigated with a DFT (TPSS functional, 6-311, G(d,p) basis set) calculation in consideration of chloroform (IEFPCM) continuum model in cooperation with PD Dr. Martin Breugst. The axial-axial aryl substituents chair conformation was a result of lower energy in comparison to equatorial-equatorial chair conformation ($\Delta\Delta G = 3.3 \text{ kJ mol}^{-1}$) and considerable boat conformations ($\Delta\Delta G \geq 7.1 \text{ kJ mol}^{-1}$). Rationalization of the findings were the steric repulsion avoidance between the Boc substituent and the PMP substituent aside from an energy lowering interaction of the nitrogen lone pair with an antibonding σ* orbital based around carbon no. 5 to the connected PMP substituent.

In contrast, the apparent occurrence of a significant diastereodiscrimination in this alkylation-cyanation procedure was not a feature of the related alkylation-peroxidation procedure[3] via alkenyl peroxides. When looking at the highest diastereoselectivity among the performed alkylation-cyanations, for substrates indene and pinacolone a d.r. > 19:1 was achieved (**12**). The scope of the alkylation-peroxidation methodology bore as closest comparable product, one that was formed from indene and acetone **3c**. This reaction yielded two diastereomers with a d.r. = 1.5:1.[3] In order to have a more reliable comparison between these two techniques, the alkylation-peroxidation[3] of indene was carried out with pinacolone (**17**) and the alkylation-cyanation[1] of indene was carried out with acetone (**18**) as ketone, respectively (M.L., Figure 6).

During the reactions leading to structures **17** and **18**, each reaction formed two diastereomers (à two enantiomers). In both cases, these could be separated from each other by column chromatography (see chapter 5 for details). NOESY NMR experiment (see chapter 5.5) analysis for the separated diastereomers indicated that for both structures the major diastereomer exhibited a relative *trans* relation between the substituents that were added across the double bond during the reaction.

Structure	y (*trans*) [%]	y (*cis*) [%]	y (total) [%]	d.r. (NMR)	d.r. (HPLC/GC)	Ref.
3c			59	1.5:1		3
17	34	14	48	1.7:1	1.73:1 (HPLC)	
18	54	23	77	3.6:1	3.26:1 (GC)	
12	47		47	>19:1		1

d.r. were determined from crude reaction mixtures.

Figure 6. Comparison of diastereoselectivities of bezylic peroxidation vs. cyanation.

For structure **17** the products were in sum yielded in 48%, for product **18** in 77%, respectively. For structure **17** ^{1}H NMR and high performace-liquid chromatography (HPLC, UV/Vis detection) analysis of the crude reaction mixture reflected a ratio of 1.7:1 and 1.73:1, respectively, for the two distinguishable diastereomers (for details see chapter 5.6). In respect to the known structure **3c** (d.r. = 1.5:1) the use of pinacolone instead of acetone lead to a small change in diastereomeric ratio. The use of sterically more demanding pinacolone resulted as expected in a higher diastereoselectivity in the peroxidation process.

For structure **18** ^{1}H NMR and gas chromatography (GC) analysis of the crude reaction mixture derived a ratio of 3.6:1 and 3.26:1, respectively, for the two distinguishable diastereomers (for details see chapter 5.6). For the use of acetone, the alkylation-cyanation disclosed a more than doubled diastereomer ratio, an increase in diastereoselectivity in comparison to the alkylation-peroxidation of indene (3.6:1 (**18**) vs 1.5:1 (**3c**), see also 2:1 for **5d** vs 1.2:1 for corresponding peroxidation product[3]).

The use of pinacolone instead of acetone resulted in a much stronger effect on diastereoselectivity for the alkylation-cyanation (>19:1 (**12**) vs 3.6:1 (**18**)) than in correlation to the alkylation-peroxidation.

From the observations in the alkylation-cyanation, the trends pointed towards the assumption, that especially internal alkenes could have the potential of generating a diastereoinducing environment for the cyanation process on the radical-alkene-adduct. After Dr. Wen Shao found that *trans*-stilbene was not a suitable substrate for the methodology, attempts to difunctionalize benzofuran and 1,2-dihydronaphthalene neither resulted in alkylation-cyanation.

3.2.4   Mechanistic Models

In contrast to the alkylation-peroxidation, the alkylation-cyanation procedure revealed by direct visual observation the generation of water during the reaction (separation in DCM). This gave another evidence for a condensation process in a main reaction path.

From the observations and analogies to the reported radical addition of ketones and peroxides[3], a reaction mechanism could be proposed. Brønsted acid catalyzed condensation of ketone and TBHP leads to an unstable alkenyl peroxide intermediate **I3** which by fast O–O bond cleavage

forms a resonance stabilized α-ketonyl radical **I4** (and *tert*-butoxyl radical). The alkyl radical adds to the alkene, resulting in a benzyl radical **I5** (Scheme 43).
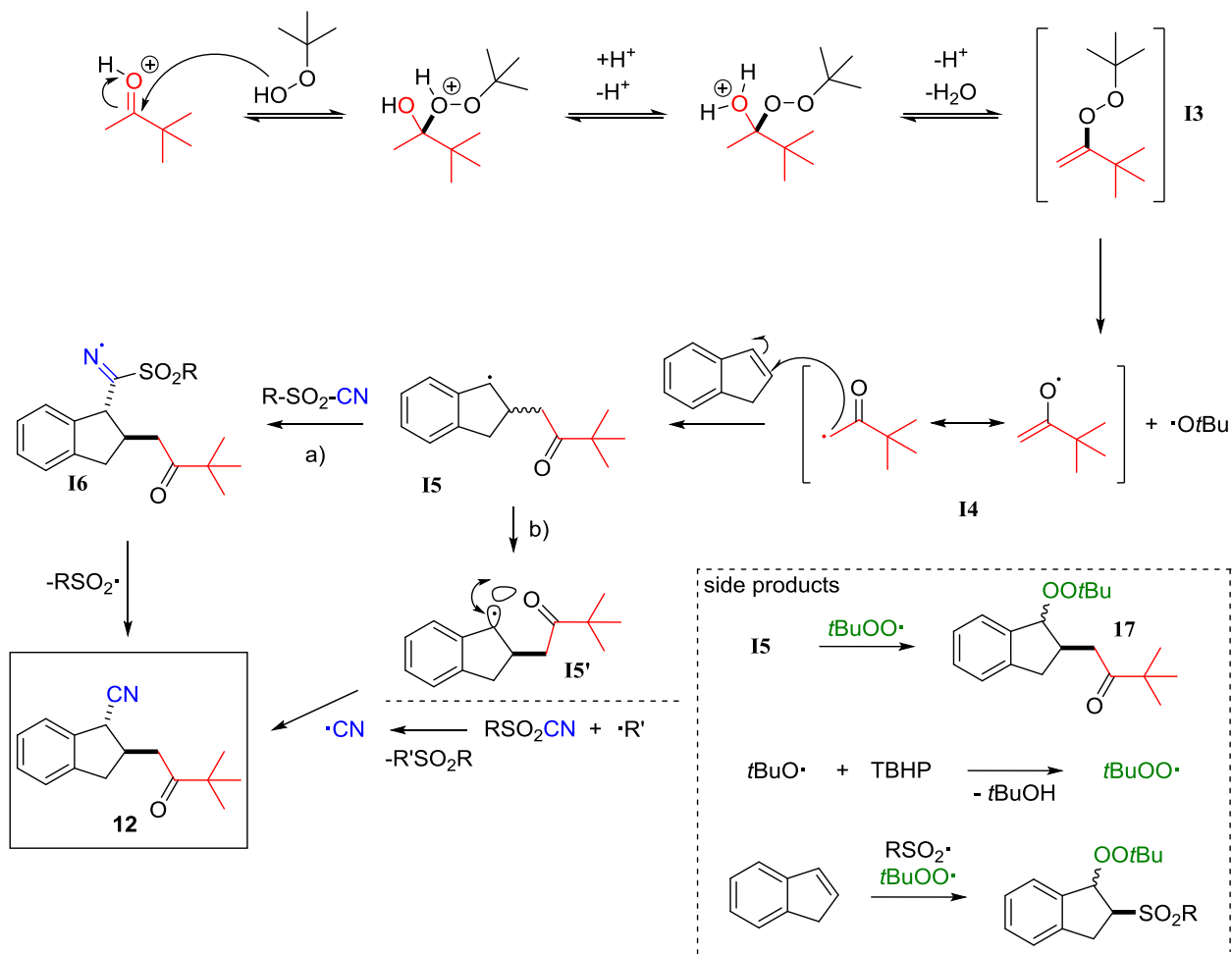
Scheme 43. Mechanistic models for radical addition of ketones and cyanide to alkenes.

Although the technique of alkylation-cyanation was not delivering high diastereoselectivites on a general basis, it was remarkable, that even some reactions with small substrate acetone presented higher d.r. than all known examples of peroxidations from the alkylation-peroxidation method. It was especially compelling and unexpected, that the alkylation-cyanation of indene with pinacolone practically resulted in the isolation of just one diastereomer. The question for the grounds of this diastereoselectivity differences between the alkylation-cyanation and the alkylation-peroxidation ultimately gives room for theories on differences in the reaction mechanisms. When regarding the peroxidation step, a low selectivity on which face a sp^2-hybridized benzyl radical intermediate **I5** combines with a rather pointy *tert*-butyl peroxyl

radical, appeared reasonable and justified this consideration a valid model. For the cyanation however, the small sized cyanidyl radical gives alone no expectation that the corresponding radical-radical-combination proceeds more biased.

The benzyl radical intermediate **I5** could add to the C–N triple bond of the sulfonyl cyanide (Scheme 43a).[144] The so formed iminyl radical **I6** centers in β-position to the sulfonyl group, which represents a homolytic leaving group[145] in such a S_H2' reaction.[143] The feature, that makes this behavior possible, is the reversibility of sulfonyl radical addition reactions to double and multiple bonds and the remarkable low exothermic of this addition.[143,146] The addition of the whole sulfonyl substrate to the benzylic radical occurs due to steric reasons more probable on the face averted to the ketone substituent on the cyclopentenyl. Alternatively a radical-radical combination of benzyl and cyanidyl radical would deliver the final cyanide (Scheme 43b). For this scenario to happen, a S_H2 reaction at the sulfur atom[147] of the sulfonyl reagent needs to proceed to release the cyanidyl radical. This is a controversial process, claimed as slow.[147] Furthermore, there would be a less strong reason for dissociating the observed diastereoselectivity differences in the alkylation-cyanation compared to the alkylation-peroxidation on such a reaction path. If the cyanation goes via a free radical, a reason which could explain the diastereoselective cyanation is a stabilizing intramolecular interaction of a ketone oxygen centered orbital with the single occupied benzylic π orbital (**I5'**, note that only one orbital lobe is depicted for sake of graphical clarity) in the less polar solvent (DCM vs MeCN). This interaction could lead to a closer proximity of the ketone substituent to the benzyl radical and by that to a diastereoinduction in the radical attack. For more information, a project of theoretic calculations on the mechanistic models was proposed and planned in cooperation with the group of PD Dr. Martin Breugst.

When analyzing different carbocyanation techniques from the literature, the actual cyanation of the radical-alkene-adduct proposingly proceeds mainly by two distinguishable means. Cyanide was proposed to be coupled with the radical-alkene-adduct by a metal catalyst[55-57], commonly Cu based, in a reductive elimination scenario (from a Cu complex bearing cyanido as well as alkyl ligand from radical-alkene-adduct). In cases of this proposal the cyanide source often was TMSCN. The other possibility was without a metal catalyst.[59-60] Here a more direct transfer of the cyanide from its substrate to the benzylic position was assumed, often without a distinct proposal how this process is realized on a molecular level (see chapter 1.2.3).

3.3 Additions of Aldehyde-derived Radicals and Nucleophilic *N*-Alkylindoles to Styrenes

Results presented in this chapter were partially published before and thus, the following contains discussions of the same meaning (Ref. [2]*)*

3.3.1 Project Plan and Inspiration

Implementing a nucleophilic attack in a radical difunctionalization of alkenes, requested the oxidation of radical-alkene-adduct **I1** into the mechanism plan (**I1a** and **I2a** in Scheme 44 are derivatives of the more general structures **I1** and **I2**, respectively).[31] Hydrogen atom transfer (HAT) to oxyl radicals is one of the most studied approaches in order to generate radicals.[148] The formal simplicity of this reaction type gives the opportunity to use common starting materials without prefunctionalization as H-donor and simple peroxides as precursors for H-acceptors.[148a] Intermolecular alkene difunctionalizations with HAT-derived radicals and a nucleophile represented a rather low developed branch among radical reactions.[101,105,108,149] Among these examples, Cu species were the most present catalysts.[101,108,149b,149e] The example of the J.-H. Li group represented the possibility of using Eosin Y as photocatalyst in combination with Fe(OTf)$_2$ in order to functionalize styrenes with 1,3-dicarbonyl nucleophiles and cycloalkane-derived radicals. However, at elevated temperatures they could yield the products without the use of Eosin Y by Fe catalysis with DTBP as oxidant.[149c] In accordance to the proposed mechanistic model in these examples, in its cycle, the photoredox catalyst needed to appeal to the oxidative formation of **I2** and the reductive formation of an oxyl radical for radical formation by HAT (Scheme 44a). Radicals added to the alkene double bond to form **I1**. Upon oxidation, the nucleophile could engange in the reaction with **I2** to obtain the difunctionalization product. Since alkoxy radicals were widely used as H-acceptors[148a,148b], and a spatially rather expanded LUMO of its precursor was anticipated as advantageous in the electron transfer, *tert*-butyl perbenzoate (TBPB) (LUMO: π^*)[150] was initially chosen as the oxidant for the project (instead of *t*BuOO*t*Bu for example). After this choice, the requirements for the photocatalyst could be deduced from the redox potentials of perester reduction and **I1**-oxidation. Note that the reduction of TBPB can also be reversible[150] and in order to constitute its avail to form a *tert*-butoxyl radical, in the following the reduction is depicted as dissociative (Scheme 44b). The Knowles group reported the reductive cleavage of TBPB with Ir(III)/Ir(II) redox pair of photocatalyst [Ir(dF-CF$_3$-ppy)$_2$(dtbpy)]PF$_6$ (reduction by SET from Ir(II)$^-$ species after reductive quenching).[151] In order to control the

radical formation from TBPB by a catalytic reduction in this project, the SET had to be performed from a photoexcited Ir(III)* species (in general, the photoexcited and low oxidation state of catalyst redox pair, Scheme 44a).
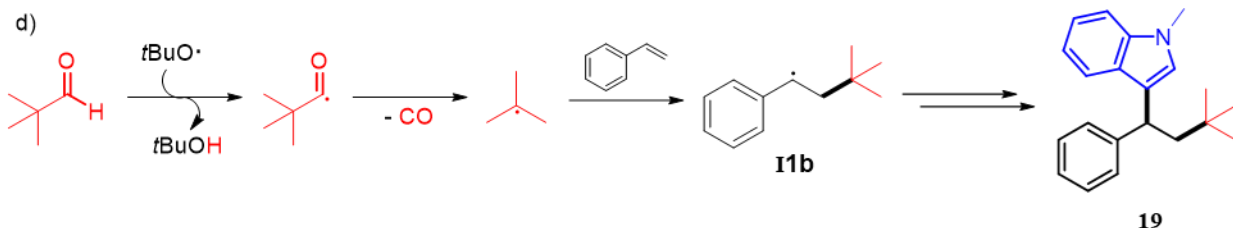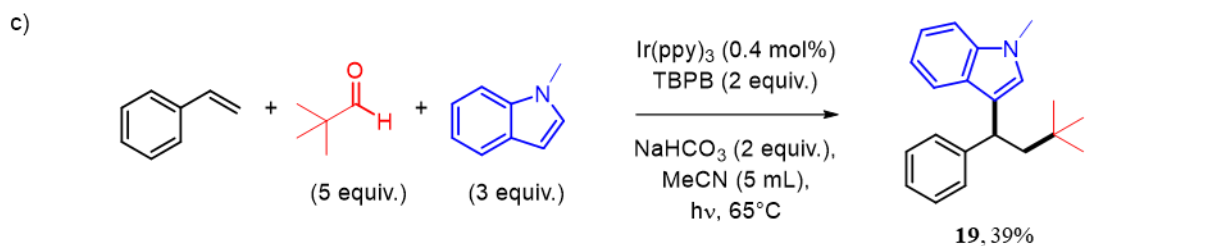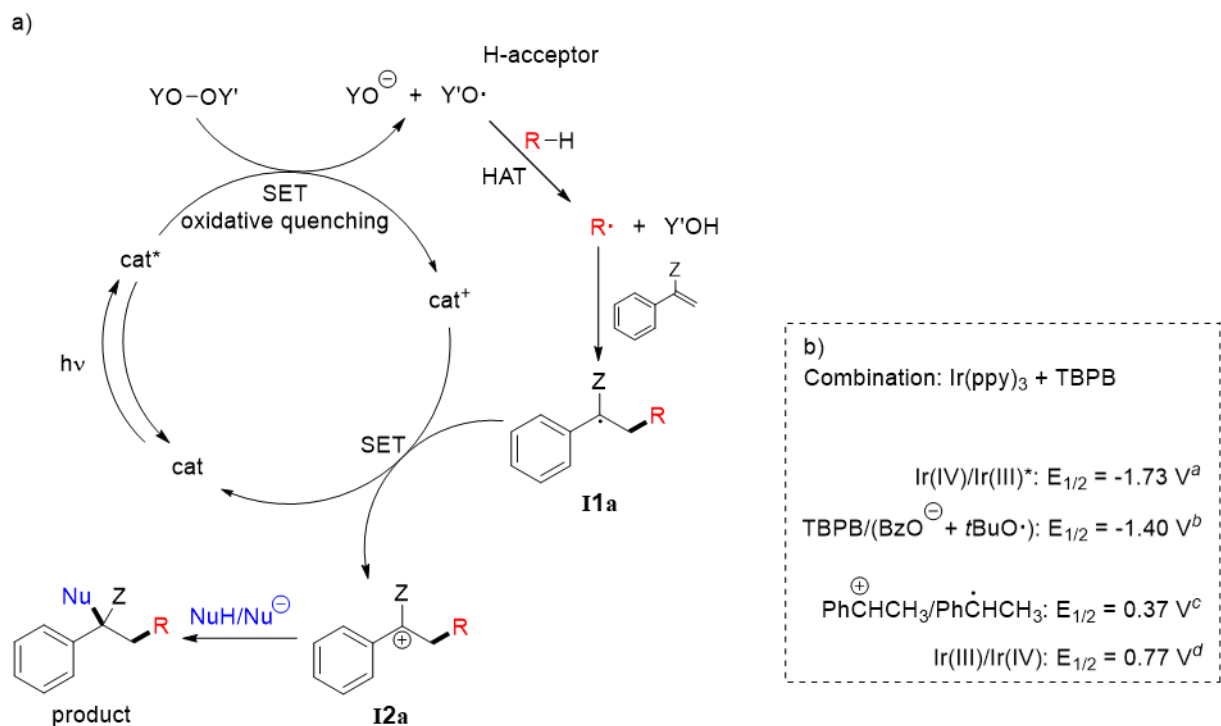
^{a}in MeCN[10]; ^{b}in DMF[152]; ^{c}in MeCN[153]; ^{d} in MeCN[10] ;all redox potentials are given vs SCE; TBPB = *tert*-butyl perbenzoate, SET = single electron transfer.

Scheme 44. Reaction plan for a photoredox catalytic radical alkene difunctionalization involving reductive H-acceptor formation and a nucleophilic functionalization step (a); Example for suitable redox chemistry in regards of catalytic radical and carbocation intermediate formation (b); Alkylation-arylation of styrene with a Ir(ppy)$_3$-TBPB system (c); Formation of decarbonylated product **19** starting from pivaldehyde (d).

A matching redox potential to realize the oxidative quenching of a Ir(III)* species, was given by Ir(ppy)$_3$ (Scheme 44b).[10b] Oxidative quenching of Ir(ppy)$_3$* by TBPB shows in theory a redox potential of about ΔE_{rct} = -1.40 V - (-1.73 V) = 0.33 V (ΔG<0). The oxidation of **I1** to **I2** by Ir(ppy)$_3$$^{+}$ shows in theory a redox potential of about ΔE_{rct} = 0.77 V - (0.37 V) = 0.40 V (ΔG<0).
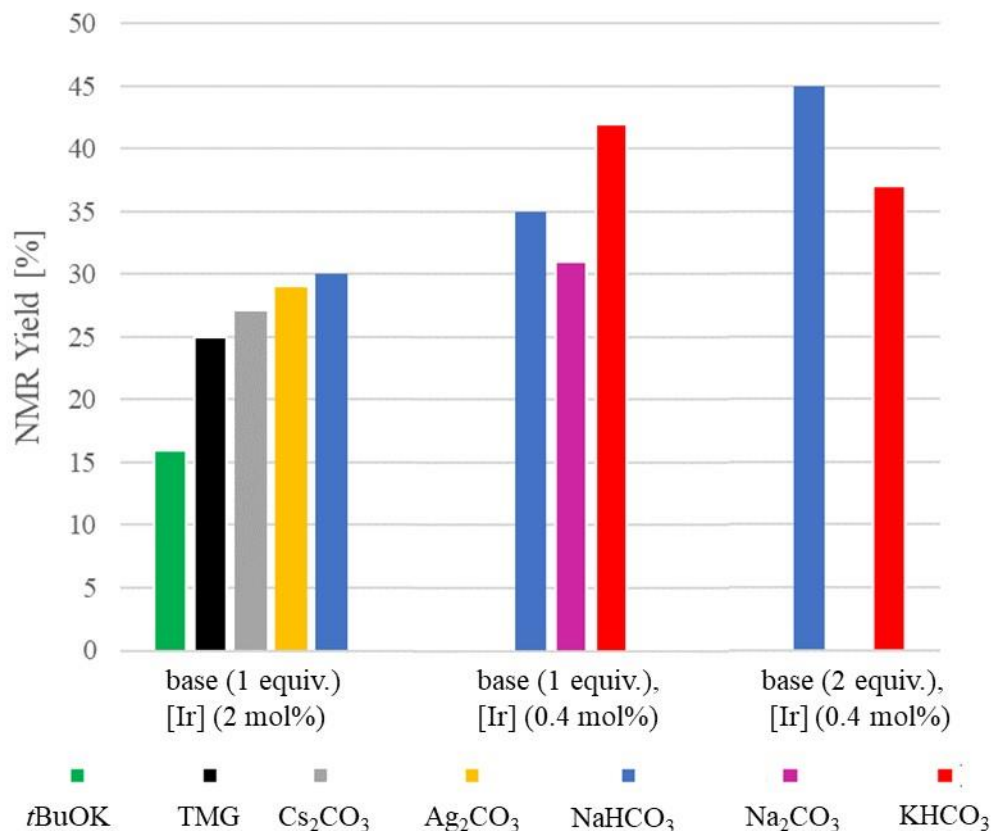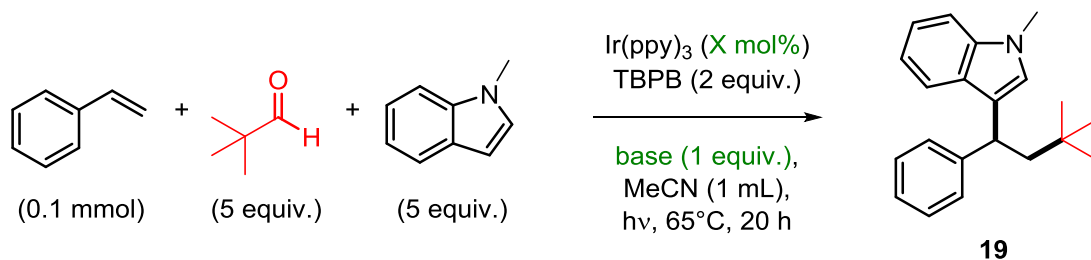
Using the system of Ir(ppy)$_3$ and TBPB in MeCN under white light irradiation (white LED, 40 W, 65°C), it was found that styrene could be difunctionalized with a *tert*-butyl radical (derived from pivaldehyde) and *N*-methylindole to yield **19** (Scheme 44c). Under optimized conditions **19** could be isolated in 39% yield (0.5 mmol scale styrene). The reaction temperature of 65°C was evoked by the heat generation of the irradiation source. Visible light irradiation and the presence of a base were each key to the reaction to be accomplished. NaHCO$_3$ was found to contribute to obtain the best yield of **19** among the evaluated conditions (see chapter 3.3.2). The formation of product **19** could be understood regarding a HAT process from pivaldehyde. The corresponding acyl radical could undergo a decarbonylation[62a-c,154] to form the *tert*-butyl radical (Scheme 44d). The so formed radical could follow the depicted reaction path (Scheme 44a and Scheme 44d) by radical addition to styrene to form **I1** and consecutively form **19** via SET and reaction with nucleophile *N*-methylindole.

From this point, studying the reaction system closely, the technique was expanded with a variety of aromatic and aliphatic aldehydes in use. The common radical added to styrenes was the acyl radical derived from the aldehyde by HAT. The acyl radicals preferentially added to α-substituted styrenes (see chapter 3.3.3).
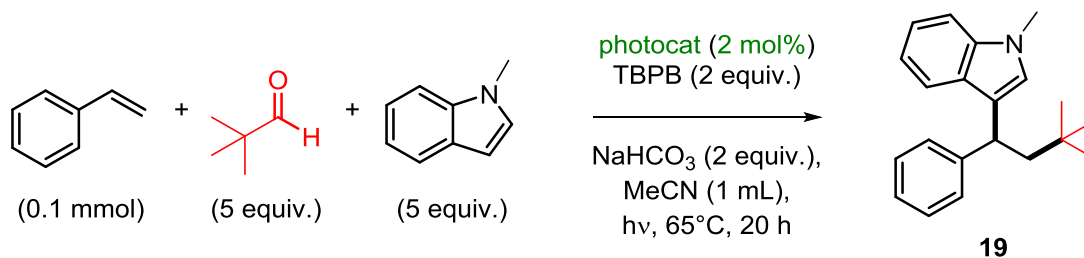
3.3.2 Assessement of Reaction Conditions

In general, the obtained products in this study showed the tendency to decompose along their mass analysis (LC/MS, GC/MS) for characterization, so that the most reliable way to quantify products from reaction mixtures was by ^{1}H NMR analysis. Furthermore, it turned out, that for longer reaction times, integrations in crude NMR mixtures were most reliable when referred to the total amount of aromatic protons in the reaction mixture, which will not change along the course of the transformations. The multicomponent mixtures display a rather complex spectrum of ^{1}H NMR, so that characteristic difunctionalization product resonances with no overlay were practically only found in cases with a benzylic proton (for α-unsubstituted styrenes). Studies that aimed for improving the reaction conditions were performed for the first found product with benzylic proton, compound **19**, synthesized from styrene, pivaldehyde and *N*-methylindole. As described, TBPB as oxidant and Ir(ppy)$_3$ as photoredox catalyst were the foundation of the system. Initial studies showed that best product yields were obtained with styrene as limiting reagent in this difunctionalization. TBPB, pivaldehyde and *N*-methylindole were kept in amounts higher than 1 equiv.. Reaction conditions were studied on a 0.1 mmol scale for styrene in a 10 mL-Schlenk tube under Ar atmosphere, starting from 2 mol% of Ir(ppy)$_3$, 2 equiv. of TBPB, 5 equiv. of aldehyde, 5 equiv. of *N*-methylindole and 1 equiv. of base (Scheme 45).

Under these conditions, base NaHCO$_3$ (30%) led to a superior NMR yield for **19** compared to the analogous reaction operated with bases *t*BuOK (16%), 1,1,3,3-tetramethyl guanidine (TMG, 25%) or Cs$_2$CO$_3$ (27%). Ag$_2$CO$_3$ (29%) provided also for a relative good NMR yield of **19**, but was for economic reasons not considered over NaHCO$_3$. From the reaction with NaHCO$_3$, product **19** was isolated in 21% yield. On a later stage of the screenings, a photoredox catalyst loading of 0.4 mol% Ir(ppy)$_3$ was found to give a higher level of product yield (Scheme 47). For this amount of catalyst, carbonate bases NaHCO$_3$, Na$_2$CO$_3$ and KHCO$_3$ were compared for their influence on NMR yield of **19**. For 1 equiv. of base, among the three bases KHCO$_3$ (42%) was giving the highest NMR yield and could be considered the best alternative to NaHCO$_3$ in the overall base evaluation. However, for the final conditions with 2 equiv. of base and 0.4 mol% of Ir(ppy)$_3$, a reaction with NaHCO$_3$ (45%) formed a higher amount of **19** than KHCO$_3$ (37%). Along a screening on the amount of NaHCO$_3$ (1-3 equiv. and 2 mol% Ir catalyst), usage of 1.5 equiv. and 2 equiv. led to the best results for the yield of **19**.

Scheme 45. Evaluating bases in styrene difunctionalization (TMG = 1,1,3,3-tetramethyl guanidine).

Studying the influence of solvents, only DCM (16%) and DCE (8%) could be identified as alternatives to MeCN (1 equiv. NaHCO$_3$, 2 mol% Ir(ppy)$_3$, 30%) in order to achieve a formation of **19** (see Supporting Information Ref. [2] for an overview). For other solvents, often high styrene conversions and partial aldehyde conversions without the formation of any difunctionalized styrene, but rather oligomerizations were observed. No concrete origin of the strong solvent dependency in such a complex system could be deduced from the screening. With reference to the redox chemistry, the critical step in the supposed cycle should be the reductive cleavage of TBPB. The influence of photoredox catalyst (2 mol%) on the difunctionalization was studied using 2 equiv. of NaHCO$_3$ (Scheme 46).

Reaction scheme: styrene (0.1 mmol) + pivaldehyde (5 equiv.) + N-methylindole (5 equiv.), with photocat (2 mol%), TBPB (2 equiv.), NaHCO₃ (2 equiv.), MeCN (1 mL), hν, 65°C, 20 h, giving product **19**.

entry#	photoredox catalyst (2-3 mol%)	NMR yield [%][a]
1	Ir(ppy)$_3$	33
2	Ru(bpy)$_3$(PF$_6$)$_2$	13
3	Eosin Y	12
4	Riboflavin	7
5	[Ir(dF-CF$_3$-ppy)$_2$(dtbpy)]PF$_6$	39
6	[Ir(ppy)$_2$(dtbpy)]PF$_6$	41
7	Fluorescein	3
8	TPPBF$_4$	0
9	Ru(bpy)$_3$Cl$_2$	0
10	Ir(dF-ppy)$_3$	0
11	[Ir(4,5'-dtbppy)$_2$(dtbpy)]PF$_6$	17
12	[Ir(dF-ppy)$_2$(dtbpy)]PF$_6$	34
13	Ir(5'-F-ppy)$_3$	43

[a]^{1}H NMR yield; ppy = "2-phenylpyridinate"($C2$, N); bpy = 2,2'-bipyridine;
TPP = triphenylpyrylium.

Scheme 46. Evaluating photoredox catalysts in styrene difunctionalization.

For an overview of catalyst structures see chapter 7.

An important control reaction in that regard, was to execute the reaction procedure without the deployment of a catalyst. The experiment showed that the reaction could proceed without catalyst (NMR yield **19**: 16%, Scheme 48, see also chapter 3.3.6.2). For catalysts TPPBF$_4$, Ru(bpy)$_3$Cl$_2$ and Ir(dF-ppy)$_3$ no difunctionalization products were formed. The reactions under use of these catalysts showed no (TPPBF$_4$) or low conversion of styrene and low conversions of aldehyde after the reaction time. Application of catalysts Ru(bpy)$_3$(PF$_6$), Eosin Y, fluorescein, riboflavin and [Ir(4,5'-dtbppy)$_2$(dtbpy)]PF$_6$ resulted in low yields of **19**. Among these reactions, the Ir catalyst was the only one enabling a high styrene conversion (88%) after 20 h reaction time. For the four other catalysts of this group, styrene conversions between 40-60% were reached after 20 h. While organic dyes and Ru based catalysts show inferiority in the transformation, especially Ir based species were able to support reaching higher NMR yields of **19**. From known redox potentials (vs SCE, in MeCN) for Ir(IV)/Ir(III)* pairs of Ir(ppy)$_3$ (E$_{1/2}$ = -1.73 V)[10] and of Ir(5'-F-ppy)$_3$ (E$_{1/2}$ = -1.46 V)[10b] a direct electron transfer upon excitation to TBPB (E$_{1/2}$ = -1.40 V)[152] is allowed. For [Ir(dF-CF$_3$-ppy)$_2$(dtbpy)]PF$_6$ and [Ir(ppy)$_2$(dtbpy)]PF$_6$ (E$_{1/2} \geq$ -0.96 V)[10b] this electron transfer would be an endergonic process.

It is left to mention that the effect of reaction medium in this multicomponent mixture could have a decisive influence on the actual redox potentials. The results allude that in some cases also Ir(III)/Ir(II) redox pairs (instead) could be involved. And these Ir(III)/Ir(II) redox pairs have somehow an advantage to Ru(bpy)$_3$$^+$, Ru(II)/Ru(I)) to occur.

It was important to investigate the influence of the catalyst loading on the product formation, to ensure an efficient usage. Thus, for the catalysts Ir(5'-F-ppy)$_3$, [Ir(ppy)$_2$(dtbpy)]PF$_6$, [Ir(dF-CF$_3$-ppy)$_2$(dtbpy)]PF$_6$ and Ir(ppy)$_3$ loadings between 0.1 mol% and 2 mol% were applied in the difunctionalization of styrene (Scheme 47). In that experiment series, it turned out that below a catalyst loading of 2 mol%, Ir(ppy)$_3$ was the best catalyst in regard of the reached NMR yield of **19**. The best result was achieved by applying a 0.4 mol% charge of Ir(ppy)$_3$ in the reaction of styrene with pivaldehyde and *N*-methylindole, manifested by a NMR yield of 45% for **19** (Scheme 47). For this reaction set-up, **19** was isolated in a 39% yield.
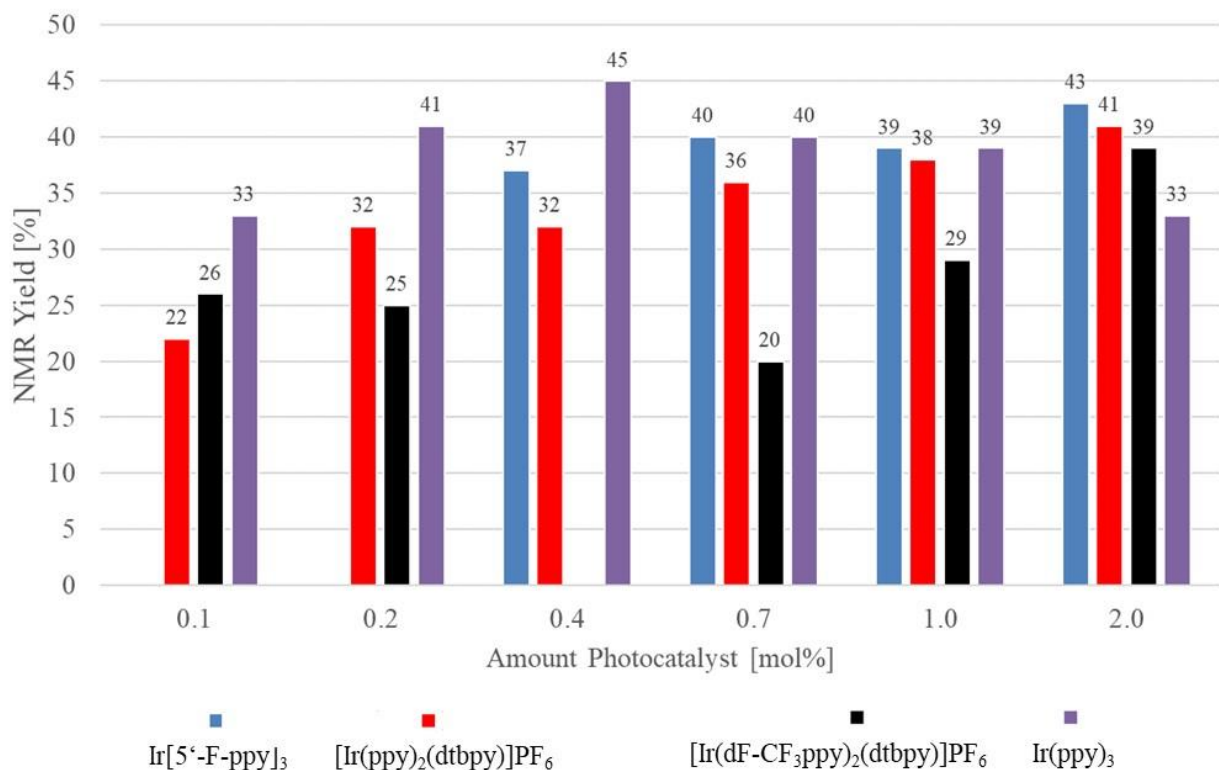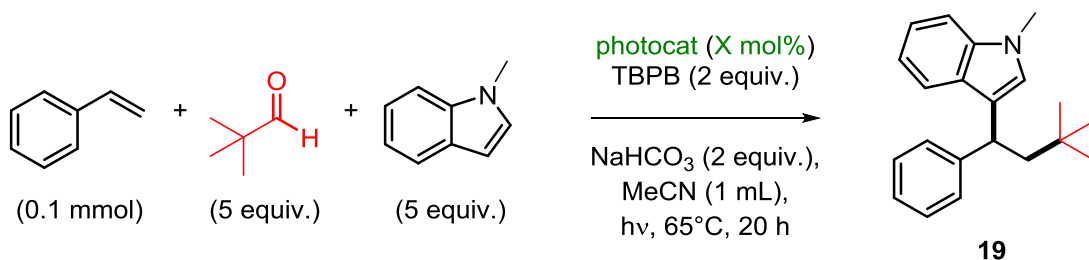
Scheme 47. Evaluating photoredox catalyst loading in styrene difunctionalization.

Photoredox catalyst Cu(dap)$_2$Cl (2 mol%) was not able to catalyze the reaction towards **19** from the reagent mixture. Attempts to catalyze the reaction in a transition metal based thermal approach (FeCl$_2$ (with or without reducing agent dimethyl aminotoluene), CuCl or CoCl$_2$, 10 mol% at 65°C) were insuccessful to form a difunctionalized styrene. In reactions with CuCl, TBPB was readily converted, but styrene kept unreacted. In reactions with FeCl$_2$, styrene and pivaldehyde showed partial conversion, while TBPB was converted only to a low degree (no TBPB conversion with dimethyl aminotoluene present). With CoCl$_2$, TBPB could be converted, but styrene and pivaldehyde showed low conversions respectively without forming noticeable products by NMR or TLC analysis.

In the photocatalytic approach a variety of metal-co-catalysts (Cu(OAc)$_2$, NiCl$_2$ glyme, PdCl$_2$, CoCl$_2$, Fe(OTf)$_3$, Fe(OAc)$_2$, Mg(OAc)$_2$, In(OTf)$_2$, In(OAc)$_3$, Sc(OTf)$_3$, ligands: phen, bpy) were

tested with the intention to improve electron transfer processes or stabilize intermediates. No particular improvement of the NMR yield of **19** could be achieved. For 2 equiv. of NaHCO$_3$ and 0.4 mol% Ir(ppy)$_3$, the amounts of TBPB (2-5 equiv., 41-45%), pivaldehyde (2-6 equiv., 37-45%) and *N*-methylindole (3-7 equiv., 40-45%) showed only low impact on the NMR yield of **19**. Also concerning the amount of solvent (0.5-2 mL, 43-45%; 3 mL (31%), 4 mL (10%)) in the 0.1 mmol scale reaction, the NMR yield of **19** showed to be of low sensitivity. When varying the oxidant (2 equiv.), *tert*-butyl peracetate (TBPA, 38%) was found as the only feasible alternative to TBPB (45%) in order to yield **19** (see Supporting Information Ref. [2]).

Along the undertaking of scaling the reaction up for the purpose of dependable synthetic isolation of reaction products, the irradiation source was varied. A blue light irradiation source (0.4 mmol scale in 4 mL vial under Ar atmosphere, blue LED, 40 W, ~30°C reaction temperature) and a blue light photoreactor (0.4 mmol scale in 4 mL vial under Ar atmosphere, blue LED, 140 W, cooling to 20°C reaction temperature) were used as concipated apparatures (for 4 mL vials) in the Ritter group, Max-Planck-Institut für Kohlenforschung, Mülheim, Germany. The reaction of styrene with pivaldehyde and *N*-methylindole led here to lower yields than on a 0.5 mmol scale in a 100 mL-Schlenk round bottom flask in the hitherto utilized white LED surrounding (40 W, 65°C).

On the 0.1 mmol scale, the reagents were checked for their necessity (Scheme 48). Not mentioned by now, the reaction could not be performed without the visible light irradiation at 65°C reaction temperature (entry 3). A thermal cleavage of TBPB could be ruled out under the found reaction conditions. Likewise, the reaction execution without the oxidant/perester (entry 4) caused the failure of difunctionalization (only small amount of styrene was converted in the mixture to indistinct products).

As Ir(ppy)$_3$ catalyst could be omitted in order to get **19**, on a low yield at full styrene conversion (entry 2), low temperature initiators BPO, AIBN and CBr$_4$ were tested. At thermal conditions (entries 5 and 6) and under white light irradiation (white LED, 65°C) conditions (entries 7, 8 and 9), it was verified that the presence of just a higher radical concentration was not sufficient to elevate the probability for the formation of **19**.
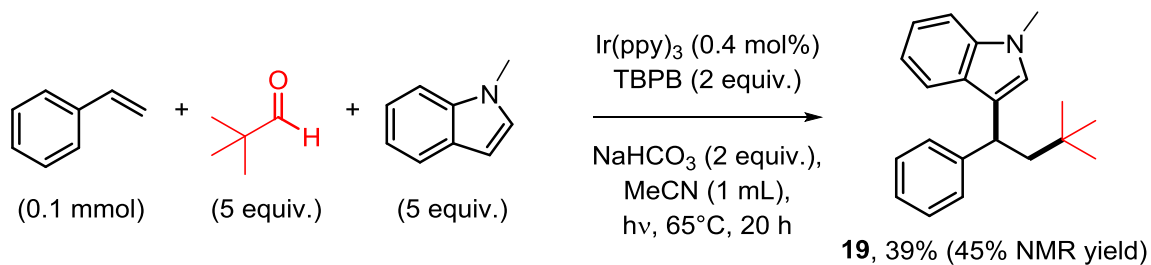
entry #	control experiment	NMR yield [%]^a
1	no base	0
2	no catalyst	16
3	no light/ 65°C	0
4	no perester	0
5	no cat/ no irradiation/ 65°C/ BPO (4 mol%)^b	0
6	no cat/no irradiation/ 65°C/ AIBN (4 mol%)^b	0
7	no cat/ irradiation/ 65°C/ BPO (4 mol%)^c	0
8	no cat/ irradiation/ 65°C/ AIBN (4 mol%)^c	0
9	no cat/ irradiation/ 65°C/ CBr$_4$ (5 mol%)^c	17

^{a}¹H NMR yield; reaction time: ^{b}12h, ^{c}14 h; BPO = benzoyl peroxide; AIBN = azo-bis(isobutyronitrile).

Scheme 48. Control experiments in styrene difunctionalization.

For a continuation of investigations, that aim for clarification on mechanism related questions in this reaction system, see chapter 3.3.6.

3.3.3 Substrate Scope

The reaction time of 20 h was chosen in the reaction condition assessements in order to have the opportunity to compare the reactions with some slower proceedings with different H-donor or nucleophile substrates or alternative conditions (see chapter 3.3.4). For the best reaction conditions of the acylation-arylation, the reaction progress was roughly finished after 10 h in most cases. A reaction time of 12 h was chosen for the synthetic application to assure full styrene conversions. In this regard, it was observed, that the difunctionalization product was stable under reaction conditions. In terms of preparative isolation, the reaction mixtures of N-alkylindole-aldehyde difunctionalizations could be described as challenging. The respective reaction mixtures contained a set of similar side products. These side products could not be identified distinctively, but were complex mixtures of indole derived species (consist of mostly aromatic protons and several N-methyl groups (300 MHz, CDCl$_3$, δ/ppm ~3.0-4.3 ppm) in ^{1}H NMR spectra). Using a lower amount of nucleophile (5 equiv.→3 equiv.) in preparative synthesis brought relief in some cases without noticeable yield detraction.

With benzaldehydes as radical source, α-substituted styrenes could be difunctionalized in combination with N-methylindole (Scheme 49). Benzaldehydes were well suited in this methodology and corresponding products (**20a-k**) were isolated in yields between 31-78%. The highest yields were obtained with *p*-methylsulfide and *p*-methoxy (71% (**20i**) and 78% (**20h**), respectively) substituents. Also heteroaromatic, electron-rich 2-thiophenecarboxaldehyde convinced as H-donor (**20k**, 75%). Electron-poorer variants like *p*-fluoro- or *p*-trifluoromethylbenzaldehyde showed also quite good yields (67% (**20f**) or 60% (**20g**), respectively), which were of same magnitude as for the unsubstituted benzaldehyde derived product (**20a**, 68%). There is no clear trend for the product yields, concerning the electronic influence of the substituent. Yet, aguebly there is an advantage in the use of electron-richer benzaldehydes, since they provided the highest yields of corresponding products. The reaction of benzaldehyde with α-methylstyrene and N-methylindole was performed without photoredox catalyst to better classify the mentioned reactivity in the absence of a catalyst. In absence of the catalyst a yield of only 9% instead of 68% was achieved. Under the catalytic conditions, p*rimary* and *secondary* aliphatic aldehydes could also be used for the radical acylation of α-methylstyrene (**21a-c**) whereas *tertiary* pivalinaldehyde led to a decarbonylated product (**22**), like in the example of plain styrene (**19**). For α-methylstyrene a higher yield was obtained than for styrene

(55% (**22**) vs. 39% (**19**)). Compared to benzaldehydes, using aliphatic aldehydes led to lower product yields (34-55%) presumably owing to more reactive radicals. Decarbonylated products from *primary* or *secondary* aldehydes could not be isolated.


20a, R' = H, 68%; 9%[a]
20b, R' = Me, 54%
20c, R' = *t*Bu, 39%
20d, R' = *i*Pr, 67%
20e, R' = Ph, 31%
20f, R' = F, 67%
20g, R' = CF$_3$, 60%
20h, R' = OMe, 78%
20i, R' = SMe, 71%

20j, 53%

20k, 75%

21a, 53%

21b, 34%

21c, 38%

22, 55%
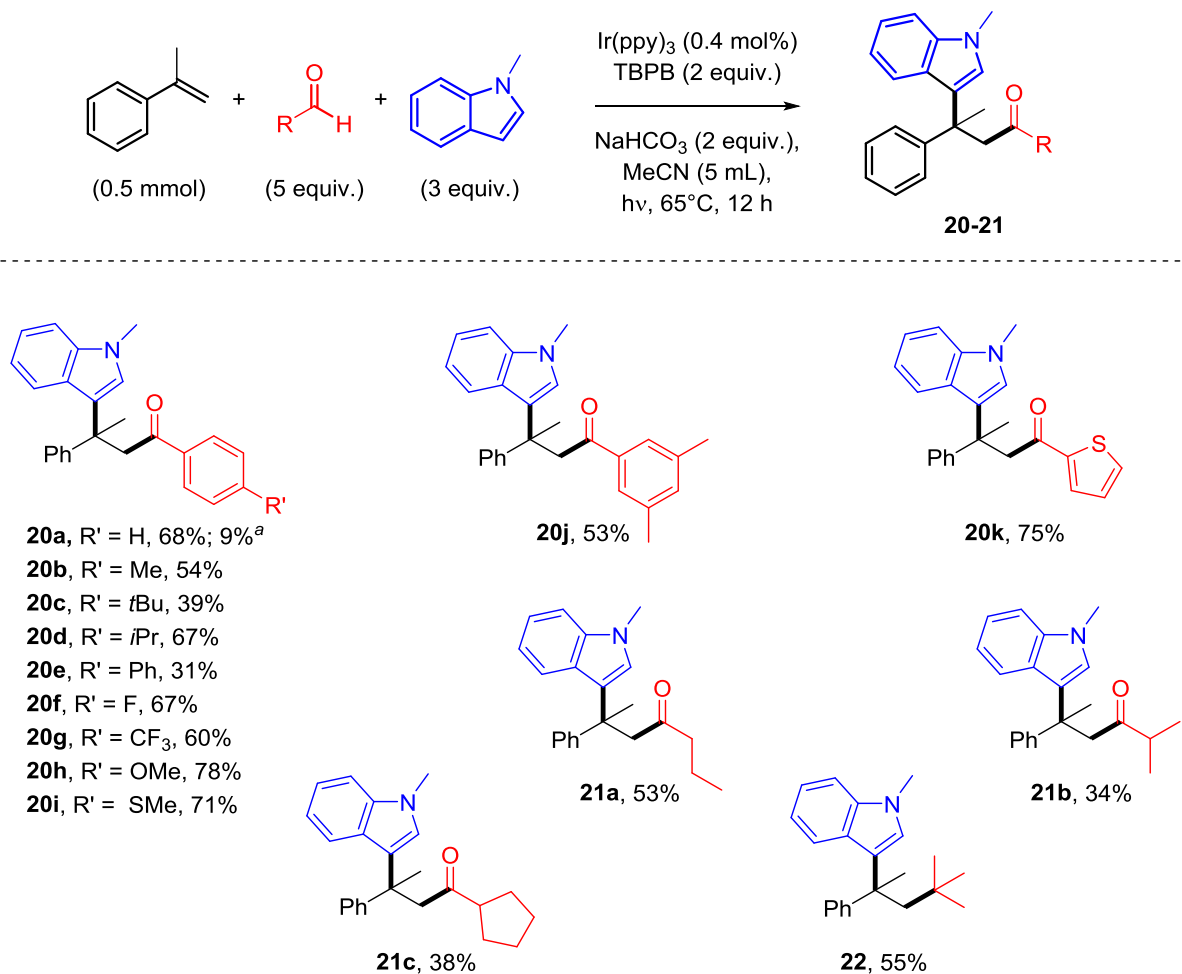
[a] in absence of photoredox catalyst.

Scheme 49. Employment of various aldehydes.

Benzaldehyde had not (together with *N*-methylindole) led to the difunctionalization product with simple styrene (**23**, with *p*-methoxystyrene: **25** in traces, Scheme 50). From the solvent screening only MeCN, DCM and DCE were found as solvents, which were suitable for the formation of **19**. Thus, some experiments with MeCN-DCM solvent combinations of different relative ratios were carried out to search for an influence on the reaction of benzaldehyde towards styrene. Furthermore some additives of Lewis bases (MeOH, H$_2$O, pyridine, THF), tetrabutylammonium salts or polarity reversal catalysts (Me$_3$NBH$_3$, PhSH, CySH; although aldehyde conversion was observed before) were tested in the reaction in MeCN. However, all experiments failed to form

the difunctionalization product of styrene with benzaldehyde and *N*-methylindole. Along with the general procedure of the methodology, *p*-methoxybenzaldehyde neither executed the difunctionalization with styrene (**24**), but instead was successfully added to *p*-methoxystyrene (**26**, 35%). *p*-Methoxystyrene proved superior to plain styrene in the reactions with benzaldehydes. *p*-Methoxybenzaldehyde proved to be more suitable in reaction with *p*-methoxystyrene than plain benzaldehyde (Scheme 50).
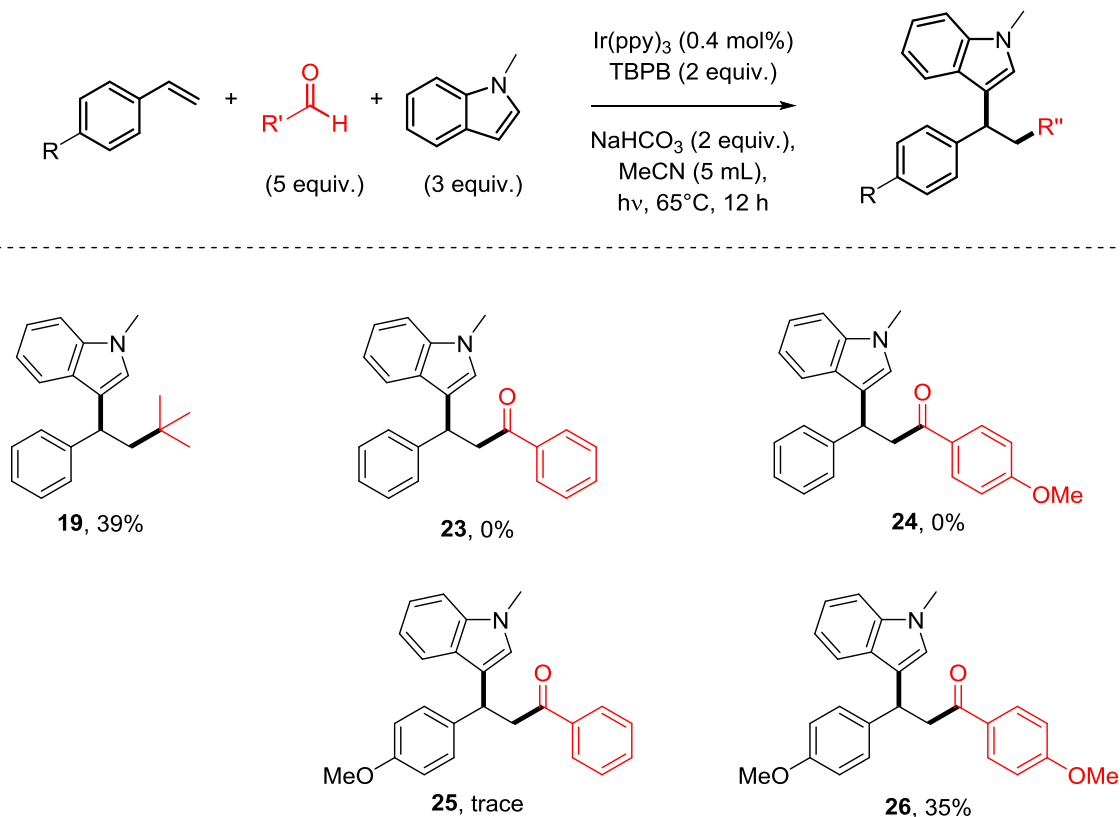
Scheme 50. Evaluating monosubstituted aromatic alkenes.

Whilst the aldehydes influence on the product formation was examined, also *p*-substituted *α*-methylstyrenes were applied in the reaction with *N*-methylindole and benzaldehyde (Scheme 51). For a fair range of evaluated *p*-substituents, the alkene difunctionalization proceeded good. For products **27a-c** relative high product yields were obtained in a narrow margin in respect to non-substituted **20a** (68-75%). An influence on product yields was remarked when analyzing the results of electron-withdrawing substituted styrenes. The difunctionalizations of *p*-fluoro-*α*-methylstyrene (**27d**) and of *p*-cyano-*α*-methylstyrene (**27f**) demonstrated lower yields in derived products (43% and 12%, respectively). More accentuated, assuming a carbocation intermediate (**I2**), among here presented alkenes, the *p*-cyano substituent is causing the strongest
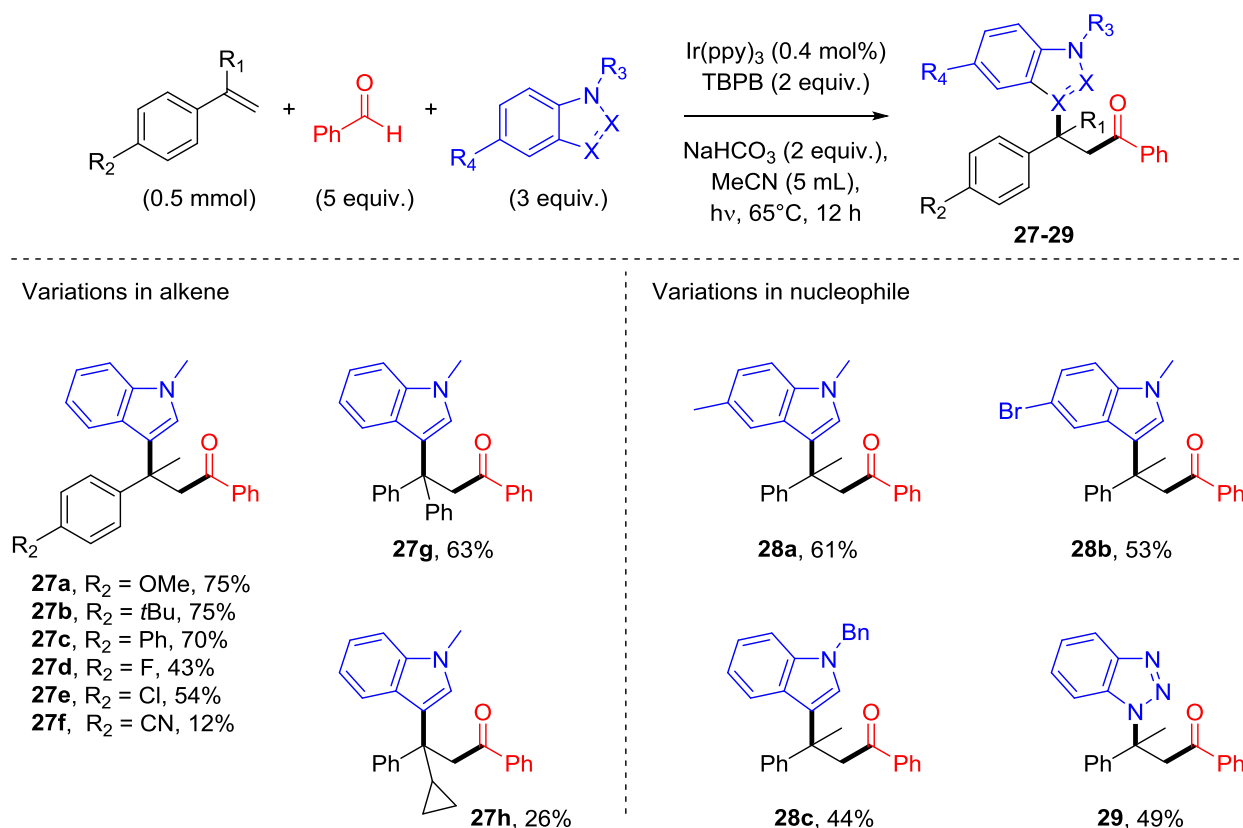
Scheme 51. Employment of various alkenes and nucleophiles.

destabilization (refer to Scheme 44a) and correspondingly produced a prominent diminished product yield (**27f**, 12%). This observation is in line with the advantageous effect of an *α*-methyl group on the styrene for product formation with benzaldehyde (and *N*-methylindole) as well as with the benefit of a *p*-methoxy substituent on styrene in difunctionalization with *p*-methoxybenzaldehyde (Scheme 50). These substrates would give well-stabilized carbocation intermediates (**I2**) due to the *tertiary* substitution as well as the electron-donating substituent, respectively. Furthermore, 1,1-diphenylethylene was effectively employed in the reaction with benzaldehyde and *N*-methylindole (**27g**, 63%) giving another example for a nucleophilic attack on a *tertiary* center. From X-ray crystallography (XRD) of **27g** the general products structure was further corroborated (see chapter 5.4 and Supporting Information of Ref. [2]). Internal styrenes did not give the desired products (see chapter 3.3.4).

Moreover, a spectrum of different nucleophiles was evaluated in the reaction of *α*-methylstyrenes with benzaldehyde (see Scheme 51). Unexpectedly, slighter variations to the indole core like in *N*-Boc-indole or 1,2-dimethylindole gave unsuccessful reaction outcomes. Pleasingly, the difunctionalization could be well established with 1,5-dimethylindole (**28a**, 61%) and also the

acceptance of the corresponding 5-bromide derivative (**28b**, 53%) to reaction conditions was demonstrated. Although *N-H* indole was incompatible to the technique, a good alternative to the *N*-methyl group was found with a *N*-benzyl protecting group on the indole (**28c**, 44%). Some more diversity could be brought to the nucleophile branch, when discovering that 1*H*-benzotriazole could be implemented (**29**, 49%) into the procedure.

Apart from these findings, the solvent MeCN was found to act as nucleophile. In the reaction that provided **19**, MeCN competed to *N*-methylindole for the attack on the benzylic carbocation intermediate **I2** (product ratio imide **30b**:*N*-methylindole **19** ≈ 1:4.5 from crude ^{1}H NMR). Omitting the indole and making MeCN the initially present nucleophile in the reaction mixture could lead to an isolated yield of **30b** as high as 53% (Scheme 52a).
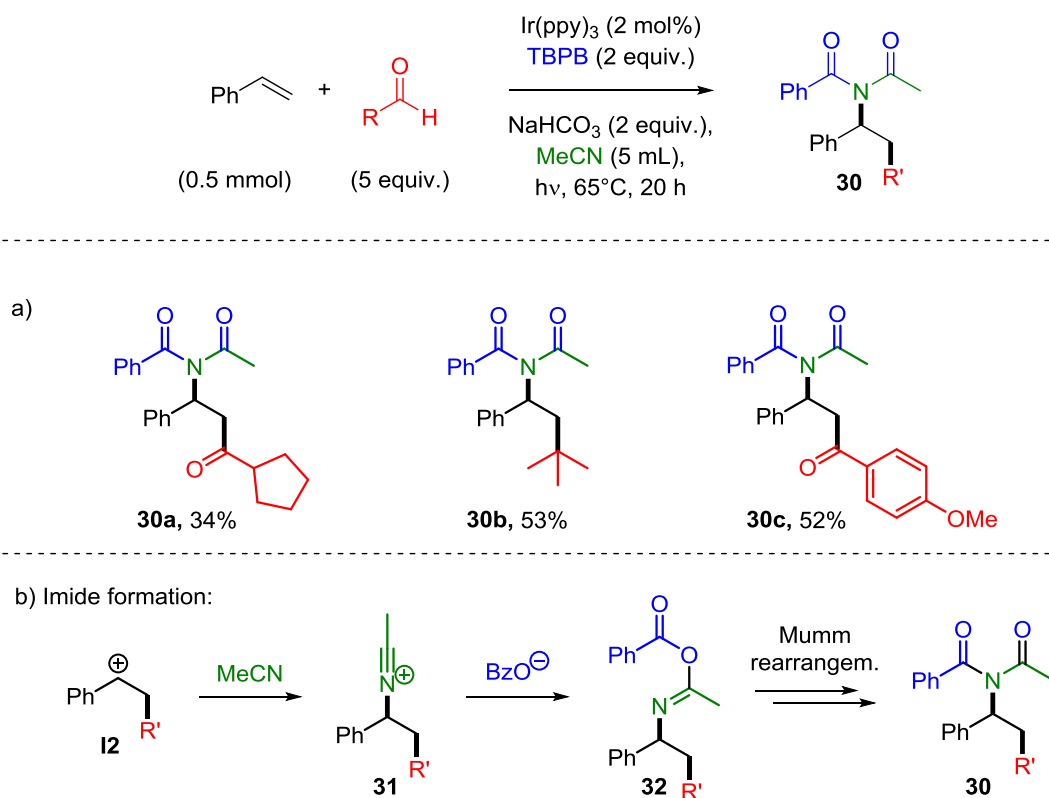
Scheme 52. Employment of acetonitrile as nucleophile.

89

Interestingly, in the presence of the benzoate anion (and absence of water) not a *N*-acetamide like for conventional Ritter reactions but a *N*-acyl benzamide functionality was introduced. This could be clarified, when assuming that after an initial attack of MeCN to **I2**, the benzoate anion attacks the electrophilic nitrilium cation **31** (Scheme 52b). The so formed imidate **32** could by intramolecular nucleophilic attack of the N-atom on the carbonyl, in a Mumm rearrangement[94], lead to imide **30**. Related imide formations were reported in intra- and intermolecular fashions.[93,155] The technique gave the possibility of formally connecting different aldehyde-derived radicals together with the imide functionality to styrene. Aliphatic cyclopentanecarboxaldehyde (**30a**, 34%) as well as aromatic *p*-methoxybenzaldehyde (**30c**, 52%) were used for imide formations (Scheme 52a).

When comparingly to the synthesis of **19** the aldehyde as well as indole were omitted, an alkyl nitrile solvent could serve as both nucleophile and H-donor. Solvent derived radicals add to the double bond of styrene and upon catalytic oxidation of radical-styrene-adduct, the formation of the respective imide was achieved. The implementation of solvent-derived radical additions, namely from propionitrile (**33a**) and *iso*-butyronitrile (**33b**), further underlined the supposed mechanism (Scheme 53a). The respective reaction in MeCN gave beyond the double adduct **33c**, two side products (Scheme 53b). For the generation of **34** the *tert*-butoxyl radical, which resulted from reductive TBPB cleavage (Scheme 53c), directly added to the styrenes double bond. For **35** a methyl radical, arguably originating from β-scission[125] of the before mentioned *tert*-butoxyl radical (Scheme 53c), added to the double bond.

The imides were obtained in medium yields for styrene (up to y = 53%). For α-substituted styrenes and 4-methoxystyrene, imide formations were not observed. A plausible reason for these results is, that MeCN as weak nucleophile was kinetically hindered to attack the more stable, *tertiary* and electron-donor substituted carbocations, respectively. Furthermore, this is in agreement with nucleophilic amidations from reported difunctionalization procedures. There was to the best of my knowledge by the time of this report no procedure for installing alkyl nitrile derived amides from 1,1-disubstituted aromatic alkenes.[98-101] Reported difunctionalizations had used mesomeric electron-donating substituted secondary carbocation amidations only scarcely.[100-101]
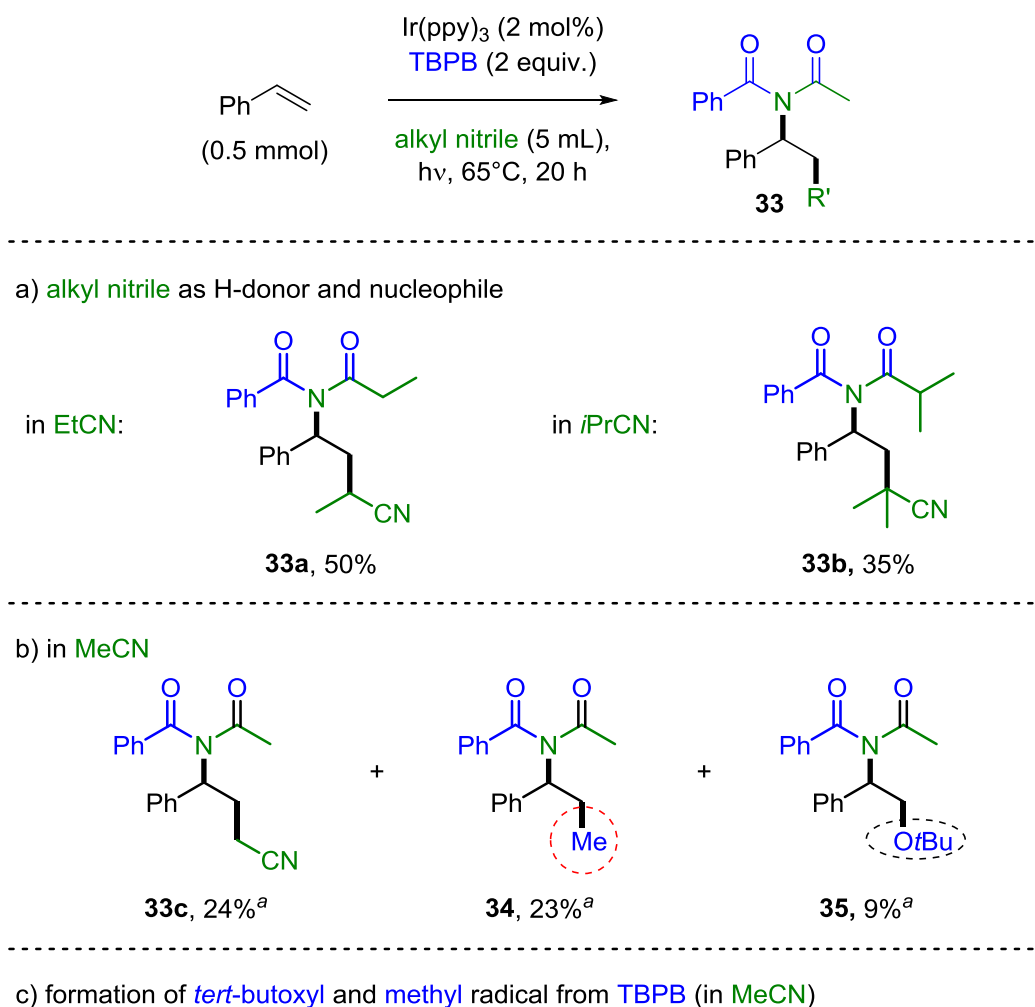
Scheme 53. Employment of alkyl nitriles as nucleophile and H-donor.

The method of alkylation-arylation is overall quite sensitive to radical scavengers. Already the addition of 1 equiv. of BHT to the reaction mixture of styrene with pivalinaldehyde and *N*-methylindole under otherwise unchanged reaction conditions led to the inhibition of the difunctionalization. No trapped radical could be isolated.

In the field of alkene difunctionalizations, limitations to methodologies have been common to the date of this thesis. When regarding procedures using indoles as nucleophile, it was striking, that they show strong limitations in the applicable alkenes and indoles/nucleophiles. Several studies

had not included unsubstituted styrene in the scope.[104,107-110] Instead most techniques were centered around the difunctionalization of methoxy-substituted styrenes. Some techniques had not shown the successful employment of α-substituted styrenes.[103-104,106,110] For the indole part, *N-H* indole derived products were not always shown in these methodology scopes.[53c,103,106-107] In conclusion, the application range of most examples in this field of difunctionalizations with indoles and the here presented results pointed towards the issue of stabilization of a supposed carbocation intermediate **I2**. Either electron-donor substitution on styrene or *tertiary* position of the carbocation helped in the stabilization, which was crucial for these techniques. In general, difunctionalization methods show less limitations regarding styrenes or in nucleophiles of one kind (see chapters 1.2.5.1 and 1.2.5.2). One methodology among difunctionalizations with indoles stood out. The groups of J.-H. Li and S. Luo showed that with their technique besides indoles fortunately also an array of N-nucleophiles and 1,3-dicarbonyl-C2-nucleophiles were added to the styrene difunctionalization scope.[105] They had used the addition of Si centered radicals in their approach. Defining for their success was probably the β-silicon effect,[156] the silicon-carbon hyperconjugation could have further stabilized **I2**.

Apart from their work, the here presented technique was to date of this thesis the only procedure, that was able to successfully functionalize a *p*-cyano-substituted styrene with an indole derivative. Pleasantly, the protocol is a powerful method to form a quaternary all carbon center upon addition of *N*-methylindoles to the benzylic position and therefore, it was able to show that various functional groups on the styrene can be employed, increasing the molecular complexity.

3.3.4 Procedural Limitations

Making use of the system Ir(ppy)$_3$ and TBPB under photocatalytic conditions, pivaldehyde (2.5 mmol) could in MeCN be transformed to imide **36** (57%, with TBPB as limiting reagent, Scheme 54a). The formation could be rationalized by the one-electron oxidation of the *tert*-butyl radical by Ir(IV)$^+$ to the respective carbocation and Ir(III), followed by consecutive nucleophilic attacks of MeCN and the benzoate anion in a Mumm rearrangement (Scheme 54b). The potential for *tert*-butyl carbocation/*tert*-butyl radical redox pair ($E_{1/2} = 0.09$ V vs SCE in MeCN[153]) testifies for a readily oxidation process with Ir(IV)/Ir(III) ($E_{1/2} = 0.77$ V vs SCE in MeCN[10], $\Delta E = 0.68$ V).

In an attempt to difunctionalize 1,1-diphenylethylene with a *tert*-butyl radical and *N*-methylindole, the only distinct product that could be isolated was imide **36** (21%, Scheme 54c). **36** could not be detected in successful difunctionalization procedures with pivaldehde (reactions forming **19**, **22**, **30b**, respectively) by TLC, although pivaldehyde and TBPB were used in excess. In addition, the difunctionalization of 1,1-diphenylethylene was accomplished with benzaldehyde and *N*-methylindole (**27g**).
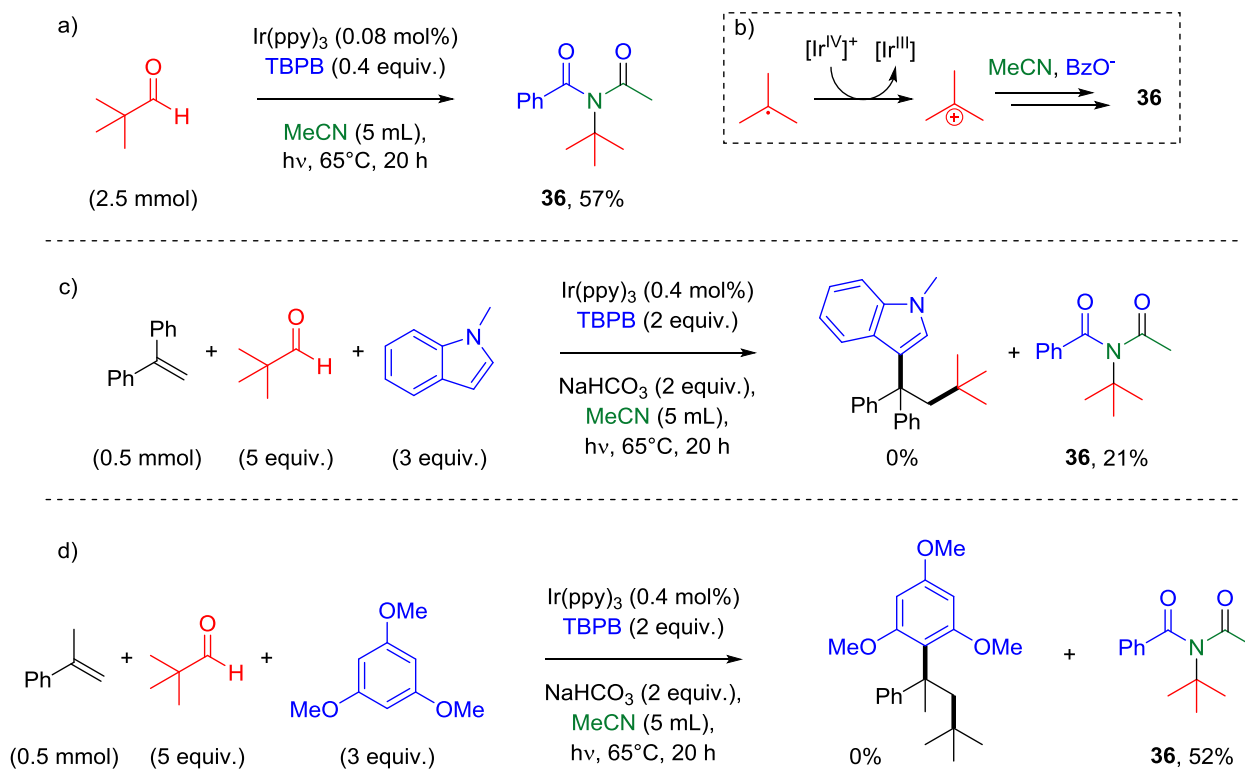
Scheme 54. Isolation of an alternative reaction product.

93

A possible reason that for 1,1-diphenylethylene a difunctionalization was possible with benzaldehyde, but not with pivaldehyde could be the steric demand of the radicals. Either *tert*-butyl radical addition or nucleophilic attack on the respective dibenzylic carbocation intermediate in β-position to a *tert*-butyl group could be considerably decelerated in comparison to corresponding steps in the difunctionalization with the benzoyl radical. Also in an attempt to use 1,3,5-trimethoxybenzene as alternative nucleophile in the α-methylstyrene difunctionalization with pivaldehyde, no difunctionalization product was found, but imide **36** could be isolated (52%, Scheme 54d). Since the radical addition of *tert*-butyl to α-methylstyrene was already accomplished in this reaction system (**22**) and the replacement of *N*-methylindole by the benzene probably had low influence on this, the inertia of 1,3,5-trimethoxybenzene as nucleophile favored finally oxidation of *tert*-butyl and imide formation.

In the following, examples of substrates for aldehyde (or H-donor), alkene and nucleophile are presented, which were found to not undergo the difunctionalization in MeCN with Ir(ppy)$_3$ and TBPB as central combination. The diversity of aldehyde substrates was exploited. On the way to implement a variety of aldehydes also some examples were found, which could not be used to difunctionalize α-methylstyrene with *N*-methylindole (Scheme 55).
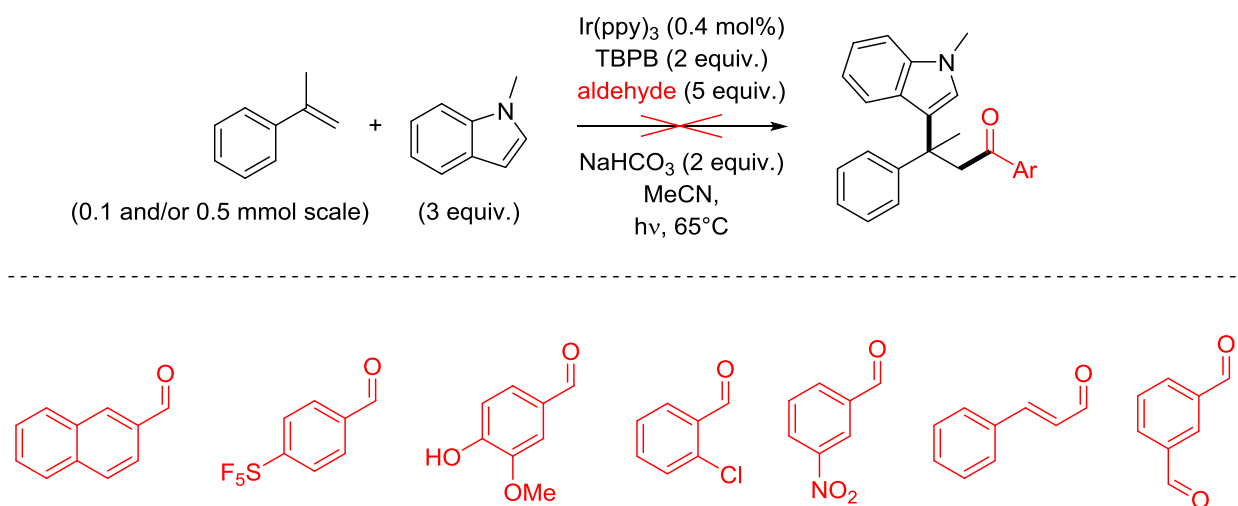

Scheme 55. Incompatible aldehyde substrates.

While vanillin, a phenolic alcohol, was likely to fail, because of the possibility to transfer the alcoholic hydrogen atom, the reasons for the unsuitability of other aldehyde remained unclear. TLC of crude reaction mixtures for the above examples mostly displayed inconspicuous. In order to not overlook possibilities, some reaction mixtures were (partially) separated by column

chromatography (in the cases with cinnamaldehyde, 1,3-benzenedicarboxaldehyde, *o*-chlorobenzaldehyde, *p*-pentafluorosulfanylbenzaldehyde). In the case of 1,3-benzenedicarboxaldehyde, the aldehyde was practically completely isolated from the mixture. From the other separations, only complex mixtures of indistinct *N*-methylindole derivatives were obtained.

Initial investigations on alternatives to aldehydes as H-donors were centered on benzyl and α-carbonyl radical precursors (Scheme 56). Among the substrates, no difunctionalization based on the corresponding C centered radicals could be implemented into the difunctionalization technique. This could have different reasons. Some observations from NMR analysis of the crude reaction mixtures (18-20 h) are described in the following. While in the application of Meldrum's acid the conversion of α-methylstyrene was highly advanced, TBPB stayed mostly unreacted. In
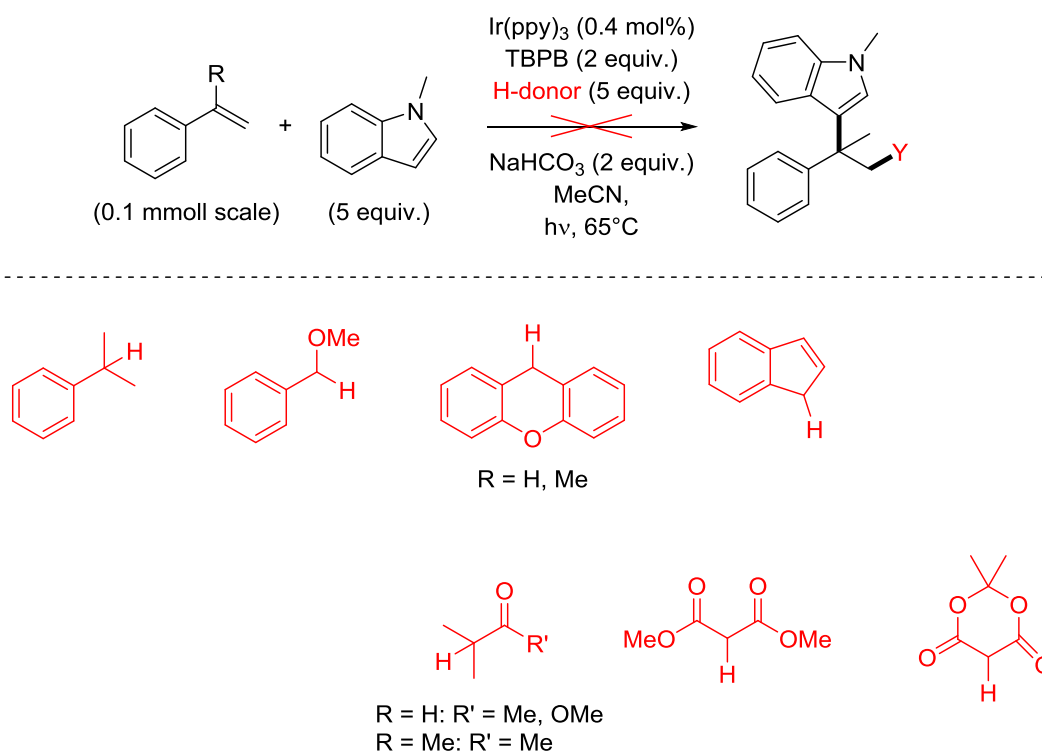
Scheme 56. Further incompatible H-donors (If not mentioned otherwise R = Me).

reactions with 3-methylbutan-2-one, TBPB and the olefin were majorly converted, but substantially, signs for a resonance set of ketone derived products (methyl groups) could not be observed. For the cumene application, the conversion of TBPB was quite advanced and α-methylstyrene was partly converted, yet in the ^{1}H NMR spectrum no set of resonances for a cumene analogue could be observed (derived methyl groups). Applying indene in the system, led

to high conversion of TBPB, but no resonance for a supposed functionalized indene (benzylic proton) was present in the crude reaction mixture. In reactions with xanthene, the redox processes seemed to be majorly influenced, since TBPB was not reacted.

In reactions with ambiguous outcome, estimated upon crude NMR analysis, and/or noticeable TLC spots (benzyl methyl ether, ethyl-2-methylpropionate, Meldrum's acid, dimethylmalonate, indene) also column chromatography was conducted. Only complex mixtures, mainly with multiple *N*-methyl groups present from supposed indole incorporations, could be isolated. No indications for styrene difunctionalizations could be observed.

In reactions with *N*-methylindole and benzaldehyde or pivaldehyde (standard conditions for TBPB, Ir(ppy)$_3$, MeCN and NaHCO$_3$ under white light irradiation over 12 h), incompatible alkenes were a group of cyclic aliphatic alkenes (cyclohexene, 1-methylcyclohexene, methylenecyclohexane with benzaldehyde), electron-deficient methyl acrylate (with pivaldehyde and benzaldehyde), electron-rich vinyl acetate (with pivaldehyde and benzaldehyde), α-bromostyrene, allylbenzene (both with benzaldehyde), (*E*)-1,3-butadien-1-ylbenzene (with pivaldehyde) and a group of internal alkenes ((*E*)-stilbene, α-methyl-(*E*)-stilbene, β-methylstyrene, indene and cyclohexen-1-ylbenzene with pivaldehyde, see Supporting Information Ref. [2] for a graphical overview on incompatible substrates). By ^{1}H NMR analysis of the crude reaction mixtures, high TBPB conversions could be determined. TLC of the reaction mixtures showed to be mostly inconspicuous. From the reactions with cyclohex-1-ene and α-bromostyrene only complex mixtures of indistinct *N*-methylindole derivatives could be isolated. From the reaction mixture containing (*E*)-stilbene, the alkene could be isolated almost quantitatively. There are some anticipations and indications from literature reports, that radical additions to internal alkenes are slower.[39,44b,45] Reported difunctionalization techniques with acyl radicals in MeCN, lack of the application of internal alkenes.[83,93]

A series of alternative nucleophiles was applied in reaction mixtures with an alkene and an aldehyde according to standard difunctionalization conditions over at least 12 h (Scheme 57).
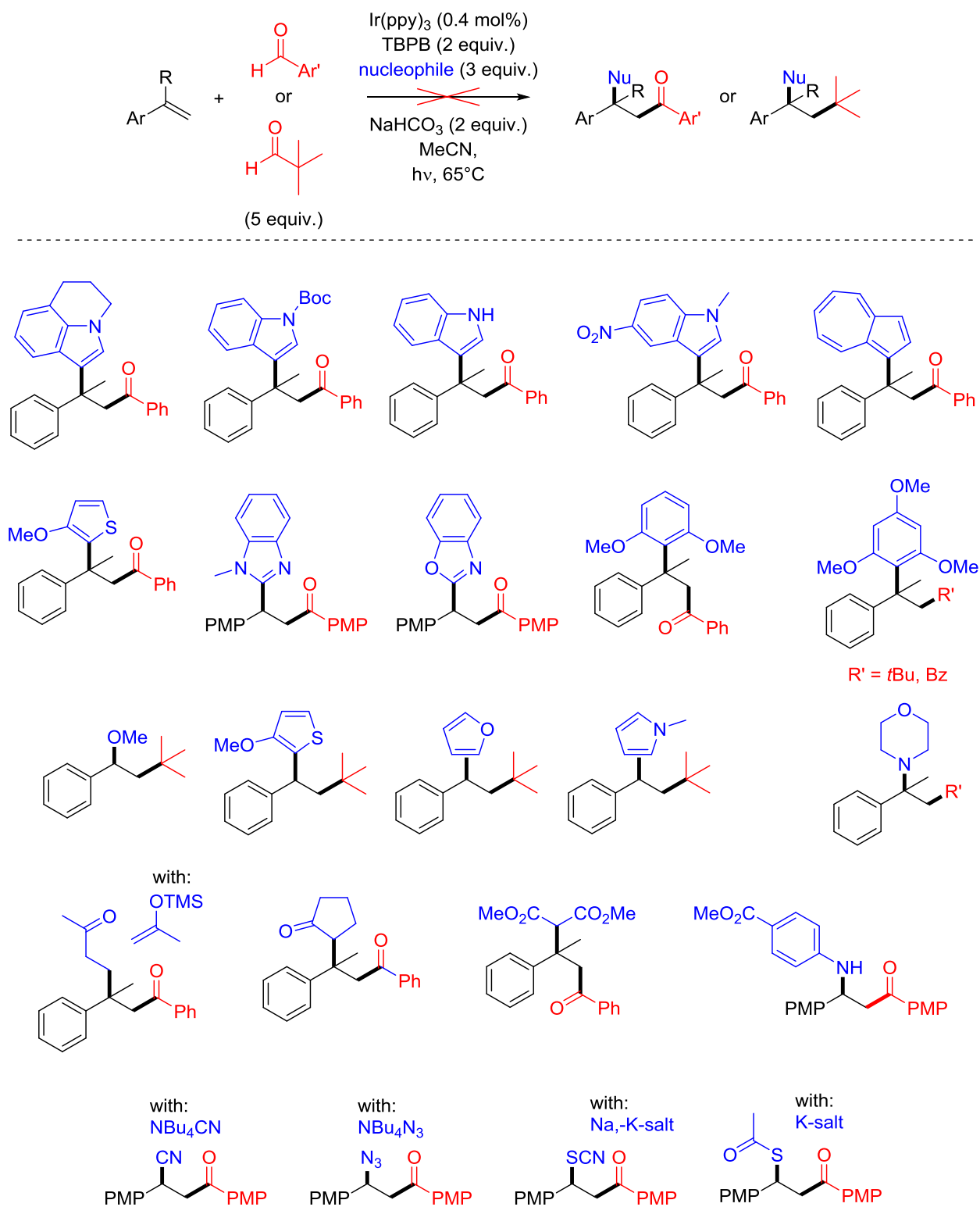

Scheme 57. Incompatible nucleophiles in difunctionalizations with styrenes and aldehydes.

In attempts with styrene and 4-methoxystyrene, the ^{1}H NMR analysis of the crude reaction mixtures after reaction times of 4-12 h revealed that no successful difunctionalizations were realized by the absence of any benzylic proton resonance (dd) in the spectra. The conversions could proceed in quite different manners. While after a reaction time of 12 h, for a reaction mixture containing NBu$_4$CN (with *p*-methoxystyrene and *p*-methoxybenzaldehyde) quite low alkene conversion was observed, for methyl *p*-aminobenzoate ~50% of each styrene and TBPB were converted and in a mixture containing NBu$_4$N$_3$, styrene was already fully converted. For cases where α-methylstyrene was used as alkene, the exclusion of the appearance of a difunctionalization process was mostly based on TLC and if unclear on column chromatography. For the use of azulene, TLC showed a promising spot, but by isolation only a complex mixture could be obtained (with rather many aliphatic protons in comparison to aromatic protons) without showing a sign for difunctionalization products. When *N*-Boc indole was applied (with α-methylstyrene and benzaldehyde), by ^{1}H NMR analysis of the crude reaction mixture, a difunctionalization process could be excluded. The absence of the *N*-methyl group gave clear insight into the shift area 2-5 ppm, where no indication for methylene groups (AB spin system) of a potential difunctionalization product could be found. For the usage of 3-methoxy thiophene (with α-methylstyrene and benzaldehyde) only a complex mixture with various (>10) 3-methoxythiophene derivatives, recognizable by the methoxy group protons was obtained by column chromatography. When applying cyclopentanone (with α-methylstyrene and benzaldehyde), column chromatography after 12 h reaction time (hexanes/EtOAc v/v = 25/1) yielded at the supposed elution volumn a colourless oil (15 mg), which was by ^{1}H NMR analysis identified as a complex mixture. Yet, the NMR analysis (300 MHz, CDCl$_3$) also revealed the presence of two doublets (δ/ppm = 4.04, 3.72; $^3J \approx 15.2$ Hz) with relatively low intensity which could belong to a possible difunctionalization product.

### 3.3.5 Further Possibilities for the System

In the reaction that led to imide **30c**, also a side product could be isolated (Scheme 58). Since the addition of benzoyl radicals to the O-end of benzaldehydes carbonyl group is known,[157] the formation of **37** could be understood as difunctionalization of *p*-methoxybenzaldehyde with a *p*-methoxybenzoyl radical and a benzoate anion as nucleophile, which are both suspected to be contained in this reaction system (see Supporting Information of Ref. [2] for more details).
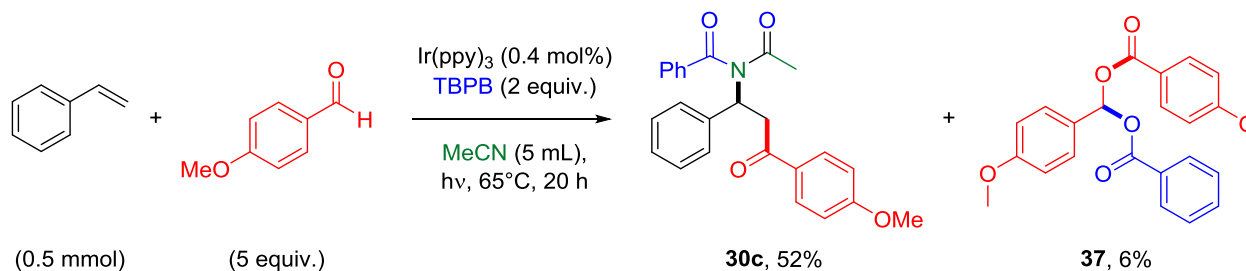
Scheme 58. Difunctionalization of a benzaldehyde as side reaction.

The reaction system gave an interesting possibility to difunctionalize the C–O double bond of benzaldehydes and generating a mixed acetale structure.

In the final phase of this whole project, some decision had to be taken in order to keep the studies in a time frame. Reactions, conducted according to the procedure of acylation-arylation or acylation-imidation, led to indications for further promising substances (Scheme 59). The products could by strong correlations of ^{1}H NMR to the expectations, assigned to structures, but were after (multiple) attempts of separation from the reaction mixture not of suitable purity to fully characterize and publish. As far as possible, the estimated yields of difunctionalization products with *p*-methyl-α-methylstyrene (**38a**, <70%), *p*-trifluoromethyl-α-methylstyrene (**38c**, <7%) and *p*-chlorobenzaldehyde (**38b**) in the presence of *N*-methylindole and for the product of cyclohexanecarboxaldehyde with MeCN as only nucleophile (**40**) in the reaction mixture are given. For the corresponding products the optimal way for isolation still is unknown. The low yield of **38c** was expected, as the electronic effect of the CF$_3$ group could provoke a destabilization of proposed intermediate **I2** (for a discussion see chapter 3.3.3).
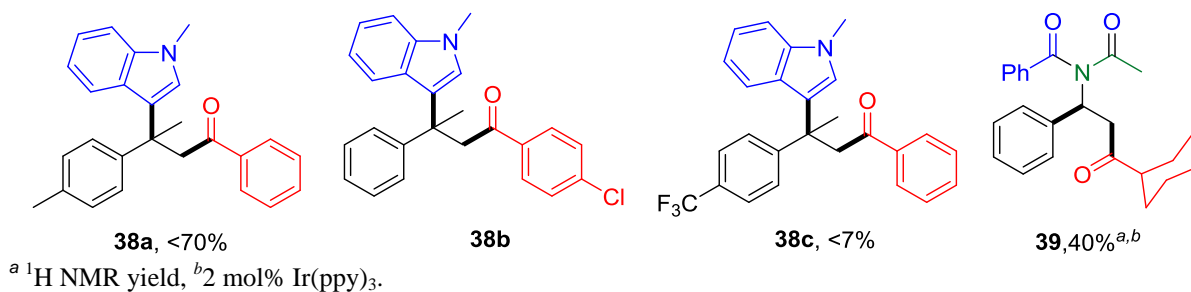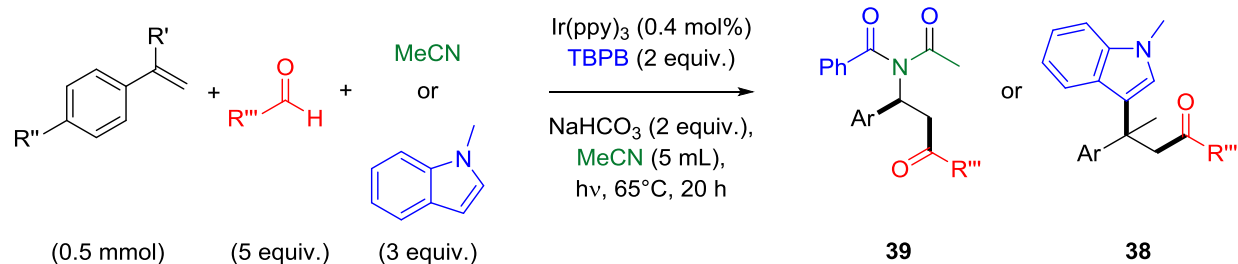
Scheme 59. Indications for further alkene difunctionalizations.

For characteristic NMR resonances, which led to the proposition of above difunctionalization products see chapter 5.7.

With the system of Ir(ppy)$_3$ and TBPB under the standard photocatalytic conditions for imide formation without extra H-donor present, styrene was transformed in iPrCN (Scheme 60). Asides the above described imide **33b** another defined product could be isolated from the reaction mixture by column chromatography.
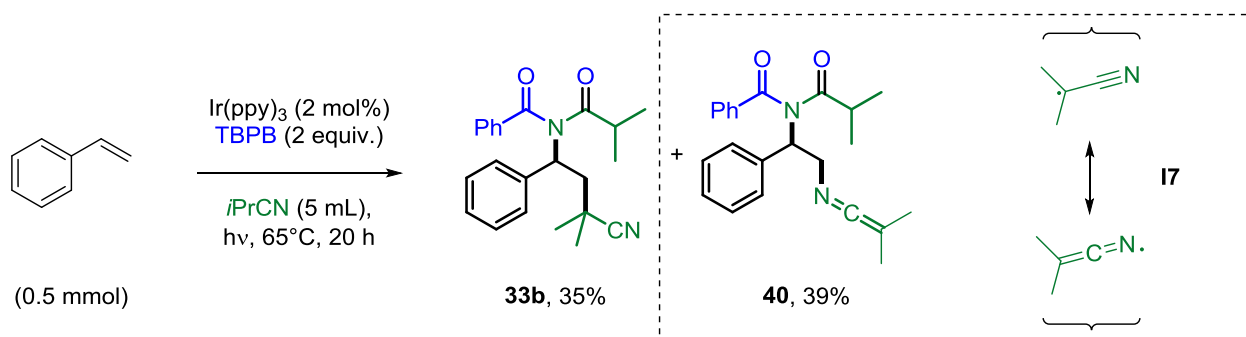
Scheme 60. Indication for a bifunctional radical.

Both isolated species were characterized by ^{1}H, ^{13}C and DEPT135 NMR experiments. For imide **33b** the NMR resembles analogue structures **33a** and **33c** in terms of chemical shifts. A high resolution molecular mass gave more evidence for the structure of **33b**. However, attempts to gain information on the molecular mass of the second product **40** by means of LC/- or GC/MS failed. Analyzing its NMR spectra, it could be stated that product **40** showed the same set of resonances as product **33b**, differing in its chemical shifts. In the ^{1}H NMR (300 MHz, CDCl$_3$) spectra doublets for methyl groups on the imide (δ/ppm = 0.77, 0.80 vs. 0.71, 0.73, no. 1+2 in Figure 7) and singlets for the second pair of methyl groups from incorporated *i*PrCN units (δ/ppm = 1.45, 1.41 vs. 1.42, 1.29, no. 3+4) showed only a slight downfield shift for **40** compared to **33b**. It is also noteworthy that these methyl groups showed for **40** a decreasing magnetic inequivalence. The differences for chemical shifts of benzylic and α-carbonyl proton (on imide)

resonances were also quite small (δ/ppm = 5.85 (dd, J = 10.2, 5.2 Hz), 2.30 (hept, J = 6.7 Hz) vs. 5.96 (dd, J = 7.5, 5.6 Hz), 2.16 (hept, J = 6.6 Hz), **40** vs. **33b**, no. 5+6). The major difference for the two products was manifested in the chemical shifts of the methylene group protons (2dd, no. 7). For **40** these
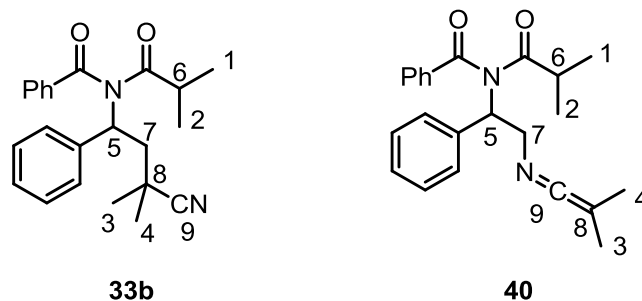

33b   **40**

Figure 7. Proton/carbon assignments for products.

protons were present at δ/ppm = 4.05 (dd, J = 9.0, 5.2 Hz) and δ/ppm = 4.54 (dd, J = 10.3, 9.0 Hz) and for **33b** at δ/ppm = 2.76 (dd, J = 14.8, 7.5 Hz) and δ/ppm = 2.62 (dd, J = 14.8, 5.6 Hz). The extra-ordinary difference in chemical shifts for the methylene protons suggested a difference in connectivity at this carbon atom, attesting a relation of constitutional isomers for the two products rather than rotational isomers. The higher chemical shifts for **40** could mean that a heteroatom is bond to the methylene group. In ^{13}C NMR spectra (75 MHz, CDCl$_3$) the two products (**40** vs. **33b**) showed particular differences in the shifts for the methylene group carbon (δ/ppm = 65.34 vs. δ/ppm = 43.65, no. 7) as well as the *quaternary* carbon (δ/ppm = 70.79 vs. δ/ppm = 31.62, no. 8) generated from radical addition. The carbons originated from cyano group in the α-cyano-isopropyl radical, showed upon incorporation rather low differences in chemical shift for the two products (δ/ppm = 120.28 vs. δ/ppm = 124.64, no. 9). Before further ways for characterization of **40** could be conducted, the product decomposed in an indistinct fashion. From NMR results, the product should consist of the same building blocks as **33b**, namely styrene, a *N*-

isobutyryl-benzamidyl unit and a α-cyano-isopropyl radical. The differences in chemical shifts most likely represent an established C–N connectivity for **40** upon radical addition to styrenes double bond. This could be rationalized by the resonance stabilization of the α-cyano-isopropyl radical. A second resonance structure could be a keteniminyl radical (**I7**, Scheme 60). This sterically less demanding radical could have a kinetic advantage over its α-cyano centered form in addition to the styrene. Since the reaction results encouraged the assumption on the formation of keteniminyl radical and on the appearance of a rather stable ketenimine that could be isolated by column chromatography, this reaction would have been the cornerstone of my next investigations. A future project could add value to the findings or conceptual approach by establishing a new way of generating N centered radicals from bulky cyano compounds with α-hydrogen atom. For an overview of resonances of proposed structure **40**, as well as a comparative depiction of ^{1}H NMR spectra of **33b** and **40** see chapter 5.7.

3.3.6 Mechanistic Investigations and Proposal

First control experiments (see chapter 3.3.2) gave information about the necessity of the base, the perester and irradiation of visible light to the system. Furthermore, low temperature radical initiators BPO, CBr$_4$, AIBN could not replace Ir(ppy)$_3$ to any extend. BPO and AIBN seemed rather to hamper the difunctionalization while CBr$_4$ showed practically no influence compared to a difunctionalization without catalyst. Noticable is yet some reaction proceeding without any catalyst present, albeit in the synthetic application far less efficient than Ir(ppy)$_3$ (y for **20a**: 9% without, 68% with catalyst, respectively). From this point, further experiments were conducted to get more information about the observed reactivities and by that, additional indications of the mechanistic basis.

3.3.6.1 Effect of Light on Radical Sources

Since visible light irradiation was indispensable for the difunctionalization to occur, the influence of this irradiation on individual reagents was verified. For this purpose a solution of pivaldehyde (0.5 mmol) in MeCN (1 mL) was stirred under Ar atmosphere for 12 h in a 10 mL-Schlenk tube, while white light irradiation was applied (white LED, 40 W, 65°C) adapted from the general procedure (for 1 mmol-styrene scale reaction without reagents other than pivaldehyde). After the irradiation time, ^{1}H NMR analysis of the mixture showed that pivaldehyde was unreactive by itself under these conditions.

Similarly a solution of TBPB (0.2 mmol) in MeCN (1 mL) was stirred under Ar atmosphere for 12 h in a 10 mL-Schlenk tube whilst irradiated with white light (white LED, 40 W, 65°C). After the irradiation time, ^{1}H NMR analysis showed only the presence of TBPB and MeCN in the mixture. The supposed radical sources of the reaction could not be activated by the light source irradiation nor heating.

3.3.6.2 Activation modes of TBPB

This finding ultimately also underpinned that a chemical reaction between TBPB and another reagent of the system is responsible for the radical formation. In consequence, reations between TBPB and Ir(ppy)$_3$ or *N*-methylindole, respectively were conducted.

To a dispersion of Ir(ppy)$_3$ (0.01 mmol, 0.25 equiv.) in MeCN-*d$_3$* (0.5 mL), TBPB (0.04 mmol, 1 equiv.) was added in a NMR tube. The tube was centered in the white light surrounding (white LED, 40 W) and the dispersion was irradiated. After a reaction time of 25 min, ^{1}H NMR analysis

revealed a 29% conversion of TBPB to benzoic acid (~28% of *tert*-butyl groups were converted to acetone, ~2% to *t*BuOH, respectively). After the measurement, the tube was irradiated again with white light to continue the reaction. Finally, after total 13.5 h of reaction time, the perester was fully converted (benzoic acid (>95%), acetone (93%), *t*BuOH (7%)). Under this reaction condition 1 equiv. of Ir(ppy)$_3$ had the potential to convert at least 4 equiv. of TBPB. This was a sign for either a catalytic or a chain decomposition of TBPB. In literature there are some examples reported about radical[158] or anion[159] related decomposition of peresters.[160] In the simple system that was investigated, a radical driven chain decomposition would mean, that either methyl radicals (derived from β-scission[125] of *tert*-butoxyl) or cyanomethyl radicals (derived from solvent by HAT) would have attacked TBPB molecules (Scheme 61a). The reaction would have yielded a corresponding alkyl benzoate. Such a product has not been detected. In a theoretic anionic decomposition scenario, benzoate, the only anionic nucleophile present, would have formed benzoic anhydride with TBPB (Scheme 61b). Since only protons of TBPB and benzoic acid (benzoate, respectively) were observed in the aromatic shift area of the NMR spectra, also this pathway seems unrealistic. (A nucleophilic attack to the peroxy group of the perester would
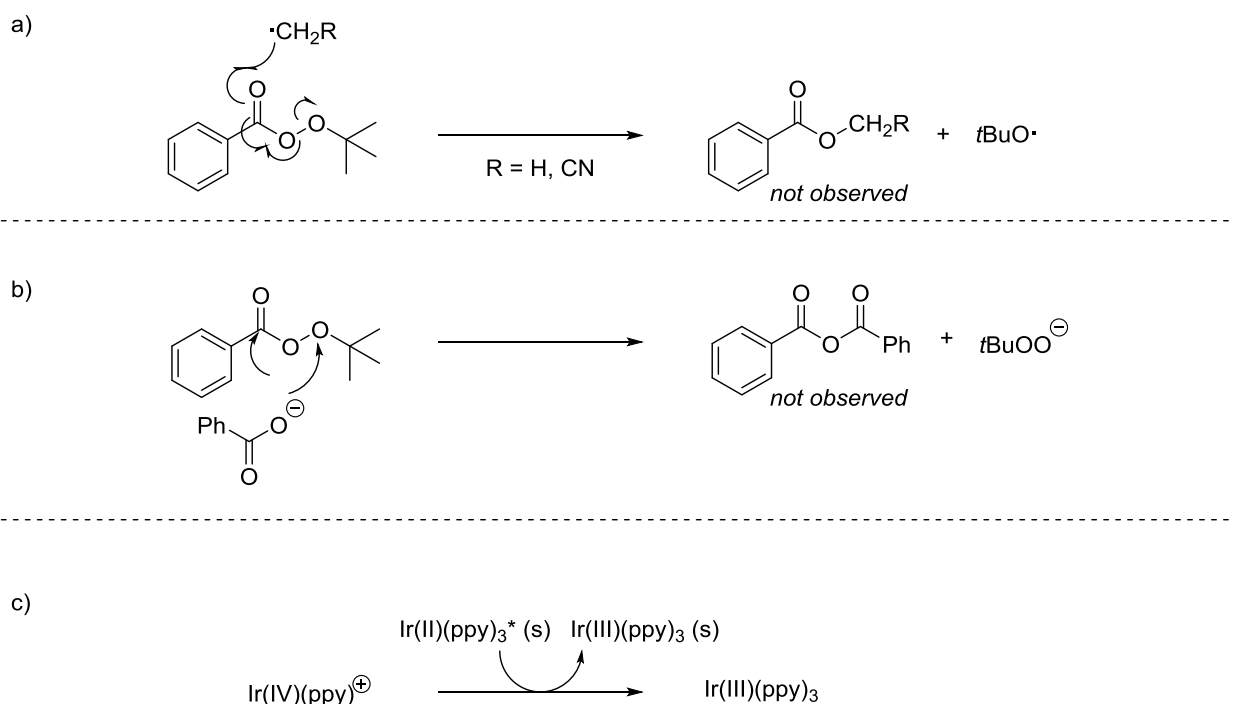
Scheme 61. Proposals for rationalizing an overstoichiometric TBPB conversion (referring to Ir(III)).

not lead to chain decomposition). A theory that would explain a catalytic decomposition of TBPB with Ir(ppy)$_3$ would base on the interaction of solid Ir(ppy)$_3$ with Ir(IV)(ppy)$_3^+$. An intermolecular electron transfer from the conduction band of undissolved Ir(ppy)$_3$ (described as Ir(II)(ppy)$_3^*$ (s)) to Ir(IV)(ppy)$_3^+$ at the interphase could recycle Ir(III)(ppy)$_3$ in solution (Ir(III)*/Ir(II): $E_{1/2} = 0.31$ V, Ir(IV)/Ir(III): $E_{1/2} = 0.77$ V vs SCE in MeCN[10], Scheme 61c). Although there was no particular report on such an electron transfer to the best of my knowledge, the benzoate anion as alternative reduction agent shows no sufficient redox potential to realize the Ir(III) recyclization (benzoate anion: $E_{1/2} = 1.64$-1.24 V vs SCE in MeCN (theo.)[161]). The lower Ir concentration under difunctionalization conditions should then contribute to a lower TBPB conversion by this means. Despite the NMR reaction featured an unexpected outcome, this NMR scale experiment was a strong indication, that TBPB can be decomposed by the photocatalyst, and most likely by the Ir(III) oxidation state.

As mentioned, also *N*-methylindole was evaluated in a NMR scale experiment on its reactivity towards TBPB. A solution of *N*-methylindole (0.15 mmol, 1.5 equiv.) and TBPB (0.1 mmol, 1 equiv.) in MeCN-*d$_3$* (0.5 mL) was irradiated with white light (white LED, 40 W) in a NMR tube. While after 2 h 20 min only about 1% of TBPB was converted, after a reaction time of 13 h the NMR yields of benzoic acid (25%), acetone (~8%) and *t*BuOH (~10%) were perceptibly higher. The reaction was also carried out with the NMR tube wrapped into dark while heated up to approximately the same reaction temperature by the irradiation source. After 13h of heating, this reaction mixture presented conversions of less than 1% of TBPB to *t*BuOH and acetone each. It was found that *N*-methylindole could promote the cleavage of TBPB under white light irradiation. However, this reaction was rather slow, but arguably is the cause of the remarked activity in styrene difunctionalizations with aldehydes and *N*-methylindole in absence of the photoredox catalyst. Due to the minor TBPB conversion compared to full conversion in the difunctionalization procedure after 12 h, the proportion of product formation that is based on purely *N*-methylindole initiation and chain propagation with TBPB in the regular procedure should be quite low.

Although *N*-methylindole was not necessary for difunctionalizations like the described imide formations had proven, as control experiment for this perspective *N*-methylindole was deployed as an additive to a major nucleophile in some reactions, which previously failed the difunctionalization. These control experiments showed no improvement to this outcome and were

yet considered since the cleavage of one TBPB molecule by *N*-methylindole could mean, that a system of Ir(III)/Ir(II) could be enabled instead of the Ir(III)/Ir(IV) proposal. Such a change in redox system could lead to further possibilities to make reactions suddenly viable.

3.3.6.3 Luminescence Quenching Experiments

Luminescence emission was measured for freshly prepared Ir(ppy)$_3$ stock solutions in MeCN for excitation irradiation of $\lambda_{ex} = 315$ nm at emission irradiation of around $\lambda_{em} = 525$ nm. Excitation and measuring bandwidth were each adjusted to 2 nm. The stock solutions were varied in their content of TBPB.

For solutions with a constant Ir concentration $c = 2 \cdot 10^{-5}$ M and a TBPB concentration in the range of $c = 1\text{-}4 \cdot 10^{-3}$ there was no diminishing of emission intensity (compared to the emission spectrum for $c(\text{TBPB}) = 0$ M) observed. This result was in accordance with experiments of the Knowles group with Ir(dF-CF$_3$-ppy)$_2$(dtbpy)(PF$_6$) and TBPB in DMA.[151]

The luminescence measurements were then carried out for solutions in which Ir and TBPB concentrations were closer to the actual conditions of the difunctionalization procedure. The solutions were adjusted to a constant Ir concentration of $c = 4.6 \cdot 10^{-4}$ M and a variation of TBPB concentrations in the range of $c = 0.1\text{-}1.48$ M along the measuring series. The emission intensity of the corresponding Ir(ppy)$_3$ ($c = 4.6 \cdot 10^{-4}$ M) solution in MeCN without TBPB present is referred to as I$_0$.

Figure 8 depicts an overlay of the emission spectra ($\lambda_{em} = 450\text{-}600$ nm) of the Ir solutions which differ in the content of TBPB additive. The measured emission intensity was dependent on the TBPB concentration. The higher the TBPB concentration, the lower the emission intensity (for higher resolution of the lower intensity spectra see chapter 5.7). The cause of this observation is the ability of TBPB to shorten the luminescence life-time of Ir(ppy)$_3$ by an interaction.
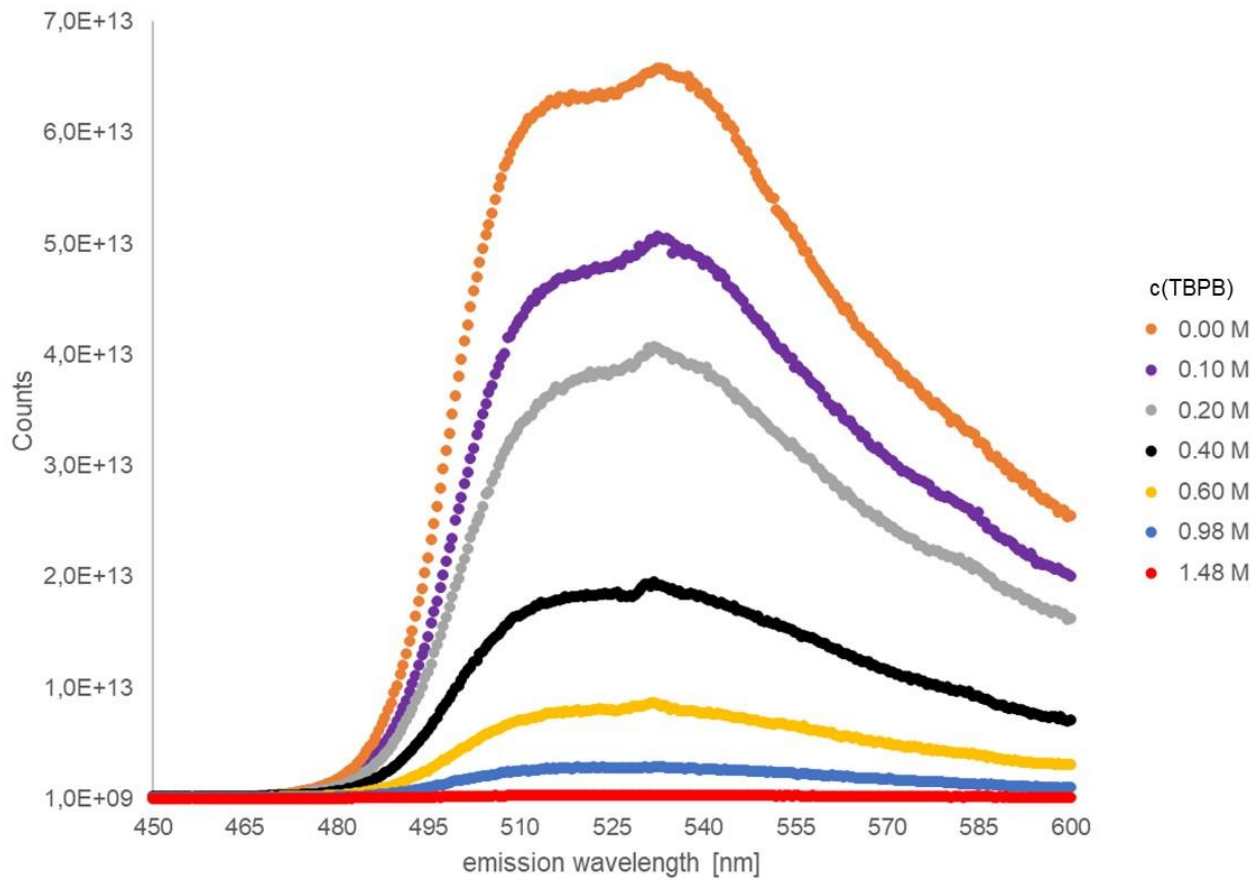
Figure 8. Emission spectra of Ir(ppy)$_3$ (c = 4.6 · 10^{-4} M) stock solutions containing different amounts of TBPB.

For a more elaborated overview on this behavior a Stern-Volmer analysis was executed, showing the ratio of I_0/I in dependency of the concentration of TBPB (c(TBPB), Figure 9 and Figure 10). Errors for I_0/I and c(TBPB) were determined on the basis of measurement inaccurancy of the
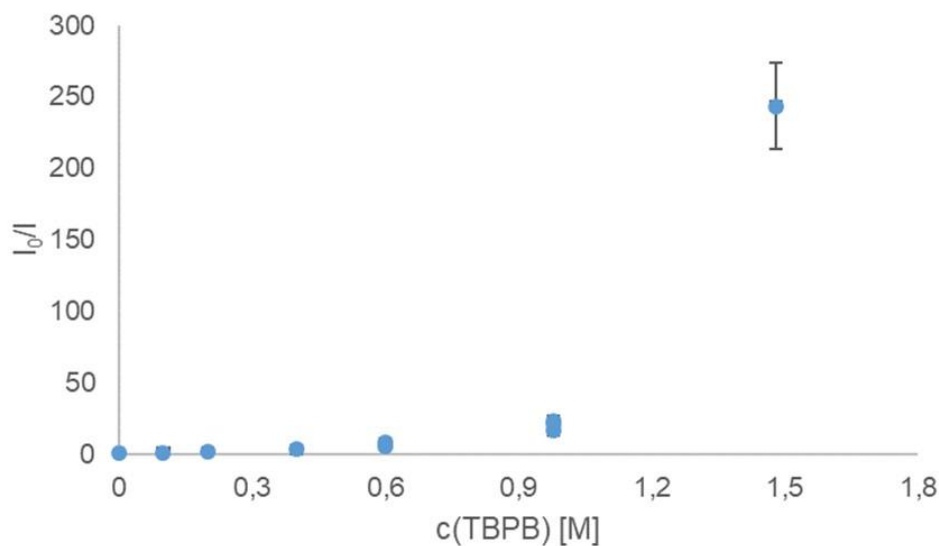

Figure 9. Stern-Volmer analysis for luminescence attenuation at λ_{em} = 525 nm of Ir(ppy)$_3$ (c = 4.6 · 10^{-4}M) stock solution containing TBPB (c = 0-1.48 M).
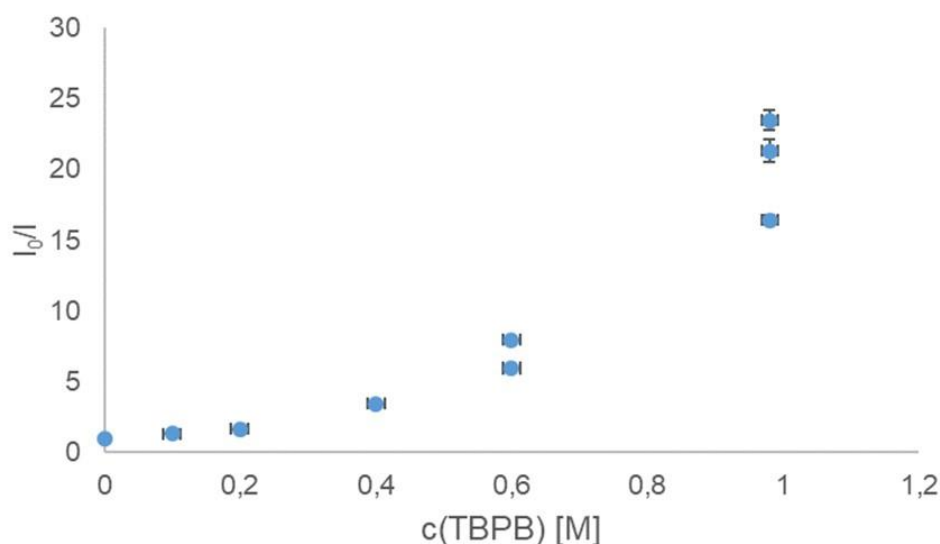
Figure 10. Stern-Volmer analysis for luminescence attenuation at λ_{em} = 525 nm of Ir(ppy)$_3$ (c = 4.6 · 10^{-4}M) stock solution containing TBPB (c = 0-0.98 M).

used Eppendorf pipette and assessement of intensity differences at maximum λ_{em} (±2 nm), respectively by calculation of error propagation (for more details see Supporting Information Ref. [2]).

For an ideal case of dynamic luminescence quenching, the ratio of I_0/I depends linearly on the concentration of the quencher. In the here analyzed luminescence quenching process, the decrease in luminescence intensity is not linearly dependent on the quencher, but of higher potency. This so-called positive deviation of the quenching process could originate from different processes.[162] Consensus in literature on such cases is that besides a dynamic luminescence quenching, also static quenching is in action.[162a,162c,163] There are different kinds and propositions on static luminescence quenching. On the one hand, the reaction of quencher with photoemitter by forming a new covalent bond could change the excitation and luminescence properties. Further, the formation of photoemitter-quencher-complexes could be a variant of static luminescence quenching.[162b,162c,163] For these examples normally a change in the emission spectra is observed.[162a] This could not be confirmed in the case of $Ir(ppy)_3$ with TBPB. On the other hand, at higher quencher concentrations the occurring proximity of photoemitter to quencher in the solution could lead to a more or less immediate quenching that deviates the quenching kinetics from the dynamic quenching model.[162a] On the background of this, it seems likely that the excited state $Ir(ppy)_3^*$ could be quenched by TBPB and that in the evaluated range of TBPB concentration, quenching proceeds rather fast upon Ir excitation because of an established proximity between donor and acceptor molecules.

3.3.6.4 Light-Switch Experiments

Besides a catalytic activity, there was also the possibility that $Ir(ppy)_3$ acted as initiator instead. Along this scenario, after one molecule of TBPB got cleaved, further propagation could proceed by electron transfer from benzyl intermediate **I1** to another TBPB molecule to form the benzylic carbocation intermediate and reductively cleave TBPB to benzoate anion and H-acceptor *tert*-butoxyl radical. If this reaction pathway would be the mechanism in act, the reaction would proceed after an initial irradiation phase with a substantial degree in the absence of light, and with a rather similar rate in comparison to the up-lighted reaction mixture. In order to pursue the enlightment of this issue, two reactions on a NMR scale were carried out, alternating phases of irradiation and darkening of the reaction mixture over a total reaction time of 140-150 min. After each phase of irradiation or darkening, the reaction progress was verified by ^{1}H NMR analysis.

For the first NMR experiment, Ir(ppy)$_3$ (4.6 · 10^{-4} mmol, 0.5 mol%) and NaHCO$_3$ (0.2 mmol, 2 equiv.) were dispersed in MeCN-d_3 (1.0 mL). Styrene (0.1 mmol, 1 equiv.), *N*-methylindole (0.5 mmol, 5 equiv.), pivaldehyde (0.5 mmo, 5 equiv.) and TBPB (0.2 mmol, 2 equiv.) were added to the dispersion in the NMR tube. Before irradiation and NMR measurements, the mixture was rigorously shaken. For the irradiation phases the sample was placed in the center of the white light sheating that was used for the synthetic difunctionalization procedure (white LED, 40 W, Δ). For the alternating dark phases, the NMR tube was wrapped in aluminum foil while placed also in the photo reactor, where it was heated to a nearly same reaction temperature (Δ, Figure 11).
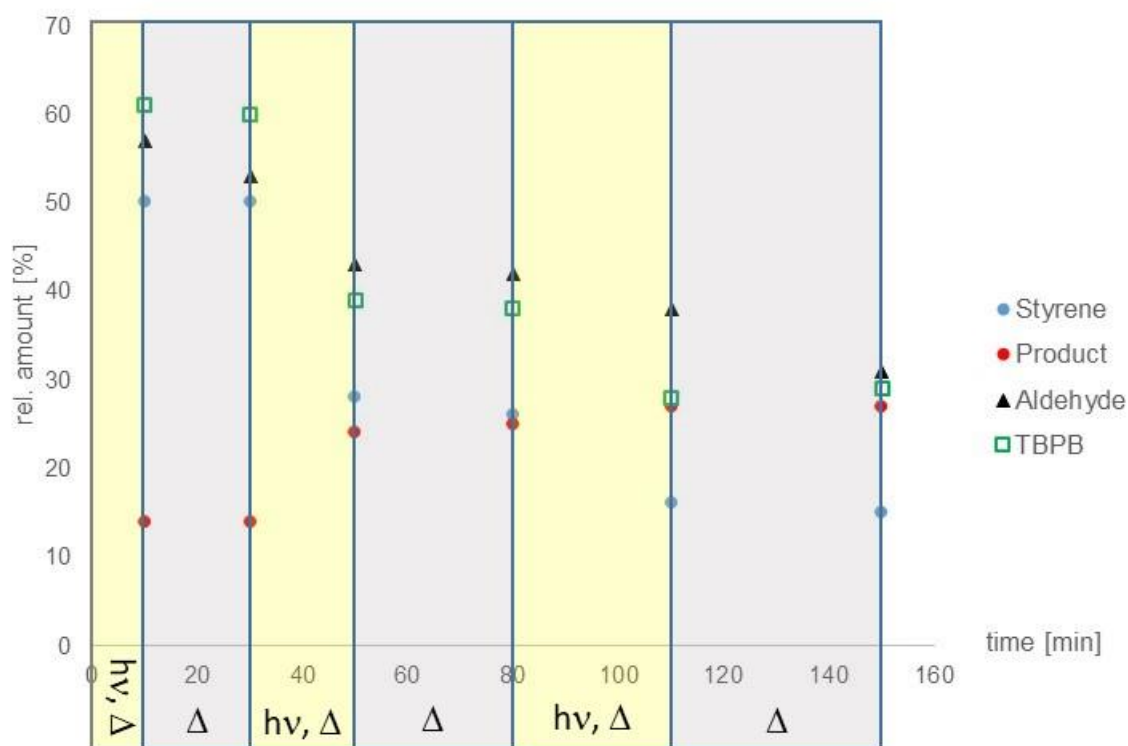
Figure 11. Light-switch experiment for styrene difunctionalization with pivaldehyde and *N*-methylindole, in which irradiation and dark phase were both heated to the same temperature.

The phases are represented by yellow or grey underlay, respectively in Figure 11 and Figure 12. After a first irradiation phase of 10 min, a NMR yield of 14% for the difunctionalization product could be determined. Conversions were progressed to 50% for styrene, 43% for pivaldehyde and 39% for TBPB at that time. The reaction was conducted in a following dark phase of 20 min, a irradiation phase of 20 min, another dark phase of 30 min and an irradiation phase of 30 min

110

before performing a final dark phase of 40 min. The ^{1}H NMR measuring time was not counted into the reaction times, measuring was performed immediately after each irradiation and dark phase. Quantification revealed that product formation was restricted to irradiation phases (1st irradiation phase: 0%→14%; 2nd irradiation phase: 14%→24%; 3rd irradiation phase: 25%→27%), while no product formation was observed during dark phases. For the starting materials styrene, pivaldehyde and TBPB, the conversions proceed mostly during the irradiation phases. Lower conversion of the reagents could be observed during the dark phases. Especially, the pivaldehyde conversion progressed without irradiation needed (1st dark phase: 43%→47%; 2nd dark phase: 57%→58%; 3rd dark phase: 62%→69%).

For the second NMR experiment, the reaction mixture was prepared in the same manner. The main difference in reaction conduction was that during the dark phases, the reaction mixture was kept at r.t.. Therefore, measuring times were also counted as reaction time during dark phases. After a first irradiation phase of 10 min, 16% of difunctionalization product were formed. For starting materials conversions of 35% for styrene, 33% for pivaldehyde and 32% for TBPB were determined. The irradiation phase was followed by a 20 min dark phase, another 20 min of irradiation phase, further 30 min of dark phase, 30 min of an irradiation phase and a final dark phase of 30 min (Figure 12). For the product formation the irradiation was authoritative (1st irradiation phase: 0%→16%; 2nd irradiation phase: 16%→26%; 3rd irradiation phase: 27%→30%) while in the dark phases product formation was observed in the magnitude below measurement accuracy and especially in the first dark phase a striking difference to the previous and subsequent irradiation phases was demonstrated. For the starting material conversions strinkingly low progress was determined in the dark phases, alluding to the same trend as for the product formation and the first NMR light-switch experiment. Merely, the conversion of pivaldehyde in the dark phases was noticeable (3rd dark phase: 48%→52%).

The experiments were carried out without stirring for a heterogeneous reaction mixture, so that observed conversions were not strictly representative for corresponding reaction progression in screening or synthetic application mentioned above, but rather deliver an approximation of quantitative reaction results during the irradiation phases.

Overall the light-switch experiments state that the difunctionalization reaction of styrene with pivaldehyde and *N*-methylindole in MeCN solution proceeds only if visible light irradiation is

applied in the presence of Ir(ppy)₃. And the reaction does not progress in the absence of light after a phase of irradiation, neither at r.t. nor at elevated temperature (temperature of irradiation phase). It could be observed that starting materials, especially pivaldehyde could be transformed during the exclusion of irradiation, but not in favor of difunctionalization. Therefore, the reaction is in competition to some radical chain processes, but is itself based on catalysis. Ir(ppy)₃ is photocatalytically active in the formation of product **19**.
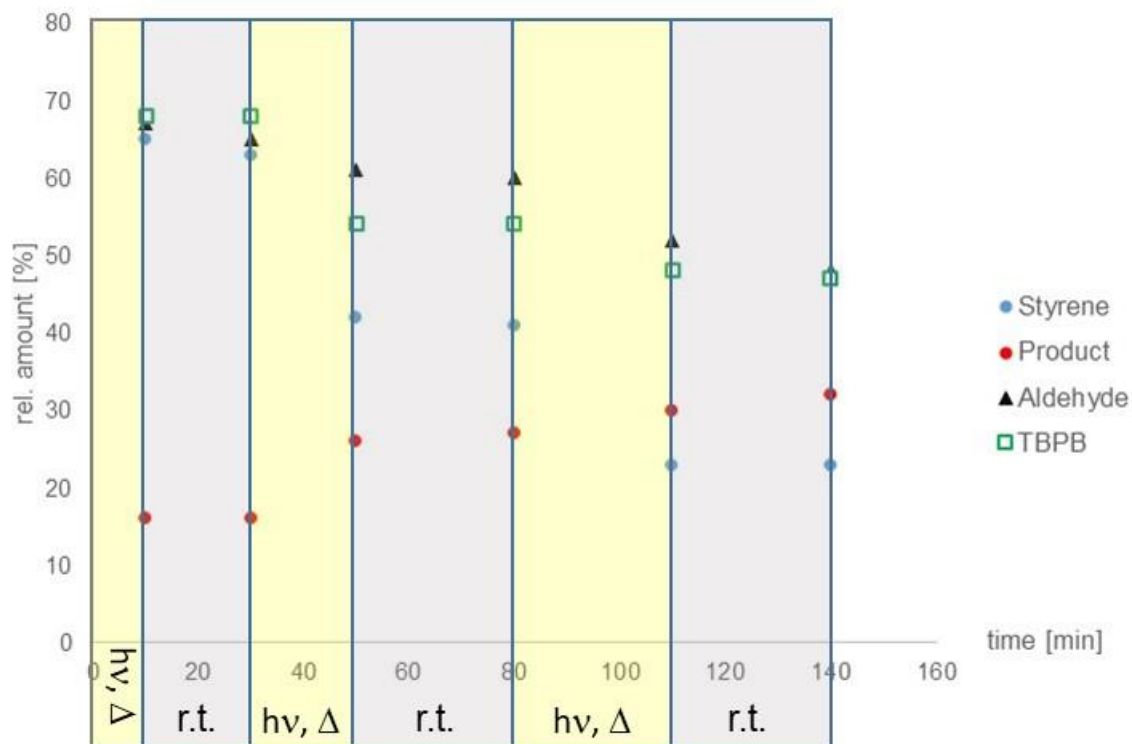
Figure 12. Light-switch experiment for styrene difunctionalization with pivaldehyde and *N*-methylindole, in which the dark phase was held at r.t..

4 Conclusion

4.1 Artemisinin as Radical Initiator in Aqueous Acrylamide Polymerization

Artemisinin was used together with hydrochloric acid and iron species as co-initiators to start radical polymerizations of acrylamide in aqueous medium at 37°C. The three individual components of the initiator combination were by themselves, or as combination of two, incapable to start an acrylamide radical chain reaction. Artemisinin and hydrochloric acid could efficiently be used in amounts of 0.5 mol% and 1 mol%, respectively, referring to acrylamide. In this system, iron species were already potent in trace amounts, like as impurity in reagents of common commercial purity.
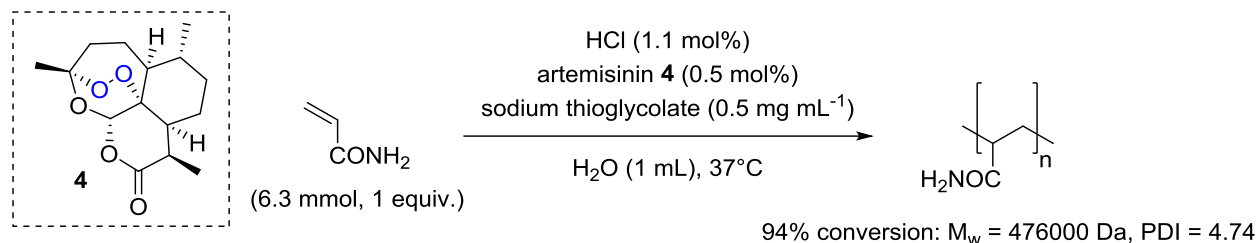
^{a} traces of iron species necessary

Its necessity to the polymerization application was verified as the iron chelator deferoxamine (DFO) could inhibit every polymerization procedure found in this study. Hydrochloric acid has a special status in this system. Applying HCl of high purity (trace metal grade, <1 ppb Fe), the polymerization would still proceed to some extend in presence of trace iron impurities from the other reagents, while analogous hydrobromic or hydroiodic acid (of common commercial purity grade) were both inactive as co-initiator. Along the studies, only methanephosphonic acid and *o*-benzsulfonimide were found as potential alternatives to HCl. In order to form water soluble polyacrylamides with assumingly lower degree of branching a chain transfer agent, sodium thioglycolate, was used as described in literature.[132a] For an acrylamide (6.3 mmol, 1 equiv.) solution in deionized water (1 mL) and in the presence of sodium thioglycolate (0.5 mg mL^{-1})[132a], artemisinin (0.5 mol%) and just HCl (1.1 mol%) of ACS purity grade (0.2 ppm Fe) without extra iron addition, were applied to reach high monomer conversion of 89% after 17.5 h. Average molecular weights of M_w = 476000 Da and a broad distribution (PDI = 4.74) were determined by gel permeation chromatography (GPC, Polymer Standards Service GmbH) for the resulting polymer mixture. With 5,5-dimethylpyrrolidinone-*N*-oxide (DMPO) present, a radical formed from the initiator system of artemisinin and HCl (0.2 ppm Fe) in aqueous medium could be

observed as DMPO-adduct by *electron paramagnetic resonance* (EPR) spectroscopy (Dr. Sonia Chabbra, Dr. Shannon Bonke, group of Dr. Alexander Schnegg at MPI für Energiekonversion, Mülheim). The unknown radical-adduct was characterized by $g_{iso} = 2.0061$, $^{H}A_{iso} = 58.2$ MHz and $^{N}A_{iso} = 43.2$ MHz. So far, attempts of preparative radical trapping were unsuccessful, but a future identification of the formed radical could contribute to a better understanding of the radical chemistry of artemisinin.

4.2   Free-Radical Alkene Difunctionalizations with Ketone-derived and Cyanidyl Radicals

A method for alkylation-cyanation of alkenes was discovered by Dr. Wen Shao, relying on α-ketonyl radical formation from ketones with *tert*-butylhydroperoxide (TBHP) by Brønsted acid catalysis. Previously the aforementioned radical formation was applied to form γ-peroxyketones by addition of α-ketonyl and *tert*-butylperoxyl radicals to styrenes in the group.[3] The alkylation-cyanation procedure was carried out in dichloromethane (DCM) at 50°C. The radical formation was achieved by methanesulfonic acid (MsOH)-catalyzed condensation of ketone and TBHP and O–O bond cleavage of the resulting alkenyl peroxide.[51] The cyanation of radical-alkene-adduct intermediate succeeded with methanesulfonyl cyanide (MsCN) to form the corresponding γ-cyanoketone.
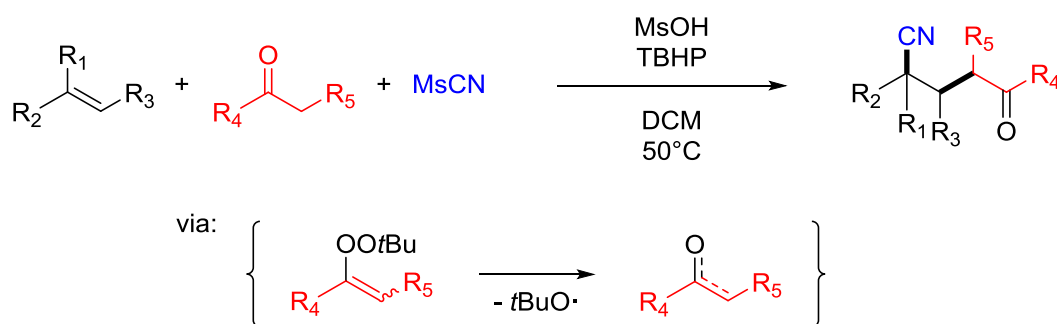
After I joined the project, we explored the application of aliphatic alkenes in this method. We could establish a series of aliphatic alkenes bearing different functional groups and in addition (*R*)-limonene could be functionalized at the exo-cyclic double bond. Furthermore, Wen Shao proved that γ-cyanoketones could be transformed by ensuing sequences of reduction-cyclization or hydrogenation-cyclization to the corresponding lactones or piperidines. Characterization of piperidines **16** by 2D NMR analysis (CDCl$_3$) revealed that in the major diastereomer the aryl substituents had a relative *trans* configuration. Interestingly, the analysis also showed the
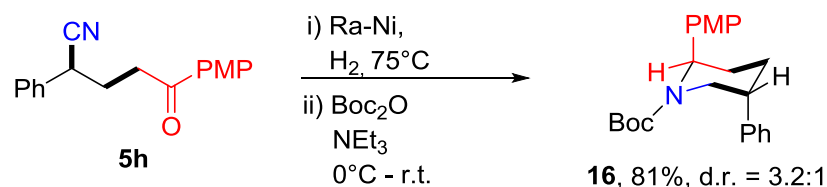
preferential axial orientation of the two aryl substituents. Theoretical calculations (DFT, PD Dr. Martin Breugst, Universität zu Köln) approved, that the axial-axial conformation is energetically beneficial, arguably due to steric repulsion between *tert*-butoxycarbonyl (Boc) and *p*-methoxyphenyl (PMP) groups and a complementary interaction of piperidines nitrogen lone pair with the adjacent σ* orbital of the C–PMP bond.[1] For difunctionalizations of indene, the alkylation-cyanation showed higher diastereoselectivities compared to the related alkylation-peroxidation procedure (up to d.r.>19:1 vs. up to 1.7:1). We believed that this is caused by mechanistic differences between the radical peroxidation and the cyanation process. The higher diastereoselectivity of the cyanation could be rationaliazed by the addition of the benzyl radical intermediate to the C–N triple bond of the sulfonyl cyanide compared to a radical-radical-combination for the respective peroxidation process. The ability of sulfonyl groups to act as homolytic leaving groups in β-position to radicals is consistent to this mechanistic proposal.[143,145] Calculations were planned with PD Dr. Martin Breugst for future investigations of the cyanation process.

4.3   Additions of Aldehyde-derived Radicals and Nucleophilic *N* Alkylindoles to Styrenes

A vicinal acylation-arylation technique for styrenes was developed, able to use straightforward aldehydes as H-donors and thus for radical acylation. *N*-Alkylindoles or 1*H*-benzotriazol served as nucleophiles to form the second σ bond from the C–C double bond in one reaction. Further, the technique was implemented by using photoredox catalyst Ir(ppy)$_3$, *tert*-butyl perbenzoate (TBPB) as oxidant and source of *tert*-butoxyl radicals. The employment of a base was necessary in order to obtain the difunctionalization product. NaHCO$_3$ was used in the technique and the reactions were carried out under argon gas atmosphere in acetonitrile at 65°C.
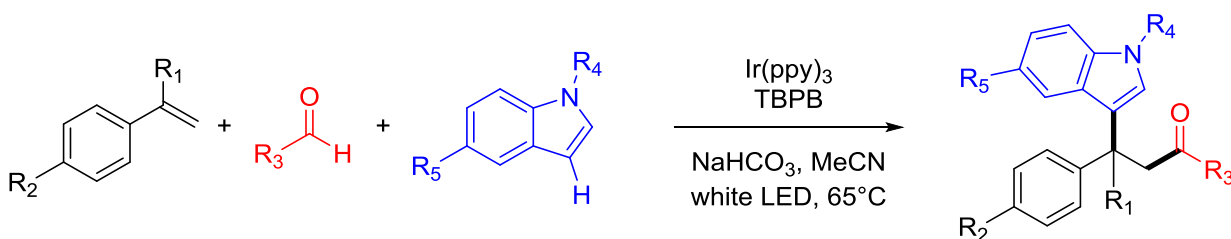
The photoredox catalyzed methodology was outlined from the reduction potentials of Ir(ppy)$_3$[10] and *tert*-butyl perbenzoate (TBPB)[152], which characterize an electron transfer from photoexcited Ir(III)* to TBPB as exergonic process and enabled a system of Ir(IV)/Ir(III) to act. In experiments, this was supported by quenching the luminescence of Ir(III)(ppy)$_3$* with TBPB in acetonitrile. A Stern-Volmer analysis revealed that dynamic as well as static quenching processes might be involved. The reductive cleavage of TBPB was needed for the generation of H-acceptors *tert*-butoxyl radicals. Thus, the applied radicals in the difunctionalization were formed by hydrogen atom transfer (HAT). Recyclization to Ir(III) followed upon an electron transfer from radical-addition-adduct of the styrene (benzyl radical), while forming a benzylic carbocation intermediate.[10,153] This cation in turn engaged in a reaction with a nucleophile. White light LED irradiation delivered the excitation energy of the catalyst and the light source generated the heat for a reaction temperature of 65°C in the vessel as well. The
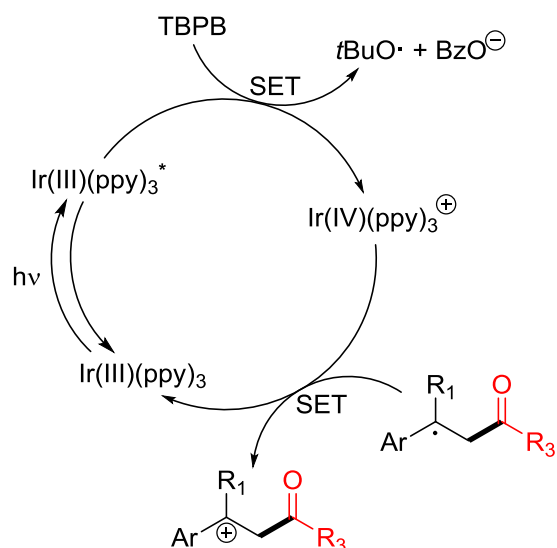
transformation proceeds also at room temperature and a thermal or an irradiative perester cleavage were not observed at 65°C and white light irradiation. The approach realized the first difunctionalization technique of adding acyl radicals generated from aldehydes together with a nucleophile to an alkene. In general, many different substituted benzaldehydes were shown to work fine in this procedure. Moreover, aliphatic aldehydes were suitable substrates. Interestingly, for pivaldehyde only the decarbonylated[154] product could be isolated, while for aldehydes with less substituted α-carbonyl centers no indication for decarbonylation could be observed. Radical alkene difunctionalization techniques showed up to the date of this thesis firm limitations. Discussing difunctionalizations implementing indole nucleophiles, all actual literature reports demonstrated that best results were received with electron-donor substituted styrenes and the successful use of electron-withdrawing substituted styrenes was rare. This indicated the importance for stabilization of a benzylic carbocation intermediate. In the here presented method, this was manifested by the preference of benzaldehydes to form products with *p*-methoxy- or α-substituted-styrenes. For instance, this could be harnessed to form a variety of *N*-methylindole-derived products bearing an all-carbon quaternary center. In most reactions with substrate combinations, that are incompatible to the technique, no alternative reaction product could be isolated, impeding rationalization[164] and leaving space for future works in this field of chemistry for deeper understanding. In addition, when dispensing *N*-alkylindole from the reaction mixture, alkyl nitrile solvents were found to fulfill the role of nucleophiles. The present benzoate anion (from TBPB cleavage) led to the formation of imides. This could be explained by the consecutive nucleophilic attack of the anion to the nitrilium cation and a Mumm rearrangement[94]. The possibility to use some chemically different nucleophiles further supported the inclusion of a carbocation intermediate in the reaction mechanism. Among the imide preparations a product bearing a *tert*-butoxyl group had been synthesized, further indicating the presence of the corresponding radical in the reaction system.

5   Experimental Section

5.1   General Methods

If not stated otherwise, chemicals were used as received from commercial distributors. Solvents used for column chromatography (hexanes, ethylacetate, dichloromethane) were of technical grade. Organic solvents used in reactions and reaction optimizations were used dried (MeCN, dimethylformamide (DMF), dimethylacetamide (DMA) commercially available; dichloromethane, diethyl ether, tetrahydrofuran, methanol were dried by distillation methods in-house) and stored under argon atmosphere. Water as reaction solvent was used as received from local deionization process of Max-Planck-Institut für Kohlenforschung, Mülheim/Ruhr, Germany.

Methylsulfonyl cyanide (MeSO$_2$CN)[59], substituted *N*-methylindoles[165], substituted α-methylstyrenes[166] were synthesized in adaption of known procedures.

Parts of the following synthesis, characterizations and descriptions can be found in published articles.[1-2]

γ-Peroxyketone **17** was synthesized according to the difunctionalization procedure by the Klußmann group.[3] γ-Cyanoketone **18** was synthesized according to the procedure by the Klußmann group.[1] Polymerizations of acrylamide in aqueous medium were carried out, leaning on a procedure by Bovey and Tiers.[132a]

Thin-layer chromatography was used for determining reaction progression and product separation procedures on Macherey-Nagel Polygram Sil G/UV254 thin-layer plates. Spots were visualized by UV-light irradiation and/or staining with an acidic cerium ammonium molybdate, an acidic *p*-anislaldehyde, an acidic vanillin and/or a basic KMnO$_4$.

For column chromatography, Merck Silica Gel 60 (40-63 μm) was used as stationary phase. Yields are given for pure, isolated compounds and referred to limiting reagents of the specific reaction, if not stated otherwise.

Preparative thin-layer chromatography (PTLC) were performed with POLYGRAM Sil G UV254 (500 μm) from Macheney-Nagel or Silica Gel GF (1500 μm) from Miles Scientific

High performance-liquid chromatography (HPLC) for reaction and diastereomer analysis were carried out on a Shimadzu LC-20A HPLC system.

Gas chromatography (GC) analysis was performed on a Agilent Technologies 6890N Network GC System equipped with a MN Optima 5 Accent capillyry column (0.32 mm x 30 m x 0.25 µm) and a flame ionization detector using *n*-heptadecane as internal standard. Probes contained 3-5 µL reaction mixture with DCM (~1 mL), when for analysis 1 µL was injected by autosampler. The device was coupled with an Agilent Technologies 5975C VL MSD mass detector for GC-MS measurements.

^{1}H, ^{13}C nuclear magnetic resonance (NMR) spectra were resolved from probe measurements on Bruker AV300, AV400, AV500 or AV600 spectrometers. Listings of probe signals are connected to the measurement's frequency and solvent in the following. All chemical shifts are given downfield relative to TMS and are referred to a resonance of residual solvent protons.[167] ^{19}F NMR spectra were resolved from probe measurements on Bruker AV300 or AV500 spectrometers.

High resolution mass spectra were gained by probe measurement on a Bruker APEX III FTICR-MS or a Finnigan SSQ 7000 quadrupole MS or Finnigan MAT 95 double focusing sector field-MS device.

Luminescence measurings were performed on an Edinburgh Instruments FS5 Spectroflurometer equipped with a Xenon arc lamp (150 W, CW, ozone-free) as light source. Monochromators were of Czerny-Turner design with plane gratings and the emission detector a Photomultiplier R928P arranged in a 90° angle with the sample and light source. The samples were measured as solutions in a square quartz cuvette (dimensions: 10 mm x 10 mm) at room temperature (r.t.).

Gel permeation chromatography (GPC) spectra were derived from probe measurements over PSS Suprema columns (30°C, modified acrylate copolymer, 10 µm pore size, 8 mm inner diameter, series of 1 guard column (50 mm length) and 3 Ultrahigh columns (300 mm length each)) in cooperation with the company polymer standard solutions (PSS) in Mainz, Germany. As eluent a solution of $NaNO_3$ (0.1 M) in deionized water was used. The PSS SECcurity 1260 HPLC pump produced a flow rate of 1 mL min^{-1}. Samples (50 µL of diluted rection mixtue (~3 mg mL^{-1} in eluent with 0.05% ethylene glycol as internal standard)) were injected by PSS SECcurity 1260 Autosampler. PSS SECcurity 1260 Differential Refractometer RID was used as detector and the

spectra were analyzed on PSS WinGPC UniChrom (version 8.33). Molar masses refer to computed numerical solutions based on a calibration curve with solutions of pullulan of different molar masses (180-2350000000 Da).

Electron paramagnetic resonance (EPR) spectra were resolved from probe measurements on a X-band spectrometer from Magnettech GmbH of type MS5000 at 40°C/313 K in cooperation with the Schnegg group at the Max-Planck-Institut für Energiekonversion in Mülheim/Ruhr, Germany. The resonances were recorded at microwave frequency of 9.4753 GHz adjusted at a microwave power of 10 mW. Furthermore a field sweep of 15 mT, centered at 337.5 mT, a modulation amplitude of 0.1 mT and a sweep time of 30 s were applied. Samples of aqueous media were measured in a EPR tubes of 1.6 mm (o.d.). Spectra were recorded every two minutes. The EasySpin Software was used for simulations.

5.2 General Synthesis Procedures

5.2.1 Polymerization of Acrylamide
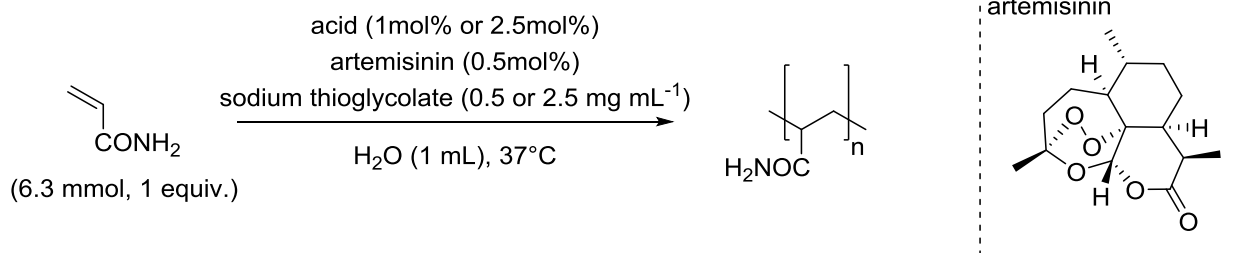
Scheme 62. Artemisinin initiated polymerization of acrylamide.

To a mixture of acrylamide (450 mg, 6.33 mmol, 1.0 equiv.), artemisinin (8.9 mg, 0.032 mmol, 0.5 mol%) and sodium tosylate as internal standard, an aqueous stock solution of sodium 2-mercapto acetate (1 mL, 10 mg/20 mL or 50 mg/20 mL, respectively, as chain-transfer agent) was added in a GC vial. While acrylamide fully dissolves, artemisinin mostly stays undissolved. After the addition of acid (aqueous HCl solution, methylphosphonic acid or *o*-benzodisulfonimide; 0.07 mmol or 0.16 mmol, 1 mol% or 2.5 mol%, respectively) and closure of the vial, the reaction mixture was allowed to react at 37°C without stirring for 16-18 h. After samples for NMR analysis were taken, the reaction mixtures were stored at -20°C.

Note that iron needs to be present in traces. For concentrated HCl of J.T. Baker with ACS grade purity contains 0.2 ppm Fe.

5.2.2 General Procedure of γ-Cyanoketones
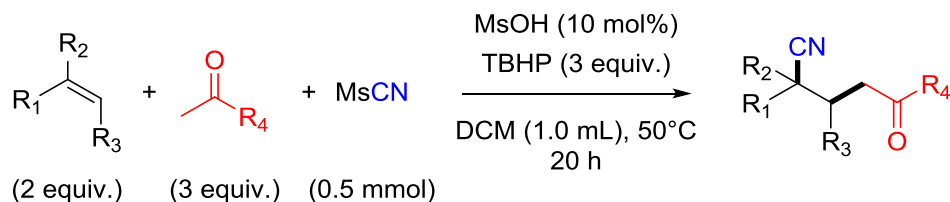
Scheme 63. General formation of γ-cyanoketones

Methanesulfonyl cyanide (0.5 mmol, 1.0 equiv.), alkene (1.0 mmol, 2.0 equiv.), ketone (1.5 mmol, 3.0 equiv.) and tBuOOH (TBHP, 5.5 M solution in decane, 1.5 mmol, 3.0 equiv.) were dissolved in dry DCM (1.0 mL) under Ar gas atmosphere in a 10 mL Schlenk-tube. Methanesulfonic acid (0.05 mmol, 10 mol%) was finally added and after sealing the tube, the reaction mixture was stirred overnight at 50°C (about 20 h).

The cooled down reaction mixture was diluted with EtOAc, transferred and all volatiles were removed under reduced pressure. The residue has been purified by column chromatography on silica gel, using mixtures of hexanes/EtOAc to afford the desired γ-cyanoketone. (In cases of vinylarenes sometimes together with the sulfonyl peroxide).

5.2.3 General Procedure of β-(Indol-3-yl)ketones
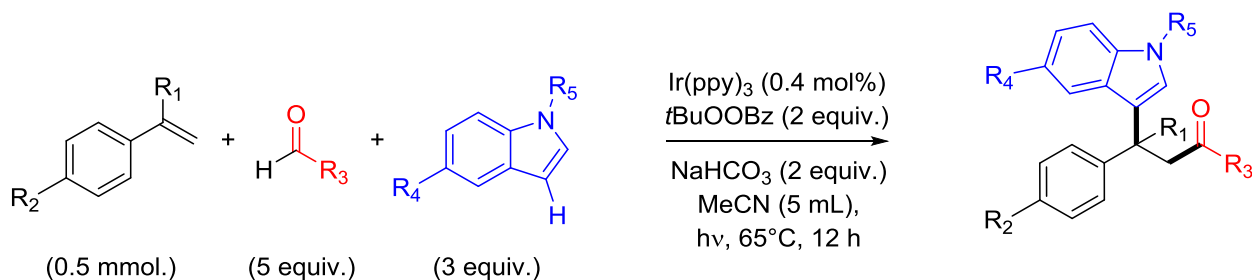
Scheme 64. General formation of β-(indol-3-yl)ketones

Tris(2-phenylpyridinato-$C2,N$-)iridium (III) (Ir(ppy)$_3$, 1.3 mg, 0.004 equiv.) and sodium hydrogencarbonate (84 mg, 1 mmol, 2 equiv.) were dispersed in dry acetonitrile (5 mL) under Ar gas atmosphere in a Schlenk-round-bottom-flask (100 mL, 0.5 mmol scale). Subsequently the corresponding styrene (0.5 mmol, 1 equiv.), N-methylindole (1.5 mmol, 3 equiv.), aldehyde (2.5 mmol, 5 equiv.) and TBPB (1 mmol, 2 equiv.) were added to the yellow dispersion. The
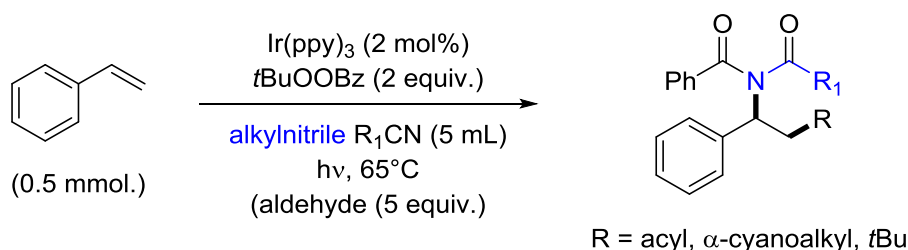
reaction mixture was stirred while irradiated with white light (40 W white LED) for 12 h. The irradiation power produced a reaction temperature of around 65°C.

The reaction mixture was diluted, dried under reduced pressure (after addition of some silica) and the residue was purified by column chromatography using eluent mixtures of hexanes/EtOAc.

The indole compounds often have showed to decompose when stored in solution.

For pivaldehyde the corresponding decarbonylated product has been isolated.

5.2.4 General Procedure of Imides

Reagents over arrow: Ir(ppy)$_3$ (2 mol%) / tBuOOBz (2 equiv.) / alkylnitrile R$_1$CN (5 mL) / hν, 65°C / (aldehyde (5 equiv.))

Starting material label: (0.5 mmol.)

Product label: R = acyl, α-cyanoalkyl, tBu

Scheme 65. General formation of imides.

Tris(2-phenylpyridinato-*C2,N*-)iridium (III) (Ir(ppy)$_3$, 0.02 equiv.) was dispersed in dry alkylnitrile (1 mL, 0.1 mmol scale /5 mL, 0.5 mmol scale, respectively) under Ar gas atmosphere in a Schlenk-tube (10 mL)/Schlenk-round-bottom-flask (100 mL), respectively. This was followed by adding styrene (1 equiv.), (aldehyde if required (5 equiv.)) and TBPB (2 equiv.) to the yellow dispersion. The reaction mixture was stirred while irradiated with white light (40 W white LED) for 20 h. The irradiation power produced a reaction temperature of around 65°C.

The reaction mixture was diluted and transferred, dried under reduced pressure (after addition of some silica) and the residue was purified by column chromatography using mixtures of hexanes/EtOAc as eluent.

5.3 Synthesis Products and Characterization
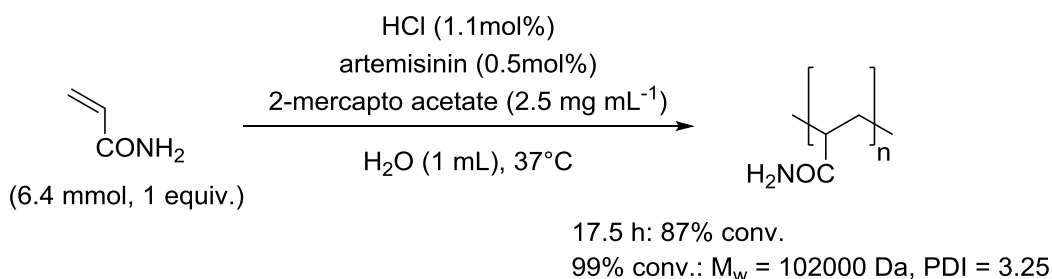
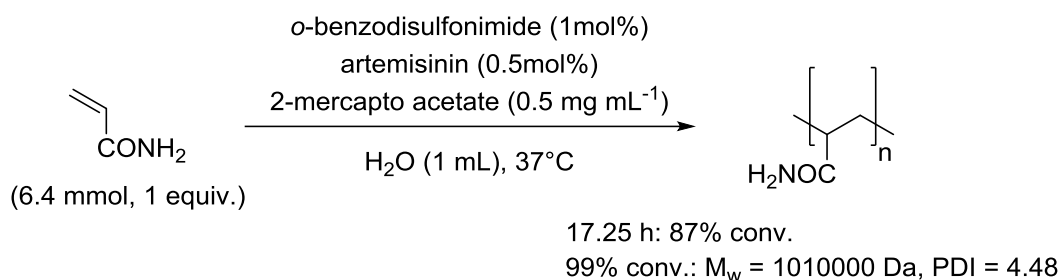### 5.3.1 Polyacrylamide Products

Polyacrylamide LB008
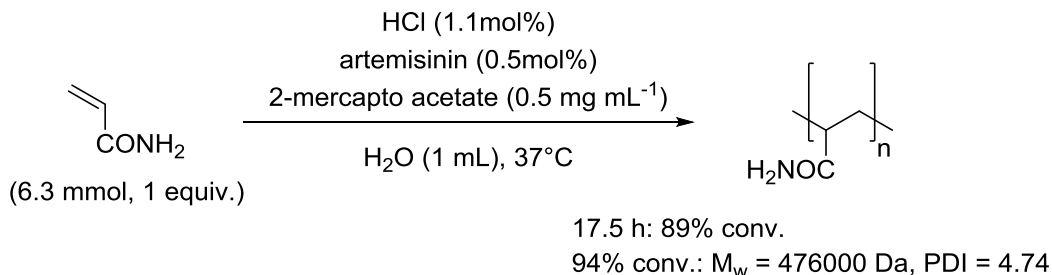
Scheme 66. Acrylamide polymerization with HCl and low transfer agent concentration.

The general procedure for polymerization of acrylamide using an aqueous solution of HCl (37 wt%, 6 µL, 1.1 mol%) as acid and sodium 2-mercapto acetate in a concentration of 0.5 g mL^{-1} as chain-transfer-agent led to the conversion of 89% of acrylamide to polyacrylamide after 17.5 h. After reaching 94% conversion the sample was send to Polymer Standard Solutions for analysis by GPC. The polymer sample featured $M_n = 100000$ Da, $M_w = 476000$ Da, $M_z = 1620000$ Da and a PDI = 4.74.

Polyacrylamide LB010

Scheme 67. Acrylamide polymerization with HCl and high transfer agent concentration.

The general procedure for polymerization of acrylamide using an aqueous solution of HCl (37 wt%, 6 µL, 1.1 mol%) as acid and sodium 2-mercapto acetate in a concentration of 2.5 g mL^{-1} as chain-transfer-agent led to the conversion of 87% of acrylamide to polyacrylamide after 17.5 h. After reaching 99% conversion the sample was send to Polymer Standard Solutions for analysis

by GPC. The polymer sample featured M_n = 31400 Da, M_w = 102000 Da, M_z = 206000 Da and a PDI = 3.25.

Polyacrylamide LB080

Scheme 68. Acrylamide polymerization with *o*-benzodisulfonimide.

The general procedure for polymerization of acrylamide using *o*-benzodisulfonamide (14 mg, 1.0 mol%) as acid and sodium 2-mercapto acetate in a concentration of 0.5 g mL^{-1} as chain-transfer-agent led to the conversion of 87% of acrylamide to polyacrylamide after 17.25 h. After reaching 99% conversion the sample was send to Polymer Standard Solutions for analysis by GPC. The polymer sample featured M_n = 225000 Da, M_w = 1010000 Da, M_z = 3990000 Da and a PDI = 4.48.

Polyacrylamide LB114
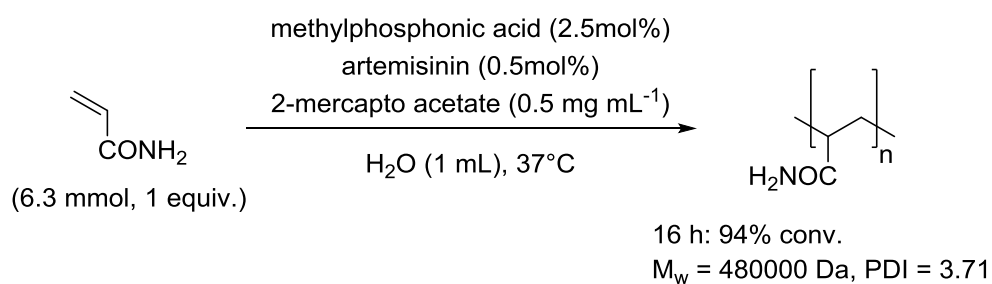
Scheme 69. Acrylamide polymerization with methylphosphonic acid (higher conc.).

The general procedure for polymerization of acrylamide using methylphosphonic acid (14.9 mg, 2.5 mol%) as acid and 2-mercapto acetate in a concentration of 0.5 g mL^{-1} as chain-transfer-agent led to the conversion of 94% of acrylamide to polyacrylamide after 16 h. The sample was send to Polymer Standard Solutions for analysis by GPC. The polymer sample featured M_n = 129000 Da, M_w = 480000 Da, M_z = 1160000 Da and a PDI = 3.71.

4-Methyl-5-oxo-2-phenylheptanenitrile (5l)
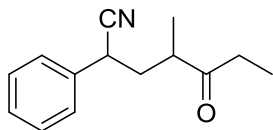
The general procedure for γ-cyanoketones by using 3-pentanone as ketone, styrene as alkene and a mixture of hexane/EtOAc (v/v = 7/1) as eluent for column chromatography lead to the isolation of **5l** as colorless viscous oil (40.2 mg, 37% yield) in a d.r. = 1.0:1 as determined by crude NMR analysis.

^{1}H NMR (501 MHz, CDCl$_3$, 1st diastereomere): δ/ppm 7.38 − 7.21 (m, 5H), 3.74 (dd, J = 11.0, 5.4 Hz, 1H), 2.95 − 2.80 (m, 1H), 2.57 (dq, J = 17.8, 7.3 Hz, 1H), 2.40 (dq, J = 17.8, 7.3 Hz, 1H), 2.22 (ddd, J = 13.7, 10.3, 5.4 Hz, 1H), 1.70 (ddd, J = 13.7, 11.0, 3.8 Hz, 1H), 1.11 (d, J = 7.2 Hz, 3H), 1.03 (t, J = 7.3 Hz, 3H).

^{13}C NMR (126 MHz, CDCl$_3$, 1st diastereomere): δ/ppm 213.7, 135.9, 129.1, 128.1, 127.1, 120.6, 43.8, 38.8, 35.6, 34.9, 18.0, 7.8.

HRMS (ESI) calculated for [C$_{14}$H$_{17}$NONa]$^+$: 238.120233, Found: 238.120330.

^{1}H NMR (501 MHz, CDCl$_3$, 2nd diastereomere): δ 7.33 − 7.24 (m, 3H), 7.21 − 7.18 (m, 1H), 3.77 (dd, J = 8.7, 7.3 Hz, 1H), 2.61 − 2.52 (m, 1H), 2.45 (dq, J = 17.9, 7.3 Hz, 1H), 2.34 − 2.21 (m, 2H), 1.76 (ddd, J = 14.1, 7.1 Hz, 1H), 1.10 (d, J = 7.1 Hz, 3H), 0.95 (t, J = 7.3 Hz, 3H).

^{13}C NMR (126 MHz, CDCl$_3$, 2nd diastereomere): δ 213.1, 135.3, 129.2, 128.3, 127.4, 120.5, 43.1, 37.9, 35.0, 34.4, 16.8, 7.7.

HRMS (ESI): calculated for [C$_{14}$H$_{17}$NONa]$^+$: 238.120233, found: 238.120300 .

2-(4,4-Dimethyl-3-oxopentyl)heptanedinitrile (7a)
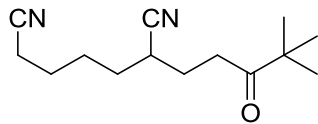
The general procedure for γ-cyanoketones by using pinacolone as ketone, 3-cyanohex-1-ene as alkene and mixture of hexane/EtOAc (v/v = 4/1→2/1) for column chromatography, led to the isolation of **7a** as colorless oil (63.8 mg, 58% yield).

^{1}H NMR (501 MHz, CDCl$_3$): δ/ppm 2.73 – 2.61 (m, 2H), 2.63 – 2.52 (m, 1H), 2.32 (t, J = 6.8 Hz, 2H), 1.96 – 1.78 (m, 1H), 1.70 – 1.52 (m, 7H), 1.10 (s, 9H).

^{13}C NMR (126 MHz, CDCl$_3$): δ/ppm 214.49, 121.41, 119.22, 44.18, 33.53, 31.76, 30.73, 26.41, 26.31, 26.29, 24.94, 17.04.

HRMS (ESI): calculated for [C$_{14}$H$_{22}$N$_2$ONa]$^+$: 257.162431, found: 257.162500.
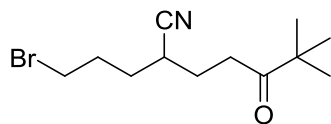
2-Isopentyl-6,6-dimethyl-5-oxoheptanenitrile (7b)
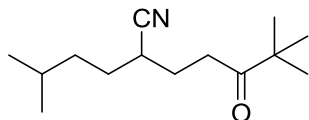
The general procedure for γ-cyanoketones by using pinacolone as ketone, 5-methylhex-1-ene as alkene and a mixture of hexane/EtOAc (v/v = 9/1) for column chromatography,lead to the isolation of **7b** as colorless oil (20.0 mg, 18% yield).

^{1}H NMR (501 MHz, CDCl$_3$): δ/ppm 2.75 – 2.59 (m, 2H), 2.55 – 2.45 (m, 1H), 1.91 – 1.81 (m, 1H), 1.70 – 1.63 (m, 1H), 1.57 – 1.46 (m, 3H), 1.39 – 1.31 (m, 1H), 1.30 – 1.20 (m, 1H), 1.09 (s, 9H), 0.84 (d, J = 2.4 Hz, 3H), 0.83 (d, J = 2.4 Hz, 3H).

^{13}C NMR (126 MHz, CDCl$_3$): δ/ppm 214.60, 121.98, 44.18, 36.15, 33.67, 31.21, 30.44, 27.72, 26.41, 26.39, 22.49, 22.26.

HRMS (ESI): calculated for [C$_{14}$H$_{25}$NONa]$^+$: 246.182833, Found: 246.182540.

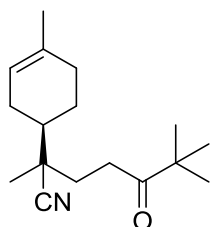## 2-(3-Bromopropyl)-6,6-dimethyl-5-oxoheptanenitrile (7c)

The general procedure for γ-cyanoketones by using pinacolone as ketone, 5-bromopent-1-ene as alkene and a mixture of hexane/EtOAc (v/v = 7/1) for column chromatography, led to the isolation of **7c** as yellow oil (31.4 mg, 23% yield).

^{1}H NMR (501 MHz, CDCl$_3$): δ/ppm 3.38 (t, J = 6.4 Hz, 2H), 2.73 − 2.62 (m, 2H), 2.63 − 2.55 (m, 1H), 2.11 − 1.99 (m, 1H), 1.98 − 1.84 (m, 2H), 1.79 − 1.65 (m, 3H), 1.10 (s, 9H).

^{13}C NMR (126 MHz, CDCl$_3$): δ/ppm 214.43, 121.34, 77.30, 77.04, 76.79, 44.18, 33.49, 32.35, 30.96, 30.92, 30.21, 29.91, 26.46, 26.42, 26.29.

HRMS (ESI): calculated for [C$_{12}$H$_{20}$NOBrNa]$^{+}$: 296.062058, found: 296.062070.

## 2,6,6-trimethyl-2-((R)-4-methylcyclohex-3-en-1-yl)-5-oxoheptanenitrile (7d)

The general procedure for γ-cyanoketones by using pinacolone as ketone, (R)-limonene as alkene and a mixture of hexane/EtOAc (v/v = 15/1) for column chromatography, led to the isolation of **7d** as colourless, viscous oil that solidifies upon freezing (d.r. = 1:1 from ^{1}H NMR, 29.0 mg, 22% yield).

^{1}H NMR (300 MHz, CDCl$_3$, 2 diastereoisomers): δ/ppm 5.50 − 5.09 (m, 1H), 2.72 − 2.50 (m, 2H), 2.17 − 1.77 (m, 6H), 1.73 − 1.52 (m, 1H), 1.59 (br, 3H), 1.45 − 1.27 (m, 1H), 1.21 (s, 3H of 1st diastereoisomer), 1.19 (s, 3H of 2nd diastereoisomer), 1.10 (s, 9H).

13C NMR (75 MHz, CDCl₃, 2 diastereoisomers): δ/ppm 214.59 (C, two diastereoisomers) , 134.40 (*C*=CH, diastereoisomer 1), 134.12 (*C*=CH, diastereoisomer 2), 123.89 (CN, diastereoisomer 1), 123.73 (CN, diasteoisomer 2), 119.73 (*C*H=C, diastereoisomer 1), 119.46 (*C*H=C, diastereoisomer 2), 44.48 (C, two diastereoisomers), 41.12 (C, diastereoisomer 1), 40.79 (C, diastereoisomer 2), 40.00 (CH, diastereosiomer 2), 39.90 (CH, diastereoisomer 1), 32.32 (CH₂, diastereoisomer 1), 32.29 (CH₂, diastereoisomer 2), 31.02 (CH₂, diastereoisomer 2), 30.78 (CH₂, diastereoisomer 1), 30.74 (CH₂, diastereoisomer 2), 30.50 (CH₂, diastereoisomer 1), 27.46 (CH₂, diastereoisomer 1), 26.60 (CH₃, two diastereoisomers), 26.26 (CH₂, diastereoisomer 2), 25.16 (CH₂, diastereoisomer 2), 24.14 (CH₂, diastereoisomer 1), 23.31(CH₃, diastereoisomer 1), 23.29 (CH₃, diastereoisomer 2), 21.12 (CH₃, diastereoisomer 2), 20.47 (CH₃, diastereoisomer 1).

HRMS (ESI): calculated for $[C_{17}H_{27}NONa]^{+}$: 284.198483, found: 284.198700.

2-(2-oxopropyl)-2,3-dihydro-1*H*-indene-1-carbonitrile (18)
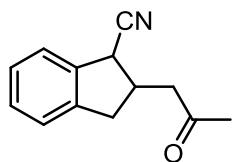
The general procedure for γ-cyanoketones by using acetone as ketone, indene as alkene and a mixture of hexane/EtOAc (v/v =7/1→5/1) for column chromatography, led to the isolation of two diastereomers **18**, each as colourless oil (minor diastereomer: 23 mg, 0.12 mmol, 23%; major diastereomer: 54 mg, 0.27 mmol, 54%).

From ¹H NMR analysis of the crude reaction mixture a d.r. = 3.6:1, from GC analysis d.r. = 3.26:1 was procured.

Minor Diastereomer (cis):

1H NMR (501 MHz, CDCl₃): δ/ppm 7.38 (d, $J = 6.7$ Hz, 1H), 7.31 − 7.21 (m, 3H), 4.35 (d, $J = 7.7$ Hz, 1H), 3.22 − 3.08 (m, 2H), 3.02 (dd, $J = 18.4, 7.8$ Hz, 1H), 2.87 − 2.73 (m, 2H), 2.23 (s, 3H).

13C NMR (126 MHz, CDCl₃): δ/ppm 206.8, 142.1, 137.1, 128.9, 127.6, 125.2, 124.9, 118.8, 45.7, 39.1, 37.7, 37.4, 30.5.

HRMS (GC-CI): calculated for $[C_{13}H_{13}N_1O_1+H]^+$: 200.106989, found: 200.106890.

Major Diastereomer (trans):

^{1}H NMR (501 MHz, CDCl$_3$): δ 7.42 – 7.38 (m, 1H), 7.30 – 7.21 (m, 3H), 3.88 (d, *J* = 9.1 Hz, 1H), 3.35 (dd, *J* = 15.8, 7.8 Hz, 1H), 3.18 – 3.07 (m, 1H), 2.96 (dd, J = 17.5, 4.8 Hz, 1H), 2.73 (dd, *J* = 17.5, 8.8 Hz, 1H), 2.62 (dd, J = 15.8, 8.8 Hz, 1H), 2.22 (s, 3H).

^{13}C NMR (126 MHz, CDCl$_3$): δ 206.3, 142.0, 136.8, 128.9, 127.5, 125.1, 124.3, 120.3, 46.8, 41.8, 40.2, 37.7, 30.4, 26.7.

HRMS (GC-EI): calculated for $[C_{13}H_{13}N_1O_1]^+$: 199.099164, found: 199.099250.

5.3.3 β-(Indol-3-yl)ketone Products

**3-(3,3-Dimethyl-1-phenylbutyl)-1-methyl-1*H*-indole (19)**
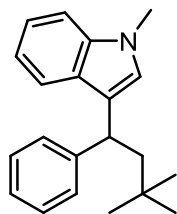
The general procedure for β-(Indol-3-yl)ketones using pivaldehyde in the reaction and a solvent mixture of hexanes/EtOAc (v/v = 200/1) as eluent in column chromatography lead to the isolation of this product as pale yellow oil (57 mg, 0.20 mmol, 39%).

^{1}H NMR (501 MHz, CDCl$_3$): δ/ppm 7.60 (d, *J* = 7.9 Hz, 1H), 7.37 (d, *J* = 7.6 Hz, 2H), 7.28 – 7.23 (m, 3H), 7.18 (t, *J* = 7.6 Hz, 1H), 7.14 (t, *J* = 7.3 Hz, 1H), 7.06 (t, *J* = 7.4 Hz, 1H), 6.77 (s, 1H), 4.34 (dd, *J* = 7.9, 5.3 Hz, 1H), 3.71 (s, 3H), 2.19 (dd, *J* = 14.1, 5.3 Hz, 1H), 2.09 (dd, *J* = 14.1, 7.9 Hz, 1H), 0.88 (s, 9H).

^{13}C NMR (126 MHz, CDCl$_3$): δ/ppm 147.0, 137.3, 128.4, 128.2, 127.2, 126.1, 125.8, 121.6, 120.9, 119.5, 118.7, 109.3, 50.1, 39.6, 32.8, 31.7, 30.4.

HRMS (ESI): calculated for $[C_{21}H_{25}N+H]^+$: 292.2060; found: 292.2060.

3-(1-Methyl-1*H*-indol-3-yl)-1,3-diphenylbutan-1-one (20a)
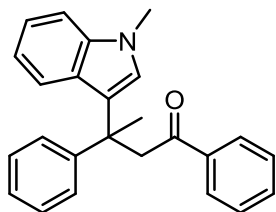
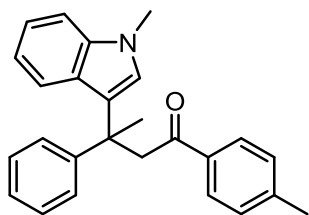The general procedure for β-(Indol-3-yl)ketones using a solvent mixture of hexanes/EtOAc (v/v = 40/1→25/1) as eluent in column chromatography lead to the isolation of the product **20a** as yellow oil (120 mg, 0.34 mmol, 68%).

^{1}H NMR (501 MHz, CDCl$_3$): δ/ppm 7.61 − 7.55 (m, 2H), 7.42 − 7.35 (m, 2H), 7.39 − 7.31 (m, 1H), 7.29 − 7.21 (m, 2H), 7.21 − 7.13 (m, 4H), 7.15 − 7.08 (m, 1H), 6.99 (d, J = 8.1 Hz, 1H), 6.91 − 6.83 (m, 1H), 6.86 (s, 1H), 4.01 (d, J = 14.1 Hz, 1H), 3.73 (d, J = 14.1 Hz, 1H), 3.66 (s, 3H), 1.98 (s, 3H).

^{13}C NMR (126 MHz, CDCl$_3$): δ/ppm 200.1, 148.3, 138.3, 137.8, 132.2, 128.2, 127.9, 127.9, 126.9, 126.7, 126.3, 126.1, 122.3, 121.4, 121.3, 118.7, 109.3, 48.5, 42.2, 32.7, 28.3.

HRMS (ESI): calculated for [C$_{25}$H$_{23}$NONa]$^+$: 376.1672; found: 376.1671.

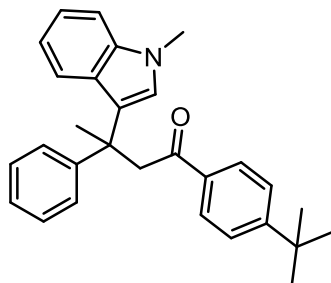### 3-(1-Methyl-1*H*-indol-3-yl)-3-phenyl-1-(*p*-tolyl)butan-1-one (20b)

The general procedure for β-(Indol-3-yl)ketones using a solvent mixture of hexanes/EtOAc (v/v = 40/1→25/1) lead to the isolation of the product **20b** as yellow oil (99 mg, 0.27 mmol, 54%).

^{1}H NMR (501 MHz, CDCl$_3$): δ/ppm 7.51 (d, J = 8.2 Hz, 2H), 7.41 − 7.34 (m, 2H), 7.24 (t, J = 7.6 Hz, 2H), 7.21 − 7.12 (m, 2H), 7.15 − 7.08 (m, 1H), 7.02 − 6.95 (m, 3H), 6.89 − 6.84 (m, 1H), 6.86 (s, 1H), 3.94 (d, J = 14.3 Hz, 1H), 3.72 (d, J = 14.3 Hz, 1H), 3.67 (s, 3H), 2.30 (s, 3H), 1.98 (s, 3H).

¹³C NMR (126 MHz, CDCl₃): δ/ppm 199.5, 148.3, 143.0, 137.8, 135.9, 128.6, 128.2, 128.1, 126.9, 126.7, 126.4, 126.0, 122.5, 121.31, 121.30, 118.6, 109.3, 48.5, 42.2, 32.7, 28.3, 21.6.

HRMS (ESI): calculated for [C₂₆H₂₅NONa]⁺: 390.1828; found: 390.1825

## 1-(4-(*Tert*-butyl)phenyl)-3-(1-methyl-1*H*-indol-3-yl)-3-phenylbutan-1-one (20c)

The general procedure for β-(Indol-3-yl)ketones using a solvent mixture of hexanes/EtOAc (v/v = 40/1→22/1) lead to the isolation of the product **20c** as yellow oil (79 mg, 0.29 mmol, 39%).

¹H NMR (501 MHz, CDCl₃): δ/ppm 7.54 – 7.48 (m, 2H), 7.39 (dd, *J* = 8.2, 1.1 Hz, 2H), 7.28 – 7.22 (m, 2H), 7.19 – 7.13 (m, 4H), 7.13 – 7.08 (m, 1H), 6.98 (d, *J* = 8.2 Hz, 1H), 6.89 – 6.85 (m, 1H), 6.84 (s, 1H), 4.01 (d, *J* = 14.0 Hz, 1H), 3.67 (d, *J* = 14.0 Hz, 1H), 3.63 (s, 3H), 1.96 (s, 3H), 1.27 (s, 9H).

¹³C NMR (126 MHz, CDCl₃): δ/ppm 199.8, 155.7, 148.5, 137.8, 135.8, 128.2, 127.8, 126.9, 126.8, 126.4, 126.0, 124.7, 122.2, 121.31, 121.30, 118.6, 109.2, 48.4, 42.2, 35.0, 32.6, 31.2, 28.4.

HRMS (ESI): calculated for [C₂₉H₃₁NONa]⁺: 432.2298; found: 432.2296.

## 1-(4-Isopropylphenyl)-3-(1-methyl-1*H*-indol-3-yl)-3-phenylbutan-1-one (20d)
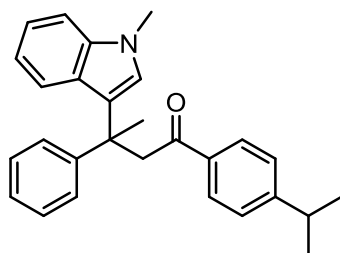
The general procedure for β-(Indol-3-yl)ketones using a solvent mixture of hexanes/EtOAc (v/v = 40/1→22/1) for column chromatography and a solvent mixture of hexanes/DCM (v/v = 50/50) for a subsequent thin layer chromatography lead to the isolation of the product **20d** as white solid (132 mg, 0.36 mmol, 67%).

¹H NMR (501 MHz, CDCl₃): δ/ppm 7.49 (d, J = 8.2 Hz, 2H), 7.38 − 7.34 (m, 2H), 7.23 (t, J = 7.6 Hz, 2H), 7.17 − 7.13 (m, 2H), 7.11 − 7.07 (m, 1H), 6.97 (dd, J = 14.5, 8.2 Hz, 3H), 6.87 − 6.83 (m, 1H), 6.83 (s, 1H), 3.97 (d, J = 14.1 Hz, 1H), 3.66 (d, J = 14.1 Hz, 1H), 3.64 (s, 3H), 2.82 (h, J = 6.9 Hz, 1H), 1.95 (s, 3H), 1.18 (d, J = 6.9 Hz, 6H).

¹³C NMR (126 MHz, CDCl₃): δ/ppm 199.8, 153.6, 148.4, 137.8, 136.3, 128.2, 128.1, 126.9, 126.8, 126.4, 126.0, 125.9, 122.3, 121.3 (2C), 118.6, 109.3, 48.4, 42.2, 34.2, 32.7, 28.4, 23.84, 23.80.

HRMS (ESI): calculated for [C₂₈H₂₉NONa]⁺: 418.2141; found: 418.2140.

1-([1,1'-Biphenyl]-4-yl)-3-(1-methyl-1*H*-indol-3-yl)-3-phenylbutan-1-one (20e)
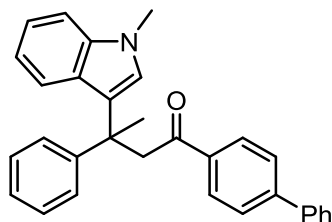
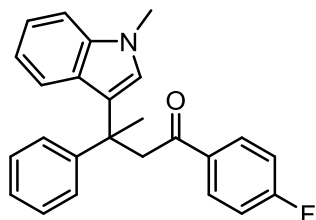The general procedure for β-(Indol-3-yl)ketones using a solvent mixture of hexanes/EtOAc (v/v = 40/1→25/1) for column chromatography lead to the isolation of the product **20e** as yellow oil (68 mg, 0.l6 mmol, 31%).

¹H NMR (501 MHz, CDCl₃): δ/ppm 7.62 − 7.56 (m, 2H), 7.55 − 7.49 (m, 2H), 7.48 − 7.41 (m, 2H), 7.42 − 7.36 (m, 3H), 7.36 − 7.31 (m, 2H), 7.29 − 7.22 (m, 2H), 7.21 − 7.14 (m, 1H), 7.16 − 7.08 (m, 2H), 6.97 (d, J = 8.0 Hz, 1H), 6.88 (ddd, J = 8.0, 6.4, 1.6 Hz, 1H), 6.85 (s, 1H), 4.05 (d, J = 13.7 Hz, 1H), 3.69 (d, J = 13.7 Hz, 1H), 3.62 (s, 3H), 1.97 (s, 3H).

¹³C NMR (126 MHz, CDCl₃): δ/ppm 200.0, 148.4, 144.8, 140.2, 137.8, 137.0, 129.0, 128.4, 128.2, 128.1, 127.3, 126.9, 126.8, 126.44, 126.43, 126.1, 122.1, 121.4, 121.3, 118.7, 109.3, 48.5, 42.4, 32.7, 28.5.

HRMS (ESI): calculated for $[C_{28}H_{29}NONa]^+$: 452.1985; found: 452.1986.

1-(4-Fluorophenyl)-3-(1-methyl-1*H*-indol-3-yl)-3-phenylbutan-1-one (20f)

The general procedure for β-(Indol-3-yl)ketones using a solvent mixture of hexanes/EtOAc (v/v = 40/1→13/1) for column chromatography and a solvent mixture of hexanes/EtOAc (v/v = 70/1) for a subsequent thin layer chromatography lead to the isolation of the product **20f** as white solid (124 mg, 0.33 mmol, 67%).

¹H NMR (501 MHz, CDCl₃): δ/ppm 7.55 – 7.49 (m, 2H), 7.38 – 7.32 (m, 2H), 7.27 – 7.19 (m, 2H), 7.19 – 7.13 (m, 2H), 7.14 – 7.07 (m, 1H), 6.93 (d, *J* = 8.0 Hz, 1H), 6.86 (ddd, *J* = 8.0, 6.9, 1.0 Hz, 1H), 6.84 (s, 1H), 6.81 – 6.72 (m, 2H), 3.96 (d, *J* = 13.6 Hz, 1H), 3.65 (s, 3H), 3.63 (d, (*J* = 13.6 Hz), 1H), 1.93 (s, 3H).

¹³C NMR (126 MHz, CDCl₃): δ/ppm 198.8, 165.2 (d, *J* = 253.8 Hz), 148.2, 137.8, 134.7 (d, *J* = 3.1 Hz), 130.4 (d, *J* = 9.1 Hz), 128.3, 126.8, 126.7, 126.3, 126.2, 122.0, 121.4 (d, *J* = 28.6 Hz), 118.8, 114.8, 114.7, 109.3, 48.4, 42.4, 32.7, 28.5.

¹⁹F NMR (471 MHz, CDCl₃): δ -106.85.

HRMS (ESI): calculated for $[C_{25}H_{22}NOFNa]^+$: 394.1578; found: 394.1576.

3-(1-Methyl-1*H*-indol-3-yl)-3-phenyl-1-(4-(trifluoromethyl)phenyl)butan-1-one (20g)
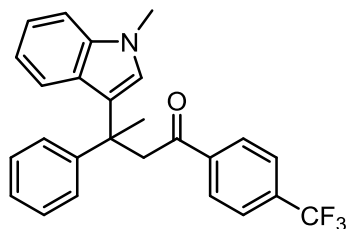
The general procedure for β-(Indol-3-yl)ketones using a solvent mixture of hexanes/EtOAc (v/v = 100/1→15/1) as eluent in column chromatography followed by a preparative thin layer chromatography with an eluent of hexanes/EtOAc (v/v = 70/1) lead to the isolation of the product **20g** as colourless oil (127 mg, 0.30 mmol, 60%).

^{1}H NMR (501 MHz, CDCl$_3$): δ/ppm 7.46 (d, J = 8.1 Hz, 1H), 7.36 (d, J = 7.5 Hz, 1H), 7.25 (t, J = 8.5 Hz, 2H), 7.18 (t, J = 7.2 Hz, 1H), 7.13 − 7.05 (m, 1H), 6.91 − 6.83 (m, 1H), 6.78 (s, 0H), 4.09 (d, J = 12.9 Hz, 0H), 3.59 (d, J = 15.1 Hz, 1H), 1.89 (s, 1H).

^{13}C NMR (126 MHz, CDCl$_3$): δ/ppm 200.4, 148.2, 140.9, 137.8, 133.2 (q, J = 32.5 Hz), 128.46, 127.87, 126.9, 126.8, 126.41, 126.40, 124.5 (q, J = 3.7 Hz), 121.7, 121.3 (2C), 119.0, 109.4, 48.7, 42.5, 32.7, 28.8

^{19}F NMR (282 MHz, CDCl$_3$): δ/ppm -63.09.

HRMS (ESI): calculated for [C$_{26}$H$_{22}$F$_3$NONa]$^+$: 444.1546; found: 444.1546.

1-(4-Methoxyphenyl)-3-(1-methyl-1*H*-indol-3-yl)-3-phenylbutan-1-one (20h)
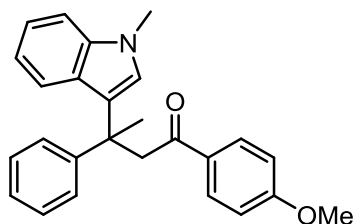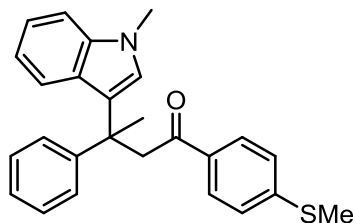

The general procedure for β-(Indol-3-yl)ketones using a solvent mixture of hexanes/EtOAc (v/v = 40/1→9/1) as eluent in column chromatography lead to the isolation of the product **20h** as white solid (150 mg, 0.39 mmol, 78%).

^{1}H NMR (501 MHz, CDCl$_3$): δ/ppm 7.55 (d, J = 8.9 Hz, 2H), 7.38 − 7.34 (m, 3H), 7.23 (t, J = 7.6 Hz, 2H), 7.19 − 7.13 (m, 2H), 7.10 (t, J = 7.6 Hz, 1H), 6.97 (d, J = 8.0 Hz, 1H), 6.88 − 6.83 (m, 2H), 6.63 (d, J = 8.9 Hz, 3H), 3.91 (d, J = 14.0 Hz, 1H), 3.77 (s, 3H), 3.66 (s, 3H), 3.65 (d, J = 14.0 Hz, 1H), 1.95 (s, 3H).

^{13}C NMR (126 MHz, CDCl$_3$): δ/ppm 198.5, 162.9, 148.4, 137.8, 131.5, 130.2, 128.2, 126.9, 126.7, 126.4, 126.0, 122.5, 121.35, 121.34, 118.7, 113.0, 109.3, 55.5, 48.2, 42.3, 32.7, 28.3.

HRMS (ESI): calculated for [C$_{26}$H$_{25}$NO$_2$Na]$^+$: 406.1777; found: 406.1773.

3-(1-Methyl-1*H*-indol-3-yl)-1-(4-(methylthio)phenyl)-3-phenylbutan-1-one (20i)
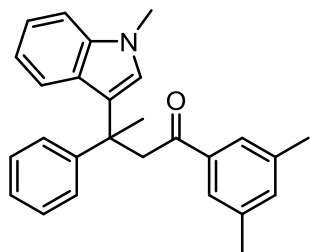

The general procedure for β-(Indol-3-yl)ketones using a solvent mixture of hexanes/EtOAc (v/v = 40/1→9/1) as eluent in column chromatography lead to the isolation of the product **20i** as white solid (142 mg, 0.36 mmol, 71%).

¹H NMR (300 MHz, CDCl₃): δ/ppm 7.48 – 7.42 (m, 2H), 7.41 – 7.32 (m, 2H), 7.28 – 7.20 (m, 2H), 7.20 – 7.14 (m, 2H), 7.14 – 7.07 (m, 1H), 6.98 – 6.91 (m, 3H), 6.89 – 6.83 (m, 1H), 6.83 (s, 1H), 3.94 (d, *J* = 13.8 Hz, 1H), 3.64 (s, 3H), 3.64 (d, *J* = 13.8 Hz, 1H), 2.43 (s, 3H), 1.94 (s, 3H).

¹³C NMR (75 MHz, CDCl₃): δ/ppm 199.2, 148.3, 144.6, 137.8, 134.7, 128.3, 128.2, 126.9, 126.8, 126.4, 126.1, 124.4, 122.2, 121.4, 121.3, 118.7, 109.3, 48.3, 42.4, 32.7, 28.4, 14.9.

HRMS (ESI): calculated for $[C_{26}H_{25}NOSNa]^+$: 422.1549; found: 422.1546.

**1-(3,5-Dimethylphenyl)-3-(1-methyl-1*H*-indol-3-yl)-3-phenylbutan-1-one (20j)**

The general procedure for β-(Indol-3-yl)ketones using a solvent mixture of hexanes/EtOAc (v/v = 40/1→20/1) for column chromatography and a solvent mixture of hexanes/DCM (v/v = 70/30) for a subsequent thin layer chromatography lead to the isolation of the product **20j** as yellow oil (101 mg, 0.26 mmol, 53%).

¹H NMR (501 MHz, CDCl₃): δ/ppm 7.40 – 7.35 (m, 2H), 7.28 – 7.21 (m, 2H), 7.21 – 7.13 (m, 2H), 7.14 – 7.07 (m, 3H), 7.00 – 6.94 (m, 2H), 6.87 (ddd, *J* = 8.0, 7.0, 0.9 Hz, 1H), 6.82 (s, 1H), 4.00 (d, *J* = 13.7 Hz, 1H), 3.64 (s, 3H), 3.63 (d, *J* = 13.7 Hz, 1H), 2.13 (s, 6H), 1.94 (s, 3H).

¹³C NMR (126 MHz, CDCl₃): δ/ppm 200.8, 148.5, 138.4, 137.8, 137.5, 133.8, 128.2, 126.9, 126.8, 126.5, 126.0, 125.8, 122.2, 121.4, 121.3, 118.7, 109.2, 48.6, 42.2, 32.7, 28.4, 21.1.

HRMS (GC-CI): calculated for $[C_{27}H_{28}NO+H]^+$: 382.2165; found: 382.2166.

3-(1-Methyl-1*H*-indol-3-yl)-3-phenyl-1-(thiophen-2-yl)butan-1-one (20k)
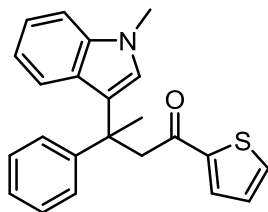
The general procedure for β-(Indol-3-yl)ketones using a solvent mixture of hexanes/EtOAc (v/v = 40/1→9/1) as eluent in column chromatography lead to the isolation of the product **20k** as white solid (133 mg, 0.37 mmol, 75%).

¹H NMR (501 MHz, CDCl₃): δ/ppm 7.41 (dd, *J* = 4.9, 1.0 Hz, 1H), 7.38 – 7.34 (m, 2H), 7.25 – 7.18 (m, 3H), 7.18 – 7.13 (m, 1H), 7.13 – 7.09 (m, 1H), 7.04 (dd, *J* = 3.8, 1.0 Hz, 1H), 6.94 – 6.92 (m, 1H), 6.92 (s, 1H), 6.89 – 6.82 (m, 1H), 6.73 (dd, *J* = 4.9, 3.9 Hz, 1H), 3.85 (d, *J* = 13.4 Hz, 1H), 3.68 (s, 3H), 3.61 (d, *J* = 13.4 Hz, 1H), 1.96 (s, 3H).

¹³C NMR (126 MHz, CDCl₃): δ/ppm 192.6, 148.1, 145.9, 137.9, 133.2, 131.9, 128.3, 127.6, 126.9, 126.8, 126.4, 126.1, 122.1, 121.4, 121.3, 118.7, 109.3, 49.6, 42.6, 32.8, 28.5.

HRMS (ESI): calculated for $[C_{23}H_{21}NOS+H]^+$: 360.1417; found: 360.1413.
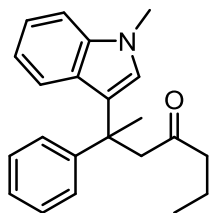
2-(1-Methyl-1*H*-indol-3-yl)-2-phenylheptan-4-one (21a)

The general procedure for β-(Indol-3-yl)ketones using a solvent mixture of hexanes/EtOAc (v/v = 40/1→22/1) as eluent in column chromatography lead to the isolation of the product **21a** as yellow oil (84 mg, 0.26 mmol, 53%).

^{1}H NMR (501 MHz, CDCl$_3$): δ/ppm 7.33 – 7.29 (m, 2H), 7.28 – 7.23 (m, 3H), 7.21 – 7.14 (m, 2H), 7.16 – 7.11 (m, 1H), 6.95 (d, J = 8.1 Hz, 1H), 6.94 (s, 1H), 6.89 – 6.84 (m, 1H), 3.75 (s, 3H), 3.38 (d, J = 12.8 Hz, 1H), 3.15 (d, J = 12.8 Hz, 1H), 1.88 (s, 3H), 1.79 (dt, J = 17.4, 7.0 Hz, 1H), 1.69 (dt, J = 17.4, 7.1 Hz, 1H), 1.31 – 1.23 (m, 2H), 0.57 (t, J = 7.4 Hz, 3H).

^{13}C NMR (126 MHz, CDCl$_3$): δ/ppm 210.9, 148.2, 137.8, 128.2, 126.7, 126.6, 126.3, 126.1, 121.8, 121.5, 121.2, 118.7, 109.4, 52.8, 46.7, 42.0, 32.8, 28.4, 16.8, 13.5.

HRMS (ESI): calculated for [C$_{22}$H$_{25}$NONa]$^+$: 342.1828; found: 342.1823.

2-Methyl-5-(1-methyl-1H-indol-3-yl)-5-phenylhexan-3-one (21b)
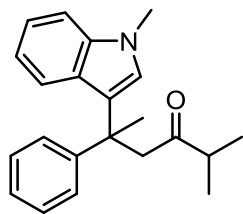

The general procedure for β-(Indol-3-yl)ketones using a solvent mixture of hexanes/EtOAc (v/v = 40/1→25/1) as eluent in column chromatography lead to the isolation of the product **21b** as yellow oil (54 mg, 0.17 mmol, 34%).

^{1}H NMR (501 MHz, CDCl$_3$): δ/ppm 7.32 – 7.28 (m, 1H), 7.28 – 7.21 (m, 3H), 7.18 – 7.14 (m, 1H), 7.14 – 7.10 (m, 1H), 6.95 – 6.90 (m, 2H), 6.87 – 6.82 (m, 1H), 3.76 (s, 3H), 3.43 (d, J = 13.4 Hz, 1H), 3.23 (d, J = 13.4 Hz, 1H), 1.94 – 1.83 (m, 4H), 0.78 (d, J = 6.9 Hz, 3H), 0.70 (d, J = 6.8 Hz, 3H).

^{13}C NMR (126 MHz, CDCl$_3$): δ/ppm 214.4, 148.3, 137.8, 128.2, 126.8, 126.5, 126.3, 126.1, 122.2, 121.4, 121.2, 118.7, 109.4, 51.1, 42.0, 32.8, 28.3, 18.1, 17.6.

HRMS (ESI): calculated for [C$_{22}$H$_{25}$NONa]$^+$: 342.1828; found: 342.1827.

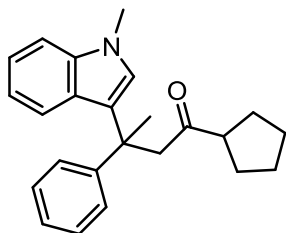## 1-Cyclopentyl-3-(1-methyl-1*H*-indol-3-yl)-3-phenylbutan-1-one (21c)
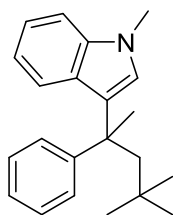

The general procedure for β-(Indol-3-yl)ketones using a solvent mixture of hexanes/EtOAc (v/v = 50/1→25/1) as eluent in column chromatography lead to the isolation of the product **21c** as pale yellow oil (65 mg, 0.19 mmol, 38%).

^{1}H NMR (501 MHz, CDCl$_3$): δ/ppm 7.34 − 7.30 (m, 2H), 7.28 − 7.23 (m, 3H), 7.21 − 7.13 (m, 1H), 7.13 (ddd, *J* = 8.1, 7.1, 1.0 Hz, 1H), 6.96 (d, *J* = 8.0 Hz, 2H), 6.94 (s, 1H), 6.86 (ddd, *J* = 8.0, 7.0, 0.9 Hz, 1H), 3.76 (s, 3H), 3.44 (d, *J* = 13.7 Hz, 1H), 3.26 (d, *J* = 13.7 Hz, 1H), 2.25 − 2.15 (m, 1H), 1.90 (s, 3H), 1.53 − 1.43 (m, 5H), 1.39 − 1.27 (m, 3H).

^{13}C NMR (126 MHz, CDCl$_3$): δ/ppm 212.9, 148.2, 137.8, 128.2, 126.5, 126.3, 126.0, 122.3, 121.4, 121.2, 118.6, 109.3, 52.7, 52.5, 42.0, 32.8, 29.0, 28.4, 28.3, 26.0.

HRMS (ESI): calculated for [C$_{24}$H$_{27}$NONa]$^+$: 368.1985; found: 368.1982.

3-(4,4-Dimethyl-2-phenylpentan-2-yl)-1-methyl-1*H*-indole (22)

The general procedure for β-(Indol-3-yl)ketones using pivaldehyde in the reaction and a solvent mixture of hexanes/EtOAc (v/v = 200/1) as eluent in column chromatography, and a mixture of hexanes/DCM (v/v = 30/1) for a subsequent thin layer chromatography lead to the isolation of this product **22** as pale yellow oil (584 mg, 0.27 mmol, 55%).

^{1}H NMR (501 MHz, CDCl$_3$): δ/ppm 7.44 − 7.40 (m, 2H), 7.28 − 7.22 (m, 3H), 7.19 − 7.10 (m, 2H), 7.04 (d, *J* = 8.1 Hz, 1H), 6.93 (s, 1H), 6.86 (ddd, *J* = 8.1, 7.1, 0.9 Hz, 1H), 3.77 (s, 3H), 2.43 (d, *J* = 14.1 Hz, 1H), 2.34 (d, *J* = 14.1 Hz, 1H), 1.92 (s, 3H), 0.79 (s, 9H).

¹³C NMR (126 MHz, CDCl₃): δ/ppm 149.8, 137.9, 127.9, 127.7, 126.8, 126.11, 126.05, 125.6, 121.9, 121.2, 118.4, 109.2, 53.7, 43.3, 32.9, 32.8, 32.1, 28.8.

HRMS (GC-EI): calculated for [C₂₂H₂₇N]⁺: 305.2138; found: 305.2138.

### 1,3-Bis(4-methoxyphenyl)-3-(1-methyl-1*H*-indol-3-yl)propan-1-one (26)
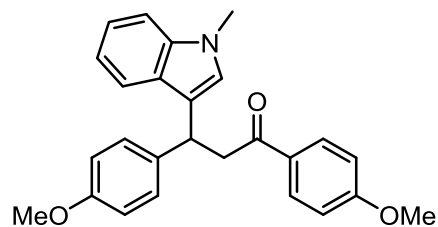
The general procedure for β-(Indol-3-yl)ketones using solvent mixtures of hexanes/EtOAc (v/v = 30/1→7/3) for column chromatography lead to the isolation of the product **26** as white solid (71 mg, 0.18 mmol, 35%).

¹H NMR (501 MHz, CDCl₃): δ/ppm 7.95 – 7.90 (m, 2H), 7.48 – 7.42 (m, 1H), 7.29 – 7.23 (m, 3H), 7.21 – 7.15 (m, 1H), 7.05 – 6.99 (m, 1H), 6.93 – 6.88 (m, 2H), 6.84 – 6.77 (m, 3H), 5.01 (t, *J* = 7.2 Hz, 1H), 3.86 (s, 3H), 3.75 (s, 3H), 3.72 (s, 3H), 3.75 – 3.62 (m, 2H).

¹³C NMR (126 MHz, CDCl₃): δ/ppm 197.3, 163.5, 158.0, 137.5, 136.8, 130.5, 130.4, 128.9, 127.1, 126.3, 121.8, 119.8, 118.9, 118.4, 113.9, 113.8, 109.3, 55.6, 55.3, 45.3, 37.6, 32.8.

HRMS (ESI): calculated for [C₂₆H₂₅NO₃Na]⁺: 422.1727; found: 422.1725.

### 3-(4-Methoxyphenyl)-3-(1-methyl-1*H*-indol-3-yl)-1-phenylbutan-1-one (27a)
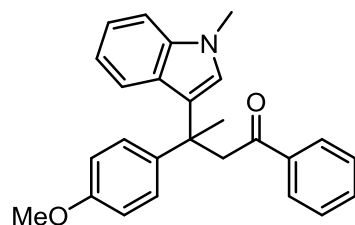
The general procedure for β-(Indol-3-yl)ketones using mixtures of hexanes/EtOAc (v/v = 40/1→20/1) as eluent for column chromatography lead to the isolation of the product **27a** as yellow oil (144 mg, 0.38 mmol, 75%).

¹H NMR (501 MHz, CDCl₃): δ/ppm 7.50 – 7.44 (m, 2H), 7.28 – 7.21 (m, 1H), 7.19 – 7.13 (m, 2H), 7.10 – 7.03 (m, 3H), 7.05 – 6.98 (m, 1H), 6.98 – 6.90 (m, 3H), 6.78 (ddd, J = 8.0, 6.8, 1.2 Hz, 1H), 6.73 (s, 1H), 3.90 (d, J = 14.1 Hz, 1H), 3.59 (d, J = 14.1 Hz, 1H), 3.55 (s, 3H), 2.20 (s, 3H), 1.85 (s, 3H).

¹³C NMR (126 MHz, CDCl₃): δ/ppm 200.2, 145.3, 138.4, 137.8, 135.4, 132.2, 128.9, 127.9 (2C), 126.7, 126.70, 126.4, 122.4, 121.4, 121.3, 118.6, 109.3 48.6, 41.9, 32.7, 28.4, 21.1.

HRMS (ESI): calculated for $[C_{26}H_{25}NO_2Na]^+$: 406.1777; found: 406.1776.

3-(4-(*Tert*-butyl)phenyl)-3-(1-methyl-1*H*-indol-3-yl)-1-phenylbutan-1-one (27b)
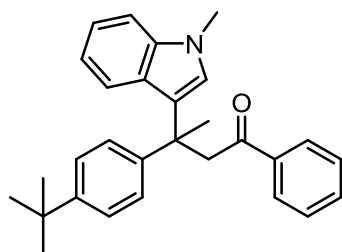
The general procedure for β-(Indol-3-yl)ketones using solvent mixtures of hexanes/EtOAc (v/v = 40/1→25/1) for column chromatography and a solvent mixture of DCM/hexanes (v/v = 70/30) for subsequent preparative thin layer chromatography lead to the isolation of the product **27b** as white solid (154 mg, 0.38 mmol, 75%).

¹H NMR (501 MHz, CDCl₃): δ/ppm 7.56 – 7.51 (m, 2H), 7.35 – 7.31 (m, 1H), 7.28 – 7.25 (m, 2H), 7.24 – 7.20 (m, 2H), 7.19 – 7.14 (m, 2H), 7.14 – 7.10 (m, 2H), 7.02 (d, J = 8.0 Hz, 1H), 6.90 – 6.85 (m, 2H), 3.95 (d, J = 13.8 Hz, 1H), 3.72 (d, J = 13.8 Hz, 1H), 3.67 (s, 3H), 1.96 (s, 3H), 1.27 (s, 9H).

¹³C NMR (126 MHz, CDCl₃): δ/ppm 200.4, 148.6, 145.0, 138.4, 137.8, 132.1, 127.9, 127.8, 126.7, 126.47, 126.45, 125.0, 122.4, 121.5, 121.3, 118.5, 109.3, 48.8, 42.0, 34.4, 32.7, 31.5, 28.3.

HRMS (ESI): calculated for $[C_{29}H_{31}NONa]^+$: 432.2298; found: 432.2298.

3-([1,1'-Biphenyl]-4-yl)-3-(1-methyl-1*H*-indol-3-yl)-1-phenylbutan-1-one (27c)
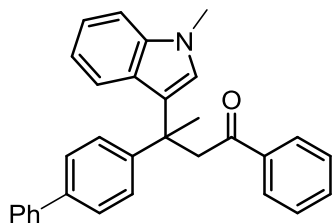

The general procedure for β-(Indol-3-yl)ketones using solvent mixtures of hexanes/EtOAc (v/v = 40/1→25/1) as eluent in column chromatography and a mixture of hexanes/DCM (v/v = 80/20) in a subsequent preparative thin layer chromatography lead to the isolation of the product **27c** as white solid (150 mg, 0.35 mmol, 70%).

^{1}H NMR (501 MHz, CDCl$_3$): δ/ppm 7.63 – 7.54 (m, 4H), 7.51 – 7.42 (m, 4H), 7.45 – 7.38 (m, 2H), 7.39 – 7.29 (m, 2H), 7.21 – 7.15 (m, 3H), 7.15 – 7.10 (m, 1H), 7.08 (d, *J* = 8.1 Hz, 1H), 6.93 – 6.86 (m, 1H), 6.89 (s, 1H), 4.02 (d, *J* = 14.1 Hz, 1H), 3.78 (d, *J* = 14.1 Hz, 1H), 3.68 (s, 3H), 2.02 (s, 3H).

^{13}C NMR (126 MHz, CDCl$_3$): δ/ppm 200.1, 147.3, 141.0, 138.7, 138.3, 137.8, 132.2, 128.8, 127.9, 127.9, 127.3, 127.1, 127.1, 126.8, 126.7, 126.3, 122.2, 121.41, 121.36, 118.7, 109.3, 48.7, 42.1, 32.7, 28.3.

HRMS (ESI): calculated for [C$_{31}$H$_{27}$NONa]$^+$: 452.1985; found: 452.1984.

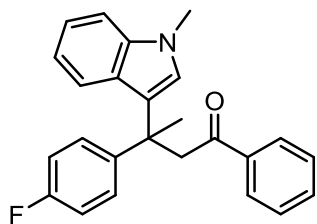**3-(4-Fluorophenyl)-3-(1-methyl-1*H*-indol-3-yl)-1-phenylbutan-1-one (27d)**

The general procedure for β-(Indol-3-yl)ketones using solvent mixtures of hexanes/EtOAc (v/v = 40/1→22/1) as eluent in column chromatography lead to the isolation of the product **27d** as yellow oil (80 mg, 0.23 mmol, 43%).

¹H NMR (501 MHz, CDCl₃): δ/ppm 7.60 (dd, J = 8.3, 1.2 Hz, 2H), 7.40 – 7.35 (m, 1H), 7.35 – 7.30 (m, 2H), 7.22 – 7.16 (m, 3H), 7.16 – 7.11 (m, 1H), 6.97 (d, J = 8.0 Hz, 1H), 6.94 – 6.86 (m, 4H), 3.95 (d, J = 14.2 Hz, 1H), 3.72 (d, J = 14.2 Hz, 1H), 3.67 (s, 3H), 1.97 (s, 3H).

¹³C NMR (126 MHz, CDCl₃): δ/ppm 199.8, 162.2, 160.3, 143.8 (d, ^4J = 3.2 Hz), 138.0 (d, ^1J = 50.6 Hz), 132.4, 128.5 (d, ^3J = 7.9 Hz), 128.0, 127.9, 126.5, 126.1, 122.3, 121.5, 121.2, 118.8, 114.8 (d, ^2J = 20.9 Hz), 109.4, 48.7, 41.8, 32.7, 28.3.

¹⁹F NMR (471 MHz, CDCl₃): δ/ppm -117.7.

HRMS (ESI): calculated for [C₂₅H₂₂NOFNa]⁺: 394.1578; found: 394.1574.

3-(4-Chlorophenyl)-3-(1-methyl-1*H*-indol-3-yl)-1-phenylbutan-1-one (27e)
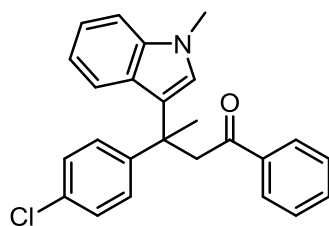
The general procedure for β-(Indol-3-yl)ketones using solvent mixtures of hexanes/EtOAc (v/v = 40/1→25/1) as eluent in column chromatography lead to the isolation of the product **27e** as yellow oil (107 mg, 0.28 mmol, 54%).

¹H NMR (300 MHz, CDCl₃): δ/ppm 7.66 – 7.57 (m, 2H), 7.42 – 7.35 (m, 1H), 7.34 – 7.28 (m, 2H), 7.24 – 7.17 (m, 5H), 7.17 – 7.10 (m, 1H), 7.00 (d, J = 8.0 Hz, 1H), 6.95 – 6.88 (m, 1H), 6.86 (s, 1H), 3.97 (d, J = 14.4 Hz, 1H), 3.71 (d, J = 14.4 Hz, 1H), 3.67 (s, 3H), 1.96 (s, 3H).

¹³C NMR (75 MHz, CDCl₃): δ/ppm 199.5, 146.8, 138.2, 137.8, 132.4, 131.8, 128.5, 128.3, 128.0, 127.9 126.6, 126.1, 122.0, 121.5, 121.1, 118.8, 109.4, 48.5, 41.9, 32.7, 28.2.

HRMS (ESI): calculated for [C₂₅H₂₂NOClNa]⁺: 410.1282; found: 410.1282.

4-(2-(1-Methyl-1*H*-indol-3-yl)-4-oxo-4-phenylbutan-2-yl)benzonitrile (27f)

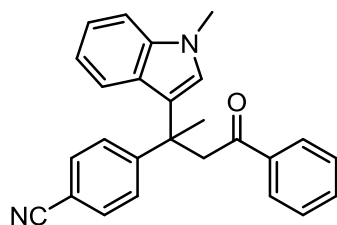

The general procedure for β-(Indol-3-yl)ketones using mixtures of hexanes/EtOAc (v/v = 9/1→4/1) as eluent for column chromatography and a mixture of hexanes/DCM (v/v = 30/70) in a subsequent preparative thin layer chromatography lead to the isolation of the product **27f** as yellow oil (22 mg, 0.058 mmol, 12%).

¹H NMR (500 MHz, CDCl₃): δ/ppm 7.66 – 7.60 (m, 2H), 7.54 – 7.45 (m, 4H), 7.43 – 7.38 (m, 1H), 7.26 – 7.18 (m, 3H), 7.14 (ddd, *J* = 8.2, 5.2, 2.9 Hz, 1H), 6.93 – 6.84 (m, 3H), 3.97 (d, *J* = 14.9 Hz, 1H), 3.75 (d, *J* = 14.9 Hz, 1H), 3.70 (s, 3H), 1.98 (s, 3H).

¹³C NMR (126 MHz, CDCl₃): δ/ppm 198.0, 152.8, 137.02, 136.95, 131.9, 131.1, 127.3, 127.1, 127.0, 125.6, 124.9, 120.9, 120.6, 119.9, 118.3, 118.2, 109.0, 108.7, 47.5, 41.6, 31.9, 26.8.

HRMS (ESI): calculated for $[C_{26}H_{22}N_2ONa]^+$: 401.1624; found: 401.1622.

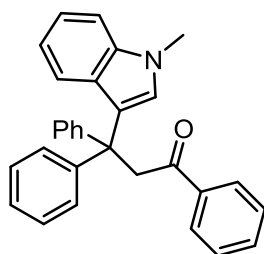**3-(1-Methyl-1*H*-indol-3-yl)-1,3,3-triphenylpropan-1-one (27g)**

The general procedure for β-(Indol-3-yl)ketones using mixtures of hexanes/EtOAc (v/v = 17/1→12/1) as eluent for column chromatography lead to the isolation of the product **27g** as white solid (128 mg, 0.31 mmol, 63%). By recrystallization from THF/pentane suitable crystals for X-ray diffractometry analysis were obtained.

¹H NMR (501 MHz, CDCl₃): δ/ppm 7.81 – 7.76 (m, 2H), 7.50 – 7.42 (m, 1H), 7.37 – 7.29 (m, 6H), 7.28 – 7.20 (m, 5H), 7.22 – 7.14 (m, 2H), 7.11 (ddd, *J* = 8.1, 6.7, 0.9 Hz, 1H), 6.91 (d, *J* = 8.0 Hz, 1H), 6.83 (ddd, *J* = 8.0, 6.8, 1.0 Hz, 1H), 6.75 (s, 1H), 4.49 (s, 2H), 3.70 (s, 3H).

¹³C NMR (126 MHz, CDCl₃): δ/ppm 197.8, 146.5, 138.2, 137.7, 132.7, 129.6, 128.9, 128.4, 127.9 (2C), 127.2, 126.1, 121.8, 121.2, 121.2, 118.8, 109.4, 51.5, 49.6, 32.9.

HRMS (ESI): calculated for $[C_{30}H_{25}NONa]^+$: 438.1828; found: 438.1832.

3-Cyclopropyl-3-(1-methyl-1*H*-indol-3-yl)-1,3-diphenylpropan-1-one (27h)
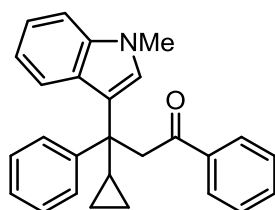
The general procedure for β-(Indol-3-yl)ketones a solvent mixture of hexanes/EtOAc (v/v = 200/1) as eluent in column chromatography lead to the isolation of this product **27h** as pale yellow oil (50 mg, 0.13 mmol, 26%).

¹H NMR (501 MHz, CDCl₃): δ/ppm 7.62 – 7.58 (m, 2H), 7.38 – 7.31 (m, 3H), 7.24 – 7.19 (m, 2H), 7.19 – 7.14 (m, 3H), 7.11 (d, J = 8.2 Hz, 1H), 7.05 (s, 1H), 7.06 – 7.02 (m, 1H), 6.76 (td, J = 7.5, 6.9, 1.0 Hz, 1H), 6.68 (d, J = 8.2 Hz, 1H), 4.12 (d, J = 13.8 Hz, 1H), 3.83 (d, J = 13.8 Hz, 1H), 3.68 (s, 3H), 2.14 – 2.06 (m, 1H), 0.51 – 0.38 (m, 2H), 0.04 – -0.05 (m, 2H).+

¹³C NMR (126 MHz, CDCl₃): δ/ppm 200.2, 144.3, 138.7, 137.4, 132.1, 128.8, 127.87, 127.85, 127.6, 127.2, 126.3, 121.7, 121.1, 119.2, 118.6, 109.2, 48.8, 46.3, 32.8, 18.8, 2.1.

HRMS (ESI): calculated for $[C_{27}H_{25}NONa]^+$: 402.1828; found: 402.1833.

3-(1,5-Dimethyl-1*H*-indol-3-yl)-1,3-diphenylbutan-1-one (28a)
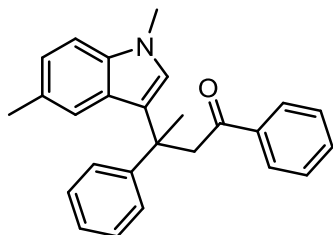
The general procedure for β-(Indol-3-yl)ketones using column chromatography with an eluent of hexanes/EtOAc (v/v = 40/1→27/1), followed by a preparative thin layer chromatography with eluent hexanes/DCM (v/v = 75/25) lead to the isolation of the product **28a** as yellow oil (112 mg, 0.30 mmol, 61%).

^{1}H NMR (501 MHz, CDCl$_3$): δ/ppm 7.59 (dd, *J* = 8.4, 1.2 Hz, 2H), 7.40 – 7.32 (m, 3H), 7.27 – 7.20 (m, 2H), 7.20 – 7.13 (m, 3H), 7.06 (d, *J* = 8.3 Hz, 1H), 6.93 (dd, *J* = 8.3, 1.3 Hz, 1H), 6.80 – 6.75 (m, 2H), 3.96 (d, *J* = 14.3 Hz, 1H), 3.73 (d, *J* = 14.3 Hz, 1H), 3.63 (s, 3H), 2.27 (s, 3H), 1.96 (s, 3H).

^{13}C NMR (126 MHz, CDCl$_3$): δ/ppm 200.1, 148.2, 138.4, 136.3, 132.2, 128.2, 127.9, 127.9, 127.7, 126.9, 126.8, 126.5, 126.0, 123.0, 121.8, 121.0, 109.0, 48.7, 42.2, 32.7, 28.2, 21.7.

HRMS (ESI): calculated for [C$_{26}$H$_{25}$NONa]$^+$: 390.1828; found: 390.1822.

3-(5-Bromo-1-methyl-1*H*-indol-3-yl)-1,3-diphenylbutan-1-one (28b)
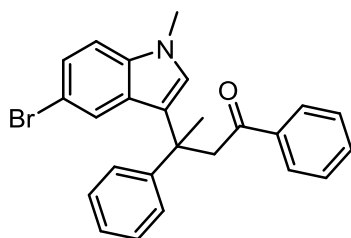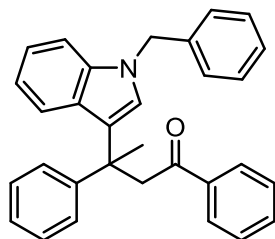

The general procedure for β-(Indol-3-yl)ketones using column chromatography with an eluent of hexanes/EtOAc (v/v = 40/1→18/1), followed by a preparative thin layer chromatography with eluent hexanes/DCM (v/v = 75/25) lead to the isolation of the product **28b** as yellow oil (114 mg, 0.26 mmol, 53%).

^{1}H NMR (501 MHz, CDCl$_3$): δ/ppm 7.59 – 7.53 (m, 1H), 7.37 – 7.31 (m, 2H), 7.28 – 7.23 (m, 2H), 7.20 – 7.14 (m, 4H), 7.05 (d, J = 1.8 Hz, 1H), 7.00 (d, J = 8.7 Hz, 1H), 6.85 (s, 1H), 3.96 (d, J = 14.1 Hz, 1H), 3.66 (d, J = 14.1 Hz, 1H), 3.62 (s, 2H), 1.93 (s, 2H).

^{13}C NMR (126 MHz, CDCl$_3$): δ/ppm 199.9, 147.8, 138.3, 136.4, 132.3, 128.4, 128.04, 128.01, 127.95, 127.85, 126.7, 126.3, 124.3, 123.6, 121.7, 112.1, 110.8, 48.3, 42.1, 32.9, 28.5.

HRMS (ESI): calculated for [C$_{25}$H$_{22}$BrNONa]$^+$: 454.0777; found: 454.0773.

3-(1-Benzyl-1H-indol-3-yl)-1,3-diphenylbutan-1-one (28c)

The general procedure for β-(Indol-3-yl)ketones using mixtures of hexanes/EtOAc (v/v = 40/1→27/1) as eluent for column chromatography lead to the isolation of the product **28c** as white solid (93 mg, 0.21 mmol, 44%).

^{1}H NMR (501 MHz, CD$_2$Cl$_2$): δ/ppm 7.68 – 7.62 (m, 2H), 7.43 – 7.37 (m, 3H), 7.34 – 7.23 (m, 5H), 7.26 – 7.14 (m, 2H), 7.14 (d, J = 8.3 Hz, 1H), 7.07 (s, 1H), 7.06 – 6.97 (m, 4H), 6.87 – 6.80 (m, 1H), 5.25 (s, 2H), 4.03 (d, J = 14.2 Hz, 1H), 3.76 (d, J = 14.2 Hz, 1H), 1.96 (s, 3H).

^{13}C NMR (126 MHz, CD$_2$Cl$_2$): δ/ppm 199.7, 148.8, 138.6, 138.3, 137.7, 132.6, 129.1, 128.37, 128.35, 128.2, 127.8, 127.2, 127.0, 126.9, 126.5, 126.3, 123.2, 121.8, 121.5, 119.1, 110.2, 50.3, 48.3, 42.4, 28.4.

HRMS (ESI): calculated for [C$_{31}$H$_{27}$NONa]$^+$: 452.1985; found: 452.1989.

3-(1*H*-benzo[d][1,2,3]triazol-1-yl)-1,3-diphenylbutan-1-one (29)
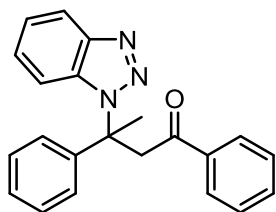
The general procedure for β-(Indol-3-yl)ketones using benzotriazole as nucleophile instead of an indole and mixtures of hexanes/EtOAc (v/v = 9/1→4/1) as eluent for column chromatography, followed by a preparative thin layer chromatography with eluent DCM lead to the isolation of the product **29** as white solid (83 mg, 0.24 mmol, 49%).

^{1}H NMR (501 MHz, CDCl$_3$): δ/ppm 8.04 (d, J = 8.4 Hz, 1H), 7.90 – 7.83 (m, 2H), 7.53 – 7.48 (m, 1H), 7.41 – 7.36 (m, 2H), 7.34 – 7.28 (m, 3H), 7.28 – 7.24 (m, 3H), 7.18 (ddd, J = 8.0, 7.0, 1.0 Hz, 1H), 6.72 (d, J = 8.5 Hz, 1H), 4.61 (d, J = 16.7 Hz, 1H), 4.32 (d, J = 16.7 Hz, 1H), 2.41 (s, 3H).

^{13}C NMR (126 MHz, CDCl$_3$): δ/ppm 196.1, 146.9, 142.4, 137.5, 133.3, 132.1, 128.9, 128.6, 128.3, 128.1, 127.0, 126.4, 123.9, 120.1, 112.3, 66.7, 49.2, 26.1.

HRMS (ESI): calculated for [C$_{22}$H$_{19}$N$_3$ONa]$^+$: 364.1420; found: 364.1421.

5.3.4 Imide Products

N-Acetyl-N-(3-cyclopentyl-3-oxo-1-phenylpropyl)benzamide (30a)
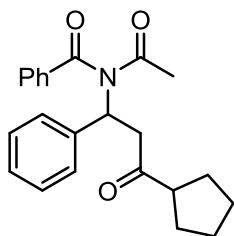
The general procedure for imide synthesis using for column chromatography an eluent of hexanes/EtOAc (v/v = 100/10→85/15), combined with a further purification by preparative thin layer chromatography an eluent of DCM/hexanes (v/v = 95/5) lead to the isolation of the product. The substance **30a** was obtained as colourless oil (62 mg, 0.17 mmol, 34%).

¹H NMR (300 MHz, CDCl₃): δ 7.61 – 7.56 (m, 2H), 7.55 – 7.48 (m, 1H), 7.48 – 7.37 (m, 4H), 7.35 – 7.28 (m, 2H), 7.27 – 7.19 (m, 1H), 6.07 (dd, *J* = 9.5, 5.3 Hz, 1H), 3.86 (dd, *J* = 18.0, 9.5 Hz, 1H), 3.25 (dd, *J* = 18.0, 5.3 Hz, 1H), 2.95 – 2.80 (m, 1H), 1.89 (s, 3H), 1.81 – 1.63 (m, 4H), 1.62 – 1.47 (m, 4H).

¹³C NMR (75 MHz, CDCl₃): δ/ppm 210.7, 174.6, 173.9, 139.7, 136.8, 132.8, 129.1, 128.9, 128.6, 127.8, 127.7, 56.3, 51.8, 44.4, 29.1, 28.9, 27.7, 26.1, 26.0.

HRMS (ESI): calculated for $[C_{23}H_{25}NO_3Na]^+$: 386.1727; found: 386.1726.

_N_-Acetyl-_N_-(3,3-dimethyl-1-phenylbutyl)benzamide (30b)

The general procedure for imide synthesis using pivaldehyde in the reaction, acetonitrile as solvent and a mixtures of hexanes/EtOAc (v/v = 95/5→/15) as eluent in chromatography lead to the isolation of this substance **30b** as white solid (0.1 mmol scale: 17 mg, 0.053 mmol, 53%; 0.5 mmol scale: 79 mg, 0.24 mmol, 49%)

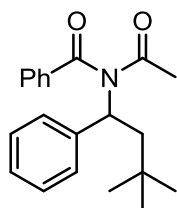**¹H NMR (501 MHz, CDCl₃):** δ/ppm 7.53 – 7.44 (m, 5H), 7.38 – 7.31 (m, 2H), 7.28 – 7.21 (m, 2H), 7.21 – 7.14 (m, 1H), 5.85 (dd, *J* = 7.0, 5.4 Hz ,1H), 2.44 (dd, *J* = 14.7, 7.0 Hz, 1H), 2.17 (dd, *J* = 14.7, 5.4 Hz, 1H), 1.73 (s, 3H), 0.90 (s, 9H).

¹³C NMR (126 MHz, CDCl₃): δ/ppm 174.7, 172.9, 141.0, 137.3, 132.9, 129.0, 128.92, 128.87, 128.3, 127.6, 57.9, 45.8, 31.0, 20.0, 28.1.

HRMS (ESI): calculated for $[C_{21}H_{25}N_1O_2Na]+$: 346.1777; found: 346.1776.

N-Acetyl-N-(3-(4-methoxyphenyl)-3-oxo-1-phenylpropyl)benzamide (30c)
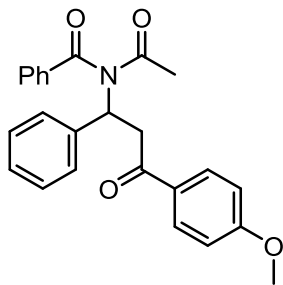
The general procedure for imide synthesis using for column chromatography an eluent of hexanes/EtOAc (v/v = 6/1→7/3) lead to the isolation of the product. The substance **30c** was obtained as pale yellow oil (104 mg, 0.26 mmol, 52%).

^{1}H NMR (501 MHz, CDCl$_3$): δ/ppm 8.01 – 7.94 (m, 2H), 7.62 – 7.57 (m, 2H), 7.55 – 7.47 (m, 3H), 7.37 (t, J = 7.6 Hz, 2H), 7.33 (t, J = 7.6 Hz, 2H), 7.27 – 7.21 (m, 1H), 6.95 – 6.88 (m, 2H), 6.26 (dd, J = 9.2, 5.3 Hz, 1H), 4.39 (dd, J = 17.6, 9.2 Hz, 1H), 3.85 (s, 3H), 3.72 (dd, J = 17.6, 5.3 Hz, 1H), 1.88 (s, 3H).

^{13}C NMR (126 MHz, CDCl$_3$): δ/ppm 196.2, 174.7, 173.9, 163.8, 139.7, 136.8, 132.8, 130.6, 129.9, 129.0, 128.9, 128.6, 127.8, 127.7, 113.9, 56.7, 55.6, 40.9, 27.7.

HRMS (ESI): calculated for [C$_{25}$H$_{23}$NO$_4$Na]$^+$: 424.1519; found: 424.1520.

N-(3-Cyano-1-phenylbutyl)-N-propionylbenzamide (33a)
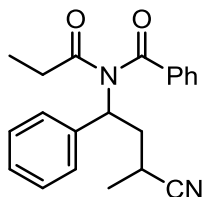
From product mixture after column chromatography d.r. ~1.4/1

The general procedure for imide synthesis using propionitrile as solvent and a mixture of hexanes/EtOAc (v/v = 19/1→6/1) as eluent in column chromatography lead to the isolation of the substances as colourless oil (0.5 mmol scale: d.r. 1.4/1, 80 mg, 0.24 mmol, 50%).

Via preparative HPLC (Chiralpak IA 5 μm, IA00CG-QD002, 250 mm Chiralpak, 10 mm diameter, eluent: n-heptane/ethanol (v/v = 99/1)) the major diastereoisomer **33a** was separated as colourless oil (19 mg, 0.057 mmol, 11%).

Major Diastereoisomer:

^{1}H NMR (501 MHz, CDCl$_3$): δ/ppm 7.55 – 7.51 (m, 3H), 7.49 – 7.44 (m, 2H), 7.42 – 7.37 (m, 2H), 7.34 – 7.29 (m, 2H), 7.29 – 7.23 (m, 1H), 5.86 (dd, J = 10.1, 6.0 Hz, 1H), 2.84 (ddd, J = 13.9, 10.1, 5.6 Hz, 1H), 2.76 – 2.67 (m, 1H), 2.44 (ddd, J = 13.9, 9.4, 6.0 Hz, 1H), 2.13 – 1.99 (m, 2H), 1.40 (d, J = 7.0 Hz, 3H), 0.89 (t, J = 7.3 Hz, 3H).

^{13}C NMR (126 MHz, CDCl$_3$): δ/ppm 177.9, 174.5, 138.5, 136.6, 133.3, 129.2, 128.9, 128.8, 128.29, 128.25, 122.4, 58.5, 37.2, 33.5, 23.4, 18.2, 9.9.

HRMS (ESI): calculated for [C$_{21}$H$_{22}$N$_2$O$_2$Na]$^+$: 357.1573; found: 357.1574.

N-(3-Cyano-3-methyl-1-phenylbutyl)-N-isobutyrylbenzamide (33b)
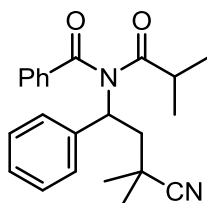
The general procedure for imide synthesis using isobutyronitrile as solvent and a mixture of DCM/hexanes (v/v = 95/5) as eluent in column chromatography lead to the isolation of substance **33b** as colourless oil (0.5 mmol scale: 64 mg, 0.18 mmol, 35%).

^{1}H NMR (300 MHz, CDCl$_3$): δ/ppm 7.59 – 7.48 (m, 5H), 7.43 – 7.36 (m, 2H), 7.34 – 7.21 (m, 3H), 5.96 (dd, J = 7.5, 5.6 Hz, 1H), 2.77 (dd, J = 14.8, 7.5 Hz, 1H), 2.62 (dd, J = 14.8, 5.6 Hz, 1H), 2.16 (hept, J = 6.6 Hz, 1H), 1.42 (s, 3H), 1.29 (s, 3H), 0.73 (d, J = 6.6 Hz, 3H), 0.71 (d, J = 6.6 Hz, 3H).

^{13}C NMR (75 MHz, CDCl$_3$): δ/ppm 181.9, 173.9, 139.0, 137.0, 133.0, 129.3, 129.1, 128.9, 128.6, 128.4, 124.6, 57.7, 43.7, 39.0, 31.6, 28.0, 26.9, 19.6, 18.9.

HRMS (ESI): calculated for [C$_{11}$H$_{12}$Cl$_4$Na]$^+$: 385.1886; found: 385.1887.

N-Acetyl-*N*-(3-cyano-1-phenylpropyl)benzamide (33c)

The general procedure for imide synthesis using acetonitrile as solvent and a mixture of hexanes/EtOAc (v/v = 95/5→80/20) as eluent in column chromatography lead to the isolation of substance **33c** as colourless oil (0.1 mmol scale: 7.4 mg, 0.024 mmol, 24%).

^{1}H NMR (400 MHz, CDCl$_3$): δ/ppm 7.56 − 7.48 (m, 3H), 7.46 − 7.41 (m, 2H), 7.41 − 7.36 (m, 2H), 7.33 − 7.28 (m, 2H), 7.27 − 7.22 (m, 1H), 5.78 (dd, *J* = 8.8, 7.0 Hz, 1H), 2.90 − 2.75 (m, 1H), 2.68 − 2.54 (m, 1H), 2.50 − 2.36 (m, 2H), 1.83 (s, 3H).

^{13}C NMR (101 MHz, CDCl$_3$): δ/ppm 173.6, 171.8, 136.8, 135.3, 132.5, 128.2, 128.0, 127.8, 127.4, 118.1, 58.1, 27.3, 26.5, 14.3.

HRMS (ESI): calculated for [C$_{19}$H$_{18}$N$_2$O$_2$Na]$^+$: 329.1260; found: 329.1257.
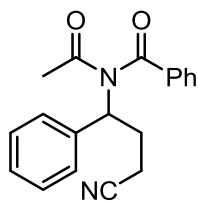
N-Acetyl-*N*-(1-phenylpropyl)benzamide (34)

The general procedure for imide synthesis using acetonitrile as solvent and a mixture of hexanes/EtOAc (v/v = 95/5) as eluent in column chromatography, and a mixture of hexanes/EtOAc (v/v = 98/2) for a subsequent preparative thin layer chromatography lead to the isolation of substance **34** as colourless solid (0.1 mmol scale: 6.6 mg, 0.23 mmol, 23%).

^{1}H NMR (501 MHz, CDCl$_3$): δ/ppm 7.63 − 7.57 (m, 2H), 7.56 − 7.49 (m, 1H), 7.47 (d, *J* = 7.4 Hz, 2H), 7.44 − 7.37 (m, 2H), 7.33 − 7.26 (m, 2H), 7.26 − 7.18 (m, 1H), 5.67 − 5.59 (m, 1H), 2.46 − 2.33 (m, 1H), 2.33 − 2.20 (m, 1H), 1.84 (s, 3H), 1.00 (t, *J* = 7.4 Hz, 3H).

¹³C NMR (126 MHz, CDCl₃): δ/ppm 174.6, 173.4, 139.9, 137.0, 133.0, 129.0 (2C), 128.39, 128.38, 127.6, 62.3, 27.7, 25.3, 11.9.

HRMS (ESI): calculated for $[C_{18}H_{19}N_1O_2Na]^+$: 304.1308; found: 304.1306.

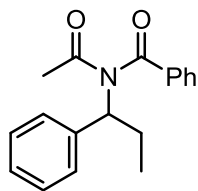**N-Acetyl-N-(2-(*tert*-butoxy)-1-phenylethyl)benzamide (35)**
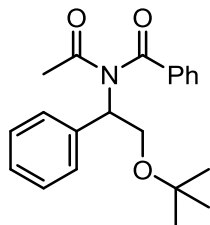
The general procedure for imide synthesis using acetonitrile as solvent and a mixture of hexanes/EtOAc (v/v = 95/5) as eluent in column chromatography, and a mixture of hexanes/EtOAc (v/v = 98/2) for a subsequent preparative thin layer chromatography lead to the isolation of substance **35** as colourless oil (0.1 mmol scale: 3.1 mg, 0.009 mmol, 9%).

¹H NMR (501 MHz, CDCl₃): δ/ppm 7.77 − 7.71 (m, 2H), 7.51 − 7.44 (m, 3H), 7.39 − 7.34 (m, 2H), 7.29 − 7.24 (m, 2H), 7.23 − 7.16 (m, 1H), 5.62 (dd, *J* = 10.5, 5.1 Hz, 1H), 4.08 (dd, *J* = 10.5, 9.2 Hz, 1H), 3.66 (dd, *J* = 9.2, 5.1 Hz, 1H), 1.80 (s, 3H), 0.97 (s, 9H).

¹³C NMR (126 MHz, CDCl₃): δ/ppm 174.3, 173.1, 138.4, 137.1, 132.8, 129.7, 128.7, 128.5, 128.2, 127.7, 73.7, 61.6, 61.4, 27.4, 27.2

HRMS (ESI): calculated for $[C_{21}H_{25}N_1O_3Na]^+$: 362.1727; found: 362.1727.

5.3.5 Other Products

2,3,4,4a,5,6,6a,11,11a,11b-decahydro-1*H*-indeno[1,2-c]quinolin-5-ium chloride (15)
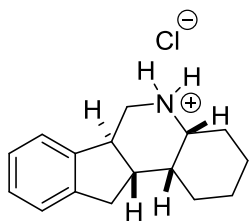
A stock solution of hydrogen chloride in methanol (1.52 M, 0.50 mL) was prepared by dropwise addition of acetyl chloride (54 µL) to stirred methanol (0.50 mL).

The stock solution of hydrogen chloride (0.10 mL, 5.6 equiv.) was added to *tert*-butyl 1,2,3,4,4a,6,6a,11,11a,11b-decahydro-5*H*-indeno[1,2-*c*]quinoline-5-carboxylate (**14**) (8.8 mg, 0.027 mmol, 1.0 equiv.). The resulting solution was stirred for 5 h at r.t.. The yielded white precipitate (7.1 mg, 0.027 mmol, 97%) was separated by filtration, dried *in vacuo* and recrystalized from MeOH/Et$_2$O by gas phase diffusion. The single crystals of **15** (6.2 mg, 0.024 mmol, 82%) were suitable for X-ray diffractometry.

^{1}H NMR (501 MHz, CDCl$_3$): δ/ppm 7.30 – 7.23 (m, 1H), 7.23 – 7.12 (m, 3H), 4.58 (s, 1H), 4.01 (dd, *J* = 11.3, 3.5 Hz, 1H), 3.55 – 3.45 (m, 1H), 3.20 (td, *J* = 12.0, 3.6 Hz, 1H), 3.16 – 3.06 (m, 1H), 2.76 (d, *J* = 9.2 Hz, 2H), 2.34 – 2.16 (m, 2H), 2.07 – 1.65 (m, 5H), 1.64 – 1.48 (m, 2H), 1.48 – 1.36 (m, 1H).

^{13}C NMR (126 MHz, CDCl$_3$): δ/ppm 144.46, 142.44, 128.37, 127.51, 126.00, 123.02, 58.30, 52.47, 49.45, 40.74, 37.88, 33.60, 29.86, 25.79, 22.29, 20.80.

HRMS (ESI): calculated for C$_{16}$H$_{22}$N$^+$ [M-Cl]$^+$: 228.174674, found: 228.174490.

1-(1-(tert-butylperoxy)-2,3-dihydro-1*H*-inden-2-yl)-3,3-dimethylbutan-2-one (17)
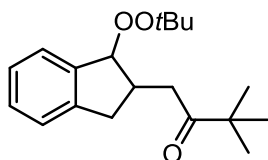
In a 10mL-Schlenk tube indene (59 μL, 0.5 mmol, 1.0 equiv.) was dissolved in MeCN (2.0 mL) under Ar gas atmosphere. Pinacolone (314 μL, 2.5 mmol, 5.0 equiv.) and a solution of TBHP (5.5 M in decane, 364 μL, 2.0 mmol, 4.0 equiv.) were added. After the addition of catalytic pTsOH (10.4 mg, 0.054 mmol, 0.11 equiv.) the reaction mixture was stirred at 50°C for 13 h.

By HPLC separation a diasteremer ratio of 1.73:1 was observed from the crude reaction mixture. For a comparable reaction mixture by crude NMR a d.r. = 1.7:1 was obtained.

The cooled down mixture was diluted and all volatiles were removed *in vacuo* (after the addition of some silica). The collected residue was purified by column chromatography using a mixture of hexanes/EtOAc as eluent (v/v = 99/1 –> 94/6). The diastereomers of **17** were each obtained as colourless oil (1st diastereomer: 22 mg, 0.072 mmol, 14%; 2nd diastereomer: 51 mg, 0.17 mmol, 34%).

1st Diastereomer (minor, cis):

^{1}H NMR (500 MHz, CDCl$_3$): δ 7.45 (d, J = 7.4 Hz, 1H), 7.29 – 7.22 (m, 1H), 7.23 – 7.16 (m, 2H), 5.35 (d, J = 5.7 Hz, 1H), 3.14 (dd, J = 18.3, 6.9 Hz, 1H), 3.03 – 2.92 (m, 2H), 2.77 – 2.67 (m, 2H), 1.19 (s, 9H), 1.15 (s, 9H).

^{13}C NMR (126 MHz, CDCl$_3$): δ 215.6, 144.4, 141.2, 128.9, 126.8, 126.2, 124.7, 87.1, 80.3, 44.2, 39.3, 37.1, 36.2, 26.9, 26.6.

HRMS (ESI): calculated for [C$_{19}$H$_{28}$O$_3$Na]$^+$: 327.193064, found: 327.193080.

2nd Diastereomer (major, trans):

^{1}H NMR (300 MHz, CDCl$_3$): δ 7.47 (dd, J = 8.0, 1.3 Hz, 1H), 7.31 – 7.17 (m, 3H), 5.17 (d, J = 4.1 Hz, 1H), 3.35 (dd, J = 16.3, 7.9 Hz, 1H), 3.05 – 2.93 (m, 1H), 2.91 (dd, J = 17.4, 4.1 Hz, 1H), 2.62 (dd, J = 17.4, 9.9 Hz, 1H), 2.39 (dd, J = 16.3, 5.1 Hz, 1H), 1.26 (s, 9H), 1.14 (s, 9H).

^{13}C NMR (75 MHz, CDCl$_3$): δ 214.9, 143.7, 139.9, 129.1, 126.5, 126.3, 125.2, 91.8, 80.4, 44.2, 41.0, 40.2, 37.1, 26.7, 26.6.

HRMS (ESI): calculated for [C$_{19}$H$_{28}$O$_3$Na]$^+$: 327.193064, found: 327.193600.

N-Acetyl-N-(*tert*-butyl)benzamide (36)
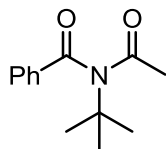
This product was derived in attempted difunctionalization reactions with 1,3,5-trimethoxybenzene as nucleophile instead of indoles and pivaldehyde according to the general procedure for β-(Indol-3-yl)ketones. For a discussion, see chapter 3.3.4 above.

Tris(2-phenylpyridinato-*C2,N*-)iridium (III) (1.4 mg, , 0.02 equiv.) was dispersed in dry acetonitrile (5 mL) under Ar gas atmosphere in a Schlenk-round-bottom-flask (100 mL, 0.5 mmol scale). Then, α-methylstyrene (65 µL, 0.5 mmol, 1 equiv.), 1,3,5-trimethoxybenzene (252 mg, 1.5 mmol, 3 equiv.), pivaldehyde (271 µL, 2.5 mmol, 5 equiv.) and TBPB (196 µL, 1.03 mmol, 2 equiv.) were added to the yellow dispersion. The reaction mixture was stirred and irradiated with white light (40 W white LED) for 20 h. The irradiation power produced a reaction temperature of 65°C.

The reaction mixture was diluted, transferred and dried under reduced pressure (after addition of some silica). The residue was purified by column chromatography using eluent mixtures of hexanes/EtOAc (v/v = 19/1→4/1). The product **36** was yielded as colourless oil (118 mg, 0.54 mmol, 52%)

^{1}H NMR (300 MHz, CDCl$_3$): δ/ppm 8.05 − 7.95 (m, 2H), 7.71 − 7.59 (m, 1H), 7.58 − 7.46 (m, 2H), 1.84 (s, 2H), 1.50 (s, 7H).

^{13}C NMR (75 MHz, CDCl$_3$): δ/ppm 176.5, 168.5, 135.8, 134.6, 130.6, 129.4, 58.6, 28.6, 26.0.

^{15}N NMR (HMBC, 51 MHz, CDCl$_3$): δ/ppm -212.8.

HRMS (ESI): calculated for [C$_{13}$H$_{17}$NO$_2$+H]$^+$: 220.1332; found: 220.1333.

(Benzoyloxy)(4-methoxyphenyl)methyl 4-methoxybenzoate (37)
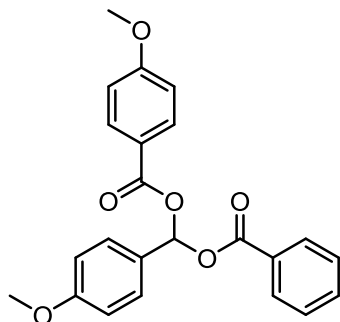
The product was isolated as a side product in the synthesis of *N*-acetyl-*N*-(3-(4-methoxyphenyl)-3-oxo-1-phenylpropyl)benzamide **30c**. It was obtained by column chromatography with a mixture of hexanes/EtOAc (v/v = 13/1→6/1) as eluent. The dicarboxylate **37** is a yellow oil (24 mg, 0.061 mmol, 6%). For a discussion on the formation see chapter 3.3.5 above.

^{1}H NMR (501 MHz, CDCl$_3$): δ/ppm 8.14 (s, 1H), 8.12 – 8.08 (m, 2H), 8.07 – 8.02 (m, 2H), 7.65 (d, *J* = 8.7 Hz, 2H), 7.57 (t, *J* = 7.4 Hz, 1H), 7.44 (t, *J* = 7.8 Hz, 2H), 6.97 (dd, *J* = 9.3, 2.2 Hz, 2H), 6.92 (d, *J* = 8.9 Hz, 2H), 3.85 (s, 3H), 3.83 (s, 3H).

^{13}C NMR (126 MHz, CDCl$_3$): δ/ppm 164.6, 164.3, 164.0, 160.8, 133.6, 132.3, 130.2, 129.5, 128.6, 128.4 (2C), 121.7, 114.2, 113.9, 90.7, 55.6, 55.5.

HRMS (ESI): calculated for $[C_{23}H_{20}O_6Na]^+$: 415.1152; found: 415.1157.

5.4 Crystallographic Data

X-Ray Structure of **15**/ CCDC-1878410. The substance was recrystalized from MeOH/Et$_2$O (see above).
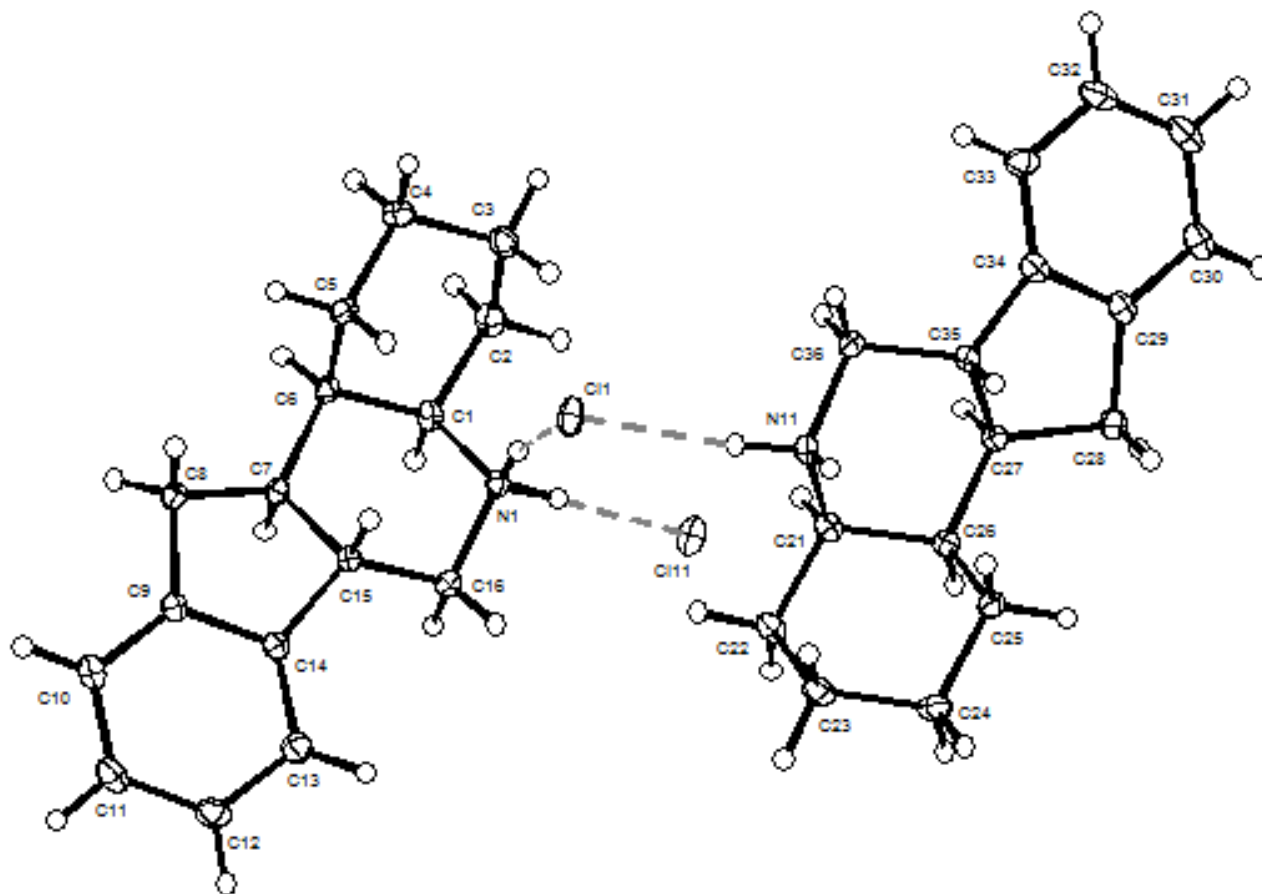
Table 1. Crystal data and structure refinement of 15.

Identification code	CCDC-1878410
Empirical formula	$C_{16} H_{22} Cl N$
Color	colorless
Formula weight	263.79 g · mol^{-1}
Temperature	100(2) K
Wavelength	0.71073 Å
Crystal system	MONOCLINIC
Space group	**P2$_1$/n, (no. 14)**
Unit cell dimensions	a = 11.4837(13) Å $\quad$ α= 90°.
	b = 7.6493(9) Å $\quad$ β= 90.774(2)°.
	c = 31.513(4) Å $\quad$ γ = 90°.
Volume	2768.0(5) Å^3
Z	8
Density (calculated)	1.266 Mg · m^{-3}
Absorption coefficient	0.259 mm^{-1}
F(000)	1136 e
Crystal size	0.051 x 0.042 x 0.023 mm^3
θ range for data collection	1.292 to 31.250°.
Index ranges	-16 ≤ h ≤ 16, -11≤ k ≤ 11, -46 ≤ l ≤ 45
Reflections collected	73006
Independent reflections	8928 [R$_{int}$ = 0.0750]
Reflections with I>2σ(I)	6540
Completeness to θ = 25.242°	100.0 %
Absorption correction	Gaussian
Max. and min. transmission	1.00 and 0.99
Refinement method	Full-matrix least-squares on F^2
Data / restraints / parameters	8928 / 0 / 373
Goodness-of-fit on F^2	1.026
Final R indices [I>2 σ (I)]	R$_1$ = 0.0444 $\quad$ wR^2 = 0.0994
R indices (all data)	R$_1$ = 0.0717 $\quad$ wR^2 = 0.1108
Largest diff. peak and hole	0.4 and -0.3 e · Å^{-3}

Table 2.   Bond lengths [Å] and angles [°] of 15.

N(1)-C(1)	1.5127(19)	N(1)-C(16)	1.4982(18)
C(1)-C(2)	1.525(2)	C(1)-C(6)	1.5417(19)
C(2)-C(3)	1.525(2)	C(3)-C(4)	1.527(2)
C(4)-C(5)	1.528(2)	C(5)-C(6)	1.531(2)
C(6)-C(7)	1.5260(19)	C(7)-C(8)	1.5419(18)
C(7)-C(15)	1.5381(19)	C(8)-C(9)	1.515(2)
C(9)-C(10)	1.3912(19)	C(9)-C(14)	1.4048(19)
C(10)-C(11)	1.392(2)	C(11)-C(12)	1.389(2)
C(12)-C(13)	1.398(2)	C(13)-C(14)	1.383(2)
C(14)-C(15)	1.5124(19)	C(15)-C(16)	1.5111(19)
N(11)-C(21)	1.5121(19)	N(11)-C(36)	1.4961(18)
C(21)-C(22)	1.5255(19)	C(21)-C(26)	1.5369(19)
C(22)-C(23)	1.530(2)	C(23)-C(24)	1.527(2)
C(24)-C(25)	1.529(2)	C(25)-C(26)	1.532(2)
C(26)-C(27)	1.5203(19)	C(27)-C(28)	1.5407(18)
C(27)-C(35)	1.5393(19)	C(28)-C(29)	1.515(2)
C(29)-C(30)	1.3885(19)	C(29)-C(34)	1.403(2)
C(30)-C(31)	1.394(2)	C(31)-C(32)	1.387(2)
C(32)-C(33)	1.402(2)	C(33)-C(34)	1.387(2)
C(34)-C(35)	1.5119(19)	C(35)-C(36)	1.5112(18)
C(16)-N(1)-C(1)	114.05(11)	N(1)-C(1)-C(2)	109.46(11)
N(1)-C(1)-C(6)	111.08(11)	C(2)-C(1)-C(6)	112.63(12)
C(1)-C(2)-C(3)	112.90(12)	C(2)-C(3)-C(4)	110.49(12)
C(3)-C(4)-C(5)	110.40(12)	C(4)-C(5)-C(6)	111.02(12)
C(5)-C(6)-C(1)	111.73(11)	C(7)-C(6)-C(1)	107.23(11)
C(7)-C(6)-C(5)	115.75(11)	C(6)-C(7)-C(8)	121.97(12)
C(6)-C(7)-C(15)	112.81(11)	C(15)-C(7)-C(8)	102.41(11)
C(9)-C(8)-C(7)	100.45(11)	C(10)-C(9)-C(8)	129.92(13)
C(10)-C(9)-C(14)	119.97(14)	C(14)-C(9)-C(8)	110.08(12)

C(9)-C(10)-C(11)	118.91(13)	C(12)-C(11)-C(10)	120.74(13)
C(11)-C(12)-C(13)	120.71(15)	C(14)-C(13)-C(12)	118.42(14)
C(9)-C(14)-C(15)	108.30(12)	C(13)-C(14)-C(9)	121.15(13)
C(13)-C(14)-C(15)	130.55(13)	C(14)-C(15)-C(7)	101.04(11)
C(16)-C(15)-C(7)	110.98(11)	C(16)-C(15)-C(14)	119.29(12)
N(1)-C(16)-C(15)	107.56(11)	C(36)-N(11)-C(21)	113.38(11)
N(11)-C(21)-C(22)	110.27(11)	N(11)-C(21)-C(26)	110.74(11)
C(22)-C(21)-C(26)	112.34(12)	C(21)-C(22)-C(23)	113.27(12)
C(24)-C(23)-C(22)	110.85(12)	C(23)-C(24)-C(25)	111.17(12)
C(24)-C(25)-C(26)	110.85(12)	C(25)-C(26)-C(21)	111.61(11)
C(27)-C(26)-C(21)	107.50(11)	C(27)-C(26)-C(25)	115.42(11)
C(26)-C(27)-C(28)	121.80(12)	C(26)-C(27)-C(35)	113.39(11)
C(35)-C(27)-C(28)	102.03(11)	C(29)-C(28)-C(27)	100.52(11)
C(30)-C(29)-C(28)	129.76(14)	C(30)-C(29)-C(34)	120.26(14)
C(34)-C(29)-C(28)	109.95(12)	C(29)-C(30)-C(31)	118.77(14)
C(32)-C(31)-C(30)	121.02(14)	C(31)-C(32)-C(33)	120.47(15)
C(34)-C(33)-C(32)	118.49(14)	C(29)-C(34)-C(35)	108.19(13)
C(33)-C(34)-C(29)	120.96(13)	C(33)-C(34)-C(35)	130.84(13)
C(34)-C(35)-C(27)	100.70(10)	C(36)-C(35)-C(27)	111.60(11)
C(36)-C(35)-C(34)	120.37(12)	N(11)-C(36)-C(35)	107.38(11)

Table 3. Selected torsion angles [°] of 15.

H(1)-C(1)-N(1)-C(16)	-57.5(11)
H(1)-C(1)-C(2)-C(3)	172.2(12)
H(1)-C(1)-C(6)-C(5)	-173.3(12)
H(1)-C(1)-C(6)-H(6)	-56.3(15)
H(6)-C(6)-C(1)-N(1)	-169.6(10)
H(6)-C(6)-C(1)-H(1)	-56.3(15)
H(6)-C(6)-C(1)-C(2)	67.2(10)
H(6)-C(6)-C(5)-C(4)	-60.2(9)
H(7)-C(7)-C(6)-C(5)	174.4(9)
H(7)-C(7)-C(6)-H(6)	52.1(13)
H(7)-C(7)-C(15)-H(15)	175.6(13)
H(7)-C(7)-C(15)-C(16)	57.2(8)
H(15)-C(15)-C(7)-C(6)	59.2(10)
H(15)-C(15)-C(7)-H(7)	175.6(13)
H(15)-C(15)-C(14)-C(13)	-91.9(10)
H(15)-C(15)-C(16)-N(1)	-63.1(10)

X-Ray structure of **27g**/ CCDC No.: 1978887. The substance was recrystallized from THF/pentane (see above).
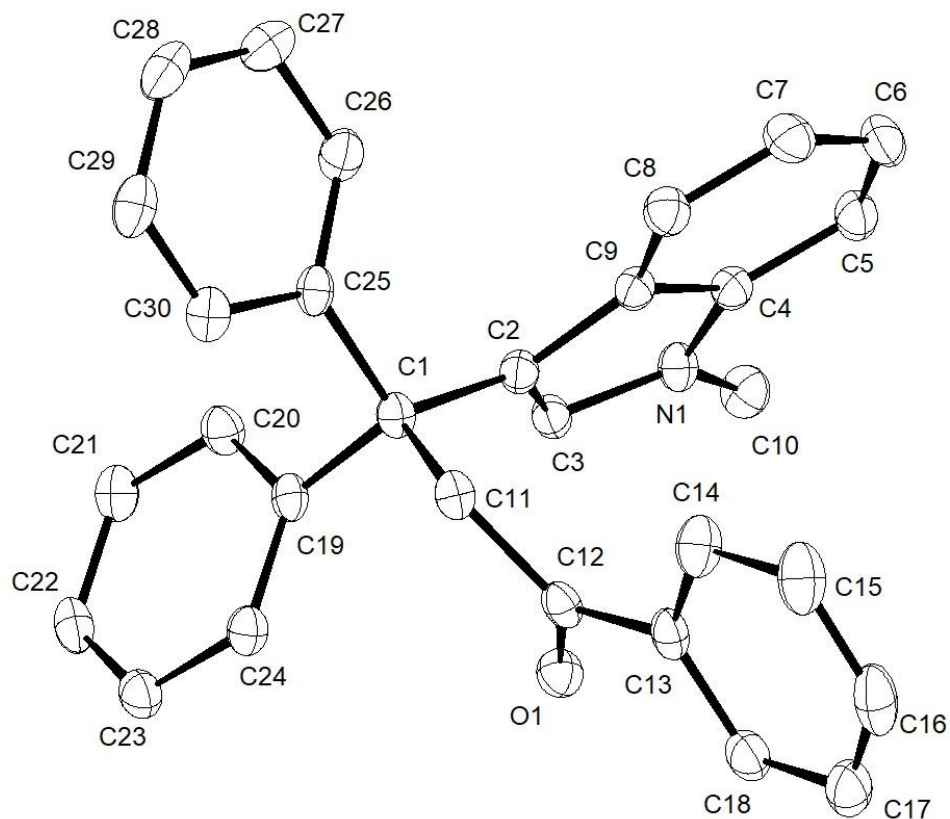
In addition, the structure contained disordered solvent molecules, which could not be refined in a satisfactory manner. With the squeeze application, the solvent voids were deleted from the structure.

The structure shows with the C1–C2 bond a connectivity of an indol-3-yl moiety with the benzylic position of the former 1,1-diphenylethylene.

Table 4. Crystal data and structure refinement of 27g.

Identification code	CCDC No.: 1978887
Empirical formula	$C_{30} H_{25} N O$
Color	colorless
Formula weight	415.51 g $\cdot$ mol^{-1}
Temperature	100(2) K
Wavelength	1.54178 Å
Crystal system	TRICLINIC
Space group	**P1, (no. 2)**
Unit cell dimensions	a = 8.0782(3) α=84.7090(10)°.
	b = 12.2475(4) Å β=76.419(2)°.
	c = 13.2367(4) Å γ =75.461(2)°.
Volume	1231.46(7) Å^3
Z	2
Density (calculated)	1.121 Mg $\cdot$ m^{-3}
Absorption coefficient	0.518 mm^{-1}
F(000)	440 e
Crystal size	0.230 x 0.142 x 0.034 mm^3
θ range for data collection	5.800 to 61.163°.
Index ranges	-9 ≤ h ≤ 9, -13≤ k ≤ 13, -15 ≤ l ≤ 15
Reflections collected	30886
Independent reflections	3638 [R$_{int}$ = 0.0498]
Reflections with I>2σ(I)	3136
Completeness to θ = 61.163°	96.0 %
Absorption correction	Gaussian
Max. and min. transmission	0.99 and 0.94
Refinement method	Full-matrix least-squares on F^2
Data / restraints / parameters	3638 / 0 / 290
Goodness-of-fit on F^2	1.083
Final R indices [I>2σ(I)]	R$_1$ = 0.0337 wR^2 = 0.0903
R indices (all data)	R$_1$ = 0.0384 wR^2 = 0.0922
Largest diff. peak and hole	0.1 and -0.2 e $\cdot$ Å^{-3}

Table 5. Bond lengths [Å] and angles [°] of 27g.

_____

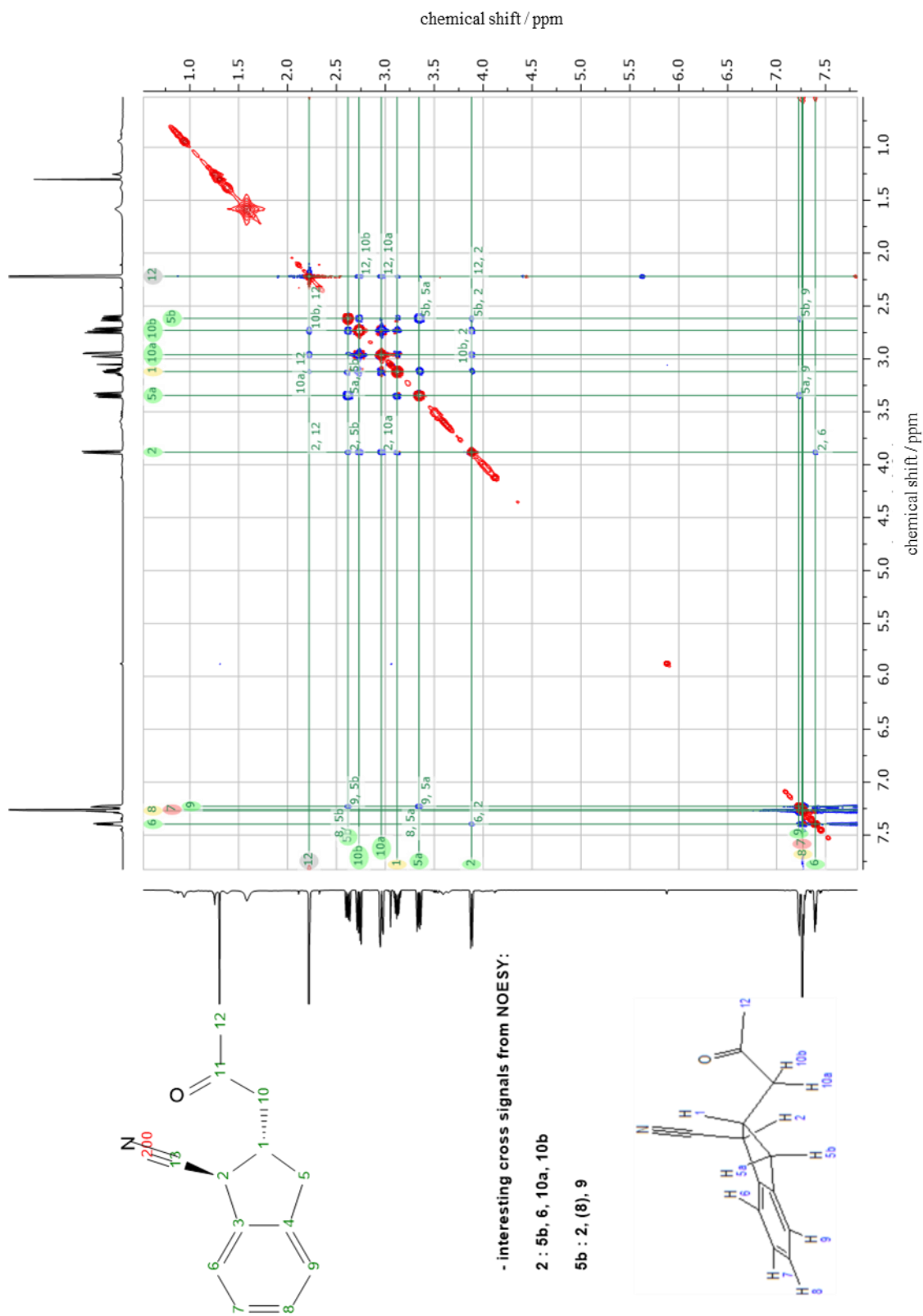| O(1)-C(12)	1.2228(15)	N(1)-C(3)	1.3749(16)
N(1)-C(4)	1.3780(17)	N(1)-C(10)	1.4518(16)
C(1)-C(2)	1.5231(16)	C(1)-C(11)	1.5642(16)
C(1)-C(19)	1.5379(17)	C(1)-C(25)	1.5500(17)
C(2)-C(3)	1.3683(17)	C(2)-C(9)	1.4448(18)
C(4)-C(5)	1.3928(18)	C(4)-C(9)	1.4180(17)
C(5)-C(6)	1.377(2)	C(6)-C(7)	1.4033(19)
C(7)-C(8)	1.3820(19)	C(8)-C(9)	1.4090(18)
C(11)-C(12)	1.5137(17)	C(12)-C(13)	1.5001(18)
C(13)-C(14)	1.3975(19)	C(13)-C(18)	1.4000(19)
C(14)-C(15)	1.387(2)	C(15)-C(16)	1.381(2)
C(16)-C(17)	1.388(2)	C(17)-C(18)	1.3826(19)
C(19)-C(20)	1.3989(18)	C(19)-C(24)	1.3911(17)
C(20)-C(21)	1.3835(19)	C(21)-C(22)	1.3893(18)
C(22)-C(23)	1.3851(19)	C(23)-C(24)	1.3868(18)
C(25)-C(26)	1.3886(18)	C(25)-C(30)	1.3996(18)
C(26)-C(27)	1.3916(19)	C(27)-C(28)	1.383(2)
C(28)-C(29)	1.388(2)	C(29)-C(30)	1.3848(19)
C(3)-N(1)-C(4)	108.43(10)	C(3)-N(1)-C(10)	126.45(11)
C(4)-N(1)-C(10)	125.12(11)	C(2)-C(1)-C(11)	106.73(10)
C(2)-C(1)-C(19)	111.75(10)	C(2)-C(1)-C(25)	112.75(10)
C(19)-C(1)-C(11)	114.02(10)	C(19)-C(1)-C(25)	105.51(10)
C(25)-C(1)-C(11)	106.07(9)	C(3)-C(2)-C(1)	126.91(11)
C(3)-C(2)-C(9)	105.98(11)	C(9)-C(2)-C(1)	126.69(11)
C(2)-C(3)-N(1)	110.92(11)	N(1)-C(4)-C(5)	129.19(11)
N(1)-C(4)-C(9)	107.81(11)	C(5)-C(4)-C(9)	122.99(12)
C(6)-C(5)-C(4)	117.35(12)	C(5)-C(6)-C(7)	121.29(13)
C(8)-C(7)-C(6)	121.31(13)	C(7)-C(8)-C(9)	119.16(12)

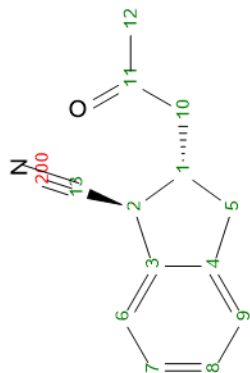|			
C(4)-C(9)-C(2)	106.86(11)	C(8)-C(9)-C(2)	135.22(12)
C(8)-C(9)-C(4)	117.90(12)	C(12)-C(11)-C(1)	116.77(10)
O(1)-C(12)-C(11)	121.70(11)	O(1)-C(12)-C(13)	119.55(11)
C(13)-C(12)-C(11)	118.70(11)	C(14)-C(13)-C(12)	123.68(12)
C(14)-C(13)-C(18)	118.43(12)	C(18)-C(13)-C(12)	117.88(11)
C(15)-C(14)-C(13)	120.78(13)	C(16)-C(15)-C(14)	119.92(14)
C(15)-C(16)-C(17)	120.18(13)	C(18)-C(17)-C(16)	120.01(14)
C(17)-C(18)-C(13)	120.67(13)	C(20)-C(19)-C(1)	118.13(11)
C(24)-C(19)-C(1)	123.80(11)	C(24)-C(19)-C(20)	117.80(12)
C(21)-C(20)-C(19)	121.33(12)	C(20)-C(21)-C(22)	120.07(12)
C(23)-C(22)-C(21)	119.24(12)	C(22)-C(23)-C(24)	120.49(12)
C(23)-C(24)-C(19)	121.05(12)	C(26)-C(25)-C(1)	122.89(11)
C(26)-C(25)-C(30)	117.82(12)	C(30)-C(25)-C(1)	119.27(11)
C(25)-C(26)-C(27)	121.08(12)	C(28)-C(27)-C(26)	120.23(13)
C(27)-C(28)-C(29)	119.55(12)	C(30)-C(29)-C(28)	119.89(12)
C(29)-C(30)-C(25)	121.35(12)		

5.5 Diastereomer Identification

Information from ^{1}H,^{1}H NOESY NMR experiments led to the differentiation of relative configurations (sometimes total configuration of one stereogenic center) at the stereogenic centers in diastereomers of structures **10**, **11**, **12**, **13**, **16**.[1]

For unpublished structures **17** and **18** the identification of relative configurations in the isolated diastereomers is shown by analogous cross signal analysis.[131]

Major diastereomer of **18**, $^{1}H,^{1}H$ NOESY NMR (500 MHz, CDCl$_3$):

- interesting cross signals from NOESY:

2 : 5b, 6, 10a, 10b

5b : 2, (8), 9

^{1}H,^{1}H NOESY NMR (500 MHz, CDCl$_3$) close-up for the major diastereomer of **18**:
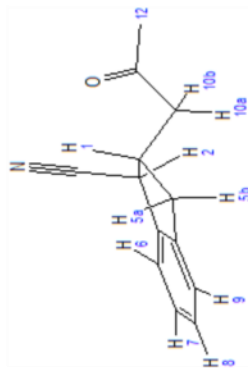
The major diastereomer of structure **18** showed meaningful cross signals (see figure above for numbering): 2↔10, 2↔ 5b (weak), 1↔5b (weaker, but also COSY artefacts present), 1↔5a.

In conclusion: 2 and 1 are oriented to different sides; 2 and 10 on the same side of the five-membered ring.

The relative configuration of the two (introduced) substituents is suggestively *trans*.

For the minor diastereomer in turn the two substituents can be assigned to a relative *cis* configuration.

^{1}H,^{1}H NOESY NMR (501 MHz, C$_6$D$_6$) for the 1st diastereomer of **17**
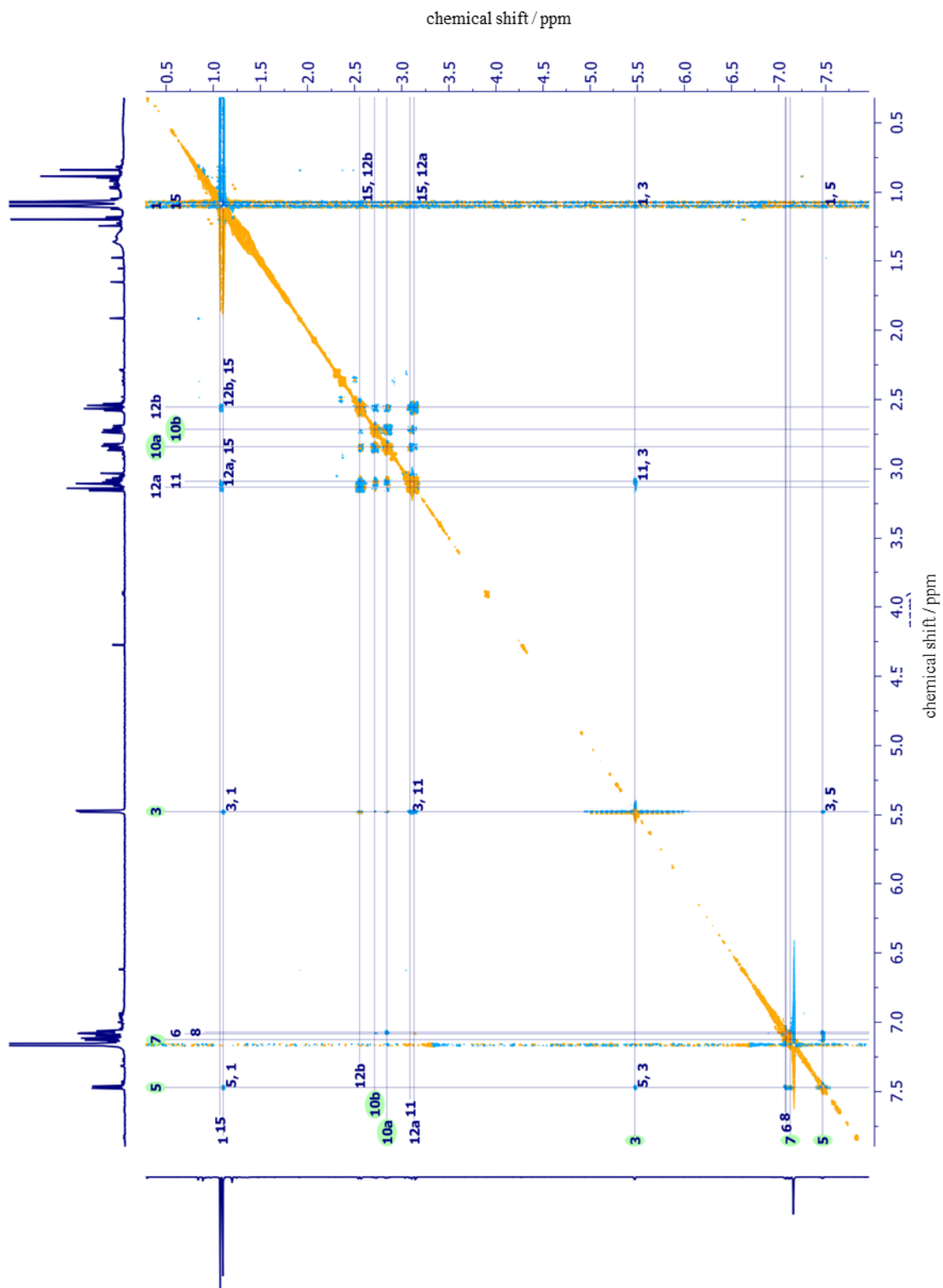
^{1}H,^{1}H NOESY NMR (501 MHz, CDCl$_3$) for the 2nd diastereomer of **17**:

Diastereomers of structure **17**:

The spectra above show NOESY NMR of the 1st and 2nd diastereomer (referred to elution sequence) of product **17**. Although the diastereomers were found in just a ratio of 1.7:1, the 1st diastereo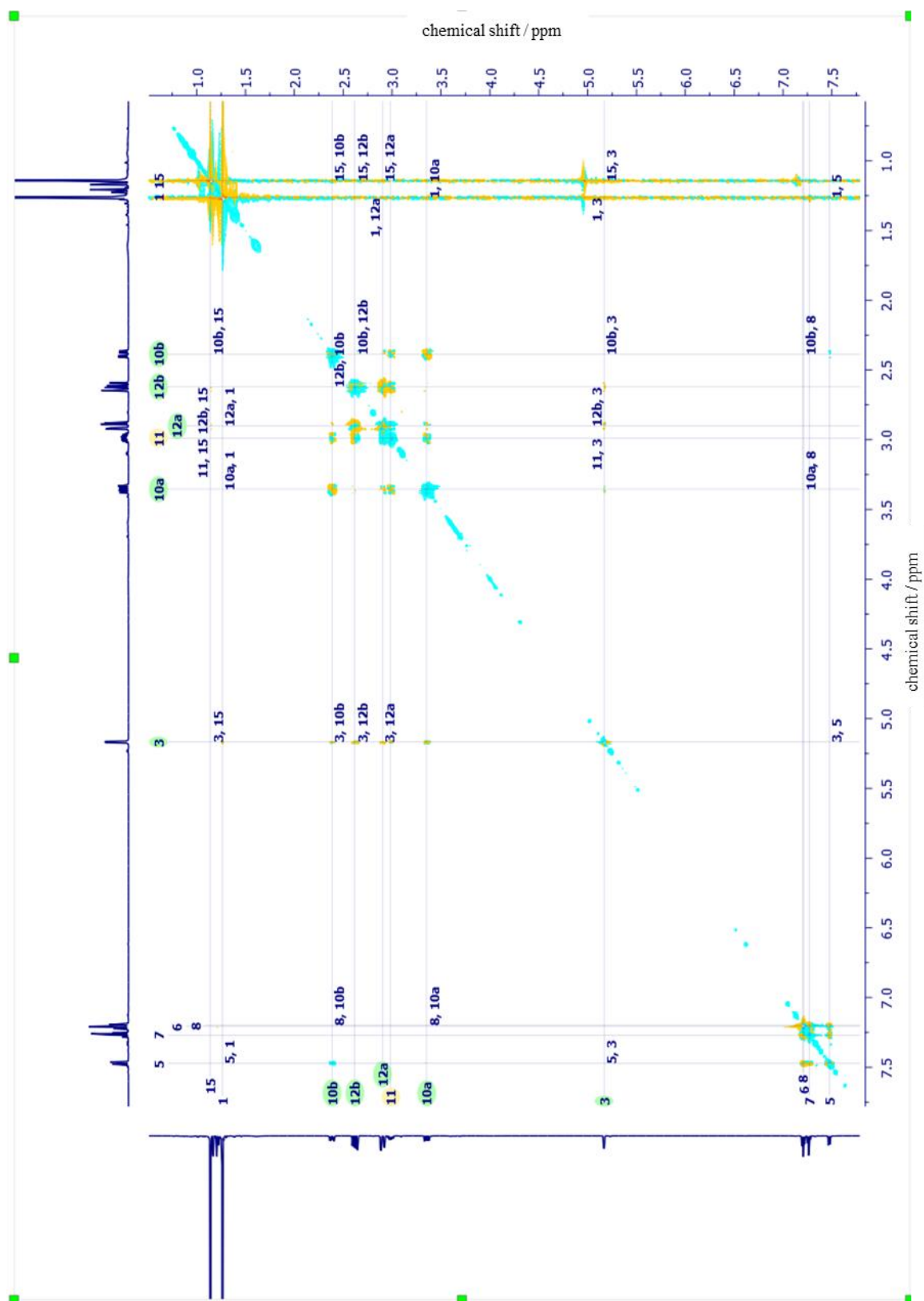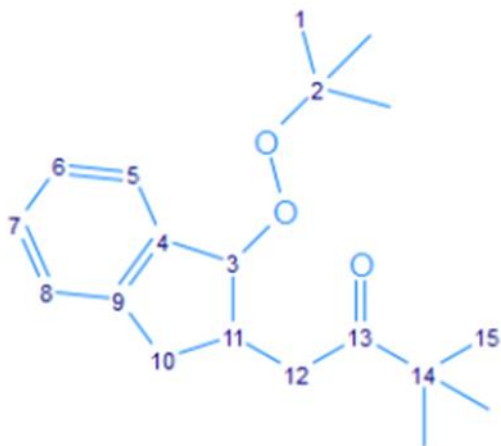mer might be called minor and the 2nd diastereomer, major diastereomer. The relative stereochemistry of the alkylation-peroxidation products **17** was a bit less clear to assign when analyzing the NOESY NMR spectra. The numbers in the spectra are corresponding to the figure on the left-hand side.

1st Diastereomer ("minor") of **17**:

The ^{1}H,^{1}H NOESY NMR experiment for this diastereomer was carried out in the solvent C_6D_6 due to better signal separations. 10 and 12 showed extensive COSY artefacts. Quite significant cross signals were observed between 3 and 11. This was an indication that the diastereomer featured a relative *cis* configuration of the two (introduced) substituents on the five-membered ring (See also 2nd diastereomer for more information).

Meaningful cross signals for 1st diastereomer ("minor") of **17**:

3↔11

2nd Diastereomer ("major") of **17**:

The cross signals show also some COSY artefacts. 10 does not give convincing information about their surroundings. When comparing both single diastereomers, for the 2nd one, it stood out that 3 shows a cross signal with 10b and 12a,b. 10b showed cross signals with 12b, while 10a showed no cross signals with 3, nor 12. This suggested that 3 is oriented to the same side of the five-membered ring as methylene group 12. In conclusion the two (introduced) substituents on the ring should have a relative *trans* configuration in the 2nd diastereomer.

172

Meaningful NOESY cross signals for 2nd diastereomer of **17**:

3: 11, 12a, 12b, 10a

10a: 1, 8

10b: 3, 8, 12b

12a: 1, 3

12b: 3, 10b

5.6 Diastereomer Ratios from Crude Reaction Mixtures

Alkylation-Peroxidation of Indene **17**:

Product **17** were not detected by GC. The crude reaction mixtures were therefore analyzed using HPLC (UV/Vis detector) and ^{1}H NMR.

HPLC analysis:

Table 6. Conditions of HPLC separation of the reaction mixture of 17.

HPLC column:	50 mm Eclipse Plus C18 1.8 μm, 4.6 mm in diameter.
MeOH/H$_2$O gradient:	70%B- 5'- 95%B
Flow/pressure/temperature:	0.5 mL min^{-1}/21 MPa/308 K
	+ 0.1 ml min^{-1} ammonium acetate solution (10 mM)
Detector:	UV, 220 nm

Chromatogram: Retention time vs. signal
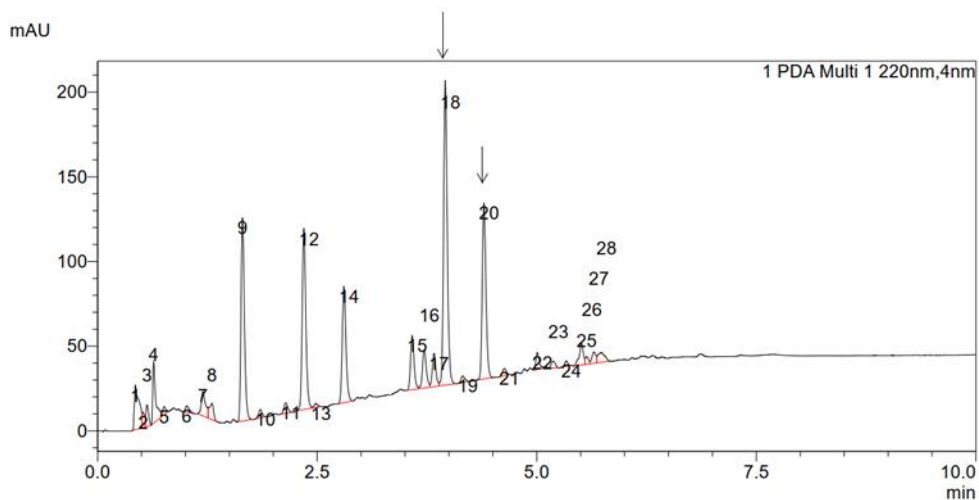
Figure 13. HPLC chromatogram of **17** in reaction mixture.

Signals numbered by 18 and 20 were by mass analysis assigned to the two diastereomers of **17**.

PDA Ch1 220nm

Peak#	Ret. Time	Area%	Name
1	0.43	4.12	
2	0.52	0.68	
3	0.56	1.18	
4	0.64	3.56	
5	0.76	0.53	
6	1.01	0.49	
7	1.20	2.08	
8	1.30	1.31	
9	1.65	13.32	
10	1.85	0.57	
11	2.14	0.80	
12	2.35	12.56	
13	2.49	0.25	
14	2.80	8.39	
15	3.58	3.71	
16	3.72	2.84	
17	3.83	2.30	
18	3.96	21.55	Produkt
19	4.16	0.51	
20	4.40	12.42	Produkt
21	4.63	0.52	
22	5.01	1.10	
23	5.19	0.54	
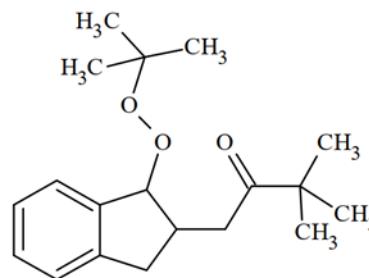
1.73 : 1

• m/z 322: M + NH$_4$ (**17**)

Peak#	Ret. Time	Area%	Name
24	5.34	0.31	
25	5.51	1.71	
26	5.57	0.46	
27	5.65	0.86	
28	5.74	1.32	
Total		100.00	

Figure 14. Signals of chromatogram of **17** in reaction mixture.

174

The two diastereomers showed from UV-detection counts integrals in the ratio 1.73:1. Assuming an identical (similar) UV absorption at the detection wavelength spectrum for the two diastereomers, this directly corresponds to the molar ratio of the isomers in the mixture after full reaction progress.

^{1}H NMR (501 MHz, CDCl$_3$) analysis of crude reaction mixture containing **17**:
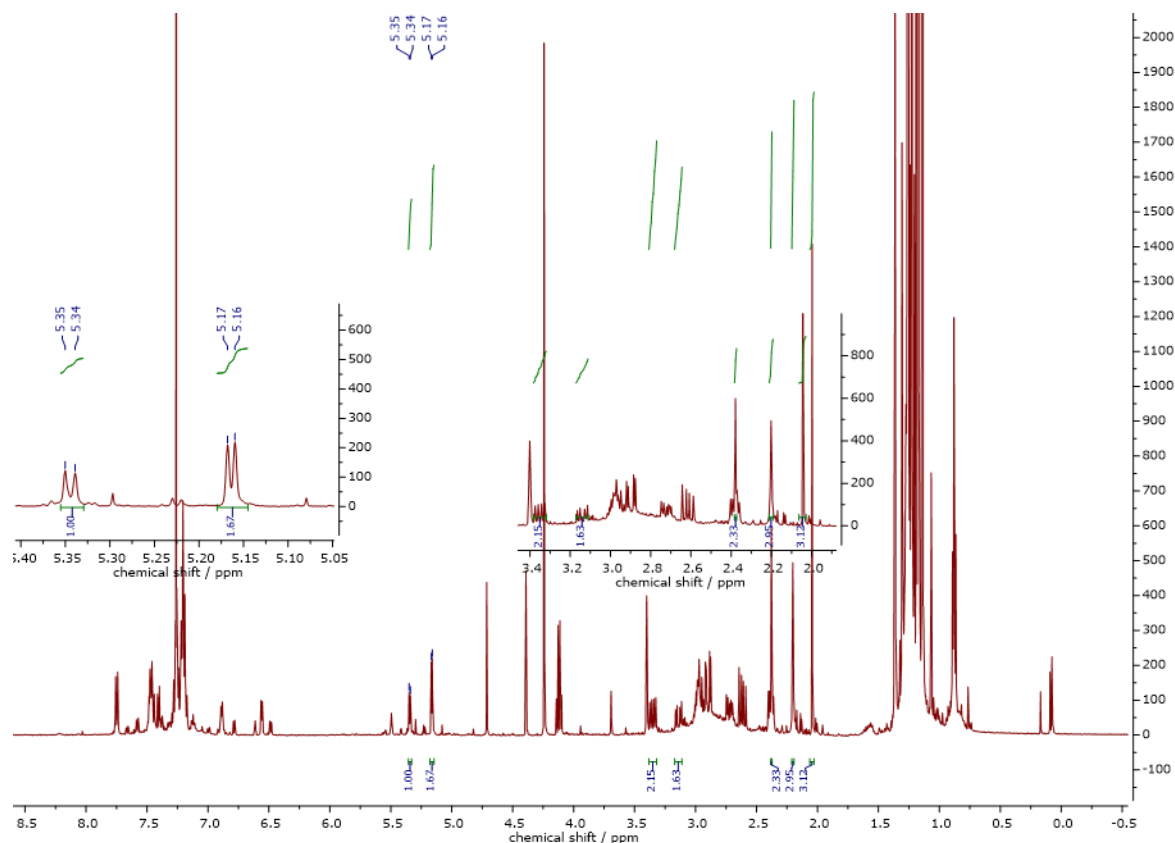
Figure 15. ^{1}H NMR of **17** in the reaction mixture.

Benzylic protons of **17** (5.35 (d) and 5.17 ppm (d), respectively) showed low overlay and hence their integrals were used to determine a molar ratio between the corresponding diastereomers formed in the reaction. The integral ratio suggested a d.r. = ~1.67:1. The results for HPLC and NMR analysis gave similar results for a d.r. around 1.7:1 (for particular reaction conditions see chapter 5.3.5; for discussion of the results see chapter 3.2.3).

Alkylation-cyanation of Indene (**18**):

Samples from a dried reaction mixture of the alkylation-cyanation of indene with acetone (**18**) were injected to a GC device (as solution in acetone).

Table 7. Conditions of gaschromatographic analysis of the reaction mixture of 18.

Column: 30 m, DB-1 0.25/0.25df G/701

Temperature: 220°C; 50°C to 220°C (5 K min^{-1}); 220°C to 320°C (5 K min^{-1}); 5 min at 320°C

Pressure: 0.50 bar (H$_2$)

Chromatogram:

From mass analysis two signals, marked as 109 and 114, in chromatogram were assigned to diastereomers of **18**. From the signal integrals the molar ratio of the two diastereomers in the reaction mixture corresponded to 3.26:1.

Table 8. Integrals of signals in GC-chromatogram of the reaction mixture containing 18.
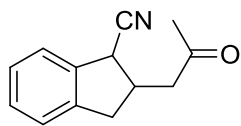
18, 199.25 u

Signal No.	Retention time [min]	Area [%]	Mol. Weight [u]
6	4.6	2.93	130.1
11	6.56	1.34	
14	8.01	2.93	142.2
19	8.59	2.05	
35	12.37	0.86	
59	17.04	8.44	
103	24.27	0.95	
104	24.44	0.70	
109	25.62	8.79	199.3
114	26.49	28.66	199.4
122	27.81	1.84	
126	28.62	1.37	
133	29.87	10.56	
151	33.96	1.31	
159	36.17	0.70	
219	42.85	1.56	
220	42.93	1.44	

The reaction mixture of **18** was also analyzed by ^{1}H NMR (501 MHz, CDCl$_3$). The benzylic protons of the two diastereomers showed low overlay in the spectrum, thus corresponding integrals were used to determine their relative molar ratio. The diastereomers showed by NMR analysis d.r. = 3.6:1 in the reaction mixture (for particular reaction conditions see chapter 5.2.2; for discussion of the results see 3.2.3).
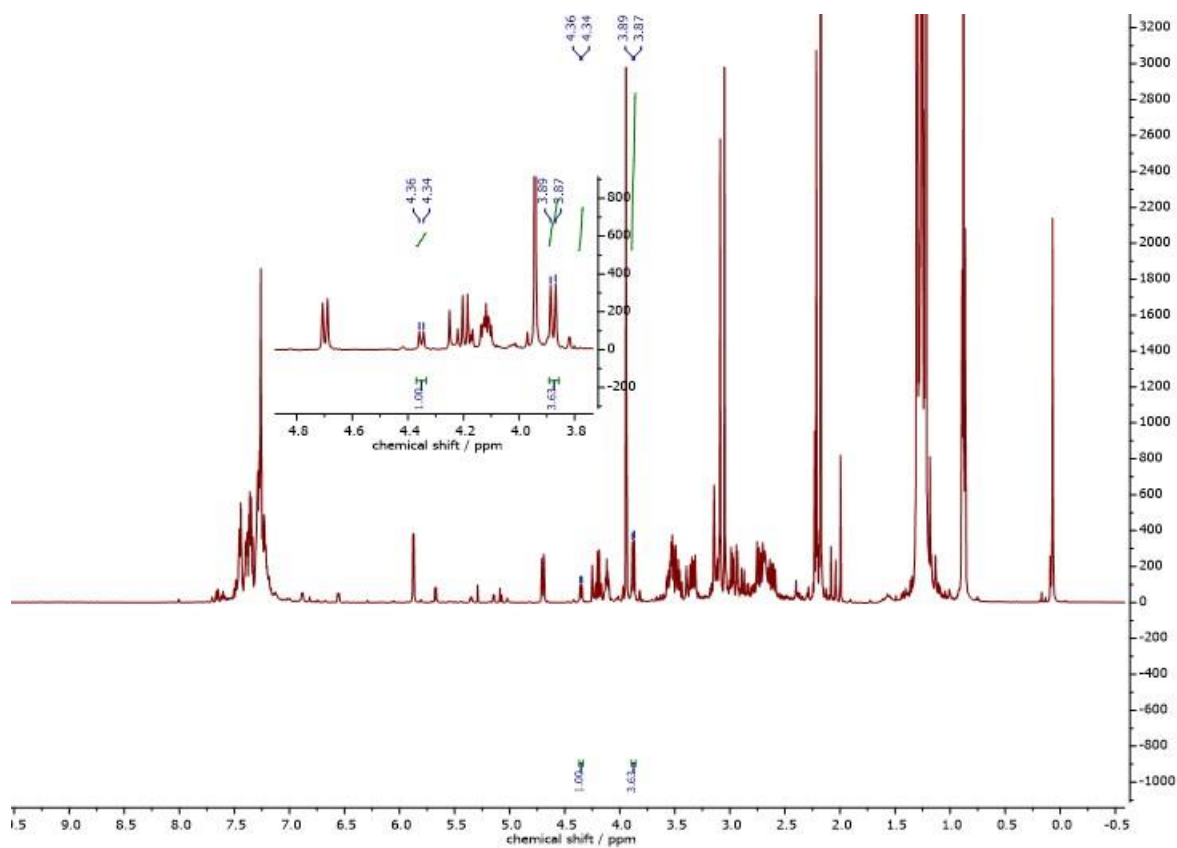

Figure 16. ^{1}H NMR of **18** in the reaction mixture.

5.7 Indications for further Difunctionalization Products

Some of the here described spectra were not immaculate and the respective compound therefore not entirely characterized. By comparison of chemical shifts with pure analogue compounds of the same study, an anticipation of the structures and thus names are given in here with reservation (see chapter 3.3.5).

3-(1-methyl-1*H*-indol-3-yl)-1-phenyl-3-(p-tolyl)butan-1-one (38a)

¹H NMR (501 MHz, CDCl₃): δ/ppm 7.59 – 7.54 (m, 2H), 7.37 – 7.32 (m, 1H), 7.27 – 7.23 (m, 2H), 7.18 – 7.13 (m, 3H), 7.13 – 7.08 (m, 1H), 7.07 – 7.00 (m, 3H), 6.90 – 6.85 (m, 1H), 6.82 (s, 1H), 4.00 (d, *J* = 14.1 Hz, 1H), 3.68 (d, *J* = 14.1 Hz, 1H), 3.64 (s, 3H), 2.29 (s, 3H), 1.94 (s, 3H).

¹³C NMR (126 MHz, CDCl₃): δ/ppm 200.23, 145.33, 138.38, 137.80, 135.42, 132.15, 128.90, 127.88 (2C), 126.72, 126.71, 126.41, 122.36, 121.38, 121.32, 118.62, 109.27, 48.58, 41.91, 32.66, 28.41, 21.06.

1-(4-chlorophenyl)-3-(1-methyl-1*H*-indol-3-yl)-3-phenylbutan-1-one (38b)

¹H NMR (501 MHz, CDCl₃): δ/ppm 7.43 – 7.38 (m, 2H), 7.36 – 7.32 (m, 2H), 7.26 – 7.21 (m, 2H), 7.19 – 7.14 (m, 2H), 7.13 – 7.09 (m, 1H), 7.07 – 7.03 (m, 2H), 6.93 – 6.90 (m, 1H), 6.89 – 6.84 (m, 1H), 6.81 (s, 1H), 3.96 (d, *J* = 13.5 Hz, 1H), 3.64 (s, 3H), 3.61 (d, *J* = 13.5 Hz, 1H), 1.91 (s, 3H).

¹³C NMR (126 MHz, CDCl₃): δ/ppm 199.35, 148.16, 138.49, 137.81, 136.58, 129.21, 128.29, 127.96, 126.79, 126.75, 126.34, 126.21, 121.80, 121.52, 121.25, 118.80, 109.37, 48.40, 42.38, 32.69, 28.49.

3-(1-methyl-1*H*-indol-3-yl)-1-phenyl-3-(4-(trifluoromethyl)phenyl)butan-1-one (38c)

¹H NMR (501 MHz, CDCl₃): δ/ppm 7.62 – 7.57 (m, 2H), 7.48 (br, 4H), 7.41 – 7.35 (m, 1H), 7.25 – 7.15 (m, 3H), 7.17 – 7.10 (m, 1H), 6.95 (d, *J* = 8.0 Hz, 1H), 6.91 – 6.88 (m, 1H), 6.87 (s, 1H), 3.98 (d, *J* = 14.6 Hz, 1H), 3.76 (d, *J* = 14.6 Hz, 1H), 3.69 (s, 3H), 1.98 (s, 3H).

¹⁹F NMR (471 MHz, CDCl₃): δ/ppm -62.31.

**N-acetyl-N-(3-cyclohexyl-3-oxo-1-phenylpropyl)benzamide (39)**

^{1}H NMR (300 MHz, CDCl$_3$): δ/ppm 7.62 – 7.56 (m, 2H), 7.55 – 7.48 (m, 1H), 7.47 – 7.36 (m, 4H), 7.34 – 7.27 (m, 2H), 7.24 – 7.20 (m, 0H), 6.04 (dd, *J* = 9.5, 5.2 Hz, 1H), 3.87 (dd, *J* = 18.1, 9.5 Hz, 1H), 3.22 (dd, *J* = 18.1, 5.2 Hz, 1H), 1.88 (s, 3H), 1.86 – 1.54 (m, 5H), 1.39 – 1.08 (m, 8H).

N-isobutyryl-N-(2-((2-methylprop-1-en-1-ylidene)amino)-1-phenylethyl)benzamide (40)

^{1}H NMR (300 MHz, CDCl$_3$): δ/ppm 7.78 – 7.66 (m, 2H), 7.59 – 7.48 (m, 3H), 7.51 – 7.39 (m, 2H), 7.40 – 7.24 (m, 3H), 5.85 (dd, *J* = 10.3, 5.2 Hz, 1H), 4.54 (dd, *J* = 10.3, 9.0 Hz, 1H), 4.05 (dd, *J* = 9.0, 5.2 Hz, 1H), 2.30 (hept, *J* = 6.7 Hz, 1H), 1.45 (s, 3H), 1.41 (s, 3H), 0.80 (d, *J* = 6.7 Hz, 3H), 0.77 (d, *J* = 6.7 Hz, 3H).

^{13}C NMR (75 MHz, CDCl$_3$): δ 181.5, 174.0, 137.1, 137.0, 133.1, 129.4, 129.0, 128.6, 128.5, 128.2, 120.3, 70.8, 65.3, 60.3, 38.5, 27.2, 26.1, 19.6, 19.0.

Below a comparative overview on ^{1}H NMR spectra (300 MHz, CDCl$_3$) of **33b** and **40** is depicted.

¹H NMR
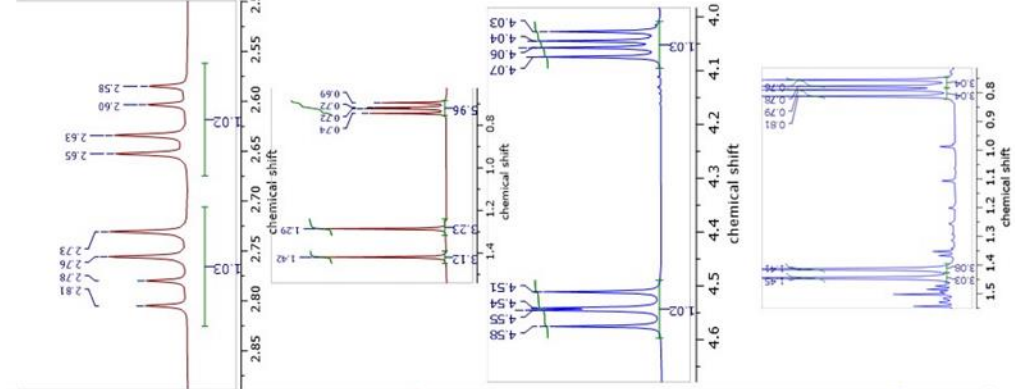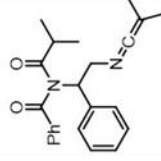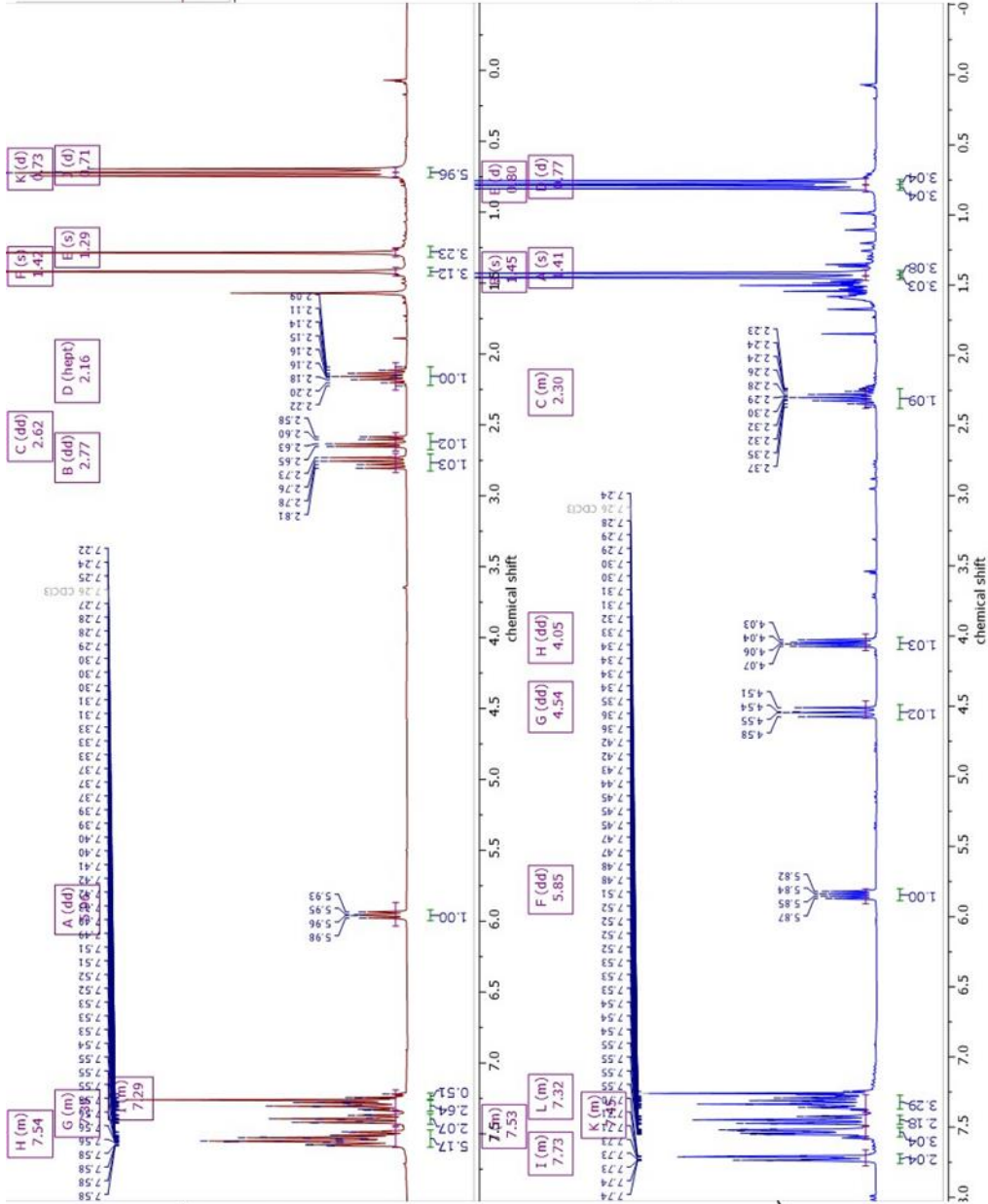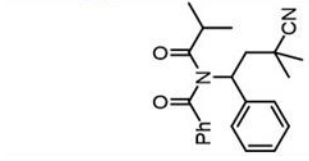
5.8 Additional View on Luminescence Quenching Spectra

Luminescence of Ir(ppy)$_3$ was excited at λ_{ex} = 315 nm and respective emission measured around λ_{em} = 525 nm. For experimental details on luminescence quenching experiments see chapter 5.1 and for further details and the discussion see chapter 3.3.6.3.

In the emission spectra of Ir(ppy)$_3$ (c = 4.6 · 10^{-4} M), TBPB concentrations of 0.60, 0.98 and 1.48 M, respectively caused intensities of lower magnitude compared to the other spectra (Figure 8). Figure 17 and Figure 18 show the curves based on a lower y-axis maximum for a better resolution.
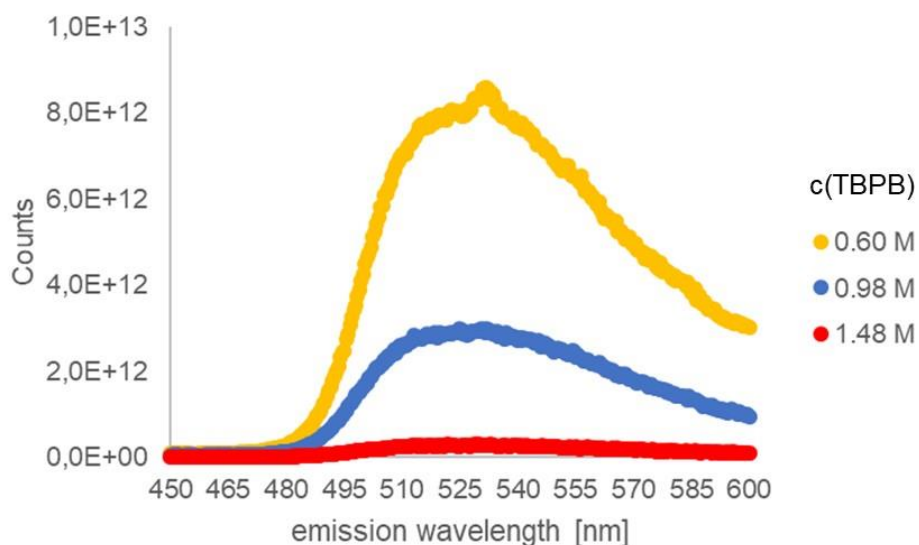

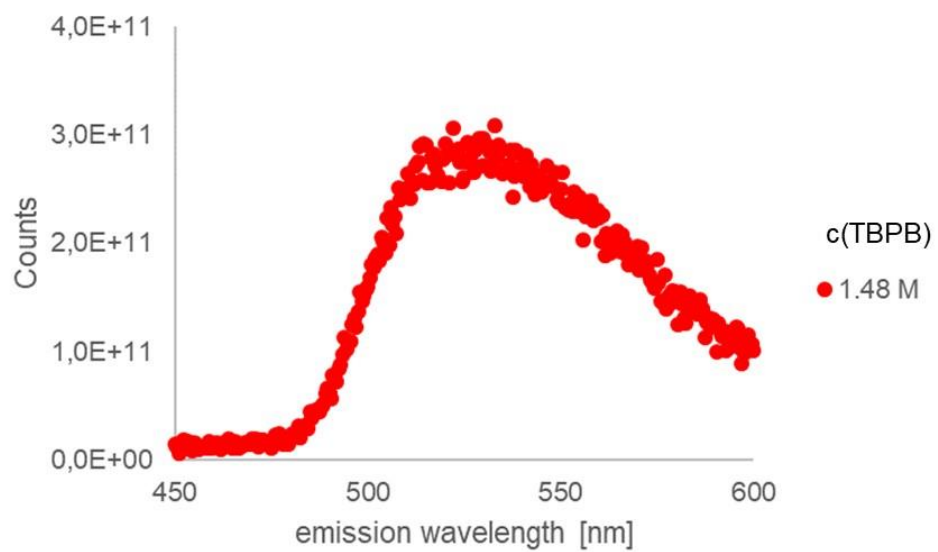Figure 17. Emission spectra of Ir(ppy)$_3$ (c = 4.6 · 10.4 M) in MeCN with high TBPB concentrations.

Figure 18. Emission spectrum of a solution of Ir(ppy)$_3$ (c = 4.6 · 10-4 M) and TBPB (c = 1.48 M) in MeCN.

6 References

(1)   Shao, W.; Lux, M.; Breugst, M.; Klussmann, M. *Org. Chem. Front.* **2019**, *6*, 1796.

(2)   Lux, M.; Klussmann, M. *Org. Lett.* **2020**, *22*, 3697.

(3)   Schweitzer-Chaput, B.; Demaerel, J.; Engler, H.; Klussmann, M. *Angew. Chem. Int. Ed.* **2014**, *53*, 8737.

(4)   Shaw, M. H.; Twilton, J.; MacMillan, D. W. C. *J. Org. Chem.* **2016**, *81*, 6898.

(5)   Balzani, V.; Bergamini, G.; Ceroni, P. *Rend. Lincei Sci. Fis. Nat.* **2017**, *28*, 125.

(6)   Balzani, V.; Bergamini, G.; Campagna, S.; Puntoriero, F. *Top. Curr. Chem.* **2007**, *280*, p 1.

(7)   (a) Balzani, V.; Moggi, L.; Manfrin, M. F.; Bolletta, F.; Gleria, M. *Science* **1975**, *189*, 852; (b) Amouyal, E. *Sol. Energy Mater. Sol. Cells* **1995**, *38*, 249;
(c) Harriman, A. *J. Photochem.* **1984**, *25*, 33.

(8)   Takeda, H.; Ishitani, O. *Coord. Chem. Rev.* **2010**, *254*, 346.

(9)   (a) Kalyanasundaram, K.; Grätzel, M. *Angew. Chem. Int. Ed.* **1979**, *18*, 701;
(b) Creutz, C.; Sutin, N. *Proc. Natl. Acad. Sci. U. S. A.* **1975**, *72*, 2858.

(10)   (a) Prier, C. K.; Rankic, D. A.; MacMillan, D. W. C. *Chem. Rev.* **2013**, *113*, 5322;
(b) Koike, T.; Akita, M. *Inorg. Chem. Front.* **2014**, *1*, 562.

(11)   Flamigni, L.; Barbieri, A.; Sabatini, C.; Ventura, B.; Barigelletti, F. In *Photochemistry and Photophysics of Coordination Compounds II*; Balzani, V., Campagna, S., Eds.; Springer Berlin Heidelberg: Berlin, Heidelberg, 2007, p 143.

(12)   (a) Colombo, M. G.; Brunold, T. C.; Riedener, T.; Guedel, H. U.; Fortsch, M.; Buergi, H.-B. *Inorg. Chem.* **1994**, *33*, 545;
(b) Fine, J.; Diri, K.; Krylov, A. I.; Nemirow, C.; Lu, Z.; Wittig, C. *Mol. Phys.* **2012**, *110*, 1849.

(13)   (a) King, K. A.; Spellane, P. J.; Watts, R. J. *J. Am. Chem. Soc.* **1985**, *107*, 1431;
(b) Maestri, M.; Balzani, V.; Deuschel-Cornioley, C.; Zelewsky, A. V. In *Advances in Photochemistry*; Volman, D. H., Hammond, G. S., Neckers, D. S., Eds.; John Wiley & Sons, Inc.: New York, 1992; Vol. 17, p 1.

(14)   (a) Marcus, R. A. *J. Chem. Phys.* **1956**, *24*, 966; (b) Marcus, R. A. *Angew. Chem. Int. Ed.* **1993**, *32*, 1111; (c) Marcus, R. A.; Sutin, N. *BBA-Bioenergetics* **1985**, *811*, 265.

(15)   Ulstrup, J.; Jortner, J. *J. Chem. Phys.* **1975**, *63*, 4358.

(16)   Atkin, P.; de Paula, J.; Keeler, J. *Atkins' Physical Chemistry*; 11th ed.; Oxford University Press: Oxford, 2017.

(17)   Garces, F. O.; King, K. A.; Watts, R. J. *Inorg. Chem.* **1988**, *27*, 3464.

(18)   Dedeian, K.; Djurovich, P. I.; Garces, F. O.; Carlson, G.; Watts, R. J. *Inorg. Chem.* **1991**, *30*, 1685.

(19)   Kärkäs, M. D.; Porco, J. A.; Stephenson, C. R. J. *Chem. Rev.* **2016**, *116*, 9683.

(20)   Ischay, M. A.; Anzovino, M. E.; Du, J.; Yoon, T. P. *J. Am. Chem. Soc.* **2008**, *130*, 12886.

(21)   Nicewicz, D. A.; MacMillan, D. W. C. *Science* **2008**, *322*, 77.

(22)   McNally, A.; Prier, C. K.; MacMillan, D. W. C. *Science* **2011**, *334*, 1114.

(23)   (a) Cukier, R. I.; Nocera, D. G. *Annu. Rev. Phys. Chem.* **1998**, *49*, 337;
         (b) Miller, D. C.; Tarantino, K. T.; Knowles, R. R. *Top. Curr. Chem.* **2016**, *374*, 30.

(24)   Tarantino, K. T.; Liu, P.; Knowles, R. R. *J. Am. Chem. Soc.* **2013**, *135*, 10022.

(25)   Choi, G. J.; Knowles, R. R. *J. Am. Chem. Soc.* **2015**, *137*, 9226.

(26)   (a) Nicholls, T. P.; Leonori, D.; Bissember, A. C. *Nat. Prod. Rep.* **2016**, *33*, 1248;
         (b) Lee, J. W.; Lee, K. N.; Ngai, M.-Y. *Angew. Chem. Int. Ed.* **2019**, *58*, 11171;
         (c) Campos, K. R.; Coleman, P. J.; Alvarez, J. C.; Dreher, S. D.; Garbaccio, R. M.; Terrett, N. K.; Tillyer, R. D.; Truppo, M. D.; Parmee, E. R. *Science* **2019**, *363*, eaat0805;
         (d) Crisenza, G. E. M.; Melchiorre, P. *Nature Commun.* **2020**, *11*, 803;
         (e) Mateus-Ruiz, J. B.; Cordero-Vargas, A. *Synthesis* **2020**, *52*, A.

(27)   Beatty, J. W.; Stephenson, C. R. J. *J. Am. Chem. Soc.* **2014**, *136*, 10270.

(28)   Müller, D. S.; Untiedt, N. L.; Dieskau, A. P.; Lackner, G. L.; Overman, L. E. *J. Am. Chem. Soc.* **2015**, *137*, 660.

(29)   Slutskyy, Y.; Jamison, C. R.; Lackner, G. L.; Müller, D. S.; Dieskau, A. P.; Untiedt, N. L.; Overman, L. E. *J. Org. Chem.* **2016**, *81*, 7029.

(30)   Xue, F.; Lu, H.; He, L.; Li, W.; Zhang, D.; Liu, X.-Y.; Qin, Y. *J. Org. Chem.* **2018**, *83*, 754.

(31)   Lan, X.-W.; Wang, N.-X.; Xing, Y. *Eur. J. Org. Chem.* **2017**, *2017*, 5821.

(32)   (a) Moir, M.; Danon, J. J.; Reekie, T. A.; Kassiou, M. *Expert Opin. Drug Discov.* **2019**, *14*, 1137;

(b) Börgel, J.; Ritter, T. *Chem* **2020**, *6*, 1877.

(33)   (a) McDonald, R. I.; Liu, G.; Stahl, S. S. *Chem. Rev.* **2011**, *111*, 2981;

(b) Yin, G.; Mu, X.; Liu, G. *Acc. Chem. Res.* **2016**, *49*, 2413;

(c) Hu, Z.; Tong, X.; Liu, G. *Org. Lett.* **2016**, *18*, 1702.

(34)   (a) Bachmann, W. E.; Wiselogle, F. Y. *J. Org. Chem.* **1936**, *01*, 354;

(b) Fischer, H. *Chem. Rev.* **2001**, *101*, 3581;

(c) Studer, A. *Chem. Eur. J.* **2001**, *7*, 1159;

(d) Griller, D.; Ingold, K. U. *Acc. Chem. Res.* **1976**, *9*, 13.

(35)   Hioe, J.; Zipse, H. In *Encyclopedia of Radicals in Chemistry, Biology and Materials*; Chatgilialoglu, C., Studer, A., Eds.; Wiley-VHC: Weinheim, 2012, p 1.

(36)   Leifert, D.; Studer, A. *Angew. Chem. Int. Ed.* **2020**, *59*, 74.

(37)   Fischer, H. *J. Am. Chem. Soc.* **1986**, *108*, 3925.

(38)   Bravo, A.; Bjørsvik, H.-R.; Fontana, F.; Liguori, L.; Minisci, F. *J. Org. Chem.* **1997**, *62*, 3849.

(39)   Fischer, H.; Radom, L. *Angew. Chem. Int. Ed.* **2001**, *40*, 1340.

(40)   Giese, B. *Angew. Chem. Int. Ed.* **1983**, *22*, 753.

(41)   (a) Tedder, J. M.; Walton, J. C. *Acc. Chem. Res.* **1976**, *9*, 183;

(b) Tedder, J. M.; Walton, J. C. *Tetrahedron* **1980**, *36*, 701.

(42)   Levy, M.; Szwarc, M. *J. Am. Chem. Soc.* **1955**, *77*, 1949.

(43)   Zipse, H.; He, J.; Houk, K. N.; Giese, B. *J. Am. Chem. Soc.* **1991**, *113*, 4324.

(44)   (a) Zytowski, T.; Fischer, H. *J. Am. Chem. Soc.* **1996**, *118*, 437;

(b) Walbiner, M.; Wu, J. Q.; Fischer, H. *Helv. Chim. Acta* **1995**, *78*, 910.

(45)   Wu, J. Q.; Beranek, I.; Fischer, H. *Helv. Chim. Acta* **1995**, *78*, 194.

(46)   Wu, J. Q.; Fischer, H. *Int. J. Chem. Kinet.* **1995**, *27*, 167.

(47)   Verschueren, R. H.; Schmauck, J.; Perryman, M. S.; Yue, H.-L.; Riegger, J.; Schweitzer-Chaput, B.; Breugst, M.; Klussmann, M. *Chem. Eur. J.* **2019**, *25*, 9088.

(48)   Hristova, D.; Gatlik, I.; Rist, G.; Dietliker, K.; Wolf, J. P.; Birbaum, J. L.; Savitsky, A.; Möbius, K.; Gescheidt, G. *Macromolecules* **2005**, *38*, 7714.

(49)   Zytowski, T.; Knühl, B.; Fischer, H. *Helv. Chim. Acta* **2000**, *83*, 658.

(50)   Schweitzer-Chaput, B.; Sud, A.; Pinter, A.; Dehn, S.; Schulze, P.; Klussmann, M. *Angew. Chem. Int. Ed.* **2013**, *52*, 13228.

(51)   Klussmann, M. *Chem. Eur. J.* **2018**, *24*, 4480.

(52)   Bell, E. R.; Raley, J. H.; Rust, F. F.; Seubold, F. H.; Vaughan, W. E. *Disscus. Faraday Soc.* **1951**, *10*, 242.

(53)   (a) Pan, G.-H.; Ouyang, X.-H.; Hu, M.; Xie, Y.-X.; Li, J.-H. *Adv. Synth. Catal.* **2017**, *359*, 2564;

         (b) Shu, W.; Merino, E.; Nevado, C. *ACS Catal.* **2018**, *8*, 6401;

         (c) Ouyang, X.-H.; Song, R.-J.; Hu, M.; Yang, Y.; Li, J.-H. *Angew. Chem. Int. Ed.* **2016**, *55*, 3187;

         (d) Yong, X.; Han, Y.-F.; Li, Y.; Song, R.-J.; Li, J.-H. *Chem. Commun.* **2018**, *54*, 12816.

(54)   Kamijo, S.; Yokosaka, S.; Inoue, M. *Tetrahedron Lett.* **2012**, *53*, 4324.

(55)   Wang, F.; Wang, D.; Wan, X.; Wu, L.; Chen, P.; Liu, G. *J. Am. Chem. Soc.* **2016**, *138*, 15547.

(56)   Zhou, S.; Zhang, G.; Fu, L.; Chen, P.; Li, Y.; Liu, G. *Org. Lett.* **2020**, *22*, 6299.

(57)   Sha, W.; Deng, L.; Ni, S.; Mei, H.; Han, J.; Pan, Y. *ACS Catal.* **2018**, *8*, 7489.

(58)   Dange, N. S.; Robert, F.; Landais, Y. *Org. Lett.* **2016**, *18*, 6156.

(59)   Hassan, H.; Pirenne, V.; Wissing, M.; Khiar, C.; Hussain, A.; Robert, F.; Landais, Y. *Chem. Eur. J.* **2017**, *23*, 4651.

(60)   Hara, R.; Khiar, C.; Dange, N. S.; Bouillac, P.; Robert, F.; Landais, Y. *Eur. J. Org. Chem.* **2018**, *2018*, 4058.

(61)   Zhu, X.; Deng, W.; Chiou, M.-F.; Ye, C.; Jian, W.; Zeng, Y.; Jiao, Y.; Ge, L.; Li, Y.; Zhang, X.; Bao, H. *J. Am. Chem. Soc.* **2019**, *141*, 548.

(62)   (a) Boger, D. L.; Mathvink, R. J. *J. Org. Chem.* **1992**, *57*, 1429;

         (b) Raviola, C.; Protti, S.; Ravelli, D.; Fagnoni, M. *Green Chem.* **2019**, *21*, 748;

         (c) Chatgilialoglu, C.; Crich, D.; Komatsu, M.; Ryu, I. *Chem. Rev.* **1999**, *99*, 1991;

         (d) Banerjee, A.; Lei, Z.; Ngai, M.-Y. *Synthesis* **2019**, *51*, 303.

(63)   Barton, D. H. R.; Jaszberenyi, J. C.; Morrell, A. I. *Tetrahedron Lett.* **1991**, *32*, 311.

(64)   Stache, E. E.; Ertel, A. B.; Rovis, T.; Doyle, A. G. *ACS Catal.* **2018**, *8*, 11134.

(65)   Nájera, C.; Yus, M. *Org. Prep. Proced. Int.* **1995**, *27*, 383.

(66)   Fujiwara, S.-i.; Shimizu, Y.; Shin-ike, T.; Kambe, N. *Org. Lett.* **2001**, *3*, 2085.

(67)   Boger, D. L.; Mathvink, R. J. *J. Am. Chem. Soc.* **1990**, *112*, 4003.

(68)   Ouchi, A.; Ando, W.; Oba, M. In *PATAI'S Chemistry of Functional Groups*; Rappoport, Z., Ed.; Wiley & Sons: New York, 2013; Vol. 4, p 1.

(69)   Horning, B. D.; MacMillan, D. W. C. *J. Am. Chem. Soc.* **2013**, *135*, 6442.

(70)   Bennasar, M. L.; Roca, T.; García-Díaz, D. *J. Org. Chem.* **2008**, *73*, 9033.

(71)   Bath, S.; Laso, N. M.; Lopez-Ruiz, H.; Quiclet-Sire, B.; Zard, S. Z. *Chem. Commun.* **2003**, 204.

(72)   Li, X.; Fang, X.; Zhuang, S.; Liu, P.; Sun, P. *Org. Lett.* **2017**, *19*, 3580.

(73)   Guo, W.; Lu, L.-Q.; Wang, Y.; Wang, Y.-N.; Chen, J.-R.; Xiao, W.-J. *Angew. Chem. Int. Ed.* **2015**, *54*, 2265.

(74)   Scheffold, R.; Orlinski, R. *J. Am. Chem. Soc.* **1983**, *105*, 7200.

(75)   Bergonzini, G.; Cassani, C.; Wallentin, C.-J. *Angew. Chem. Int. Ed.* **2015**, *54*, 14066.

(76)   Bergonzini, G.; Cassani, C.; Lorimer-Olsson, H.; Hörberg, J.; Wallentin, C.-J. *Chem. Eur. J.* **2016**, *22*, 3292.

(77)   Lei, Z.; Banerjee, A.; Kusevska, E.; Rizzo, E.; Liu, P.; Ngai, M. Y. *Angew. Chem. Int. Ed.* **2019**, *58*, 7318.

(78)   Chudasama, V.; Fitzmaurice, R. J.; Caddick, S. *Nat. Chem.* **2010**, *2*, 592.

(79)   Manna, M. K.; Bairy, G.; Jana, R. *Org. Biomol. Chem.* **2017**, *15*, 5899.

(80)   Ouyang, X.-H.; Song, R.-J.; Li, J.-H. *Eur. J. Org. Chem.* **2014**, *2014*, 3395.

(81)   Vinogradov, M. G.; Nikishin, G. I. *Russ. Chem. Rev.* **1971**, *40*, 916.

(82)   Marzo, L.; Pagire, S. K.; Reiser, O.; König, B. *Angew. Chem. Int. Ed.* **2018**, *57*, 10034.

(83)   Liu, W.; Li, Y.; Liu, K.; Li, Z. *J. Am. Chem. Soc.* **2011**, *133*, 10756.

(84)   Ashokkumar, V.; Siva, A. *Org. Biomol. Chem.* **2017**, *15*, 2551.

(85)   Zhao, L.; Wang, Y.; Ma, Z.; Wang, Y. *Inorg. Chem.* **2017**, *56*, 8166.

(86)   Jiao, Y.; Chiou, M.-F.; Li, Y.; Bao, H. *ACS Catal.* **2019**, *9*, 5191.

(87)   Ge, L.; Li, Y.; Bao, H. *Org. Lett.* **2019**, *21*, 256.

(88)   Li, J.; Wang, D. Z. *Org. Lett.* **2015**, *17*, 5260.

(89)   de Souza, G. F. P.; Bonacin, J. A.; Salles, A. G. *J. Org. Chem.* **2018**, *83*, 8331.

(90)   Liu, R.-X.; Zhang, F.; Peng, Y.; Yang, L. *Chem. Commun.* **2019**, *55*, 12080.

(91)   Wu, C.-S.; Liu, R.-X.; Ma, D.-Y.; Luo, C.-P.; Yang, L. *Org. Lett.* **2019**, *21*, 6117.

(92)   Li, W.-Y.; Wang, Q.-Q.; Yang, L. *Org. Biomol. Chem.* **2017**, *15*, 9987.

(93)   Cheng, Y.-Y.; Lei, T.; Su, L.; Fan, X.; Chen, B.; Tung, C.-H.; Wu, L.-Z. *Org. Lett.* **2019**, *21*, 8789.

(94)   Mumm, O. *Ber. Dtsch. Chem. Ges.* **1910**, *43*, 886.

(95)   Liu, Y.-Y.; Yang, X.-H.; Song, R.-J.; Luo, S.; Li, J.-H. *Nature Commun.* **2017**, *8*, 14720.

(96)   (a) Pan, G.-H.; Song, R.-J.; Xie, Y.-X.; Luo, S.; Li, J.-H. *Synthesis* **2018**, *50*, 1651; (b) Gockel, S. N.; Buchanan, T. L.; Hull, K. L. *J. Am. Chem. Soc.* **2018**, *140*, 58.

(97)   Ouyang, X.-H.; Li, Y.; Song, R.-J.; Li, J.-H. *Org. Lett.* **2018**, *20*, 6659.

(98)   Fumagalli, G.; Boyd, S.; Greaney, M. F. *Org. Lett.* **2013**, *15*, 4398.

(99)   Prasad Hari, D.; Hering, T.; König, B. *Angew. Chem. Int. Ed.* **2014**, *53*, 725.

(100)   Yasu, Y.; Koike, T.; Akita, M. *Org. Lett.* **2013**, *15*, 2136.

(101)   Zhu, N.; Wang, T.; Ge, L.; Li, Y.; Zhang, X.; Bao, H. *Org. Lett.* **2017**, *19*, 4718.

(102)   Carboni, A.; Dagousset, G.; Magnier, E.; Masson, G. *Chem. Commun.* **2014**, *50*, 14197.

(103)   Li, M.; Yang, J.; Ouyang, X.-H.; Yang, Y.; Hu, M.; Song, R.-J.; Li, J.-H. *J. Org. Chem.* **2016**, *81*, 7148.

(104)   Duan, Y.; Li, W.; Xu, P.; Zhang, M.; Cheng, Y.; Zhu, C. *Org. Chem. Front.* **2016**, *3*, 1443.

(105)   Yang, Y.; Song, R.-J.; Ouyang, X.-H.; Wang, C.-Y.; Li, J.-H.; Luo, S. *Angew. Chem. Int. Ed.* **2017**, *56*, 7916.

(106)   Ouyang, X.-H.; Cheng, J.; Li, J.-H. *Chem. Commun.* **2018**, *54*, 8745.

(107)   Ouyang, X.-H.; Hu, M.; Song, R.-J.; Li, J.-H. *Chem. Commun.* **2018**, *54*, 12345.

(108)   Su, R.; Li, Y.; Min, M.-Y.; Ouyang, X.-H.; Song, R.-J.; Li, J.-H. *Chem. Commun.* **2018**, *54*, 13511.

(109)   Klauck, F. J. R.; Yoon, H.; James, M. J.; Lautens, M.; Glorius, F. *ACS Catal.* **2019**, *9*, 236.

(110)   Min, M.-Y.; Song, R.-J.; Ouyang, X.-H.; Li, J.-H. *Chem. Commun.* **2019**, *55*, 3646.

(111)   WHO 2018.

(112)   Woodrow, C. J.; Haynes, R. K.; Krishna, S. *Postgrad. Med. J.* **2005**, *81*, 71.

(113)   Meshnick, S. R. *Int. J. Parasitol.* **2002**, *32*, 1655.

(114)   Brossi, A.; Venugopalan, B.; Dominguez Gerpe, L.; Yeh, H. J. C.; Flippen-Anderson, J. L.; Buchs, P.; Luo, X. D.; Milhous, W.; Peters, W. *J. Med. Chem.* **1988**, *31*, 645.

(115)   (a) Krungkrai, S. R.; Yuthavong, Y. *Trans. R. Soc. Trop. Med. Hyg.* **1987**, *81*, 710;

(b) Senok, A. C.; Nelson, E. A. S.; Li, K.; Oppenheimer, S. J. *Trans. R. Soc. Trop. Med. Hyg.* **1997**, *91*, 585.

(116)   (a) Wang, J.; Zhang, C.-J.; Chia, W. N.; Loh, C. C. Y.; Li, Z.; Lee, Y. M.; He, Y.; Yuan, L.-X.; Lim, T. K.; Liu, M.; Liew, C. X.; Lee, Y. Q.; Zhang, J.; Lu, N.; Lim, C. T.; Hua, Z.-C.; Liu, B.; Shen, H.-M.; Tan, K. S. W.; Lin, Q. *Nature Commun.* **2015**, *6*, 10111;

(b) O'Neill, P. M.; Barton, V. E.; Ward, S. A. *Molecules* **2010**, *15*, 1705;

(c) Ismail, H. M.; Barton, V.; Phanchana, M.; Charoensutthivarakul, S.; Wong, M. H. L.; Hemingway, J.; Biagini, G. A.; O'Neill, P. M.; Ward, S. A. *Proc. Natl. Acad. Sci. U. S. A.* **2016**, *113*, 2080;

(d) Ying-Zi, Y.; Asawamahasakda, W.; Meshnick, S. R. *Biochem. Pharmacol.* **1993**, *46*, 336.

(117)   (a) Wu, Y.; Yue, Z.-Y.; Wu, Y.-L. *Angew. Chem. Int. Ed.* **1999**, *38*, 2580;

(b) Wu, Y.; Yue, Z.-Y.; Liu, H.-H. *Helv. Chim. Acta* **2001**, *84*, 928;

(c) Wu, Y. *Acc. Chem. Res.* **2002**, *35*, 255;

(d) Wu, W.-M.; Yao, Z.-J.; Wu, Y.-L.; Jiang, K.; Wang, Y.-F.; Cehn, H.-B.; Shan, F.; Li, Y. *Chem. Commun.* **1996**, 2213.

(118)   (a) Butler, A. R.; Gilbert, B. C.; Hulme, P.; Irvine, L. R.; Renton, L.; Whitwood, A. C. *Free Radic. Res.* **1998**, *28*, 471;

(b) Meshnick, S. R.; Yang, Y. Z.; Lima, V.; Kuypers, F.; Kamchonwongpaisan, S.; Yuthavong, Y. *Antimicrob. Agents Chemother.* **1993**, *37*, 1108.

(119)   Krishna, S.; Uhlemann, A.-C.; Haynes, R. K. *Drug Resist. Update* **2004**, *7*, 233.

(120)   Posner, G. H.; Oh, C. H. *J. Am. Chem. Soc.* **1992**, *114*, 8328.

(121)   Lin, A. J.; Klayman, D. L.; Hoch, J. M.; Silverton, J. V.; George, C. F. *J. Org. Chem.* **1985**, *50*, 4504.

(122)   Susan E. Francis; David J. Sullivan, J.; Goldberg, D. E. *Annu. Rev. Microbiol.* **1997**, *51*, 97.

(123)   Zhang, S.; Gerhard, G. S. *Bioorg. Med. Chem.* **2008**, *16*, 7853.

(124)   (a) Jones-Brando, L.; D'Angelo, J.; Posner, G. H.; Yolken, R. *Antimicrob. Agents Chemother.* **2006**, *50*, 4206;
          (b) Kumar, S.; Gupta, A. K.; Pal, Y.; Dwivedi, S. K. *J. Vet. Med. Sci.* **2003**, *65*, 1171.

(125)   (a) Milas, N. A.; Surgenor, D. M. *J. Am. Chem. Soc.* **1946**, *68*, 205;
          (b) Bietti, M.; Salamone, M. *Synlett* **2014**, *25*, 1803.

(126)   Avery, M. A.; Chong, W. K. M.; Bupp, J. E. *J. Chem. Soc., Chem. Commun.* **1990**, 1487.

(127)   (a) Haynes, R. K.; Vonwiller, S. C. *Tetrahedron Lett.* **1996**, *37*, 257; (b) Haynes, R. K.; Pai, H. H.-O.; Voerste, A. *Tetrahedron Lett.* **1999**, *40*, 4715.

(128)   (a) Wondrak, G. T. *Antioxid. Redox Signal.* **2009**, *11*, 3013;
          (b) Crespo-Ortiz, M. P.; Wei, M. Q. *J. Biomed. Biotechnol.* **2012**, *2012*, 247597.

(129)   Terzić, N.; Opsenica, D.; Milić, D.; Tinant, B.; Smith, K. S.; Milhous, W. K.; Šolaja, B. A. *J. Med. Chem.* **2007**, *50*, 5118.

(130)   Posner, G. H.; Oh, C. H.; Wang, D.; Gerena, L.; Milhous, W. K.; Meshnick, S. R.; Asawamahasadka, W. *J. Med. Chem.* **1994**, *37*, 1256.

(131)   Klussmann, M. *unpublished work* **2020**.

(132)   (a) Bovey, F. A.; Tiers, G. V. D. *J. Polym. Sci. A* **1963**, *1*, 849;
          (b) Gleason, E. H.; Miller, M. L.; Sheats, G. F. *J. Polym. Sci.* **1959**, *38*, 133;
          (c) Kulicke, W. M.; Kniewske, R.; Klein, J. *Prog. Polym. Sci.* **1982**, *8*, 373.

(133)   Kattner, H.; Buback, M. *Macromol. Rapid Commun.* **2015**, *36*, 2186.

(134)   Wu, S.; Shanks, R. A. *J. Appl. Polym. Sci.* **2004**, *93*, 1493.

(135)   Flory, P. J. *J. Am. Chem. Soc.* **1940**, *62*, 1561.

(136)   (a) Liu J.-M.; Ni M.-Y.; Fan J.-F.; Tu Y.-Y.; Wu Z.-H.; Wu Y.-L.; W.-S., Z. *Acta Chim. Sinica* **1979**, *37*, 129;
          (b) Zeng, M.-Y.; Li, L.-N.; Chen, S.-F.; Li, G.-Y.; Liang, X.-T.; Chen, M.; Clardy, J. *Tetrahedron* **1983**, *39*, 2941.

(137)   (a) Duncton, M. A. J. *Med. Chem. Commun.* **2011**, *2*, 1135;
   (b) Minisci, F.; Vismara, E.; Fontana, F. *Heterocycles* **1989**, *28*, 489;

(c) Minisci, F.; Bernardi, R.; Bertini, F.; Galli, R.; Perchinummo, M. *Tetrahedron* **1971**, *27*, 3575;

(d) Caronna, T.; Gardini, G. P.; Minisci, F. *J. Chem. Soc. D* **1969**, 201;

(e) Hofmann, J.; Gans, E.; Clark, T.; Heinrich, M. R. *Chem. Eur. J.* **2017**, *23*, 9647;

(f) Guerrero, M. A.; Miranda, L. D. *Tetrahedron Lett.* **2006**, *47*, 2517.

(138)   Potts, H. A.; Smith, G. F. *J. Chem. Soc.* **1957**, 4018.

(139)   Sargent, F. P.; Gardy, E. M. *Can. J. Chem.* **1976**, *54*, 275.

(140)   Buettner, G. R. *Free Radic. Biol. Med.* **1987**, *3*, 259.

(141)   Rosen, G. M.; Rauckman, E. J. *Proc. Natl. Acad. Sci. U.S.A.* **1981**, *78*, 7346.

(142)   Davies, M. J.; Forni, L. G.; Shuter, S. L. *Chem. Biol. Interact.* **1987**, *61*, 177.

(143)   Bertrand, M. P. *Org. Prep. Proced. Int.* **1994**, *26*, 257.

(144)   Schaffner, A.-P.; Darmency, V.; Renaud, P. *Angew. Chem. Int. Ed.* **2006**, *45*, 5847.

(145)   Barton, D. H. R.; Jaszberenyi, J. C.; Tachdjian, C. *Tetrahedron Lett.* **1991**, *32*, 2703.

(146)   Bertrand, F.; Le Guyader, F.; Liguori, L.; Ouvry, G.; Quiclet-Sire, B.; Seguin, S.; Zard, S. Z. *C. R. Chimie* **2001**, *4*, 547.

(147)   Crich, D.; Hutton, T. K.; Ranganathan, K. *J. Org. Chem.* **2005**, *70*, 7672.

(148)   (a) Capaldo, L.; Ravelli, D. *Eur. J. Org. Chem.* **2017**, *2017*, 2056;

(b) Mayer, J. M. *Acc. Chem. Res.* **2011**, *44*, 36;

(c) Avila, D. V.; Brown, C. E.; Ingold, K. U.; Lusztyk, J. *J. Am. Chem. Soc.* **1993**, *115*, 466;

(d) Salamone, M.; Bietti, M. *Acc. Chem. Res.* **2015**, *48*, 2895.

(149)   (a) Xue, Q.; Xie, J.; Xu, P.; Hu, K.; Cheng, Y.; Zhu, C. *ACS Catal.* **2013**, *3*, 1365;

(b) Dong, Y.-X.; Li, Y.; Gu, C.-C.; Jiang, S.-S.; Song, R.-J.; Li, J.-H. *Org. Lett.* **2018**, *20*, 7594;

(c) Ouyang, X.-H.; Li, Y.; Song, R.-J.; Hu, M.; Luo, S.; Li, J.-H. *Sci. Adv.* **2019**, *5*, eaav9839;

(d) Klussmann, M.; Liu, S. *Chem. Commun.* **2020**, *56*, 1557;

(e) Ha, T. M.; Chatalova-Sazepin, C.; Wang, Q.; Zhu, J. *Angew. Chem. Int. Ed.* **2016**, *55*, 9249.

(150)   Antonello, S.; Maran, F. *J. Am. Chem. Soc.* **1999**, *121*, 9668.

(151)   Yayla, H. G.; Peng, F.; Mangion, I. K.; McLaughlin, M.; Campeau, L.-C.; Davies, I. W.; DiRocco, D. A.; Knowles, R. R. *Chem. Sci.* **2016**, *7*, 2066.

(152)   Baron, R.; Darchen, A.; Hauchard, D. *Electrochim. Acta* **2006**, *51*, 1336.

(153)   Wayner, D. D. M.; McPhee, D. J.; Griller, D. *J. Am. Chem. Soc.* **1988**, *110*, 132.

(154)   (a) Fischer, H.; Paul, H. *Acc. Chem. Res.* **1987**, *20*, 200;
(b) Tsentalovich, Y. P.; Fischer, H. *J. Chem. Soc., Perkin Trans. 2* **1994**, 729;
(c) Caronna, T.; Minisci, F. In *Reviews on Reactive Species in Chemical Reactions*; Freund Publishing House: Tel Aviv, 1973; Vol. 1, p 263.

(155)   (a) Qin, Q.; Han, Y.-Y.; Jiao, Y.-Y.; He, Y.; Yu, S. *Org. Lett.* **2017**, *19*, 2909;
(b) Zhang, J.; Zhang, F.; Lai, L.; Cheng, J.; Sun, J.; Wu, J. *Chem. Commun.* **2018**, *54*, 3891;
(c) Wu, D.; Cui, S.-S.; Lin, Y.; Li, L.; Yu, W. *J. Org. Chem.* **2019**, *84*, 10978.

(156)   Sommer, L. H.; Dorfman, E.; Goldberg, G. M.; Whitmore, F. C. *J. Am. Chem. Soc.* **1946**, *68*, 488.

(157)   Rust, F. F.; Seubold, F. H.; Vaughan, W. E. *J. Am. Chem. Soc.* **1948**, *70*, 3258.

(158)   Blomquist, A. T.; Ferris, A. F. *J. Am. Chem. Soc.* **1951**, *73*, 3408.

(159)   Lawesson, S.-O.; Yang, N. C. *J. Am. Chem. Soc.* **1959**, *81*, 4230.

(160)   Locklear, M.; Dussault, P. H. *Eur J Org Chem* **2020**, *2020*, 4814.

(161)   Schmidt am Busch, M.; Knapp, E.-W. *J. Am. Chem. Soc.* **2005**, *127*, 15730.

(162)   (a) Boaz, H.; Rollefson, G. K. *J. Am. Chem. Soc.* **1950**, *72*, 3435;
(b) Fraiji, L. K.; Hayes, D. M.; Werner, T. C. *J. Chem. Educ.* **1992**, *69*, 424;
(c) Lakowicz, J. R. In *Principles of Fluorescence Spectroscopy*; Lakowicz, J. R., Ed.; Springer US: Boston, MA, 2006, p 331.

(163)   Moon, A. Y.; Poland, D. C.; Scheraga, H. A. *J. Phys. Chem.* **1965**, *69*, 2960.

(164)   Studer, A.; Curran, D. P. *Nat. Chem.* **2014**, *6*, 765.

(165)   Xu, Z.-F.; Shan, L.; Zhang, W.; Cen, M.; Li, C.-Y. *Org. Chem. Front.* **2019**, *6*, 1391.

(166)   Zhang, M.-M.; Liu, F. *Org. Chem. Front.* **2018**, *5*, 3443.

(167)   Fulmer, G. R.; Miller, A. J. M.; Sherden, N. H.; Gottlieb, H. E.; Nudelman, A.; Stoltz, B. M.; Bercaw, J. E.; Goldberg, K. I. *Organometallics* **2010**, *29*, 2176.
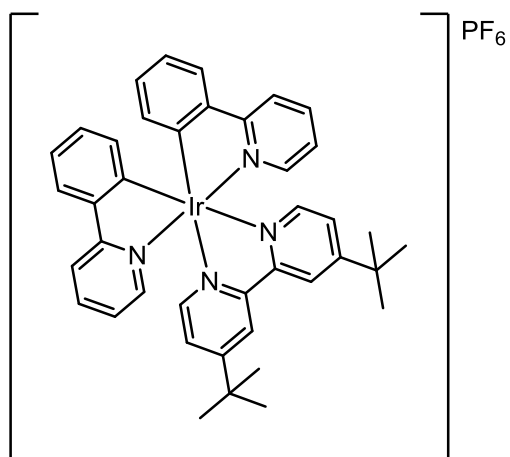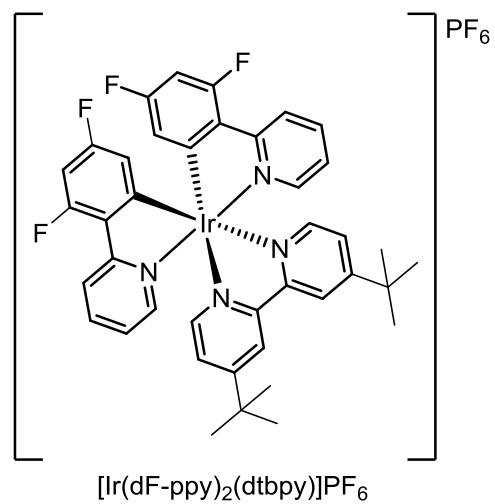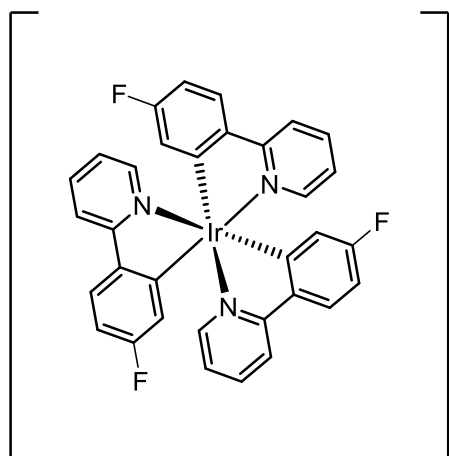
7 Catalyst Index
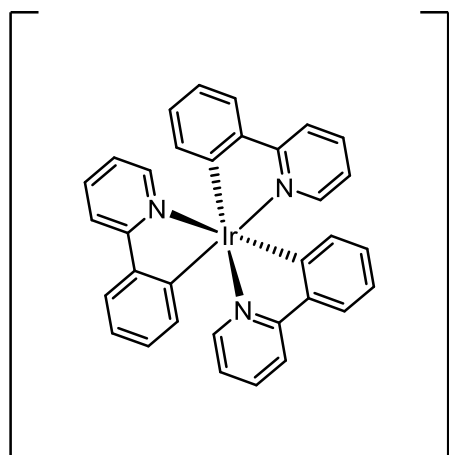
Ir(ppy)$_3$
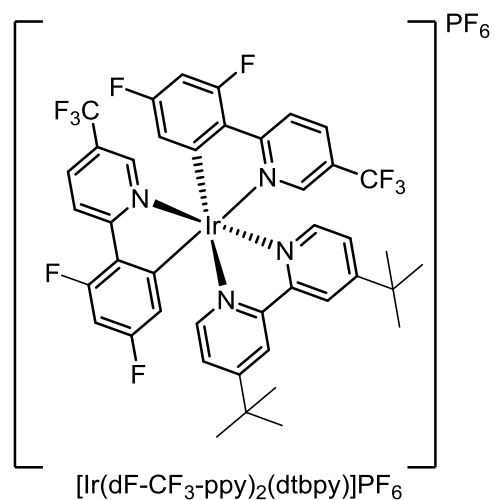
[Ir(ppy)$_2$(dtbpy)]PF$_6$

Ir(5'-F-ppy)$_3$

[Ir(dF-CF$_3$-ppy)$_2$(dtbpy)]PF$_6$

[Ir(dF-ppy)$_2$(dtbpy)]PF$_6$

8   Lebenslauf

Name: Marcel Lux

Geburtsdatum: 16. Juli 1990

Geburtsort: Siegen

Promotion Organische Chemie:

Seit Mai 2017:   Max-Planck-Institut für Kohlenforschung

Betreuer: Dr. Martin Klußmann

Voraussichtlicher Abschluss im Februar 2021

Hochschulausbildung:

WS 2014/15-November 2016:   M. Sc. Chemie (RWTH Aachen);

Abschlussarbeit mit Dr. Michael E. Tauchert

WS 2011/12- SS 2014:   B. Sc. Chemie (RWTH Aachen);

Zivildienst:

08/2010- 08/2011:   LVR-Schule am Königsforst in Rösrath

Schulausbildung:

2001 – 2010:   Freiherr-vom-Stein Gymnasium in Rösrath;

1997 – 2001:   Katholische Grundschule Rösrath

Sprachkenntnisse: Englisch: Verhandlungssicher

Französisch: Gute Kenntnisse

Mülheim an der Ruhr, der 18.12.2020